LOAD CAPACITY TESTING AND ANALYSIS OF RESIDENTIAL UNDERPINNING SYSTEMS IN EXPANSIVE CLAY ENVIRONMENT

by

WILLIAM THOMAS WITHERSPOON

Presented to the Faculty of the Graduate School of

The University of Texas at Arlington in Partial Fulfillment

of the Requirements

for the Degree of

DOCTOR OF PHILOSOPHY

THE UNIVERSITY OF TEXAS AT ARLINGTON

May 2006

ABSTRACT

LOAD CAPACITY TESTING OF RESIDENTIAL UNDERPINNING IN EXPANSIVE CLAY SOILS

Publication No._____

W. Tom Witherspoon

The University of Texas at Arlington 2006

Supervising Professor: Anand J. Puppala

For most families, owning a home is considered the major investment of their lifetime. Because this asset is so important to continued enrichment of their lives, maintenance requirements that result from home foundation problems should be addressed prior to their acquisition. Unfortunately, many house foundations are neither built to meet challenges of their expansive soil environment nor built to address moisture changes from various seasonal fluctuations. As a result of design and construction deficiencies, foundation failures may occur on a regular basis. In fact, the Department of Housing and Urban Development estimated foundation damage caused by expansive clay soil at $9 billion per year in 1981 (Jones 1981), which would make it more destructive

than any other natural disasters including tornados, hurricanes and earthquakes. More recent estimates by Witherspoon (2000), based on data collected from foundation repair contractors, places this damage total at an approximate $13 billion per year. This cost is enormous and explains the severity of concerns for home owners situated in expansive clay zones.

Since these foundations must be repaired when they fail, a large industry has grown to address the needs of homeowners everywhere. Although a foundation may rise or fall, the dominant cause of problems is foundation settlement as the clay consolidates under the load of the foundation or the clay swells and shrinks after wetting and drying. To address these problems, a repair contractor frequently will install underpinning under the perimeter of the foundation and lift the low segment(s) back to a more desirable elevation position and thus prevent the distressed segment from dropping in the future. To address the interior, a foundation repair contractor will either place underpinning under interior grade beams or lift the slab with a process called mudjacking that first fills voids and then lifts the slab with injection pressure from the grout flow. By filling voids, the load of the slab will not shift to foundation contact areas where pliable clay soils may deform over time and allow settlement of the interior slab.

Underpinning techniques, using drilled shafts have received extensive testing and research to develop standards for design and practice, whereas other methods such as hydraulically pressed piles have not been researched to determine proper design or construction practices. Since underpinnings are predominantly used to lift the distressed foundations, it is important to understand their axial load transfer mechanism. Uplift issues are not focused in this research since these are deep foundation types and can go

beyond the active depth of a test site. This research is an attempt to conduct comprehensive field studies on a variety of underpinning methods in order to understand axial load capacity of each underpinning technique at different weather conditions. Tests were conducted on each of the underpinning methods installed in expansive clays where skin friction transfer along the foundation length is the dominant load carrying mechanism.

Underpinnings including drilled straight shafts, drilled belled shafts, augercast piles, helical piers, pressed steel and pressed concrete piles were constructed utilizing the assistance of contractors who have been working with these underpinning methods. Standards of practice were followed to test the underpinning in a manner that would be fair, uniform, accurate and representative of actual site conditions. Final axial load capacity was measured by performing tests on foundations following ASTM D1143.

Actual practices for the helical anchors, pressed concrete and pressed steel pilings were reviewed to establish drive pressures available (pressed pilings) and torque drive (helical piers) for a normal residential underpinning project. In the case of drilled shafts, the normal active depth requirement for the local site expansive clay was determined, and the drilled straight shaft, drilled belled pier and augercast pile were extended beyond this active depth to be consistent and representative for local designs in this region. To allow for set-up and understand load transfer mechanisms in different climatic conditions, half of the subjects were installed in the dry season of August and September and tested in wet season of April, while another set was installed in April and tested in August.

Results of this research included a more accurate method for predicting pressed piling capacities, a skin friction value that was the same for drilled straight shafts and

augercast piles, and how the time of soil testing affects the implementation of predictive formulation for drilled shafts and augercast piles. Also, future research directions are presented to further enhance the predictions of axial capacities of underpinnings in expansive soil media.

CHAPTER 1

INTRODUCTION

1.1 Introduction

A home is usually the single most important investment that a family will make in their lifetime. It provides shelter and comfort and also enhances the quality of life. Homes are seldom built in environments or soil conditions that are perfect for construction. To complicate matters, the type of construction is many times selected solely because of economics. As a result, of the economic driving forces, foundations built on challenging soil conditions fail at an alarming rate because design and/or construction quality control does not address soil movements from these environmental factors.

Many types of foundations have been developed including: pier and beam made of wood and concrete, concrete slab-on-grade, concrete and masonry stem wall systems, and others. Each foundation system has unique advantages and deficiencies. The final section of a foundation system should always satisfy both soil and environmental conditions. Construction practices for the foundation system should also address these conditions in order to achieve a successful, stable, durable and distress free foundation system that will protect the homeowner's investment.

Soil conditions and characteristics have a major influence on the foundation design. Among soils, expansive clay soil presents the greatest challenge to engineers and

contractors. Problem clays will expand in wet conditions and shrink in dry conditions. A foundation system should be able to withstand these soil movements without cracking. For example, a slab-on-grade foundation system that is not designed rigidly enough to resist bending moments from differential soil movements, will differentially move various segments of the foundation as the bearing clay expands or shrinks with water saturation and desaturation. It should be noted that even in dry conditions, the clays can shrink and this shrinkage causes segments of the foundation to either settle or uplift due to warping of the underlying clays.

If the foundation system is a pier and beam and the piers are not terminated into strata deep enough to resist movement or belled to resist this movement, the piers may be pulled down by downward drag from expansive clay relative to the shafts or uplifted by the swelling clays pushing the piers upward as a result of uplift induced skin friction along the sides of the pier surface. Other foundation systems are often affected in a similar manner and can result in foundation distress or even failure when they are not properly designed or constructed.

The Department of Housing and Urban Development estimated the damage caused by expansive clay soil at $9 billion per year in 1981 (Jones 1981). Other experts reported similar costs (Chen 1987; Wray 1995) and a more recent study reported by this author estimates the cost to be in excess of $13 billion (Witherspoon 2000). The paramount magnitude of this financial loss makes the expansive clay induced damage greater than any other natural disasters including the combined damages caused by: tornados, hurricanes, and earthquakes (Holtz 1981).

Remedial repairs to a foundation that has been lifted by swelling clays will normally require addressing the upheaval problem and in some cases lower portions of the foundation structure will need to be elevated to relieve distress and provide a more even walking surface. In the case where a portion of the foundation has settled because of bearing clay subsidence, the normal method of repair is underpinning to provide a base to lift the perimeter and prevent future settlement (U.S. Dept. HUD 1997). To address these soil related problems, various underpinning techniques have been developed. The most commonly used remedial underpinning techniques include: drilled piers (straight and belled), augercast piles, helical anchors, pressed concrete piles, and pressed steel piles.

Drilled shafts have been studied for a long time and tested in various environments and soil conditions (O'Neill and Reese 1992 & 1999). Much of this literature work on drilled shafts has been sponsored by the Federal Highway Administration (FHWA), States' Departments of Transportation (DOTs) and the International Association of Foundation Drilling (ADSC). This research has resulted in various research reports, design guides and standard practices (O'Neill and Reese 1992 and 1999).

Because of side wall caving, casing or slurry drilling was utilized to achieve the required axial load capacity for drilled piers (Black 2005). Augercast piles were originally developed to provide an economical method of casting a drilled shaft in subsurface conditions where the water table is high in granular soil conditions. A considerable number of published articles on augercast piles are available, but estimating their capacity has been more of a site specific testing than predictive calculations that are common with drilled shafts (ADSC 2005). Since the augercast is mostly used in granular

conditions, there is not a plethora of research available in expansive clay soil that demonstrates how the piles transfers loads to foundation subsoils.

Helical anchors have been used to support vertical load capacity for a long time but their usage in remedial underpinning applications has grown over the past thirty years. While there are numerous research papers depicting axial load capacity of helical anchors, the papers that address axial load capacity in expansive clay soils are sparse. Also there are no studies where there is a comparison analysis on how these foundations perform with respect to those that are formed by either drilling operations (drilled shafts and augercast piles) or pressing operations (pressed concrete and pressed steel piles).

The pressed steel and pressed concrete pile usage in remedial underpinning has seen a dramatic growth over the past twenty years and they are in this author's experience the most popular expansive soil foundation repair system currently in practice. No published research, however, is available to determine their axial capacity in an expansive soil media and compare their performance with respect to other types of foundation installation systems used in expansive clay soil sites.

This dissertation research has attempted to address various underpinning systems installed in the expansive soil, evaluate their load transfer mechanisms and then rank them according to their performance in field conditions. Due to the extensive amount of testing and research publications on drilled shafts, it is reasonable to assume that their foundation performance will provide a good base line for use as a control, with proven results. Hence, the drilled shaft method was used for comparison with the results of other foundation systems using different construction procedures. Other analyses attempted in this research were: to deduce the load transfer mechanism of other foundation repair

systems installed with different processes and to evaluate their effectiveness when used in an expansive soil environment.

As noted earlier, the majority of research information on other underpinning systems in expansive soils is either not available or not being conducted by independent agencies, or in some cases, is still being conducted. Hence, this present research is a unique and first attempt to independently verify the load transfer mechanisms of different underpinning systems and compare their performance in relation to other foundation systems that are more commonly used in geotechnical practice. Also, the focus of this research was on axial load transfer mechanisms, and not on uplift considerations since these underpinning elements is often used to lift the distressed foundations and is normally deeper than active depths at a test site. Hence, the research was focused on axial load transfer mechanisms of the underpinning elements in expansive clays.

It should be noted here that this comparison analysis is not an attempt to either support or not support different underpinning systems. Instead, it is an attempt to better understand the loads transferred by various foundation systems and the performance of the systems currently utilized in remedial underpinning in areas of expansive soil.

Because of the growing residential foundation repair market and their reliance on underpinning systems for mitigation of movement problems, this research provided an in-depth study on actual comparisons among six common underpinning types. This information can be used by the foundation and structural engineers, along with prudent engineering judgment, in the selection of the most appropriate underpinning technique for their foundation projects in an expansive soil environment. Another positive outcome

expected is that foundation contractors can enhance their foundation underpinning systems by addressing the load transfer mechanisms reported in this research.

1.2 Research Objectives

The main objectives of this research are to:

- Determine the axial load capacity of six types of underpinning methods in expansive clay.
- Establish axial load capacity variations when they are installed and tested across seasonal changes (wet to dry and dry to wet).
- Compare load capacities among the present six underpinning techniques.
- Evaluate the currently available load prediction models for reliable estimation of load capacity of each underpinning element and determine if any modifications are necessary.
- Determine limitations of each underpinning method and their installation practices.
- Develop empirical and semi-empirical models that provide a reliable prediction of axial capacities for the helical anchors, pressed steel piles, and pressed concrete piles in expansive soil environment.

1.3 Scope of Present Research

The scope of this dissertation research is confined to the following areas:

- To study axial load capacities for commonly used residential remedial underpinning methods in expansive clay soils. Installation methods were

performed as per the acceptable and common practices followed by contractors.

- To study axial load capacities for commonly used residential remedial underpinning methods in expansive clay soils. Installation methods were performed as per the acceptable and common practices followed by contractors.
- Installation seasonal conditions were varied from 'dry to wet' and 'wet to dry' seasonal moisture conditions.
- The site chosen for this research is located in south Irving, Texas where soil borings showed that no bedrock was present for an approximate depth of 63 feet. Typically, the research results are only applicable for this type of soil condition and may not be valid for other soil conditions.
- The geographical location of this site is a semi-arid climate, which means that in a normal season moisture conditions range from extremely wet to long periods of drought. This has an effect on the present test results and should be considered when evaluating or extending the present research findings to other sites.
- Recommendations for axial load capacity are confined to the present site environmental and subsurface conditions, which may be different for other locations.
- The number of underpinning foundation subjects tested in this research may not be comprehensive enough to establish empirical formulas for future prediction of axial capacities. These equations should be considered as preliminary and could be evaluated for future modifications. Therefore, statistical formulas to determine variances and true means from the sample mean may be unrealistic.

- For the pressed piles, a driving pressure was established to emulate actual installation pressures. This procedure meant that the piles would reach varying depths and with the cross season time from installation to testing variances in final axial load would be probable.

In spite of the above limitations, one should note the challenges faced in the execution of this dissertation research provided a unique opportunity to accomplish the proposed research objectives in better understanding of axial load transfer mechanisms.

1.4 Dissertation Organization

This report consists of 8 chapters. These chapters are: Introduction (Chapter 1), Literature Review (Chapter 2), Methodology (Chapter 3), Axial Capacity Testing (Chapter 4), Empirical Capacity Predictions (Chapter 5), Comparisons between Predicted to Actual Capacity (Chapter 6), Overall Axial Capacity Comparison (Chapter 7), Summary and Conclusions (Chapter 8).

Chapter 2 provides a summary of literature review on the underpinning methods being tested in this research project. Information in the literature presented was acquired from this author's personal library, data compilation from previous research, internet searches and contributions from various practitioners, educators and contractors across the world.

Chapter 3 is a presentation of methodology that went into this research. It includes: soil borings and laboratory testing, cone penetration or CPT detailing, installation of reaction piers and beams, installation of test subjects, preparation and calibration of the test equipment and test documentation.

Chapter 4 provides a summary of test results for each element grouped into the appropriate underpinning method.

Chapter 5 provides predictive calculations of each underpinning element grouped into the appropriate underpinning method. In addition to the common predictive models, other methods and modifications are presented.

Chapter 6 is a comparison between predictions made for each underpinning element and actual load test results. The coefficient of determination provides a measure of various assumptions and predictive methods.

Chapter 7 provides an overall comparison of all the underpinning systems. This comparison includes not only axial load comparison, but also a comparison of deflection verses load for each underpinning element.

Chapter 8 presents summary and conclusions based upon the present research results. References containing sources of the literature reviews are included in the last section with an additional listing of the various contributors for their in kind and financial support of this research.

CHAPTER 2

LITERATURE REVIEW

2.1 Introduction

The available literature related to remedial underpinning techniques has been identified and collected. This literature includes: various journals, theses, dissertations, conference articles, books, reports, standards and proprietary design manuals that were made available to this engineer. This data is summarized in this chapter in the following sections:

a) Drilled Shafts- Straight

b) Drilled Shafts- Belled

c) Augercast Piles

d) Helical Anchors

e) Pressed Steel Piles

f) Pressed Concrete Piles

The first section presents the different underpinning techniques that are the subject of this research. A brief history and technical aspects of these methods is presented to provide a background for testing, evaluation and design of each method.

The second section describes load testing methods utilized to test the underpinning subjects.

2.2 Underpinning Techniques

2.2.1 Drilled Shafts- Straight

The drilled shaft underpinning method has been one of the earliest methods used for underpinning operations and has been thoroughly and comprehensively tested and reported in the literature (O'Neill and Reese 1992 and 1999). Prior to the modern drilled shaft, wells were hand dug in the ground and then filled with everything from concrete, mortar, and brick, to treated and untreated wood or rock that was compacted. This method of hand excavated caissons was very popular in the early 1900's in Chicago and the Great Lakes area where it was necessary to transfer loads to the hard clay or hardpan to support massive structures of that era. In many of these cities there was a hard pan or bedrock so close to the surface that engineers were forced to excavate to a depth suitable for the required loads (Winterkorn and Fang 1975). Since the caisson provided confirmation of termination into specific strata and verification of axial capacity, they gained popularity with engineers who were designing buildings necessary for the needs of large cities all over the world.

With the continued development of technically advanced equipment, the first machine excavation auger was constructed around 1908 that was capable of drilling 12 in. diameter shafts up to depths between 20 ft to 30 ft below the surface. During this period there is also a record of horse-driven rotary machines that were used to drill holes for the installation of shaft foundation systems in San Antonio, Texas (Greer 1969). Some of these foundation systems installed around 1920 were 25 ft deep (Greer 1969).

The early 1930's brought further development of drilled shaft equipment by Hugh B. Williams of Dallas, Texas who developed and sold light truck mounted drilling machines that were ideal for residential foundation drilling (Anon 1976). With the development of drilling machines, the drilling contractors developed bits and reamers to drill rock and the capacity for drilling very large diameter holes to great depths. Meanwhile, contractors in Europe were using drilled shafts with primary load capacity from side friction and not just end bearing as was popular in the U.S. (FHWA 1988)

Further developments included usage of casing to drill through weak and collapsible soils and prevent caving problems that prevented drilled shaft usage. Development of polymer slurries and use of oil field mineral slurry technology provided further protection against bore hole instability and opened up even greater usage of the drilled shaft.

The advent of computers and development of analytical methods and load testing programs further added to the growth and acceptance of the drilled shafts. Extensive and accepted research by Whitaker and Cooke in 1966 and Reese in 1978 improved empirical determination of load capacity of drilled shafts and provided construction quality control methods that made the drilled shaft even more versatile and accepted (Whitaker and

Cooke 1966; Reese 1978). Prof. Michael W. O'Neill of the University of Houston, who spent his life studying behavior and construction of drilled shafts in various environments and soil conditions, has been recognized as one of the pioneers for the advances in drilled shaft and deep foundation research.

As a result of the extensive research, the modern drilled shaft has become a sophisticated foundation technique whereby a vertical in situ columnar element can transmit loads to more suitable soil strata capable of supporting the intended structure, resisting lateral loads and stabilizing soil and rock in problem conditions.

Several design and construction practices for drilled shaft foundation have been documented in the FHWA Drilled Shaft Manual, which was first produced in 1988. This manual was most recently revised and edited by O'Neill and Reese in 1999 (FHWA 1999). Predictions of axial capacity of drilled shafts are developed based upon soil characteristics, which can be directly measured by conducting laboratory studies or by performing in situ field tests. Hence, the best predictions of these methods depend upon accurate characterization of soil parameters.

Since characterization of soil characteristics is the most crucial ingredient in the prediction of load capacities of foundations, an attempt is made in this research to conduct soil borings, sampling and laboratory testing along with in situ CPT logging. This soil investigation allowed the researcher to analyze load capacity of underpinning elements via laboratory determined soil properties and those determined from in situ tests using semi and empirical correlations.

Drilled shafts were originally designed for end bearing with no allowance for skin friction (Terzaghi 1943). Load tests by several researchers, however, showed that drilled

shafts carry a considerable amount of axial load in skin friction and as a result, new formulae were developed to include a skin friction component in the axial load expression (O'Neill and Reese 1999). The following is an accepted formula for calculation of axial capacity of a drilled shaft that was introduced in the 1988 FHWA Design Manual (FHWA 1988):

$$Q_T = Q_B + Q_S \quad (2.1)$$

where

Q_T = ultimate capacity of the drilled shaft (lbs)

Q_B = end bearing capacity (lbs)

Q_S = side resistance or skin friction capacity (lbs)

The calculations depicted above must then be reduced to allow for an allowable or working load for the shafts as follows:

$$Q_A = Q_T / F_S \quad (2.2)$$

where

Q_A = allowable working load (lbs)

F_S = factor of safety

Subsequent to that design manual great strides were made in further development of predictive calculations of drilled shafts as presented in the 1999 FHWA manual. The modern equations are similar but are identified as follows:

$$R_{TN} = R_{SN} + R_{BN} \quad (2.3)$$

where:

R_{TN} = total nominal ultimate capacity of the shaft (lbs)

R_{SN} = nominal ultimate side resistance of the shaft (lbs)

R_{BN} = nominal ultimate base resistance of the shaft (lbs)

For cohesive soils (not rock) that this research is being conducted, where s_u is greater than 1 tsf and the length is greater than three times the diameter, the base resistance (R_{NB}) in terms of q_{max} can be expressed as:

$$q_{max} = 9 \times s_u \quad (2.4)$$

In cohesive soils (not rock), side resistance in terms of f_{max} of each soil layer must be calculated for each strata/layer that the drilled shafts penetrates.

$$f_{maxi} = \alpha \times s_u \quad (2.5)$$

where:

f_{maxi} = side resistance for compressive loading in layer i (psi.)

α = a dimensionless correlation coefficient defined as follows:

α = 0 between the surface and 5' deep (1.5 m) or the depth of seasonal moisture change, which ever is deeper

α = 0 for a distance of the bell diameter up from the bottom of the shaft.

α = 0.55 elsewhere for $s_u / p \leq 1.5$ and varying between 0.55 and 0.45 for s_u/p between 1.5 and 2.5 as graphically depicted by Figure B-9 (FHWA 1999) p is the atmospheric pressure, which is 14.64 psi (101 kPa).

s_u = undrained shear strength for the layer being calculated. (psi)

As explained above, each layer must be considered individually and the total side resistance is the sum of resistance offered by each layer.

2.2.2 Drilled Shafts- Belled

The drilled shafts are belled or underreamed at the bottom to provide added axial capacity and prevent the pier from lifting as a result of expansive soil forces against the shaft. The normal reason for belling is that it is more economical to bell at a point below the active zone than to drill a straight shaft deep enough or socked into a rock formation to provide not only sufficient bearing capacity but also prevent uplift as a result of clay frictional forces along the area of the shaft. With belled piers the total weight of soil above the bell will not be affected by moisture changes. Therefore, there is the added factor of safety against uplift. In expansive clay soils, however, there is a need for greater reinforcement to resist tensile forces on the pier (Chen 1975).

In most cases the straight drilled shaft to a determined depth will provide a greater axial load capacity and hence be more stable. When the depth requirements are great, belling at stable and sufficiently dense strata is the more economical solution. Although confirmation of bearing strata and depth are visibly easy, the need for quality control is even more important to make sure the pier meets requirements of design. Shallow water conditions, caving sides, bells collapsing and cleanup issues may also be a consideration in residential usage.

Calculations for the drilled and belled shaft are done in the same manner with two exceptions. The area for calculating bearing resistance, q = diameter of the bell x undrained shear strength x 9 (N_c) in lieu of just the shaft diameter. Side resistance calculations are calculated at the top/roof of the bell upward and not up the total length of the shaft. Tests of belled piers suggest that when axial compression loads are applied that there is a suction created at the top of the bell that increases axial capacity of the belled

shafts by an approximate 5% (Tand et al. 2005). This factor was not included in this research.

2.2.3 Augercast Pile

The augercast pile developed in the 1940's as a result of pressure grouting open holes and holes backfilled with coarse aggregates (Neate 1988). The first patent for augercast piles was issued in 1956 with a process of pumping grout down a hollow-stem continuous flight auger as the auger is gradually extracted. Since the expiration of this patent in 1973, the augercast pile has increased in usage around the World (Neely 1989). There are two primary underpinning techniques used in Europe, the helical/screw pile and the augercast pile or continuous flight auger (CFA). (O'Neill 1994).

The equipment requirement for augercast piles is similar to drilled shafts, except that the drilling tool is a continuous auger stem with the appropriate bits at the bottom. When the auger reaches the targeted depth, grout is pumped down the hollow auger stem to push soil up as the bit is extracted out of the ground (Cernica 1995). The contractor will calculate grout volume and make sure the grout stays ahead of the extraction so that no voids will be created as a result soil caving in what is normally a wet environment prone to collapse.

Calculations to estimate axial load capacity include the side friction capacity, and this allowance for augercast piles is higher than the same for drilled shafts. To verify the axial loads estimated by the calculations, site specific axial load tests are performed prior to starting the project. Recent field testing, however, indicates that the allowance for skin friction with augercast piles may not always be advantageous for augercast piles when compared to the drilled shafts (Kitchen et al. 1995). In one recent foundation project for

the Bryant-Denny Stadium in Tuscaloosa, Alabama, the initial bid was over budget, which led to value engineering testing of drilled piers. The load tests on shafts showed that skin friction mobilized on the drilled shafts was sufficient for a direct comparison with the original augercast pile design. As a result, cost savings were realized with the use of the drilled shaft and the project was completed within the budget (Kitchens et al. 2005). Therefore, the engineer must evaluate the subsurface to determine which system is most favorable for a specific site condition.

It should be noted that in Europe, the skin friction allowances for both augercast and drilled shafts are the same (De Cock 1997). Hence, axial load estimation and comparison between drilled shafts and augercast piles should provide valuable information that can result in savings of project expenses for future projects.

While the normal environment for augercast piles has been noncohesive soils, there is a growing trend to use this method in cohesive soils where drilled shafts have long been used. One of the problems encountered in using augercast piles in cohesive soil is that soils block the auger and prevents further penetration because of this resistance to removal of spoil (Neely 1990). This research addressed this issue because of the use of relatively shallow depth of foundation and comparative testing to evaluate skin friction and end bearing components, which should add valuable data for the design engineers dealing with deep foundations.

Most augercast piles are reinforced with a single bar through the center. For purposes of a fair comparison with the drilled shaft, the same reinforcement as that of the drilled shaft was inserted into the grouted shaft immediately after completion of the augercast pile process.

2.2.4 Helical Anchors

Screw Anchors have been used for over 200 years with records dating back to the 19th century as a support for English Lighthouses (Smith 2004). First use in the U.S. appears to be in 1838 but they were not used for deep foundations because of the inability to brace them below the surface (Jacoby and Davis 1941). They also have a long history of support for power lines and as tie-back anchors. It was not until 1980, however, that interest increased for use of the helical screw anchor piles as a vertical compressive system for foundations (Bradka 1997). The most dominant manufacturer and developer of these anchors was the AB Chance Company. Helical Anchors or Screw Anchors as they are sometimes called have been used in the telecommunications industry as a foundation anchor for cell towers in very difficult environments. Over the past 20 years, however, this usage has been utilized for vertical building support in both new construction and remedial repair. In Europe there is an increase usage for helical anchors for vertical structure support because of its economy of installation and ability to match difficult subsurface conditions (O'Neill 1994).

Anchors are easy to install in low headroom conditions, they produce no vibrations and because the soil displaces in the void created by the auger flights, there is no spoil to haul-off (Smith 2004). In soft soils, the helical anchors will penetrate to greater depths, which many times will lead to buckling of the slender steel shafts during loading. Therefore, their usage has normally been restricted to foundations for temporary and mobile structures (Vyazmensky 2005).

Engineers who use helical anchors for new construction will use soil geotechnical information to not only specify the required depth but also to estimate the ultimate

capacity. With the soil data and specifying a torque requirement, it is believed that engineers can determine empirical axial capacity (Seider 2004 ; Carville, et al 1994). In normal conditions, the higher the installation torque, the higher the axial capacity. One such design factor is (Seider 2004 ; Carville, et al 1994):

$$Q = K \times T \tag{2.6}$$

where:

Q = ultimate capacity of the screw pile

K= empirical torque factor (lbs/ft-lb), (This factor depends upon soil conditions and the helical anchor shaft diameter and configuration)

T = average installation of torque (ft-lbs)

Studies by Hubbel Power Systems (A. B. Chance Company) showed a good correlation between torque to SPT and uplift capacity on helical anchors in several studies (Hoyt and Clemence 1989). While the use of the Seider formula provides strong analysis for pull-out strength, the study was attempted on vertical or axial compressive loading.

The AB Chance Company provides its installers with design programs and charts where the installation torque and blow count are read off a chart (Figure 2.1) to determine the expected axial load capacity. There are different charts for sand and clay with an estimated maximum capacity for residential foundations being 40,000 lb. (Chance 1993).

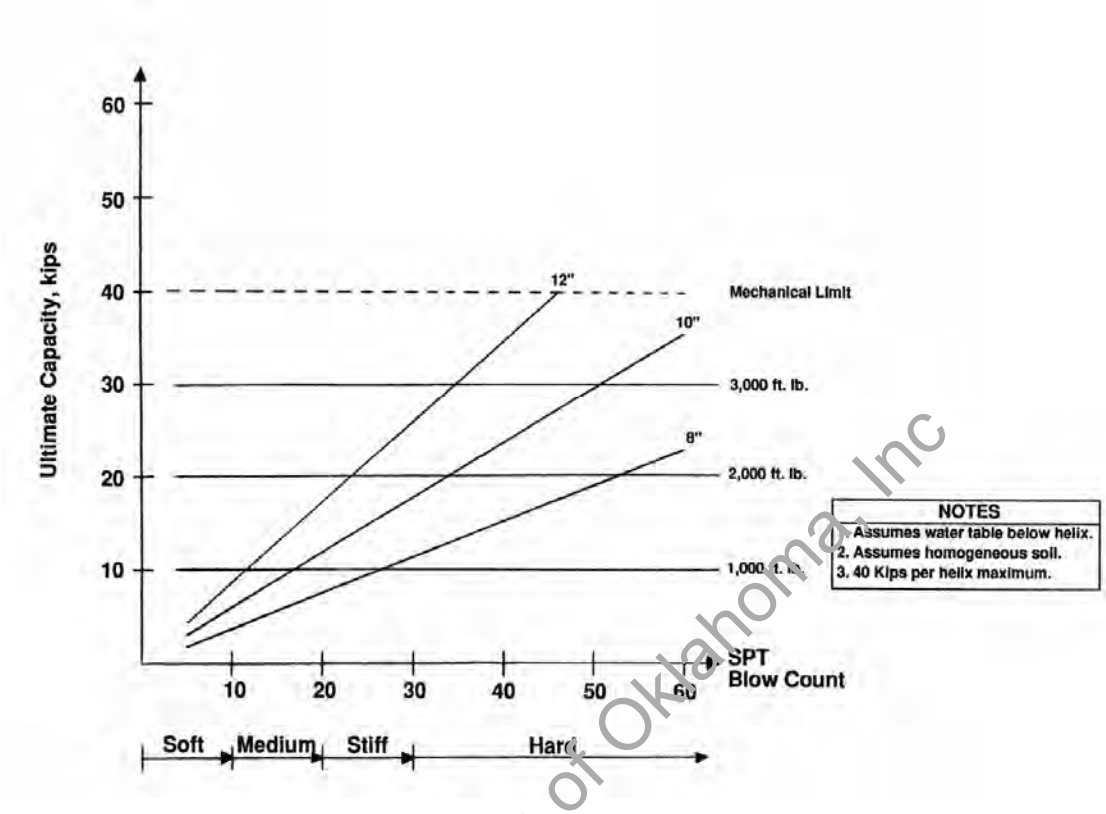

Figure 2.1 - Helical Anchor Design Chart for Clay (Chance 1993)

Single and double helix are used in remedial foundation support for residential buildings. Several charts have been developed that are predicated on torque installation pressure, pipe shaft diameter and helix diameter to provide an estimate of working load capacity (Schmidt 2004).

Although the method described above is used and accepted in industry, it has not been proven to be accurate in traditional geotechnical terms especially when the installation torque is the insitu prediction factor (Weech 2002). Torque does, however, have a correlative relationship with soil parameters and could be used for on-site quality control documentation. However, without site specific soils documentation, errors could

cause inaccurate predictions. There are two methods that are recognized because of extensive testing in a variety of soil conditions. These are the 'Cylindrical Shear Method' and the 'Individual Plate Bearing Method' (Figure 2.2), (Weech 2002).

The Cylindrical Shear Method states that the total pile capacity is:

$$Q_{total} = Q_{cyl} + Q_{end} + Q_{shaft} \quad (2.7)$$

where:

Q_{cyl} = the frictional resistance that is mobilized along the cylindrical failure surface. (lb)

$$= A_{cyl} \times S_u \quad (2.8)$$

Q_{end} = the bearing surface below the bottom place and base of pile shaft (lb)

$$= (A_{hx} + A_{tip}) N_c \times S_u \quad (2.9)$$

Q_{shaft} = the frictional resistance along the pile shaft (lb)

$$= A_{shaft} \times \alpha \times S_u \quad (2.10)$$

where:

A_{cyl} = the area of the cylindrical shear surface, which is the outer area of successive helices. (in^2)

S_u = undrained shear strength of soil (psi).

A_{hx} = net bearing area of the helix plate (in^2). With tapered helix such as being used for this test, the largest helix is used for axial compression calculation.

A_{tip} = the cross sectional area of the pile shaft (in^2).

A_{shaft} = surface area of the pile shaft (in^2).

α = the shaft adhesion factor

The Cylindrical Shear method as described above works well when the spacing to diameter ratio (S_f) is 1.5 or less (Mooney et al. 1985). This spacing produces a cylinder or wedge of resistance that acts more like a pier/pile in friction since it engages a soil column instead of individual sections of resistance. Studies that have been done indicate when the spacing ratio is greater than 1.5, the axial capacity decreased in correlation with an increase in spacing ratio above 1.5 (Narasimha et al. 1993). To respond to those inaccuracies, Mooney (Mooney et al. 1985) responded with correction factors to address the spacing engagement problem as follows:

$$Q_c = S_f(\pi D L_c)\, C_u + A_H \times C_U \times N_C + \pi d \times H_{eff} \times \alpha \times C_U \qquad (2.11)$$

where:

D = diameter of helix (in)

L_C = is the distance between top and bottom helical plates, (in)

C_U = undrained shear strength of soil, (psi)

A_H = area of helix, (in^2)

N_C = dimensionless bearing capacity factors (for this size helix $N_c = 9$)

d = diameter of the shaft, (in)

H_{eff} = effective length of pile, $H_{eff} = H - D$, (in)

α = Adhesion factor (see figure based upon undrained shear strength)

Sf = Spacing Ratio Factor

As would be expected, the depth of embedment will determine the importance of shaft adhesion. If the H/D ratio is greater than 3, then shaft friction is considered in the equation (Nasr 2004). If the spacing between the helix is greater than 3 to 1, the helix to helix shaft friction is not considered in the equation.

The helical spacing (S_f) for this research is 3 ft. Therefore, the Cylindrical Shear Method will not be a good predictor for this test and we will have to engage an empirical method that will address the shaft/helix configuration that is appropriate.

The Individual Plate Bearing Method was devised for helix plates spaced greater than two (2) times the diameter of the helical. This method assumes that individual failure occurs below each helix. In undrained conditions such as this test, total pile capacity is measured as follows:

$$Q_{ult} = Q_{end} + Q_{shaft} \quad (2.12)$$

$$= \sum(A_{hx} \times N_c \times S_u) + A_{shaft} \times \alpha \times S_u \quad (2.13)$$

where:

A_{hx} = net bearing area of the helix plate (less cross section area of pile shaft), (in^2). With tapered piles such as those being used for this test, each diameter is calculated for capacity.

N_c = is the standard bearing capacity factor that is normally assumed to be 9 for undrained analysis. It is also many times labeled as N_{cu} .

S_u = is the undrained shear strength of the soil (psi).

A_{shaft} = surface area of shaft (in^2).

α = shaft adhesion factor

It was found that using the individual bearing method with known shear strengths that under prediction were normally between 0% and 12% with a maximum variance of 22% (Narasimha et al. 1993).

As shown empirically above, increasing the number of helix should increase the ultimate vertical compressive capacity (Narasimha 1991). It is believed that the soil

column created between the helix will increase side friction and bearing capacity will subsequently be increased. The amount of increase will obviously vary with soil conditions such as shear strength and adhesion.

Another factor in anchor capacity is the pitch of the helix angle (ψ), which is the inverse tangent of the ratio between pitch (p) of the screw anchor's blade to that of the blade diameter (D) (Bradka 1997). When the pitch is increased the installation torque requirement will be increased but the depth of penetration will increase, which may increase the vertical capacity. In addition to pitch, there are manufacturers who produce sloped conical ends that because of a reduction in required installation torque will normally provide increased vertical capacity (Ghaly et al. 1991). The helix configuration used for this research is the medium pitch with a symmetrical configuration tip.

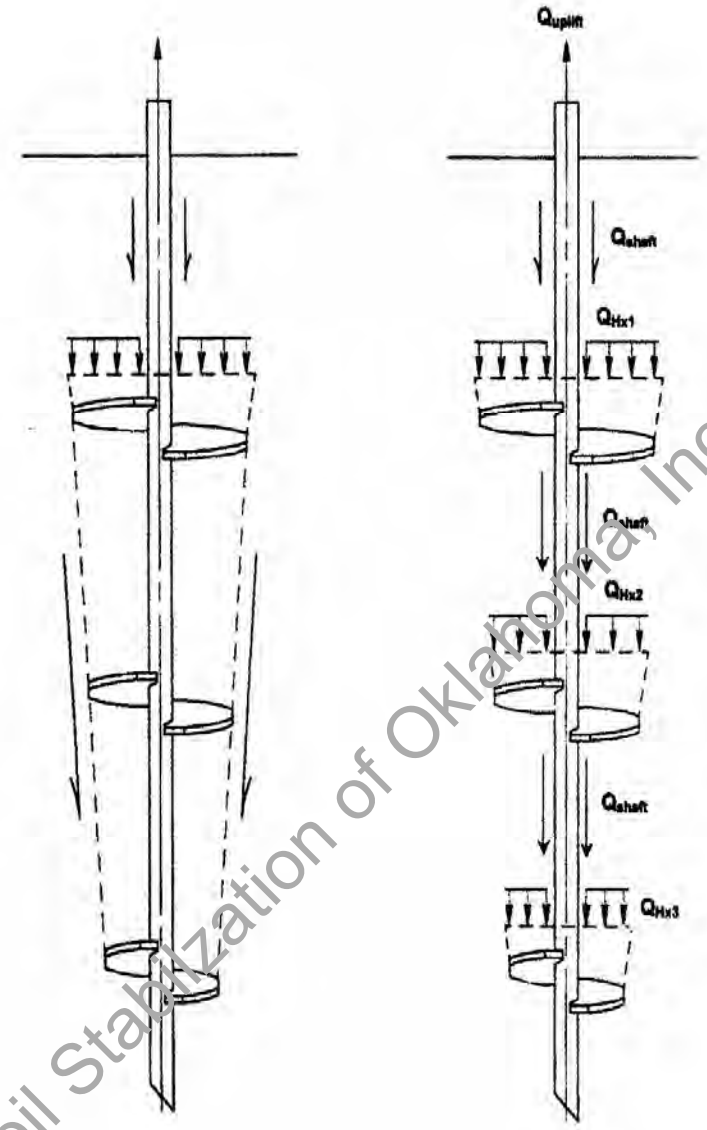

(a) (b)

Figure 2.2 – Helical Bearing Calculation Methods (Hoyt and Clemence 1989) (a) Assumed Cylindrical Shear Surface for Tapered Helix, (b) Individual Bearing Method

As with other piling systems, an increase in moisture content will produce a decrease in bearing capacity. Since this testing is in a semi-arid climate with wide swings in moisture content, some decrease in axial capacity when going from wet to dry state is

expected but with the depth to diameter ratio being so high and terminated well below the zone of seasonal moisture change, this effect is not expected (Bradka 1997).

Spacing ratio has an important bearing on vertical capacity. When the spacing is less than 1.5 diameters apart, this factor = 1. It appears, however, that this factor is more critical in determining uplift capacity than axial compression capacity.

Pore pressure increases during installation at the helix point, as a result of the upward pressure of the helix plates against the soil above, and this increased pressure leads to shortcomings in the prediction of axial load capacity. Therefore, engineers rely upon pile load tests to refine final piling design (Randolph 2003). Studies by Weech (2002) indicate that as the helix passes a soil point, a "pulse" in pore pressure is registered. When there are multiple helixes, each helix causes a pulse in pore pressure but not as great as the initial helix (Weech and Howie 2002). It was Weech's observation, however, that this increase in pore pressure decreases very quickly over a period of days. It is believed that with this pore pressure decrease that helical pile vertical capacity will increase and shear strength of the soil around and under the helical pile may be higher than prior to disturbance.

If, however, efficiency in torque installation has not been good, there may be a decrease in perceived axial capacity because of the voids created under the helix as a result of auguring in lieu of pulling into the ground. Since the time from installation to testing for this research varies between 4 and 8 months, pore pressures should decrease to a pre-installation magnitude. Therefore, we should not consider this as a factor in estimating axial capacity.

Shear strength is decreased during the installation stage because of the increase in pore pressure and disturbance of the soil. While this strength will increase over time, it will only reach a remolded strength and not a pre-disturbance strength (Weech 2002). Although there is additional disturbance with each added helix, there is not an added decrease in immediate shear strength.

Weech (2002) indicated that the peak S_u parameter underneath the lead helix be used to calculate capacity since soil shear strength between the upper helix(s) has been compromised by installation disturbance that alters the void ratio and structure of the soil. While tip resistance increases are moderate over time, resistance at the upper helix will increase after dissipation of pore pressure (Weech 2002; Weech and Howie 2002).

Weech showed that measurement of the bottom helix capacity could be done using CPT test information as presented by equation 2.14:

$$Q_{bottom\ hx} = A_{hx} \times (q_T - \sigma_{vo}) \tag{2.14}$$

where:

A = area of helix (in^2)

q_T = corrected tip resistance (psi)

σ_{vo} = effective overburden pressure (psi)

This equation works because there is a negligible amount of disturbance below the lead helix. With the CPTs used in this research, this parameter can be utilized to check against the Individual Plate Method that utilizes laboratory testing of soil samples (Weech 2002).

The amount of disturbance below the lead helix is considered to be miniscule, which equates to an index of soil destructuring of 1.0 (Weech 2002). Weech indicates the

second helix ID value, however, would range between 0.5 and 0.75, which must be considered when estimating an axial capacity. In view of an obvious inefficiency in installation rotations to penetration, the concept of disturbance is real for this project and must be considered to properly reduce capacity of the second helix and shaft friction along the depth of installation. The amount of disturbance is likely site specific and must be measured by experience and understanding of the installation process. There is not only inefficiency in the auger pulling into the stratum but also a placement issue with the second helix. In other words, the second helix is not exactly placed where with efficient rotation of the first helix into the bearing soil will encourage the second helix to follow the same auger path. In fact, the second helix is 9.4 rotations behind the first helix (30 in. /3.18 in. auger height). Therefore, the second helix will hit the same depth at a point 1.31 inches above the path of the first helix. Therefore, we have a section of disturbance that is multiplied by the higher cut of the second helix and our area of disturbance will be multiplied significantly with only the outer 1 in. plate being a virgin cut (the second helix is 12 in. diameter while the lead helix is 10 in. diameter).

Weech shows a correlation between soil sensitivity and the amount of disturbance caused by the helix tearing through the soil. Soil sensitivity is defined as:

$$S_t = S_u \text{ (undisturbed)} / S_r \text{ (remolded)} \quad (2.15)$$

Soil sensitivity, as mathematically depicted above, means that only a part of its predisturbed strength will be regained through hardening over time because of a breakdown of the original soil structure and a loss of interparticle attractive forces and bonds (Das 1997). Sensitivity has also been correlated with the Liquidity Index, as expressed by equation 2.16 (Holtz and Kovacs 1981):

$$LI = (w_n - PL)/PI \quad (2.16)$$

where:

LI = Liquidity Index of soil sample

w_n = natural water content of the same soil sample

PL = Plastic Limit

PI = Plasticity Index

Using this ratio,

LI < 1 the soil will be brittle when fractured/sheared

0 < LI < 1 the soil will behave in a plastic manner when sheared

LI > 1 the soil will behave as a liquid when sheared

Because this site is in an alluvial plane, we would expect the soil to exhibit a medium to high sensitivity. This means that because of soil disturbance caused by the leading and trailing helix, undisturbed shear strength will not be restored over time. Therefore, capacity of the second helix must be reduced to reflect these factors.

In addition to the obvious disturbance factor delineated above, there is some inefficiency between installation and axial loading. Since the helix(s) are installed by twisting, they are actually pulling themselves into the ground, which puts the pipe stem in tension. Therefore, in the case of some manufacturers product there is some amount of play/looseness in the connection. Because of this connection flexibility, there is a compression along the steel stem until force reaches the helical. As an example this engineer installed a number of helical piles in North Carolina in the past and found that each one required that they be “seated” into place using a jacking force against the house

weight that produced a plunge or downward deflection between 1 in. and 3 in. When this seating was completed the anchors could properly support the house and provide necessary axial capacity to make elevations adjustments and restore vertical stability. The stem in this situation was square steel with square connections (sometimes call knuckles) and the play was obvious when making the connection with the amount of axial connective compression deflection being large. To reduce this factor in the outcome of this research, a product was chosen that makes an inner screw connection with the stem coming together in a flat plane at each connection. While this may not completely eliminate all axial compression of the stem connections, it may prove to reduce them to an insignificant level.

Buckling of the steel stem of the helical system always is a concern with long slenderness ratios (l/r_o), however, this is only a problem in the very soft soil (Davisson 1963). While the pressed steel and concrete piles maintain a tighter fit and thus have a smaller area of disturbance, the helical anchors provide a disturbance area greater than 12 inches, which could produce enough soil strength reduction in the lateral soil support to present a problem. As long as the Standard Penetration Count (N) is greater than 4, the soil strength reduction should not be a problem in a stiff clay soil (Hoyt et al. 1995).

Several conferences and emails from installers across the U.S. and Canada showed that there is a variance of installation pressures used to advance helical anchors for foundation piling. These torques ranged between 3,000 ft-lb to 3,500 ft-lb in many of the southern states for residential installation to 5,000 ft-lb for residential and lightly loaded structures in both the U.S. and Canada. For purposes of this test, however, 5,000

ft-lb of torque will be used for installation torque as a fair approximation of the upper limit of installation pressure.

Research completed on a range of geographic installations indicates that axial capacity in cohesive soils is many times less than the same torque installation in noncohesive soils (Zhang et al. 1999). Since very few research papers were found on the helical pile applications in cohesive soils, the present research is expected to add to the database for clay soil installation and will provide further directions for future testing.

2.2.5 Pressed Steel Piles

In deep foundation system, driven piles have been used for several years (Punma 1994). The art of driving piles was well established in Roman times as recorded by Vitruvious in 59 A.D (Punma 1994). Records of pile underpinning have been confirmed in settlements that were constructed over 4000 years ago (Punma 1994). Development of piling science enabled the Romans to expand their highway and port system to meet the challenges of a vast empire for their transportation needs between cities.

The normal method for installing piles is to dynamically drive concrete or steel to a measured capacity that can be determined by the wave equation or dynamic testing such as the Gates method or other suitable electronically monitored systems that have been proven over a long history of installation (Goble et al. 1986). Dynamically driven piles provide support for many of the large and difficult environments in the World and their performance is well documented (Waters 2004 and 2004).

The first reference to pressed piles appears to be in a U.S. Patent Specification dated February 20, 1917 (U.S. Patent No. 1,217,128) with a modification by the same

patentee on June 12, 1917. These patents specified pushing of sections of steel pipe into the ground to a specified pressure and holding that pressure until the pipe stops settling. Subsequent to these patents another patent by the same patentee, Lazarus White; on October 20, 1931 (U.S. Patent No. 1,827,921) specified the spacing that must be maintained to prevent group settlement. White further indicated that each pile must be individually driven to provide adequate capacity for holding the building to be underpinned. A similar patent was filed in England as early as February 2, 1973 (London No. 1,418,164), which shows the same basic concept of pressing steel piles into the ground using the weight and resistance of the structure. The usage of this process in residential underpinning has led to a considerable number of patents that either modify equipment, piping and concrete grade beam attachments or show a process alteration.

Pile jacking as it is also known in the literature, was utilized as a remedial piling technique as far back as in 1916 by the firm of Spencer, White and Prentis, Inc. (Carson 1965), This firm, according to Carson (still an employee), developed this method for installing piling under a new structure, installing deeper piling on an existing building with piling and replacing damaged piling under an existing structure. This method was originally used for buildings but the process depicted appears to be similar to that utilized today by the residential remedial underpinning contractors. (Carson 1965).

The first regulatory reference to the pressed piling appears to be the Department of the Army's Pile Construction Manual (Department of the Army, TM5-258, March 1956, now revised in Department of The Army, FM 5-134, April 1985). This manual states "Under special conditions, it may be necessary to jack a pile into the ground. This situation generally arises when it is necessary to strengthen the foundation of an existing

structure or when regular driving would be damaging to an existing structure. In such cases, the pile is generally jacked in sections, using a hydraulic jack reacting against a heavy weight." A second reference is found in a book titled Piling Engineering which references jacking piles where headroom is limited or vibrations are not permissible (Flemming, et. al 1991).

Mention of segmental pile jacking in most books refers to the extreme expense of jacking in tight quarters and also the limited control on final depth (Prentis and White 1956); Henry 1986). Most published references indicate that the pile should be jacked down until the force reaches 150% design load and then they should recycle the loading and unloading to make sure the pile will not move when the final load is placed on the pile (Fletcher and Smoots 1974). Other references indicate that a jacking load of 50% to 67% should be held for 10 hours to make sure the pile will not settle under the working load (Dunham 1950).

While the normal pipe configuration used in remedial work is either with a guild shoe or with a point to reduce friction, some authors suggest using open end pipes so that the inner soil can be cleaned out at periodic depths to increase penetration and thus be able to achieve a specified depth (Xanthakos, et al 1994). This reference calls hydraulically driven piles as jacked piles and it refers to dynamically driven piles as driven piles (Figure 2.3).

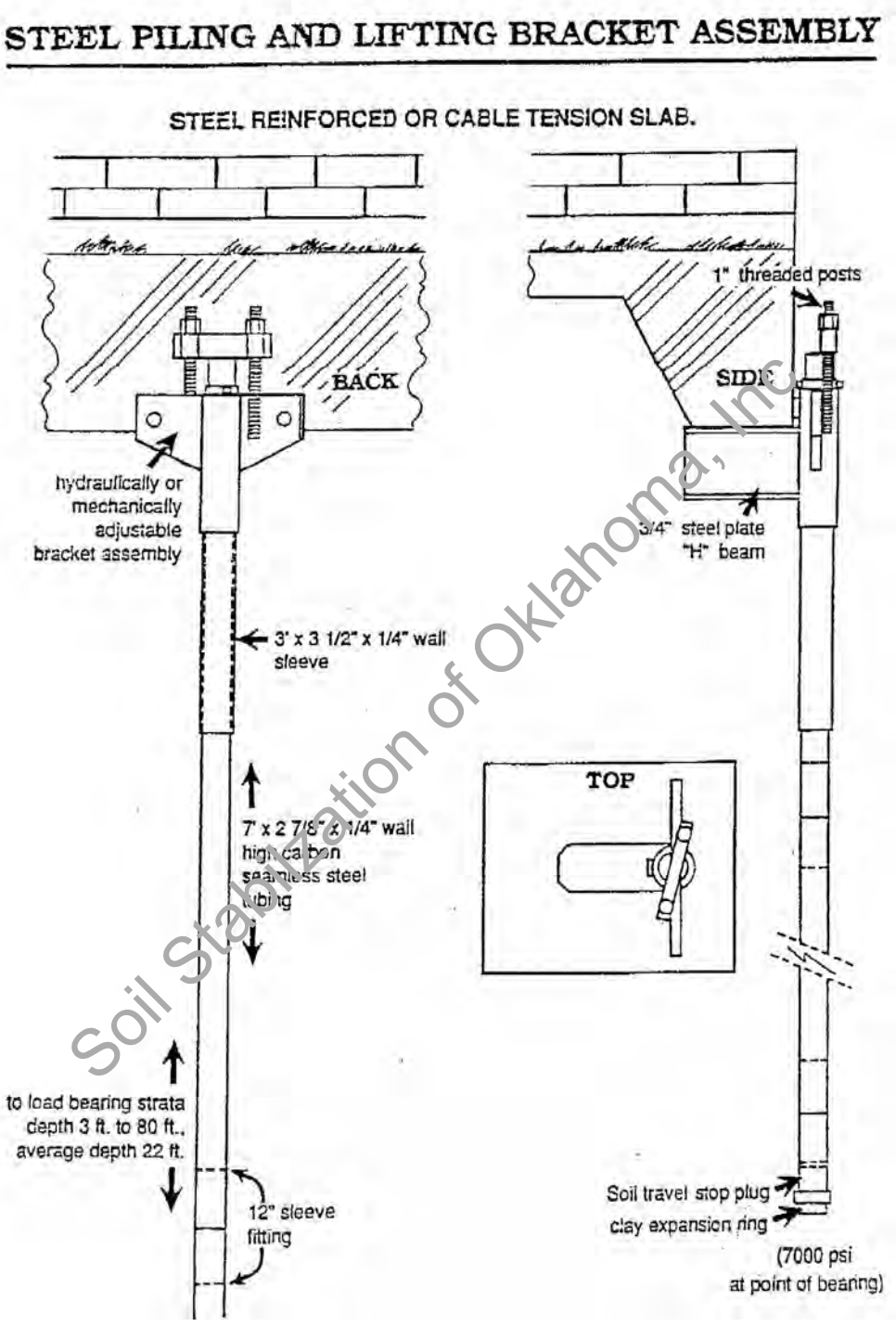

Figure 2.3 - Typical Pressed Steel Piling Attachment to House (Courtesy of Ram Jack Foundation Repair)

It is this author's experience that the use of pressed steel piling has grown over the past twenty (20) years to become one of the most frequently used methods of remedial underpinning for residential foundations. The contractor will either bolt a bracket on the grade beam to provide leverage for pushing or set a hydraulic jack under the grade beam to force the pile into the ground using the weight of the house, soil adhesion along the concrete slab and/or beams, resistance from the structure and probably the resistance of concrete bending moments or lateral friction. Regardless of the ultimate driving resistance, the pipe is forced into the ground at each location individually until the structure is lifted. Driving is then stopped to prevent damage to the grade beam, structure or veneer. Once all pilings are installed, the structure is lifted to its desired elevation by lifting at each pile and then secured on the installed piling (FRA 2005).

This engineer's inspection of actual driving and conferences with remedial contractors who employ this method shows driving forces on a one story house range from 30,000 lbs to 35,000 lbs, while driving on a two story house may reach as high as 50,000 lbs (Gregory 2005). To establish realistic installation pressures that could be not only duplicated but also consistent with actual field conditions, a driving force of 50,000 lbs was established for each of the hydraulically driven piles (Gregory 2005).

While initial capacity is provided by the drive pressure, this engineer's own experience with adjustments in foundation elevation indicates that there is some relaxation in axial capacity over time as evidenced by an additional penetration when the pile is reset in preparation for subsequent lifting of the foundation. This observation may be explained in clay soil by a process called Thixotropy, "whereby a cohesive soil stiffens while at rest and softens upon remolding" (Witherspoon 2003). This soil

relaxation may be caused by negative excess pore water pressure caused by the pile jacking that is relieved with time, causing the soil to soften. This process may occur quickly or in the case of clay over a period of 30 to 60 days (Das 1984; Coduto 1994). Another cause of soil relaxation is point seat disturbance whereby the pile driving fractures impervious strata to allow water to penetrate around the pile and softening the clay surface (ASCE 1984). Because the lead point will normally have a shear ring to reduce side friction, water may conduit along the pile to soften the surface and lessen axial load capacity.

The use of sectional piles is required to install under an eve or grade beam. Because there is a delay between driving the previous pile and setting the added pile a phenomena called "soil freeze" occurs that may prematurely stop the pile prior to reaching a more desirable depth in suitable strata (ASCE 1984). For this reason, once the driving operation begins it must continue until the targeted installation pressure has been achieved (ASCE 1984). It has been documented that "Soil Freeze" may occur sometimes within 30 minutes. Therefore, breaks should be taken between drive stages only. These factors in addition to a zone of seasonal moisture change that may reach in excess of 12 ft are some of the primary reasons for installing and testing these foundation systems in different seasonal conditions.

Since a house may lift off the piles during a wet season, there will be a loss of load on the piles during this period. To test the effect on axial capacity when the load is removed, pressure will be maintained on half of the subjects while half will have pressure removed one month after installation. This testing procedure will add even more data for load capacity maintenance.

The occurrence of lessened axial capacity over time contradicts long established phenomena such as pile set-up where axial capacity actually increases as much as 50% over time (Komurka 2004; Waters 2004). Therefore, it is possible that hydraulically driven piles may not fit recognized empirical formula developed with dynamically driven pile elements just because the method of driving into clay soils does not induce rebound action in the clay sheeting.

With an established driving pressure of 50,000 lbs, changes in soil composition that provide differences in soil shear and side friction, should cause the piles to reach varying depths. In fact, rocks, boulders, partially cemented sandy zones, thin rock layers or tree roots may provide enough resistance to prematurely stop a pile prior to reaching a depth below the active zone. A review of actual jobs and interviews with pressed piling contractors indicates that even on a small house there is always a difference in pile termination depth (Gregory 2005). With this variance in depth, applications of dynamically driven pile formulas may not be applicable in determining side friction and end bearing capacities.

While steel piles may vary somewhat in diameter, the normal width for residential underpinning is an approximate 3 in. The contractor chosen for this testing uses 2-7/8 in. diameter steel pipe in 5 ft long sections with a male and female end that will fit together to form a somewhat rigid continuous pipe without a tensile connection (Figure 2.3). Most contractors will use a lead pipe that has a driving shoe/enlarged ring at the bottom to produce less driving resistance and thereby reach greater driving depths. Because these piles are subject to some amount of bending, it is possible that they may vary from true vertical as documented (Brown 1999; Brown 2000).

Metallurgical analysis using ASTM A 370-94 reveal that the pipe used for this test has 0.221 in. wall thickness with ultimate strength of 97,000 psi, yield strength of 80,500 psi and 19% elongation. Compressive forces are therefore well within allowable stress levels for steel pipe. This large length to diameter ratio, however, does pose a concern but in dense clay soil this research engineer has not known of projects where bending failure was a problem. For unfilled pipe piles, AASHTO has established the maximum design stress at 0.25 × fy, which in the case of pressed steel pipe equals 24,250 psi with an area of 1.84 in^2. would allow 44,683 lbs of support (FHWA 1996). House loads at the perimeter are calculated at an approximate 1,000 lbs per ft. If the piles are set at a spacing of 6 ft from center to center, then the working load would be 6,000 lbs., which will yield a safe factor of safety.

Driving stresses for this type of pile are also set by AASHTO at 0.9 x fy, which would equate to 87,300 psi (FHWA 1996). This would allow a driving stress of 160,858.98 lbs, which in this test is well within the imposed 50,640 lbs applied by the installation equipment. Therefore, bending action does not appear crucial with this piling requiring 50,640 lbs of drive pressure that it be encapsulated with stiff clay soil for lateral strength. It should be noted here that the contactor selected for this test states that driving pressures have been as high as 60,000 lbs with no evidence of pipe failure. Installation on slopes, however, might induce lateral stresses that with slope failure could cause bending moments around the axis of these slender piles.

Driving depths at the corners will normally be less because there is less driving load available. A corner has an approximate ½ of the available structure and soil mass when compared with a long wall section that provides resistance at each side. Contractors

also confirm that interior pile installations under grade beams will provide much more driving load. This is because much more of the house and soil mass are available for driving resistance. With stiffer structures and 2nd story houses, drive pressures in excess of 60,000 lbs have been recorded (Gregory 2005)

2.2.6 Pressed Concrete Piles

Pressed concrete piles appear to have first been used for remedial repair in Texas in the early 1980's and were championed by a Texas engineer named Gene Wilcox. These piles are composed of cylindrical concrete sections 6 in. diameter and are 12 in. long. The sections may have an approximate 5/8 in. diameter hole through the center longitudinally. The contractor will excavate a hole under the grade beam that is an approximate 24 in. square and an approximate 24 in. below the grade beam (figure 2.4). The contractor will place a concrete pile vertically under the beam, set a hydraulic jack beneath the grade beam and press the concrete cylinder into the soil and then repeat the process until the driving pressure lifts the house (Coody 1991 et al and Dawson 2004).

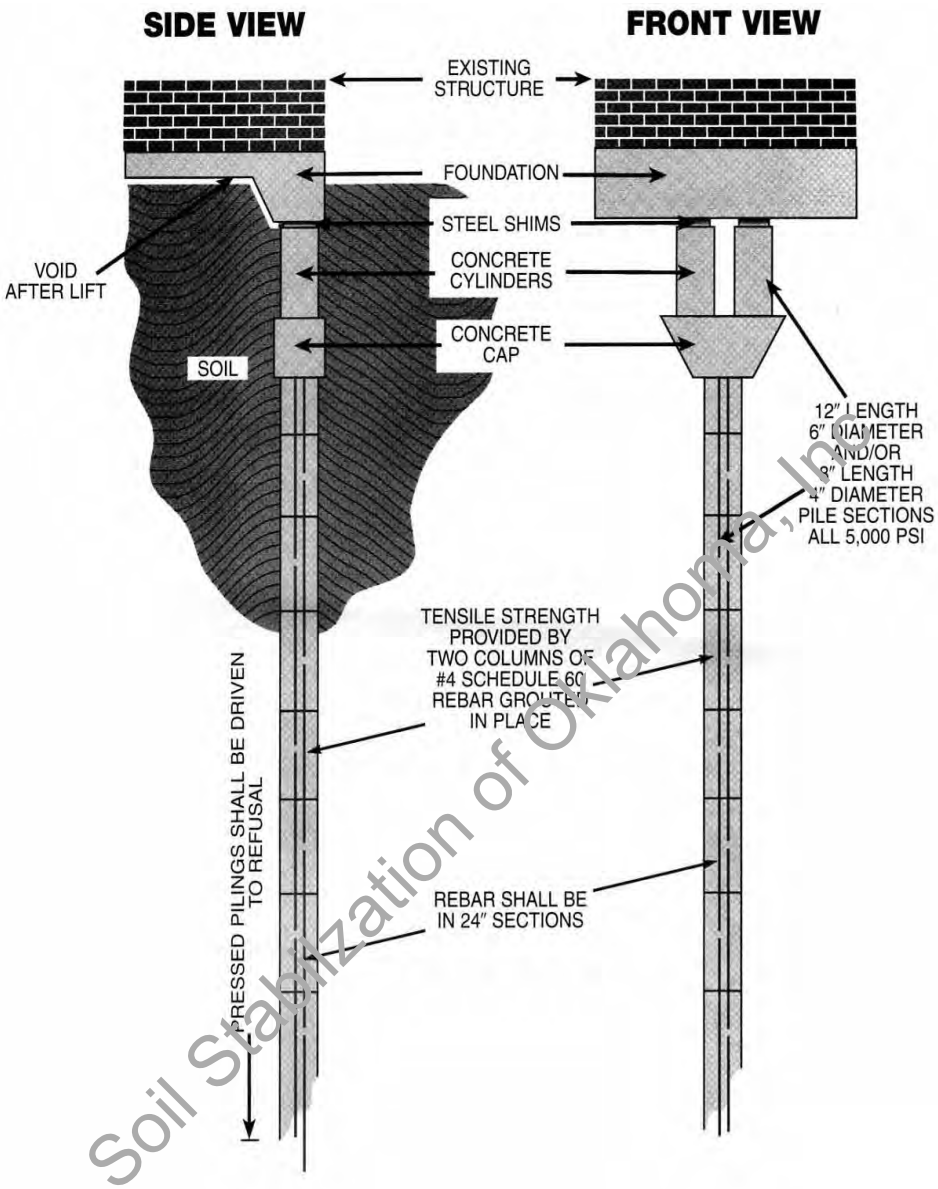

Figure 2.4 - Typical Pressed Concrete Piling Support Under House (Courtesy of Advanced Foundation Repair)

Variations in this process include; setting and grouting reinforcing steel in the hole in sections as the piles are driven, for lateral and vertical resistance, or setting a cable in the hole and pouring epoxy around the top cap piece to provide vertical resistance to separation (Gregory 2005). One contractor also installs a type of spiral cylinder to attempt to screw into the ground. There are also contractors who will jet water down the hole or around the sides to reach a greater depth (Gregory 2005). Other contractors will install a smaller section at the bottom or pointed lead cone to break through lenses and reach a greater depth. The contractor chosen for this research uses a 4 in. diameter driving shoe that they believe breaks through thin lenses and provides greater termination depth. Most contractors will install a trapezoidal cap at the top that will provide a solid driving base for the jack and allow room for setting two 6 in. diameter by 12 in. long cylinders to support the house (Figure 2.4). When the house has been raised to its desired height, the contractor will set metal shims to maintain this elevation on the installed pile.

As with the pressed steel piles, depth will vary significantly at a single house. Because the concrete piles are twice the diameter of the steel piles, there is greater amount of skin friction and end resistance offered by the pressed concrete piles. Therefore, the driving depth variance will normally be much greater than the steel pilings with exactly the same driving pressure. Another similarity with the steel piles is that at the corners of a structure the available driving pressure will be much less. This reduced pressure is found because the house mass and soil contact is ½ that of a location along a long wall. Therefore, driving depths will normally be much less at a corner than along a wall length.

Because the piles are hydraulically pressed into the ground, it is unknown if the standard dynamically driven concrete pile formulas are applicable to these elements. The variance in driving depth may also create problems when trying to empirically determine final axial capacity.

Because this method is a sectional precast pile driven hydraulically using resistance from the house, the same phenomena can develop as explained above with the pressed steel piles such as: Thixotropy, soil relaxation, soil freeze, etc. are applicable to this method. With the shorter sections there is also a greater chance of vertical alignment problems. Therefore, the installation technician must be aware of pile drift and make corrections as necessary to keep the pile vertical. With the larger diameter of pile (6 in. for the pressed concrete in lieu of 3 in. for the steel piling), there is a greater chance of obstruction influence. These obstructions may include tree roots, boulders, hard lenses, soft weathered rock etc. When these problems are identified, the installer may choose to move to the side or install steel sectional piling.

As the segmental pressed pile method has developed, changes have been implemented to overcome problems in installation and durability. One of these modifications is that all precast pile sections are now 5,000 psi concrete. It was learned early on that the compressive strength of the concrete could be ruptured during a heavy drive and when that happened there was little that could be done to mitigate damage with that individual pile. Another problem was quality control of the precast cylinders that resulted in swings in cast concrete strength. Since the amount of Portland cement in concrete is a relatively small expense in view of possible problems with cylinder failure, the manufacturers have started using a 5,000 psi concrete mix. As extensively as these

piles have been utilized over the past 20 years, it would appear stresses are well within allowable design stresses in the concrete pile.

AASHTO establishes maximum design stress of concrete piles at 0.33 f'c, which in the case of pressed concrete pile equals 1,650 psi (0.33 × 5,000 psi). 1,650 psi with an area of 28.2743 sq.in. would allow 46,652 lbs of support (FHWA, 1996). House loads at the perimeter are calculated at an approximate 1,000 lbs per ft. If the piles are set at a spacing of 6 ft o.c., then the working load would be 6,000 lbs so in theory there is a safe factor of safety. With irrigation patterns, altering drip lines, evapotranspiration influences by trees and other variations, however, loading on an individual pile may change with the expansion and contraction of soils under the foundation. Lifting at one end, for instance, might rotate the structural position enough to greatly increase the support requirement for an individual pile far in excess of the assumed 6,000 lbs. Therefore, factors of safety must be large enough to accommodate seasonal foundation shifting.

Driving stresses for this type of pile are also set by AASHTO at 0.9 fy, which would equate to 4,500 psi (FHWA 1996). For the subject of this testing, this would allow a driving stress of 127,234.35 lbs, which in this test provides a safe factor of safety. Therefore, the segmental precast pile will be well within tolerance. As a side note, in calculating 3,000 psi concrete, the allowable drive stress would be 84,822.9 lbs (3,000 psi × 28.27), which provides a factor of safety of only 1.68. With poor quality control at the manufacture's plant, it is obvious why cylinders would sometimes rupture prior to the change to 5,000 psi concrete. We must remember that an approximate 5/8 in. diameter hole sits in the center. If reinforcing steel is grouted in place, the strength reduction caused by the hole area would lessen.

2.2.7 Common Design Features for Pressed Steel and Pressed Concrete

Static analysis dictates the ultimate capacity, Q_u; of a pile in homogeneous soil is the sum of the shaft resistance Rs and toe resistance Rt:

$$Q_u = R_s + R_t \quad \text{or} \tag{2.17}$$

$$Q_u = f_s \times A_s + q_t \times A_t \tag{2.18}$$

As indicated on the soils borings and CPT, the clay is not homogeneous but has a variance in soil parameters. Therefore, the ultimate capacity will actually be:

$$Qu = \sum (f_s \times A_s) + q_t \times A_t \tag{2.19}$$

For cohesive soils, a standard method of calculating ultimate capacity is the total stress analysis, which is calculated from the undrained shear strength (τ_u or c_u) of the soil and an empirical adhesion factor (α) which is normally calculated from Figures 2.5 and 2.6 (FHWA 1996)

$$f_s = c_a = \alpha \times c_u \tag{2.20}$$

Another method used in clay soils is the Effective Stress Method, which is expressed by the following equation:

$$Fs = \beta \times \rho \tag{2.21}$$

β = Bjerrum-Burland beta coefficient = $K_s \tan \delta$

ρ = Average effective overburden pressure along the pile shaft

K_s = Earth pressure coefficient

δ = Friction angle between pile and soil

The toe resistance is determined from the formula:

$Qt = N_t \times \rho_t$

N_t = Toe bearing capacity coefficient

ρ_t = Effective overburden pressure at the pile toe

Ranges for β and N_t are a function of soil type and φ angle. (FHWA 1996).

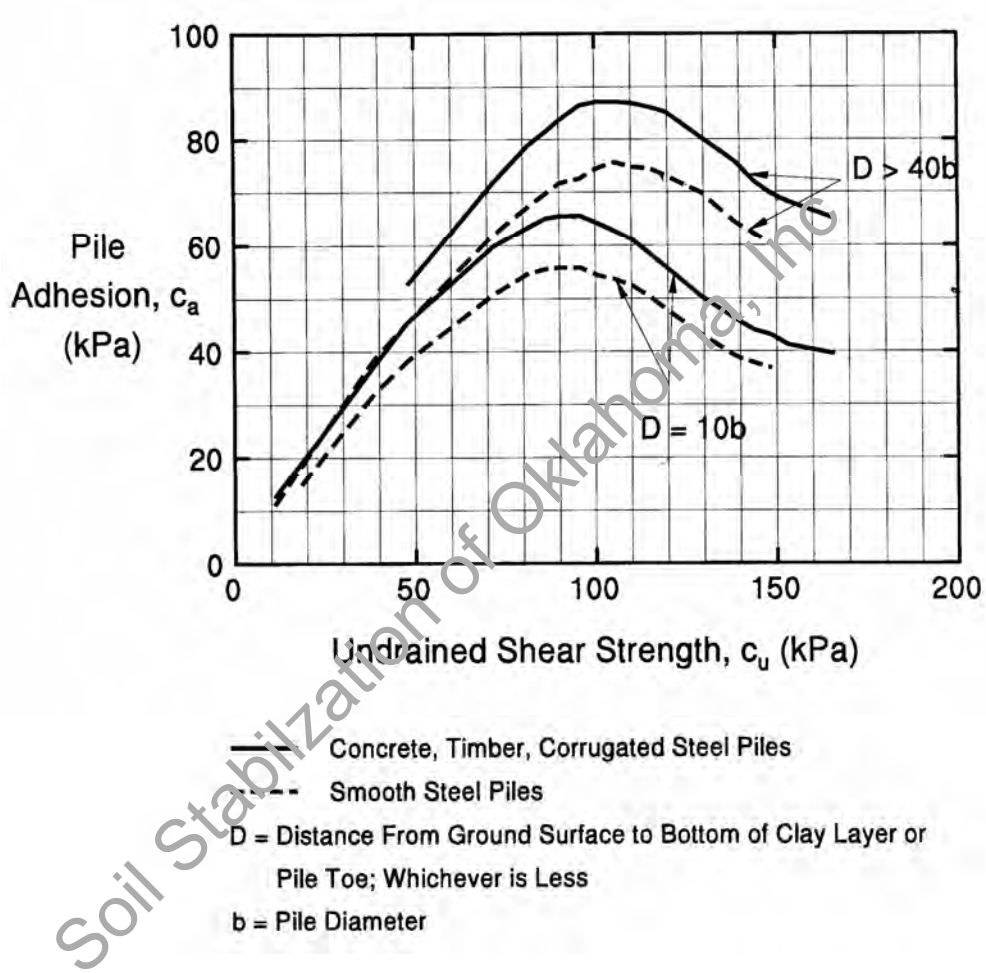

Figure 2.5 - Adhesion Values for Cohesive Soils
(Figure 9.18, FHWA 1996)

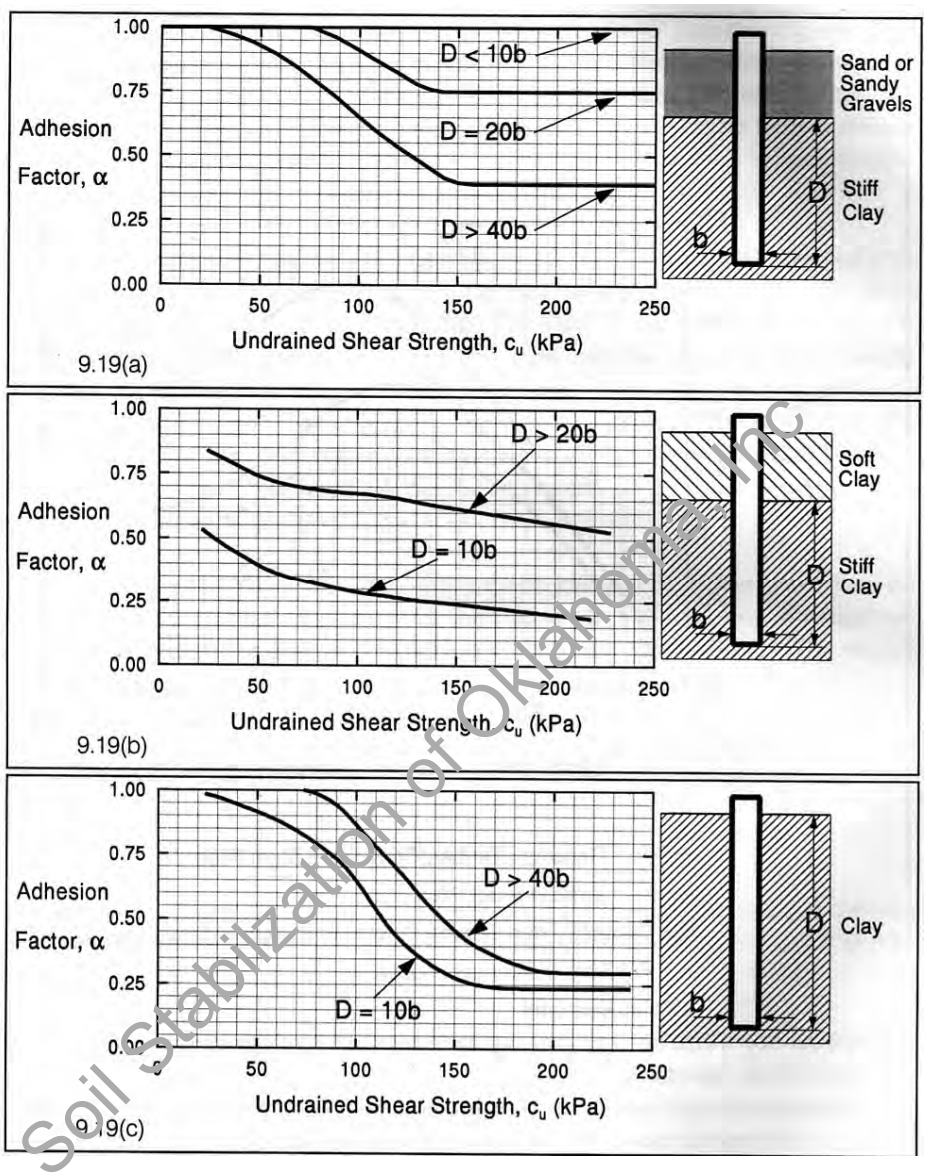

Figure 2.6 - Adhesion Factors for Driven Piles in Clay
(Figure 9.19, FHWA 1996)

Other important tools for calculating pile capacities are the SPILE and DRIVEN Computer Programs. The SPILE Computer Program, which was developed by the FHWA, uses the Nordlund (sand) and ά (cohesive) methods for determining Ultimate Static Pile Capacity and is referenced as FHWA-SA-92-044. Required parameters are soil friction angled, adhesion, pile dimensions and type.

The DRIVEN computer program follows Nordlund and ά method and is available on the FHWA web site. This program is based upon the soil profile with inputs of; soil unit weight and soil strength parameters. The pile diameter, length and type can be varied until desired ultimate and allowable loads can be estimated.

In this present thesis research, two Cone Penetration Tests (CPT) related soundings were conducted in the field, which provided direct in-situ test data of continuous layers. Semi empirical methods based upon CPT data are available to directly calculate axial capacity of foundations. This method is referred as the Schmertmann method (Schmertmann 1978). Using this method the ultimate shaft resistance in cohesionless soil can be calculated as follows:

$$Rs = K[1/2\ (f_s \times A_s)_{0\ to\ 8b} + (f_s \times A_s)_{8b\ to\ D}] \qquad (2.22)$$

where:

K = Ratio of unit pile shaft resistance to unit cone sleeve friction as a function of the pull penetration depth, D (FHWA 1996.

f_s = Average unit sleeve friction over the depth interval indicated by the subscript (psi).

A_s = Pile-soil surface area over fs depth interval (in^2).

b = Pile width or diameter (in).

D = Embedded pile length (in).

0 to 8b = Range of depths for segment from ground surfaced to a depth of 8b.

8b to D= Range of depths for segment from a depth equal to 8b to the pile toe.

The method above is based upon cone sleeve friction data. If cone sleeve friction is not available, Rs can be determined from the cone tip resistance as follows:

$$R_s = C_f \sum q_c \times A_s \quad (2.23)$$

C_f is as a function of pile type and configuration (FHWA 1996).

q_c = Average cone tip resistance along the pile length (psi).

A_s = Pile-soil surface area (in^2).

With cohesive soil, the ultimate shaft resistance is obtained from the sleeve friction values using the following:

$$R_s = \acute{\alpha} \times f_s \times A_s \quad (2.24)$$

$\acute{\alpha}$ = the ratio of pile shaft resistance to cone sleeve friction, patterned after the Tomlinson's α method (FHWA 1996). It is unknown, however, if dynamically driven pile parameters are applicable to jacked piles since tip resistance during driving may determine depth. If the depth obtained is deep, this may shift a greater portion of total shaft resistance to skin friction. If, however, tip resistance is greater, the side resistance will be small with a much greater reliance on end bearing.

It is this engineer's experience in the field and in communiqué with pressed piling contractors that driving depths may vary greatly on a single house. This is a result of high tip resistance caused by high shear strength of the clay soil, an obstruction such as a rock or tree root, or thin stiff soil layer(s) that cannot be broken through. Since this research location was chosen at a safe distance away from trees, root blocks are not anticipated. The soil from the field site is in an area free from fill that might contain rock or other debris. Therefore, there should only be shear strength resistance that will determine

driving depth. This area is, however, in an alluvial fill area where some inconsistency of stratum may be anticipated. With this inconsistency there will obviously be differences in driving depth. With the deeper piles, tip resistance will be a smaller part of total axial compression capacity and the primary factor will be skin friction. With shallow piles; however, the distribution of stresses may not be as certain (Bowles 1988).

Shear strength should only be attributed to three basic components: frictional resistance to sliding between the solid soil particles, cohesion or adhesion between the soils particles and interlocking and bridging of the solid soil particles in resistance to deformation during driving of a pile (Cernica 1995). The shear strength of a soil correlates with the effective stress. In the field this stress condition is axisymmetric (transversely isotropic) in that the principle stress equals the minor stress, which is similar to the condition that exists beneath the tip of a piling (Conduto 1994).

As evident from the description above, water content will affect shear strength in a soil (Sowers and Sowers 1961). One reason is that the bonds that hold the clay particles together are weakened as more water particles are absorbed (Marshall and Holmes 1988). In the case of pilings, the point resistance and compression index decreases in a clay soil with the increase in moisture content (McCarthy 2002). In clay soil there is an undrained condition and at this site the soil borings indicate the soil is undrained. Figure 2.7 graphically displays how when moisture content decreases that soil strengths increase and this relationship is also independent of the type of loading and degree of drainage during the loading phase (Lambe & Whitman 1979). Although this figure depicts unsaturated clay soil, the same relationship exists for drained conditions.

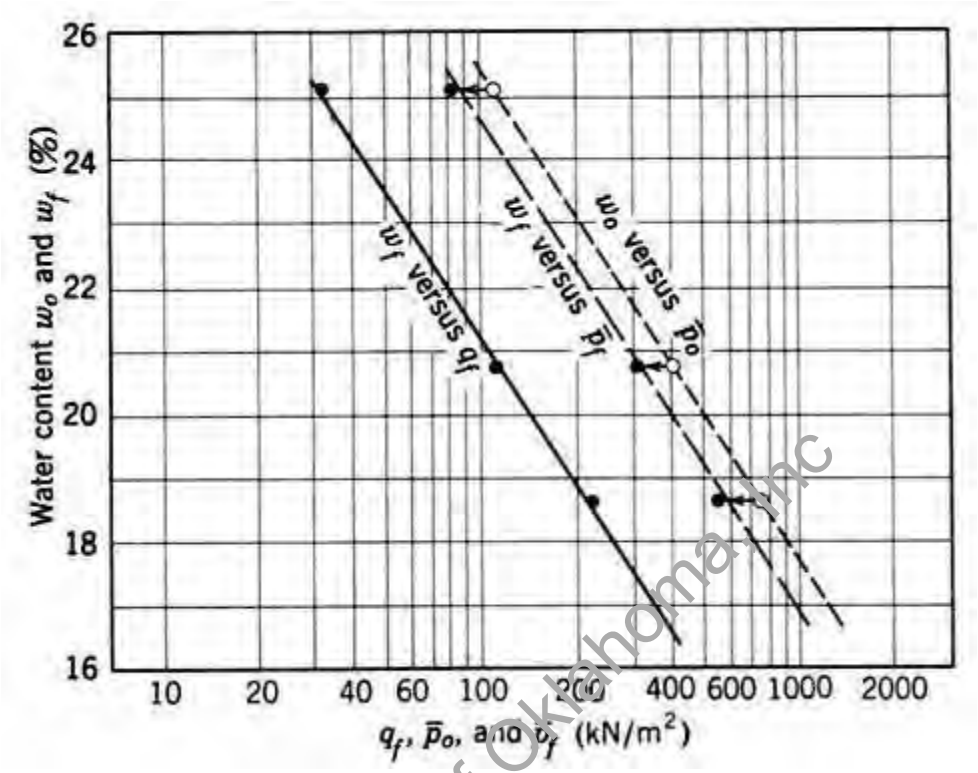

Figure 2.7 - Stress-volume relationship for normally consolidated Weald clay (Lambe and Whitman, 1979)

During the driving stage, the soil is densified, pore water pressures increase, moisture content decreases and the effective overburden is decreased, which all lead to an increase in shear strength and a decrease in skin friction. Therefore, the tip resistance is increased and in the case of shallow pilings, side friction remains a smaller component of the ultimate shaft capacity. Over time, however, pore pressure decreases and water content is restored, which reduces end bearing, increasing the effect of overburden and increases skin friction (Tomlinson 1980).

When going from a dry season of installation to a wetter season of testing, water content increases to further reduce end bearing of deep foundations. If, however, the pilings are driven below the zone of seasonal moisture change, this reduction will be less

because there is not a seasonal increase in soil moisture at those depths. With pilings driven below the active zone, skin friction may increase and the end bearing is only reduced by pore pressure restoration, which is normally a much lesser factor in tip resistance. Evaluation of the soil/pile interface must be with the fact that the clay has been remolded during the driving process. Therefore, the properties of the clay will be altered temporarily during the installation process (McCarthy 2002).

It has also been shown that shear strength in unsaturated clay soils is a function of matric suction and soil water characteristic curve (drying path). If the soil dries, the wetted area of contact decreases and soil suction increases (Marshall and Holmes 1988). With this increase in soil suction there is an increase in shear strength (Vanapalli and Fredlund 1999; Fredlund and Rahardjo 1993). It is also known that matric suction holds the soil together which results in apparent cohesion. From the soil water characteristic curve and measurement of soil matric suction, a reasonable prediction of shear strength can be obtained (Vanapalli, et al. 1999; Rahardjo and Fredlund 1999; Nishimura T. et al. 1999).

Pressed piles are sometimes jetted to help the pile reach a desired depth. With jetting, it has been reported that a loss of 50% to 85% of axial capacity may result because of this process. None of these pressed piles were jetted prior to driving; therefore, there should be no reduction in strength from initial driving load as a result of jetting.

When piles are dynamically driven in clay soil, it has been observed that an enlarged hole will form around the pile as a result of lateral vibration of the pile with the hammer blows (Tomlinson 1980). This soil action is sometimes called quake, which is

the amount of pile deformation required to activate the unrecoverable deformation of soil (Smith 1960). This concept is sometimes depicted by the Concentric Cylinder Model and conforms to the following parameters: soil deformation is believed to deflect downward in the form of cylinders around the pile shaft, the shearing condition operates in this circular pattern and decreases in a radial distance from the pile shaft as depicted in figure 2.8 (Liang and Husein 1993). Because these piles are hydraulically pressed into the soil, little or no vibration is provided. Therefore, an enlarged hole would normally not be expected.

It is this engineer's experience, however, that this enlargement is visible with the pressed concrete piles. Therefore, something else must be causing the enlargement such as remolding of the clay because of a downdrag of clay that stretches the clay layers down with the driving effort. Because this is not a dynamic driving process, the clay layer deformation is not as recoverable with the pressed piling installation and may be much more permanent. It is reported that this enlargement disappears over time as clay moisture is restored. Since this recovery can only be observed at the surface, we do not know exactly how much recovery has actually occurred below the surface and the amount of contact recovery in the form of adhesion along the pile shaft. It is also unknown if clay material from the surface adheres to the shaft and is pulled downward to alter deeper shaft resistance over time.

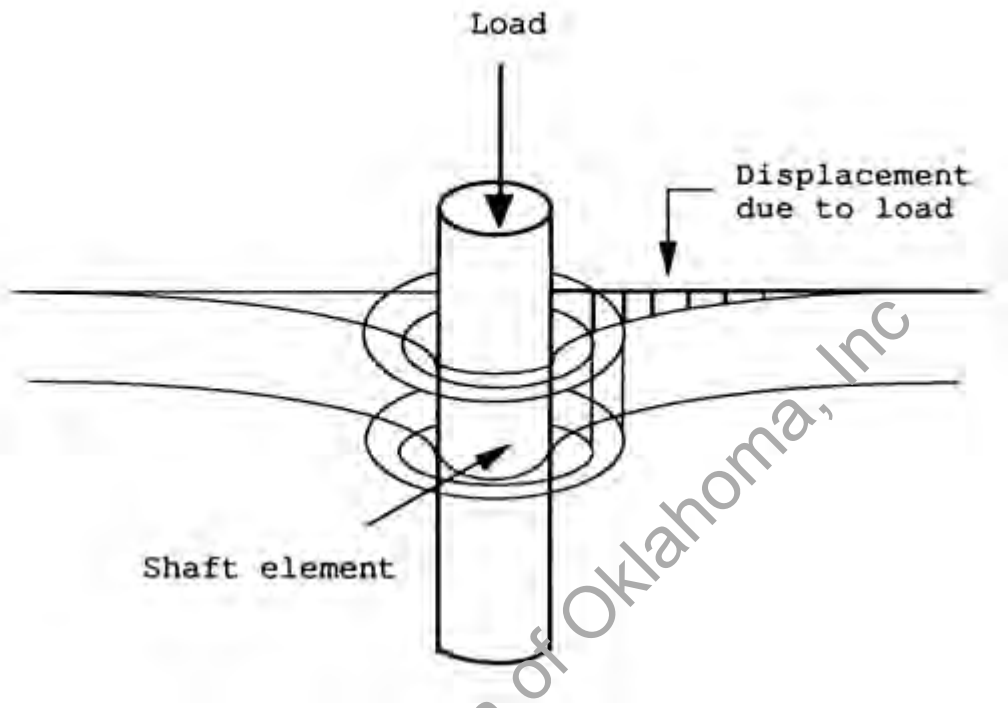

Figure 2.8 - Concept of Concentric Cylinder Model (Liang and Husein, 1993)

This deforming of the clay stratum has also been reported to include cracks in the clay along the surface of the pile that radiate outward such that adhesion is uncertain in the upper 20 pile diameters. Therefore, it is recommended that skin friction be neglected in the upper 4 ft to 6 ft (Tomlinson 1971).

The zone of seasonal moisture change may reach 12 ft to 14 ft in the Dallas/Ft. Worth Metroplex. Since it is common for the concrete pressed piles to not reach that depth, there is a chance of negative skin friction as a result of "downdrag" caused by the shrinkage settlement of clay surrounding the pile. This distribution of stress will normally increase with depth to a point where no change in moisture occurs. With the pile tip being within the active zone, there will not be adequate resistance to counteract negative

friction and a settlement may occur. It is also possible for the negative resistance to overload tip resistance and this would create downward movement (Fleming et al. 1985; Tschebotarioff 1973).

2.3 Deep Foundation Load Testing Methods

Because of the variance in underpinning types, a standard load test, ASTM D 1143-81 (Reapproved 1994) was chosen as the method for field testing. This method is referred to as the "Standard Test Method for Piles Under Static Axial Compressive Load." As described in the introduction, "This standard has been prepared to cover routine methods of testing to determine if a pile has adequate bearing capacity". This method is a static load test where in the Quick test as defined in ASTM D1143, the determined load will be applied for 2 minutes while watching the deflection gauge to determine failure.

Although cyclic loading has been used, it does not appear to contribute to the interpretation of static load bearing capacity and even makes it harder to interpret (England and Fleming 1994). Another factor in the selection of a two (2) minute static test is that some studies have shown an increase risk of influence of the time-dependent movements if left loaded for over 15 minutes and this may impair the test results (Butler and Hoy 1977).

Other sources of testing criteria were reviewed to confirm parameters for failure load. Ultimate failure is a peak load above which the foundation does not take more load and will plunge downward if the load is increased further. In other cases, the peak may not appear in the load-deforming plots; instead, a plateau type loading curve is established. In such cases, the deformation criterion should be used to establish ultimate

failure load of a foundation. For augercast piles, failure load is recorded at 3 in. of downward movement (Neely 1990) whereas ultimate loads for helical piers will produce a plunging failure (Smith 2004). According to FHWA-HI-96-033, "the failure load of a pile tested under axial compressive load is that load which produces a settlement at failure of the pile head equal to":

$$S_f = \Delta + (4.0 + 0.008b) \quad (2.24)$$

where: S_f = Settlement at failure in mm (in).

b = Pile diameter or width in mm (in).

Δ = Elastic deformation of total pile length in mm (in).

If we discount pile deformation, allowable settlement for the steel and concrete piles would be computed as:

Steel piles = 4.0 mm + 0.008(73.03) = 4.584 mm or 0.178 inches

Concrete piles= 4.0 mm + 0.008(152.4) = 5.219 mm or 0.204 inches

Therefore, it will be important to record incremental deflection to load for the entire deformation so that all failure modes will be easily measured.

Elastic deformation in a pile is computed as follows:

$$\Delta = Q_a L/(A E) \quad (2.25)$$

Where: Δ = Elastic compression of pile material (in), (mm)

Q_a= Design axial load in pile (lb), (kN)

L = Length of Pile (in), (mm)

A = Pile cross sectional area (in^2), (m^2)

E = Modulus of elasticity of pile material, (psi), (kPa)

For the steel piles used in this research, we will assume a modulus of elasticity of 207,000 MPa (30,022,813 psi), Length of 13,000 mm (44 ft), Design load of 11.24 kN (50 kips), Pipe cross sectional area of 0.00418 sq.m. (0.0451 sq.ft.).

Therefore:

$$\Delta = \frac{(11.24)(13{,}000)}{(0.0041881)(207{,}000{,}000)}$$

$$= 1.685 \text{ mm} = 0.066 \text{ inch}$$

For the concrete piles of this experiment, we will assume a modulus of elasticity of 27,800 MPa, length of 8231.7 mm (27 ft), design load of 11.24 kN (50 kips), concrete cross sectional area of 0.0182 sq.m. (0.1965 sq.ft.)

Therefore:

$$\Delta = \frac{(11.24)(8{,}231.7)}{(0.01824)(27{,}800{,}000)}$$

$$= 0.18 \text{ mm} = 0.007 \text{ inch}$$

Criteria established for settlements at failure loads were followed in the present research.

While the purpose of this testing is to determine ultimate axial capacity, there is a theory that evaluates the rebound curve (curve of deflection vs. load when the load is released), which will provide a proportion of tip bearing to skin friction resistances. This method of analysis by England (England 2000) establishes that the shaft friction quickly reaches its ultimate level while base resistance increases until failure. It is also proposed that when the load is decreased to no load that the skin friction reverses itself to counteract base resistance rebound (Davies 1987; England 2000). Elastic Shortening

must obviously be accounted for so that actual pile/soil interaction is known (Fleming 1993). This theory has relevance but should only be used as a supplementary data tool in conjunction with proven empirical methods based upon the large and diverse data pool available for a particular test. It is also important that the foundations are set in a homogeneous soil condition that certainly does not exist at this site. Another difficulty in application to this research is the usage of the ASTM 1143 Quick Load Test that can enhance the skin friction approximation because of the rapid static loading (England 1992 and 1993).

It has been mentioned that knowing the distribution of forces along the shafts would be beneficial to the total understanding of pier and pile functional performance and also that there are residual loads along the shaft that could alter an understanding of these forces (Fellenius 2002). This testing, however, only focused with the ultimate resistance of piers and piles in vertical compression. Results presented in this research show load versus deflection plots depicting the failure loads for each underpinning element (ASCE 1985).

2.4 Summary

This chapter provides a comprehensive literature review on the six most common remedial underpinning methods used in practice. Each of the six foundation types (drilled straight shafts, drilled and belled piers, augercast piles, helical anchors, pressed steel and pressed concrete piles) are presented with background information applicable to testing for determining the axial compression capacity. Available literature, including: papers, books, website reviews and conversations with field and academia experts were reviewed to gather this information.

CHAPTER 3

RESEARCH METHODOLOGY

3.1 Introduction

The experimental program of this research included testing of six 6 piling methods that are commonly used in remedial underpinning. These methods include: drilled straight shafts, drilled and belled shafts, augercast piles, helical anchors, pressed steel piles and pressed concrete piles. The intent of this research is to determine values of axial capacity for each element. With the drilled shafts and drilled belled shafts, established accepted empirical formulas (FHWA 1999) will be used to predict final axial capacity. It should be mentioned that the present assessments will attempt to evaluate these established formulae for the better prediction of axial capacities of shafts in expansive soil media under varying seasonal environment.

Published formulae for augercast piles and helical anchors will be used for their capacity prediction. Both the pressed steel and concrete piles are hydraulically driven at an established driving capacity. An attempt will be made to assess whether these capacities will remain the same or vary with respect to different seasonal changes. In other words, variations in the axial capacity with respect to load tests at different seasons will be evaluated. Seasonal variations will simulate a difference in soil conditions when

going from dry to wet to simulate summer to spring conditions and from wet to dry to simulate spring to summer conditions. Dynamic or mixed formulae for predicting axial capacity are used to compare with actual test results.

Another important variable addressed in this research is to study the effects of expansive clayey soils on axial capacities of piers, piles and screw anchors. While drilled shafts have had extensive testing in clay soils, the augercast and helical anchors have not been tested in sufficient numbers in these soil conditions. In the case of the hydraulically driven piles, no test results in clayey soils are reported or documented in the geotechnical literature to verify their capacities with respect to time. Therefore, the present testing program has been offered for the first time to understand how the capacities of various underpinnings can be estimated in expansive soil environment and also provided further understanding of the approaches that could lead to better estimation of axial capacities of these foundations.

Economics of the research project are important since it is quite expensive to construct or install deep foundation type underpinnings and then test them. Therefore, the number of test elements for each underpinning type was selected such that these tests would provide adequate information on the present trends of their capacities with respect to seasonal changes and provide confirmation or rejection of the present industrial practice of established formulae in this soil

A total of eight (8) helical anchors, six (6) drilled shafts, six (6) drilled and belled shafts, six (6) augercast piles, twelve (12) pressed steel piles and twelve (12) pressed concrete piles were constructed or installed and these foundations were tested to address the main objectives of this research project. Though a larger number of foundations

would have been preferred for testing, the present number offered sufficient information to offer explanations or corroborate the variations in their axial capacities.

3.2 Site Selection

In order to compare axial capacities, it was necessary to find a site where no bed rock was present. The site should also have sufficient free area to support various types and numbers of underpinning elements. Bed rock criterion will ensure that all pier/pile/anchor capacities derive the majority of their loads from both skin friction and end bearing in expansive clay soil. Such a site was located in South Irving, Texas and this site was available to the researcher for performing the present testing for the whole duration of the research, which is well over thirty months. Also the soil conditions at the site are proven to be ideal for this research as the soils at this site are expansive in nature. It should be mentioned that this site located in north Texas is well known for expansive clay soil deposits with Plasticity Indices ranging from 30 to 60, and the only rock being shale that can be found at depths reaching 70 ft from the surface.

The environment of Irving, Texas can be characterized as a semi-arid climate where conditions may vary from long droughts in the summer to wet conditions in the spring. For this reason, the first set of underpinning elements were installed in late August and early September of 2004. These foundations were tested in April of 2005, when conditions are normally close to the wet period of the year.

This research was planned 24 months in advance of actual implementation. Therefore, there was no way of knowing that the summer of 2004 as a wet summer with considerable rainfalls. Temperatures, however, still ran in the upper 90^{o} to 100^{o} F on the

days when reaction piers were installed. With this type of temperatures, ground conditions were close to dry conditions of the year and thus satisfied the criterion for dry seasonal conditions.

The following figures depict the width of variations in the field moisture contents from year to year and also depict the severe nature of droughts over the past fifty (50) years. The Palmer Drought Severity Index (PDSI), which is also called as a monthly index indicates the magnitude of a wet or dry spell. As noted in the Figures 3.1, 3.2 and 3.3, the variation in rainfall could be extremely severe with positive numbers indicating wet spells and negative numbers depicting dry periods. In short, this is a meteorological drought index that is used to assess the severity of a dry or wet spell. This index does not take into consideration both lake and reservoir levels or stream and river flow. It does, however, include temperature and the local available water content of the soil. All the basic terms of water balance can be calculated from the input data including: evapotranspiration, soil recharge runoff and moisture loss from the surface layer. There is no allowance for human impacts such as irrigation. Therefore, watering around a structure during dry spells may mitigate some amount of drought severity. (http://www.ncdc.noaa.gov/oa/climate/onlineprod/drought/xmgrg3.html)

The Modified Palmer Drought Severity Index is a modification that was made by the National Weather Service Climate Analysis Center for their own purposes but is only different from the standard PDSI in transition years (Heddinghause and Sabol 1991). Figure 3.1 is a 10 year plot of PMDI for the North Texas area whereas Figures 3.2 and 3.3 provide graphs of PMDI for 15 and 50 year occurrences, respectively.

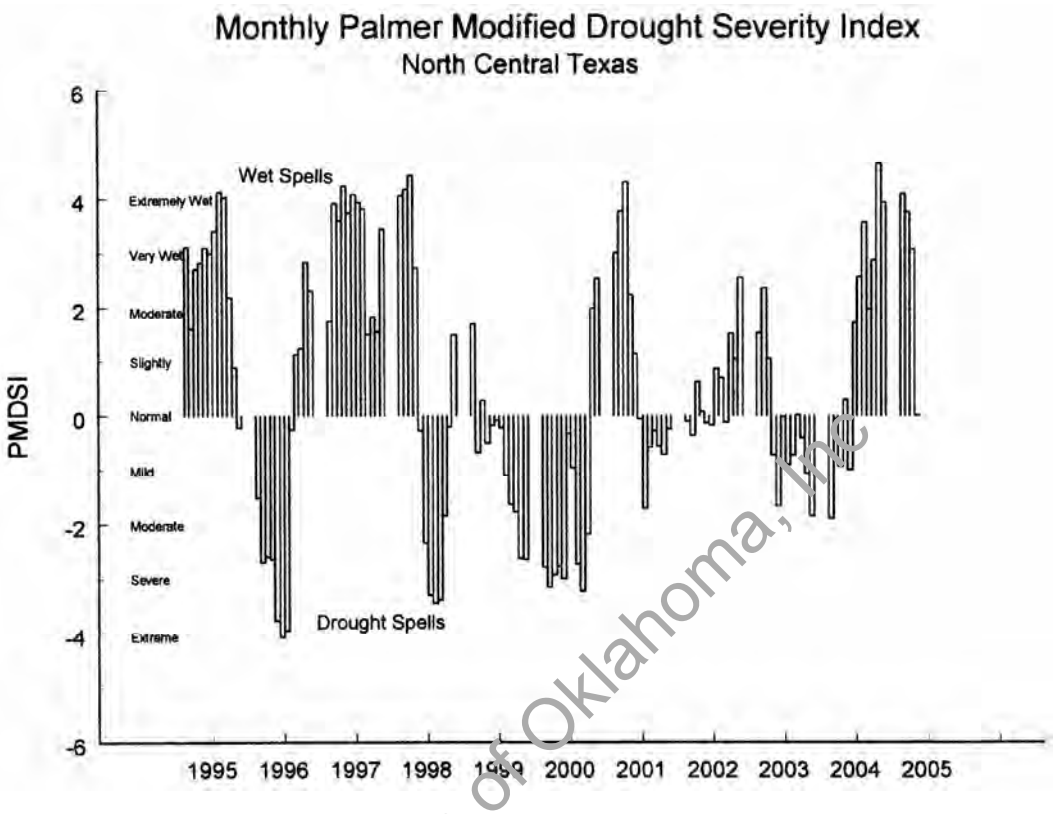

Figure 3.1- Palmer Severity Chart for the Last 10 Years.
(http//www.ncdc.noaa.gov/oa/climate/onlineprod/drought/xmgrg3.html)

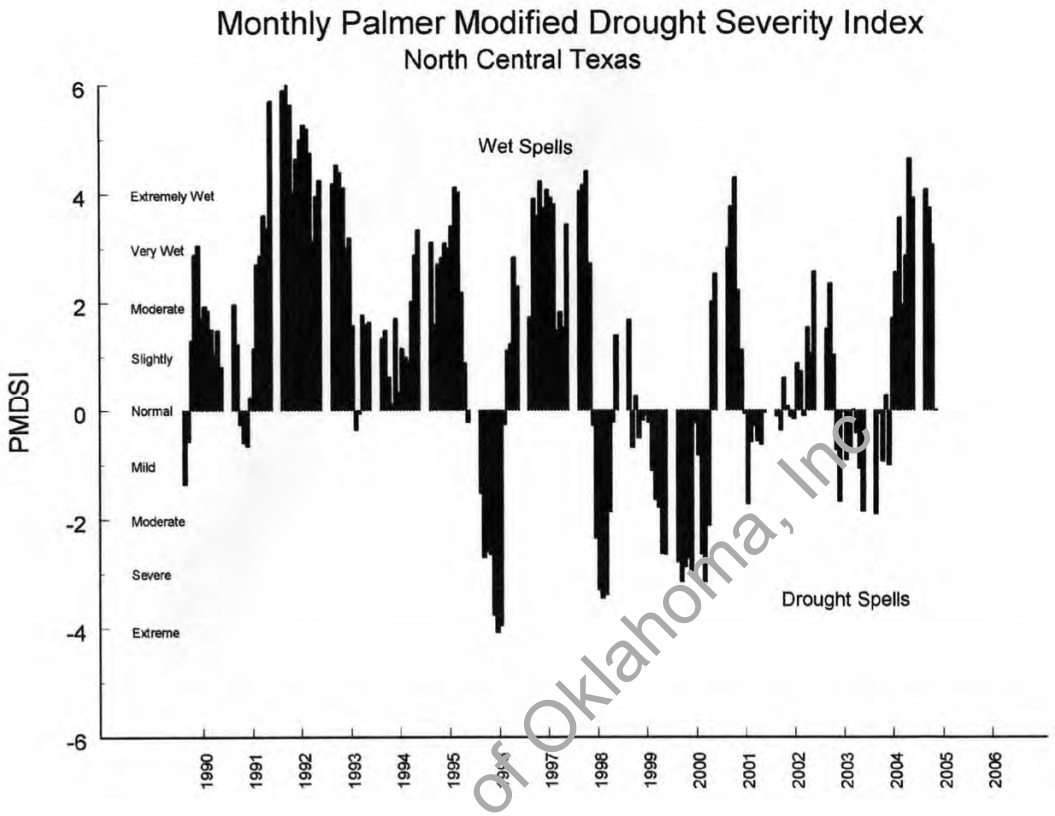

Figure 3.2 – Palmer Severity Chart for Past 15 years (http//www.ncdc.noaa.gov/oa/climate/onlineprod/drought/xmgrg3.html)

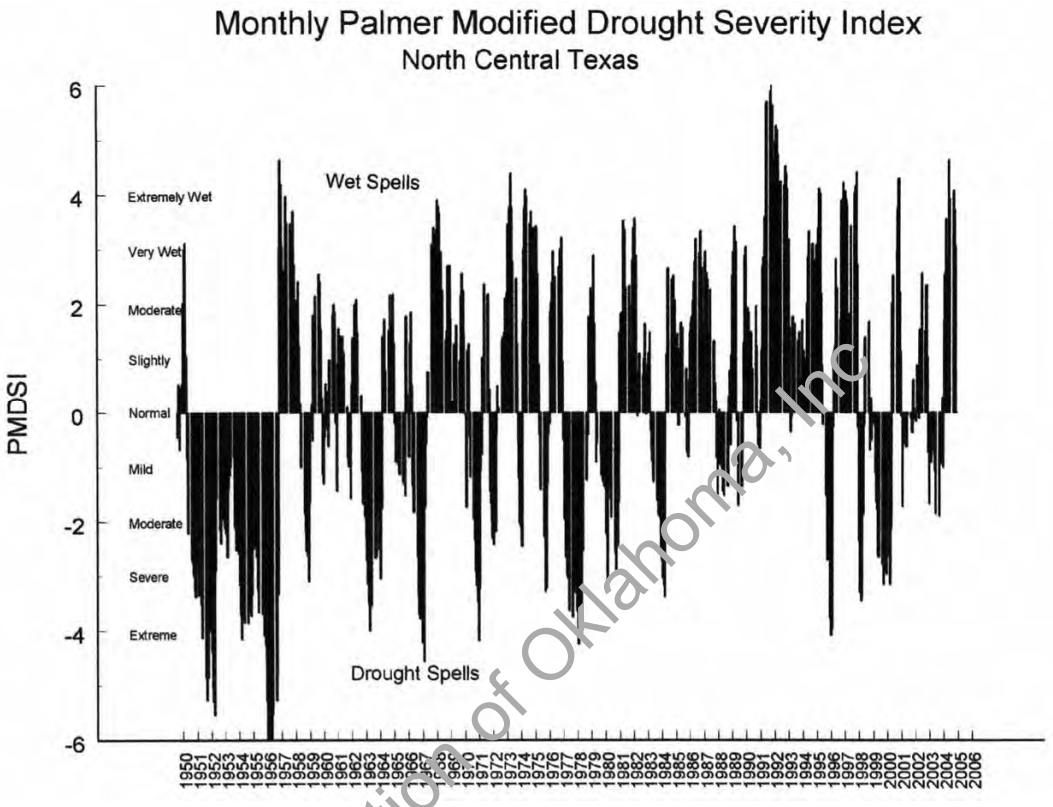

Figure 3.3 – Palmer Severity Chart for Past 55 years (http//www.ncdc.noaa.gov/oa/climate/onlineprod/drought/xmgrg3.html)

Another measurement of wide changes in moisture readings can be explained using 'Thornthwaite Moisture Index (TMI)', which has been documented since 1948. The TMI balances rainfall, potential evapotranspiration and soil water holding capacity. Negative values indicate dry climates, whereas wet climates are shown with positive numbers. As depicted on Figure 3.4, the Dallas/Ft. Worth Metroplex is located in an area with a 0 TMI, which depicts a balance between drought and very wet periods. Areas with ratings between -20 and + 20 are the susceptible to having problems with expansive clay soil because of the wide swings in moisture contents of the soils (O'Neill and

Poormoayed 1980). This method does consider water balance, where there is a storage of moisture during the wet periods and an evapotranspiration of moisture during the dry periods (Buol 1997).

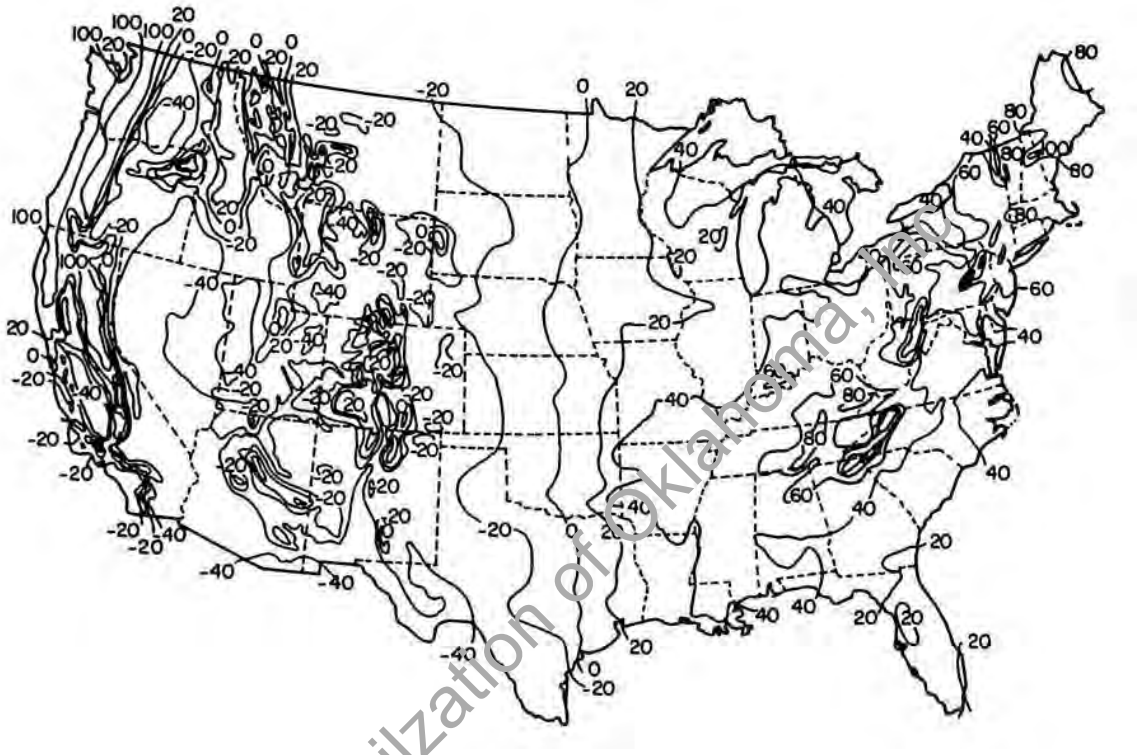

Figure 3.4 – Thornthwaite Moisture Index (Thornthwaite, 1948)

Figure 3.5 shows the location of this site with respect to the city of Irving, Texas. As noted on the map, this location is at the south end of the city and in an area near the Trinity River, which is the largest river in north Texas.

Also important to the success of this research is maintaining an environment that is both secure and fair to the different contractors participating in this testing. An attempt was made to protect the contractor's privacy by ensuring the following. No two underpinning contractors worked at the same time and tests on underpinnings were

conducted with the same privacy rule. Since this location is in locked gate surroundings, all underpinning elements at this test location were not subjected to any vandalism.

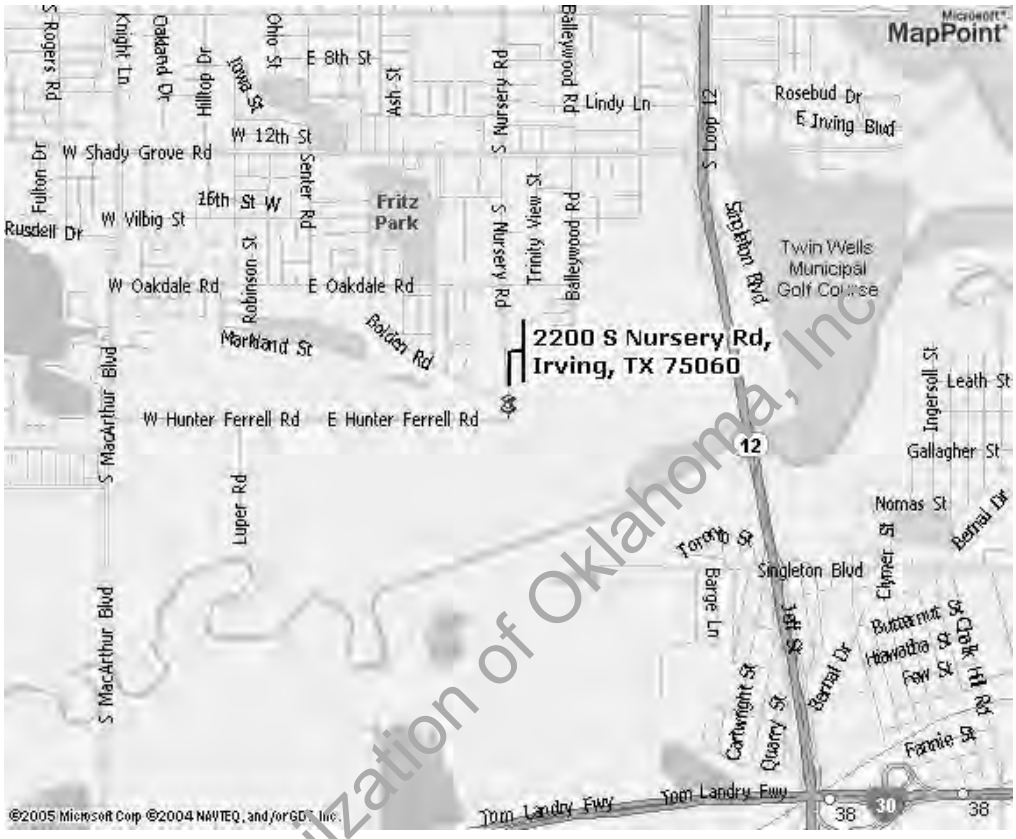

Figure 3.5 – Site Location

Figure 3.6 - A View of Test Site From the North

3.3 Subsurface Investigations

3.3.1 Site Layout and Boring Locations

The project site shown in (Figure 3.7) depicts the layout of the site and locations of borings as they relate to the test elements. The reaction pier locations were surveyed by the researcher with a transit to place the reaction piers in a true north position. This layout provided a staggering of the piers so that testing could be maximized with each pier being used as a reaction point for four (4) reaction beam directions and the potential for an additional line of reaction piers on the east or west sides for two more directions of beam placement. Care was taken to establish the pier locations with two straight lines from north to south that were staggered at 60^{o} angles to supportive piers.

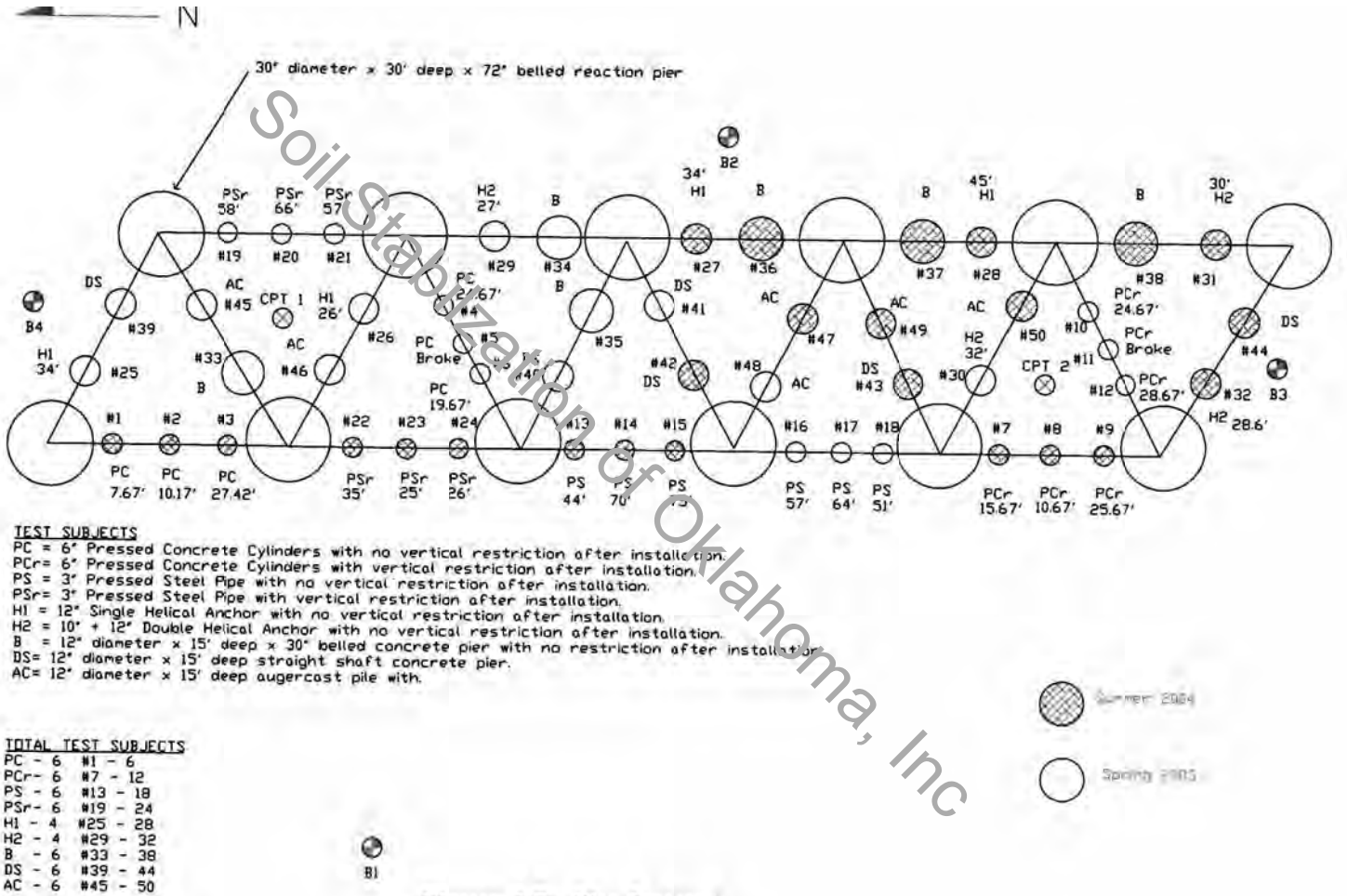

TEST SUBJECTS
PC = 6" Pressed Concrete Cylinders with no vertical restriction after installation.
PCr= 6" Pressed Concrete Cylinders with vertical restriction after installation.
PS = 3" Pressed Steel Pipe with no vertical restriction after installation.
PSr= 3" Pressed Steel Pipe with vertical restriction after installation.
H1 = 12" Single Helical Anchor with no vertical restriction after installation.
H2 = 10" + 12" Double Helical Anchor with no vertical restriction after installation.
B = 12" diameter x 15' deep x 30" belled concrete pier with no restriction after installation.
DS= 12" diameter x 15' deep straight shaft concrete pier.
AC= 12" diameter x 15' deep augercast pile with.

TOTAL TEST SUBJECTS
PC - 6 #1 - 6
PCr- 6 #7 - 12
PS - 6 #13 - 18
PSr- 6 #19 - 24
H1 - 4 #25 - 28
H2 - 4 #29 - 32
B - 6 #33 - 38
DS - 6 #39 - 44
AC - 6 #45 - 50

Figure 3.7 - Site Layout

Soil borings, which are also noted in Figure 3.7, were performed and Shelby tube samples were retrieved around the site. These samples were subjected to physical tests to provide a stratagraphic delineation of the underlying soil strata (Figure 3.7). The intent of the first boring was to explain the subsurface conditions and confirm that this site was suitable for this research testing.

The first boring was placed off to the side of the test site to make sure that there would be no contamination of subsurface conditions caused by the bored hole in a direct location with a pier or pile. Since a minimum of 50 ft depth to rock was required, the first boring was only conducted up to 50ft depth, but samples were continuously retrieved along the total depth. This test procedure provided the necessary confirmation of subsurface conditions including the homogeneity of clay and absence of water table and other conditions that might reduce the consistency of this testing (see field boring log #1, Figures 3.7 and 3.8).

Prediction of axial load capacity would only be possible if accurate subsurface geologic conditions are known, which in turn could reduce the uncertainty involved in the non-homogeneity nature of the soil and rock (ASCE 1984).

Figure 3.8 - Boring Operations Using Augering: Log #1

A total of four (4) borings were performed to make sure a good cross-section of soil strata was available that would provide soil parameters for testing (Figure 3.7). Since one of the goals of this testing was to show changes in axial capacity across wide variations of moisture content, it was also important to identify the zones of moisture changes or active depths and then compare it with depths of the piers, piles and anchors. The second log was taken at the east side of the project, 5 ft away from the beam line, and is depicted by the attached boring log #2 (Figure 3.9 and 3.10).

The third and fourth borings were located on both the north and south sides of this site to identify possible stratagraphic dipping from north to south, which was observed in

this area (see boring logs #3 and #4, Figures 3.11-3.14). It was also important to evaluate the east to west strata to better apply soil factors in the empirical calculations of the test subjects.

Another factor in determining the number of soil borings is that one of the strength characteristics used in determining pier and pile capacity is cohesion, which is the result of attractive forces between soil particles. Because of these forces, a soil may exhibit shear strength under no confining pressure condition. Therefore, where φ is negligible, clay soil's cohesion approaches as near the measured shear strength in the field conditions (in situ soil) (McNab 2003). If cohesion in clay soils is the result of capillary action, it may then disappear or reduce as the soil dries. The reason that a boring was attempted at the time of each installation and at time of testing is to correlate cohesion with axial capacity such that if the piling/pier system is above the zone of seasonal moisture changes, then these cohesion phenomena might explain changes in axial capacity.

Boring #1 was attempted to identify the suitability of this site for testing. Boring #2 was performed at the time of first half installation. Boring #3 was attempted at the time of testing of the first half of underpinning subjects, which was also the time for installing the second half of subjects. Boring #4 was done at time of testing the second half of subjects. Therefore, changes in moisture, cohesion, shear strength and the angle of internal friction were identified and properly determined to help explain changes in bearing capacity from time of installation.

Unlike the drilled piers that are normally drilled to a specified depth or strata, the pressed pilings are pushed to a specific installation pressure or at the point the house lifts.

They must then be stopped to prevent damage to the structure or the pressure exceeds driver capacity. It is this engineer's experience and is also reported by remedial repair contractors that driving depths may vary significantly, even on the same side of a house or building. Therefore, the number of borings on this site may help suggest why they vary on this project and where the lenses of clay strata are stiff enough to stop progress of the piles during installation.

3.3.2 Soil Boring Field Records

The soil borings were conducted with the assistance of Fugro South Inc., a local geotechnical engineering company, while testing of the soil samples was attempted at the UTA geotechnical laboratory in Arlington, Texas. A split spoon sampler was used for retrieving the samples in the upper 5 ft depth since this material was harder to retrieve in full. For the depths below 5 ft, a Shelby tube was used with the sample extended after retrieval by a hydraulic ram provided on the drill rig. All samples were placed in a clear plastic sample container, sealed to prevent loss of moisture, marked for location and depth and axial direction then placed in protective boxes for transport to the UTA Labs for further geotechnical tests (Figure 3.9).

Figure 3.9- Recording of Shelby Tube Samples

For the initial boring (boring #1), the objective was to test the hypothesis that a rock layer was non existent in the top 50 ft. Hence, this boring required continuous sampling of the soil strata but testing of soil samples was confined to those that showed changes in soil appearance and texture. It was also important to establish the water table location. This area is exposed to droughts in the late summer and wet conditions in the spring. The summer period at the start of underpinning installation was unseasonably wet due to several rainfalls occurring during that time. Since the first boring information was primarily to establish uniformity of soil and to prove that rock was below 50 ft, pocket penetrometer (P) readings were measured at each depth but no standard penetration tests (SPT) were attempted at this phase. It should be mentioned that the P readings were only

used to assess the homogeneity nature of the sample. These results were not used in any of the subsequent analysis.

The second boring was performed in August on the east side of the project and was extended to a depth of 63 ft, which was to a point 3 ft into the eagleford shale formation, an soft Cretaceous-aged argillaceous rock that is common for this area (O'Neill et al. 1992 and O'Neill et al. 1993). For purposes of evaluating pier capacities, this shale is considered an Intermediate Geo Material (IGM) as discussed by O'Neill (FHWA 1999). For this boring, samples were taken at 5 ft depth intervals and standard penetration tests were performed at the same depth interval. Here again, the top 5 ft of soil was collected with a split spoon sampler with soil below that point retrieved with a Shelby tube sampler.

Samples from borings #3 and #4 were retrieved in the same manner as boring #2 and these boring information is provided in Figures 3.10, 3.11, 3.12, 3.13, 3.14, 3.15, 3.16, and 3.17. Pocket penetrometer tests were measured on the samples to compliment SPT readings. The pocket penetrometer is not an accurate test, and provides qualitative information. Hence, it is not used along with other soil properties. The Standard Penetration Test (SPT) is more widely used in situ method in the Unites States and is considered as a reliable method for interpreting soil properties. Procedures for this test are detailed in ASTM D1586 method. Since the friction of walls induces resistance to the test equipment during penetration, the measured readings are often subjected to some error. Hence, the driller opens the hole with a continuous auger prior to each measurement in order to obtain an accurate measurement of actual soil conditions. Even with an experienced soil driller, the effect of overburden pressure will produce

inaccuracies in the SPT measurement. Therefore, same density soils near the surface will yield smaller N values than those with the same density soils at a deeper depth. To correct for this inaccuracy, charts have been developed to correct for the effect of overburden pressure. Formula 3.1 provides the necessary overburden correction factor, Cn. From this charts the corrected N value becomes:

$$N' = C_N \times (N) \quad (3.1)$$

Where: N'= corrected SPT N value

C_N= correction factor for overburden pressure

N= uncorrected or field SPT value.

As depicted on the field logs, stratum descriptions were made for each change in soil.

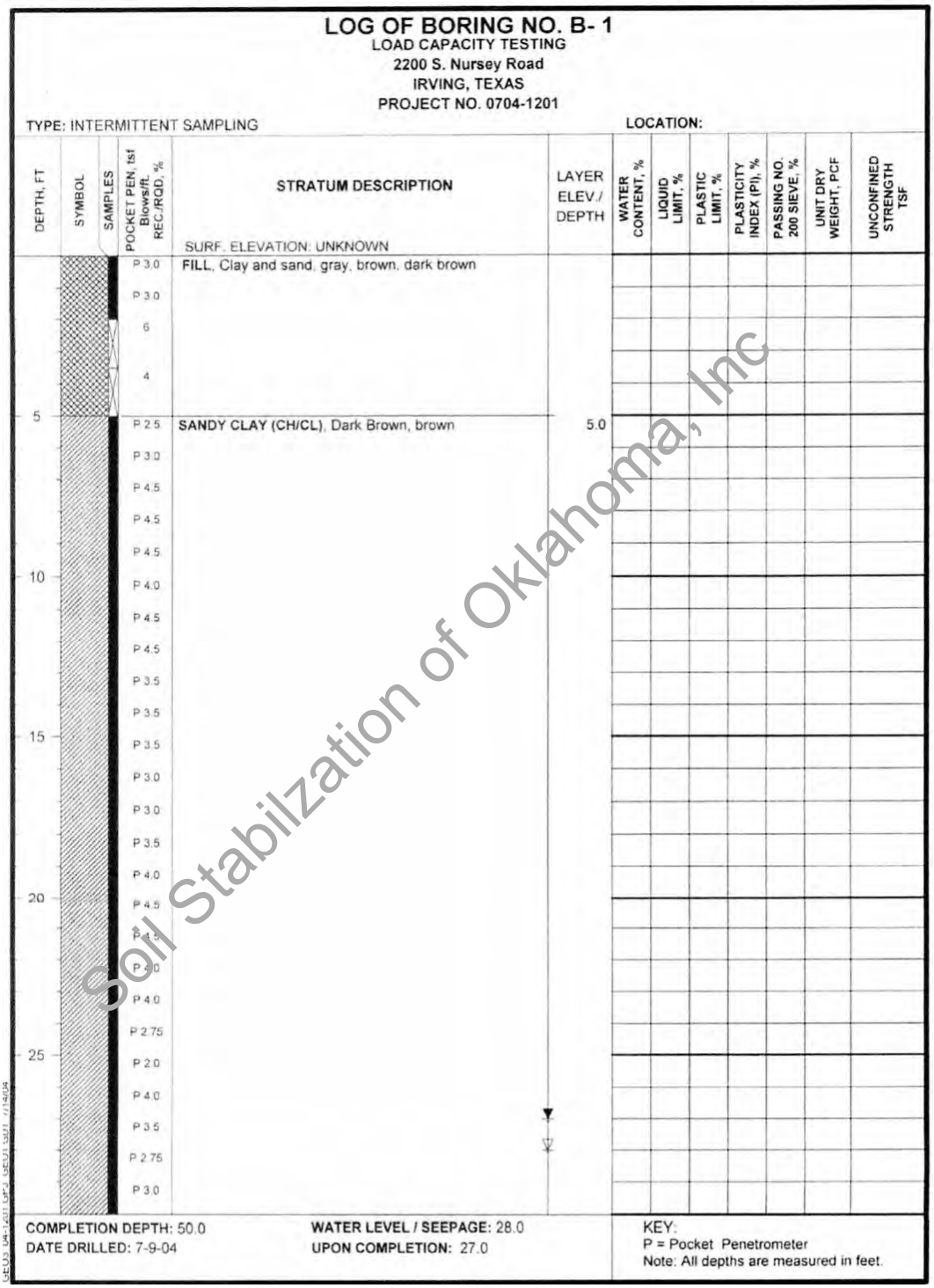

Figure 3.10 - Boring #1, Upper Soil Strata Information

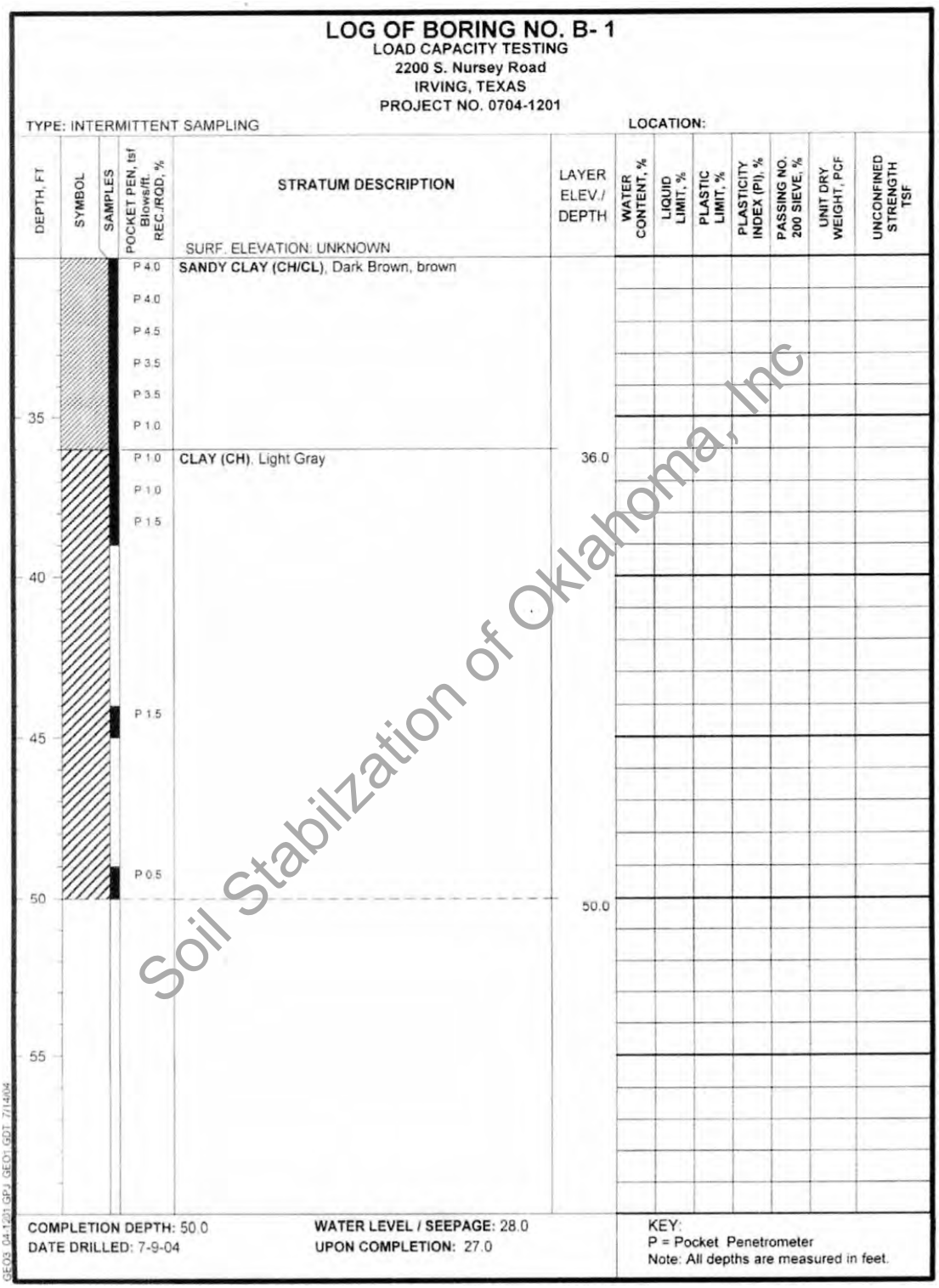

Figure 3.11 – Boring #1, Lower Soil Strata Information

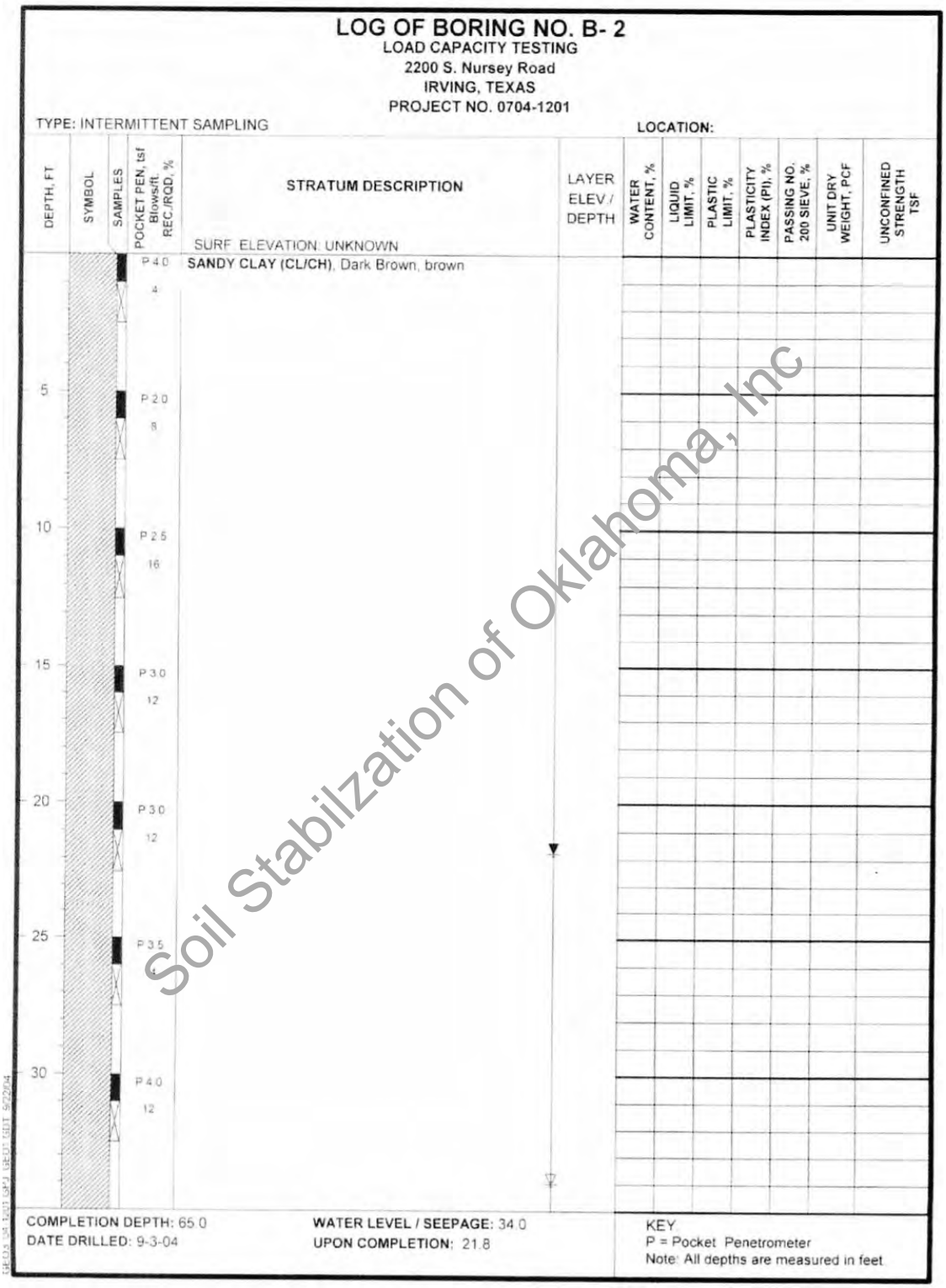

Figure 3.12- Boring #2, Upper Soil Strata Information

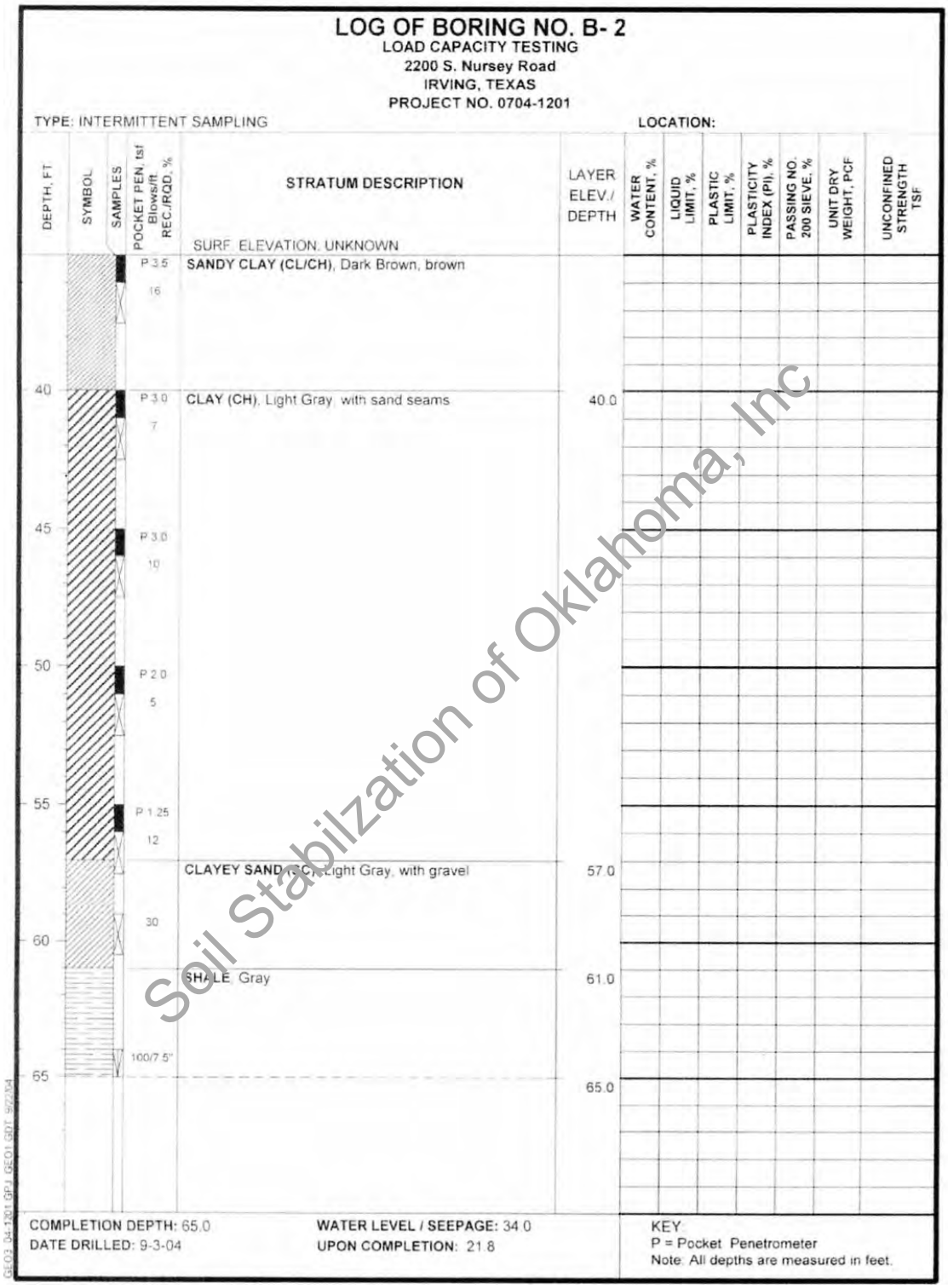

Figure 3.13- Boring #2, Lower Soil Strata Information

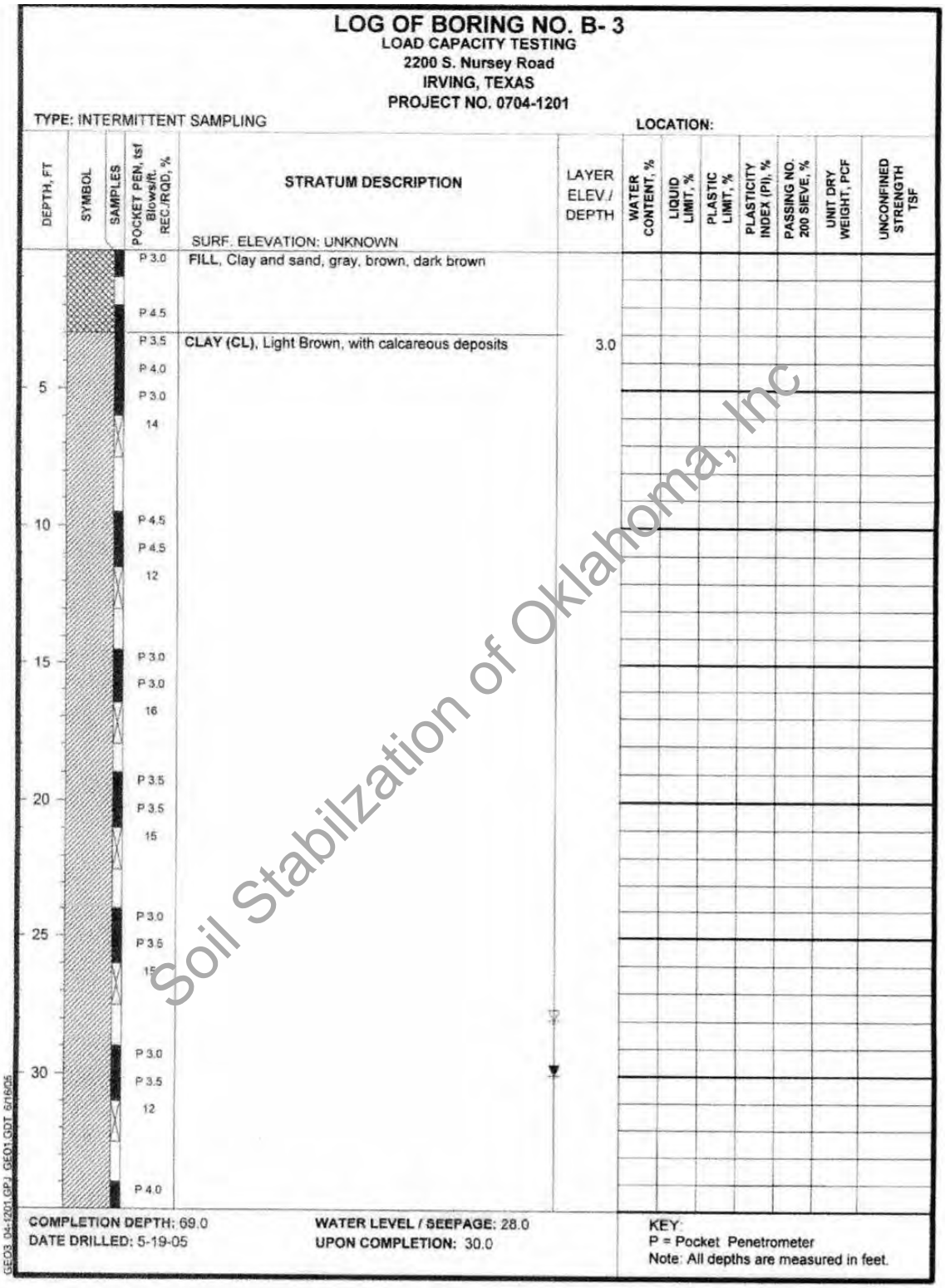

Figure 3.14- Boring #3, Upper Soil Strata Information

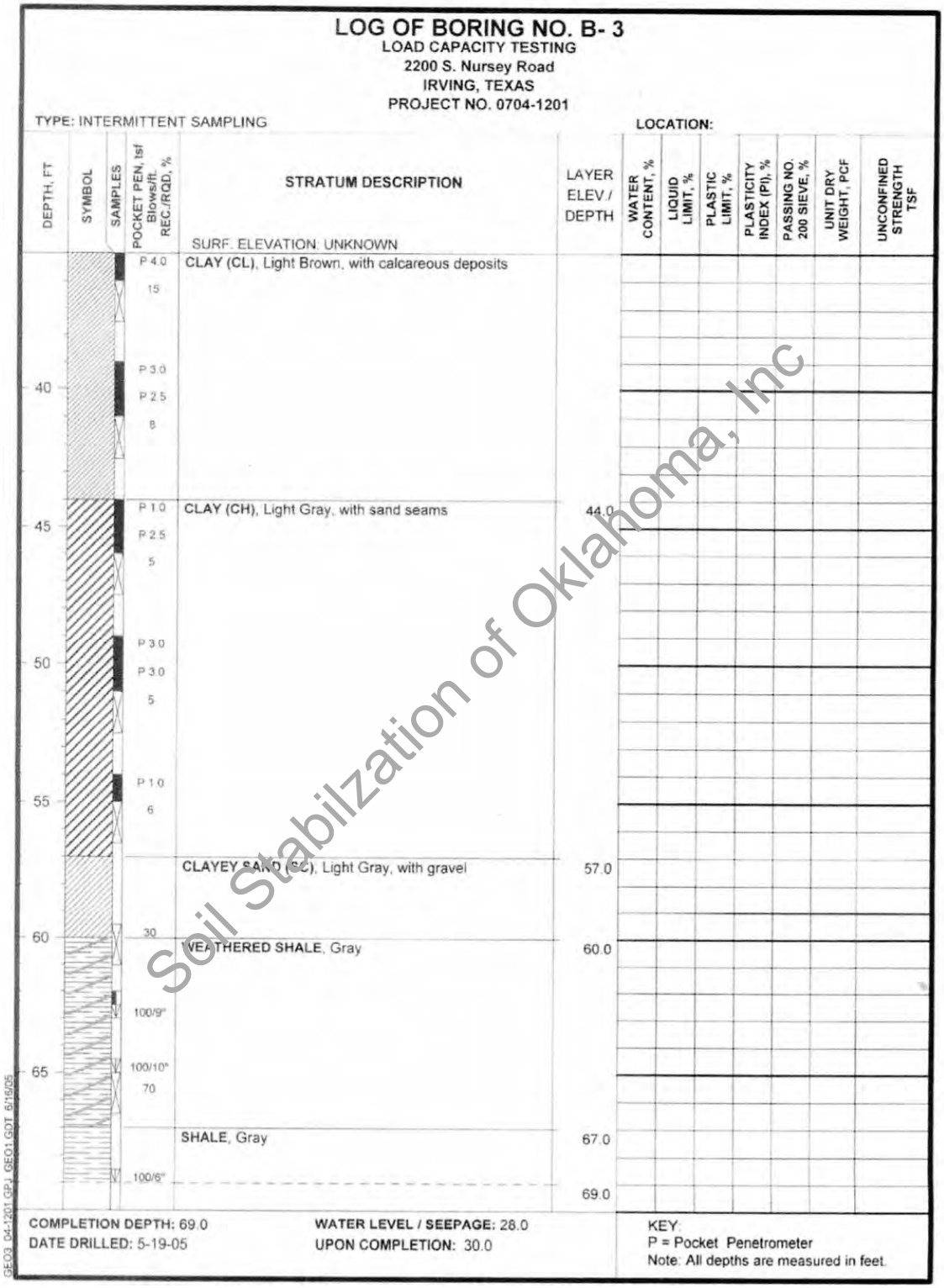

Figure 3.15- Boring #3, Lower Soil Strata Information

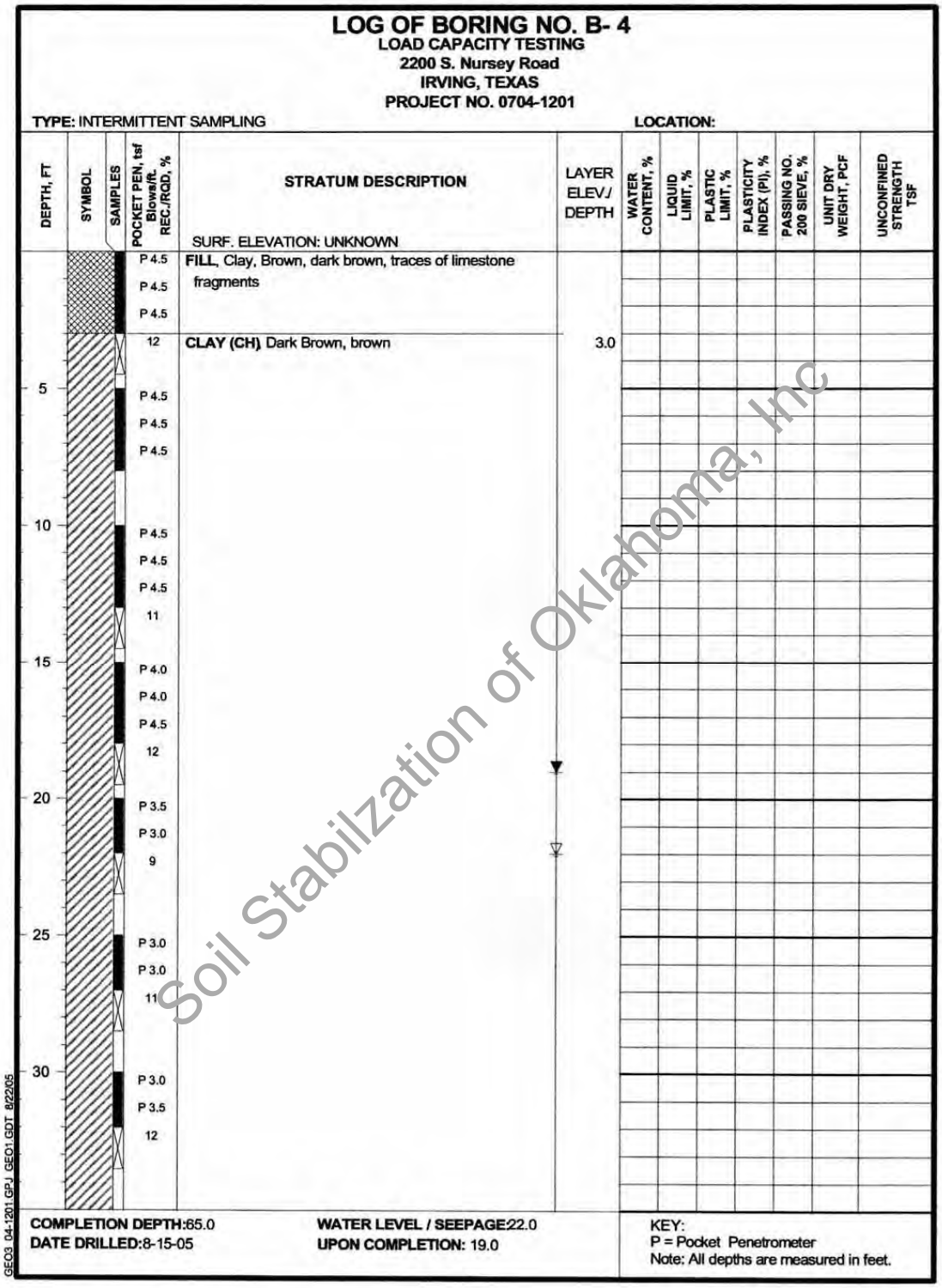

Figure 3.16- Boring #4, Upper Soil Strata Information

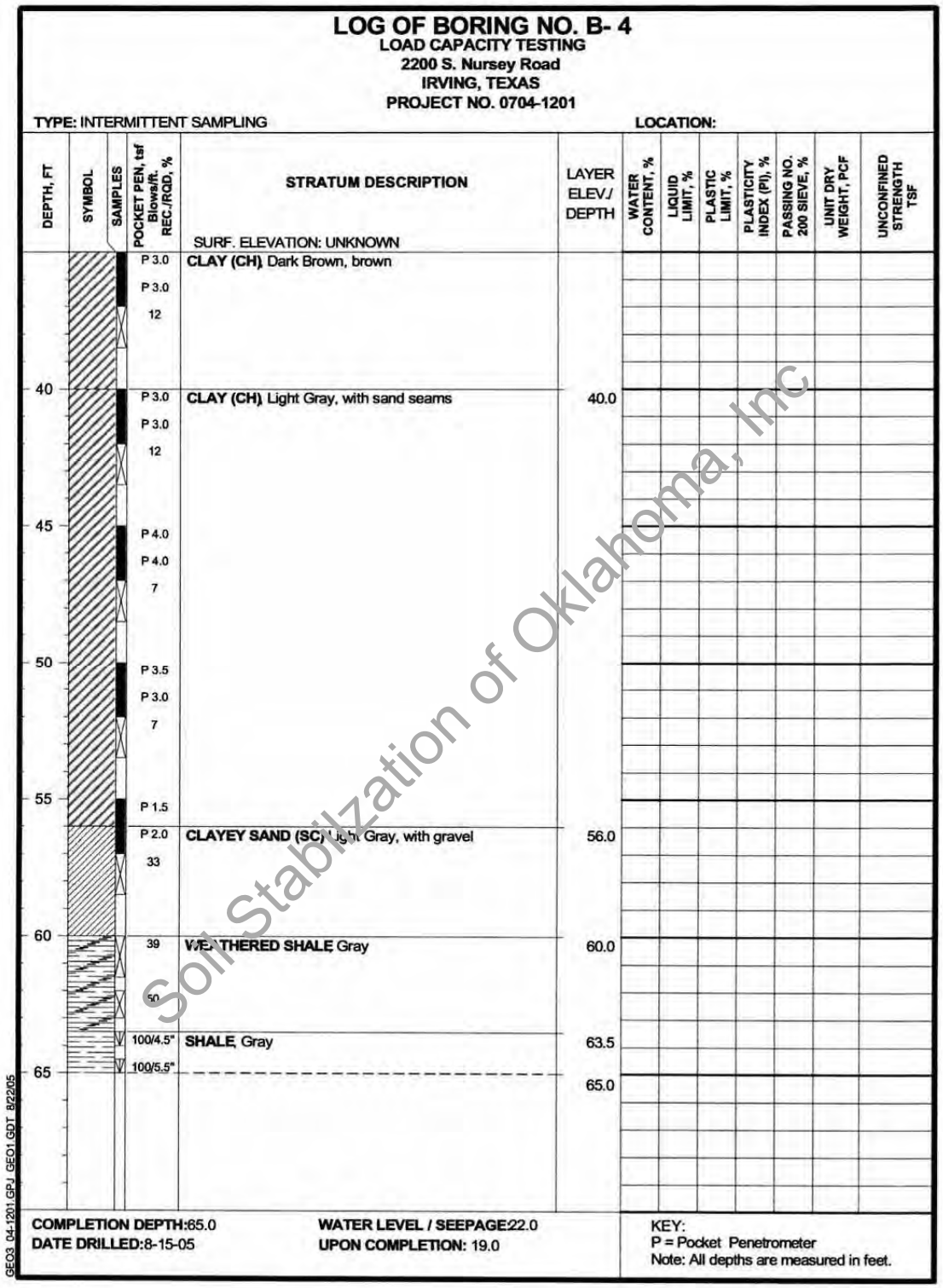

Figure 3.17- Boring #4, Lower Soil Strata Information

3.3.3 Laboratory Testing

All soil samples were transported and kept in a 100% humidity control room at the UTA soils laboratory for subsequent testing. The soil testing was performed in accordance with the American Society of Testing and Materials (ASTM) procedures. Physical and engineering soil tests performed in the laboratory included: hydrometer analysis (ASTM D 422), atterberg limits (ASTM D 4318) and Unconsolidated Undrained triaxial tests (Figure 3.18).

Wet sieve and hydrometer analyses were performed on site clay to characterize grain size of fine soils from the bore holes. More than 92% of the site soil is finer than No. 200 sieve. Atterberg limits consisting of liquid limit and plastic limits were often measured to determine the plasticity index or PI value. These tests provide general information about the plasticity nature of subsurface conditions by identifying characteristics of the clay that are sometimes helpful in determining soil strengths and shrink/swell parameters. Correlations with other important soil properties were often reported in the literature. The plasticity index (PI), which is the difference between liquid limit and plastic limit, has long been used as a standard parameter for characterizing expansiveness of clay soil. The PI values of various soil layers ranged between 25 and 40 for this site as evidenced by Table 3.1.

Table 3.1 - Atterberg Limits of Soil Samples from Borings #1 and #2

Depth	LL	PL	PI
0'-5'	40	15	35
5'-10'	52	21	31
10'-15'	49	21	28
15'-20'	39	12	27
20'-30'	49	19	30
30'-40'	45	20	25
40'-50'	46	19	26
50'-60'	58	18	40

Free vertical swell tests were performed on select soil samples in Oedometer test setups and these swell strains ranged between 14 to 28%. Triaxial tests were normally used to determine the undrained internal friction angle (φ or φ_u) and cohesion intercept (C_u), which in turn can provide shear strength of soil at various depths. These total strength or undrained soil properties (cohesion and friction angle) are used in bearing capacity expressions to predict axial capacities of pier, pile and helical anchors. Among triaxial test methods, the unconsolidated/ undrained (UU) test is a rapid test method that can provide reasonable measure of cohesion intercept and undrained friction angle in clay soils at their field moisture states, which are close to unsaturated conditions. These UU tests were made by testing soil specimens at confining pressures of 20 psi, 40 psi and 60 psi, where three samples were available and at 30 psi and 60 psi when only two specimens could be prepared from the Shelby tube samples. Results of these tests were provided in Tables 3.2, 3.3, 3.4 and 3.5 for each boring log.

Figure 3.18 - UTA Triaxial Equipment

Table 3.2 - Results of UU Triaxial Tests on Samples from Boring #1

Depth	Cu (psi)	φ (deg)
0-5'	22	11
5'-10'	14	9
10'-15'	35	8
15'-20'	22	3
20'-25'	25	8
25'-30'	28	1
30'-35'	39	1
35'-40'	20	7
40'-45'	19	4
45'-50'	20	13

Table 3.3 - Results of UU Triaxial Test on Samples from Boring #2

Depth	Cu (psi)	φ (deg)
0-5'	24	7
5'-10'	21	9
10'-15'	36	9
15'-20'	16	1
20'-25'	26	3
25'-30'	23	5
30'-35'	34	3
35'-40'	31	5
40'-45'	17	4
45'-50'	15	3
50'-55'	16	10

Table 3.4 - Results of UU Triaxial Test on Samples from Boring #3

Depth	Cu (psi)	φ (deg)	mc (%)
0-5'	7	7	20.67
5'-10'	14	13	23.88
10'-15'	32	11	23.13
15'-20'	16	5	24.11
20'-25'	26	4	22.24
25'-30'	34	5	23.12
30'-35'	31	4	22.21
35'-40'	21	5	22.98
40'-45'	19	2	23.98
45'-50'	16	7	28.78
50'-55'	14	8	32.99

Table 3.5 - Results of UU Triaxial Test on Samples from Boring #4

Depth	Cu (psi)	φ (deg)	Mc (%)
0-5'	24	8	10.30
5'-10'	25	7	22.51
10'-15'	32	10	23.53
15'-20'	16	1	23.90
20'-25'	27	3	21.85
25'-30'	34	3	22.45
30'-35'	31	5	22.64
35'-40'	21	8	23.82
40'-45'	19	11	25.11

As noted in Tables 3.2 to 3.5, cohesion and obviously shear strength of the soil varied significantly throughout the soil mass and this proved to be a factor when installing hydraulically driven piles. With the number of soil borings on this site in conjunction and along with the Cone Penetration Test profile (CPT data presented in Figure 3.20 and 3.21), a good picture of resistance lenses in the soil helped with pile axial capacity resistances.

Since triaxial testing would take months to complete for conducting tests on fully saturated cohesive soils, in situ tests utilizing piezocone penetration tests (CPTUs) were conducted to directly determine undrained shear strength or S_u parameters for depths below 10 ft in all seasons related to summer testing conditions. For the upper 10 ft in spring conditions, undrained triaxial test results on unsaturated clay samples were used to establish undrained shear strength values.

The CPT tests were conducted only once (in summer) during the project due to costs associated with this testing. Hence, UU test values on unsaturated clays were used to establish undrained shear strengths values for spring conditions.

Because shear strength varies with moisture content in the soil, this factor was measured to determine the zone of seasonal moisture change, which is commonly called the active zone. Figure3.19 shows the variance with depth for the wet season and the dry season.

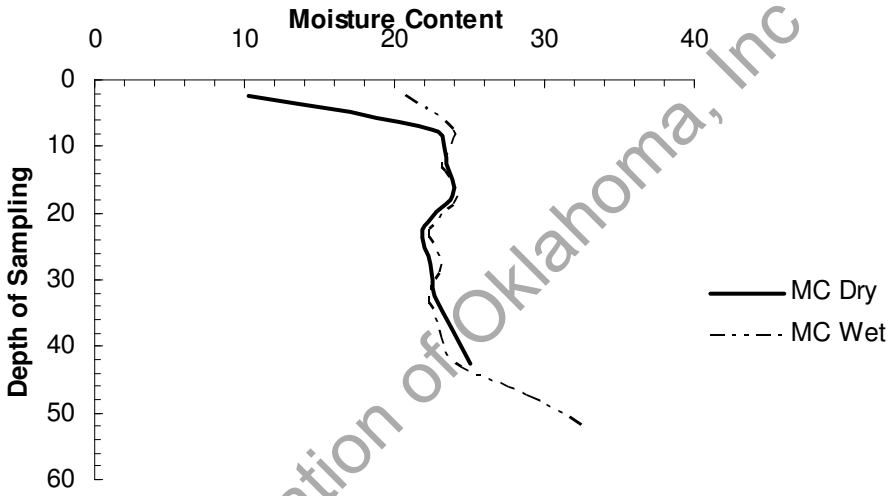

Figure 3.19 - Moisture Content verses Depth

3.3.4 Cone Penetration Testing With Pore Pressure Measurements (CPTU)

Records indicate the use of probing rods through soft/weak soils to locate firmer stratum has been practiced since 1917 (Lunne et al. 1997). It was, however, in the Netherlands that modern CPT was first recognized in 1932. CPT systems are now divided into three main types: mechanical cone penetrometers (CPT), electric cone penetrometers (CPT) and piezocone penetrometers (CPTU) (Lunne et al. 1997).

The initial mechanical probes consisted of a 0.75 in. (19 mm) steel gas pipe, inner 0.59 in. (15 mm) steel rod with a 60% point on the end. The inner rod was pushed down 5.91 in. (150 mm) and measurements of resistance were measured on a manometer. The outer sleeve was then advanced until it reached a point where point resistance would not include the side resistance. Measurements were taken every 0.66 ft (0.2 meters) so there was a continuous profile of soil. Later improvements included adding an "adhesion jacket" so that side resistance could be measured and estimations of soil classification could also be made. Although mechanical penetrometers are still used widely because of their low cost, they are operator dependent and subjective in evaluating their data (Lunne et al. 1997).

Electric cone penetrometers appear to have been developed in Berlin during World War II (Broms and Flodin 1988). Signals from the tip were transmitted to the ground surface through a cable that provided accurate and easily recorded results that eliminated false skin friction readings and continuous sampling over the entire soil stratum. Acoustic transmission of signals is also used to improve handling of the segmental rods but there is still a continuous measurement of soil parameters (Jefferies and Funegard 1993).

The advent of the piezocone accelerated accuracy and increased information from the soil including; penetration pore water pressure, sleeve pressure and a correction of cone resistance for pore water pressure caused by the penetration. Since the ratio of sleeve resistance to cone resistance is higher in clay than in cohesionless soils, the classification of soil can be predicted. In most cases, however, it is far more accurate to add soil boring information for a more precise prediction (Liu and Evett 1992). With the

increased capacity of computers, other sensors were also included that provided even better modeling of both clay and sand stratum.

Static cone resistance (q_c) is used to determine shear strength based upon effective overburden stress (p_o) and knowledge of the water table. This information also provides an estimate of the over consolidation ration (OCR), which is very useful in evaluating a site (Schmertmann 1974; Nelson and Miller 1992).

The cone penetration test (CPT) was used for the first time in the U.S. in 1965 (Briaud et al. 1991). Within ten years after this use, the mechanical test was being replaced with an electronic cone. Developments in the electronic cone progressed with the measurement of pore pressure, which provided further refinements to soil property interpretation (Briaud et al. 1991).

Two cone penetration tests were conducted with the assistance of Greg In Situ, a commercial entity that provided their services at no cost to this research project. These soundings were conducted at the inner section of the underpinning elements with one at the north end and one at the south end (Figure 3.7). Cone Penetration Testing was conducted by pushing a specially designed electronic rod with a conical tip attached into the ground. This device was capable of measuring tip, sleeve friction and pore pressure (Figure 3.13). From these measurements, interpretations are made continuously for: temperature, pore pressure, shear strength, soil unit weight, effective overburden stress at mid layer depth (σ_v).

Standard Penetration test or SPT N values were also corrected for overburden pressure, equivalent clean sand and SPT N values, undrained shear strength (S_u), coefficient of permeability (k), pore pressure parameter (Bq), end bearing (Q_t), friction

ratio (Fr), equivalent clean sand correction for q_{ct} (K_c), soil index for estimating grain characteristics (Ic), apparent fines content (%) (FC), friction angle (φ), relative density (D_r), overconsolidatation ratio (OCR), cyclic resistance ration for M=7.5 (CRR), youngs modulus (E), coefficient of lateral earth pressure at rest (K_o).

Charts labeled as Figure 3.20 and 3.21 depict measurements of conditions on this site at the two CPTU test borings. Detailed analysis of interpreted parameters of these probes are depicted in Tables 3.6 and 3.7, which provide depth (ft) measurements of q_c(tsf), q_t (tsf), fs (tsf), Rf (%), u (psi), SBT (zone).

One of the greatest advantages of the CPTU is that results can be obtained at the test spot with no waiting for laboratory testing that can take several days or a week (see photos). This method of soil sampling has become accurate and sometimes eliminates laboratory technician errors. The depth of penetration can be increased by installing helical anchors and tying down the rig to provide much more drive pressure than just the rig weight. Since the rig is mounted on tracks, there is the added advantage of all terrain drive, which allows not only slope access but also access to the very soft ground conditions. There is also a capacity for working off barges and off drilling ships in depths over 40 m.

Although cone penetration tests are best suited for softer materials, testing of fills or hard soils are possible by predrilling a hole for the cone. In situations such as course fills, it may also be necessary to add casing to keep the hole open and prevent damage to the equipment (Lunne et al. 2002). The operator must also choose a cone penetrometer that will provide the most accurate data but will fit the environment. Typically, the more sensitive the tool the more susceptible to penetration damage in very hard stratum.

Technological advances, however, have provided higher capacity cones that will perform near the top of sensitivity input (Zuidberg 1988).

The greatest drawback in cohesive soils, however, is that in stiff clays friction forces will many times limit the depth of penetration. This project was a prime example as evident by only being able to penetrate to 41 ft at the north end and 54.7 ft at the south end of the project. The volume of measurements provided by this test, however, were invaluable to understanding pressed pile termination depth differences. Also, because the cone implementation is so similar to the installation of pressed piles, application of the soil values should be extremely accurate (Abu-Farsakh and Titi 2004).

With the drilled shafts, it is assumed there is no increase in pore pressure at time of construction and studies have proved this assumption to be correct. With the driven piles, however, these same studies show axial capacity increases over time, for at least a year because of the decrease in excess pore pressure. Therefore, CPTU measurements are considered to be long-term factors that are relevant over time and not just at the instant measured. With the testing of this research project extending over 6 months, much of this correction should be mitigated (Poulos 1989).

Precision of soil measurements has been accelerated with the advent of the computers, but a better understanding of the interface of all soil parameters is even more important. This involves correction factors that provide a more accurate measurement of critical geotechnical engineering parameters necessary for better predictions of performance under different usage demands. The following are examples of some correction factors used to add accuracy to precise equipment.

3.3.4.1 Corrections of CPTU Readings: Background

Cone resistance must be corrected for pore water pressure to obtain an accurate measurement:

$$q_t = q_c + u_2 (1\text{-}a) \quad (3.2)$$

where: q_t = corrected cone resistance

q_c = measured cone resistance

u_2 = pore pressure acting being the cone

a = cone area ratio (most range from 0.55 to 0.90)

Sleeve friction must also be corrected for pore pressure but this includes not only pressure behind the cone but also behind the sleeve.

$$f_t = f_s - [(u_2)(A_{sb}) - (u_3)(A_{st})]/ A_s \quad (3.3)$$

where

f_t = corrected sleeve friction

f_s = measured sleeve friction

u_2 = pore pressure behind cone

u_3 = pore pressure behind sleeve

A_{sb} =cross sectional area at bottom of sleeve

A_{st} =cross sectional area at top of sleeve

A_s = friction sleeve surface area

Measurement of pore pressure is obviously very important and must be as accurate as possible. The filter element is used to predict pore pressure but the location for this element varies somewhat (Lunne et al. 1997). Consensus of opinion, is that the most accurate and precise location is just behind the cone.

Axial loading was found to influence pore pressure readings but engineers found that they could modify the filter paper and calibrate the cone to mitigate these malfunctions. As a result, most cones are designed to avoid these problems (Bruzzi and Battaglio 1987).

Temperature at both the ground surface and within the cone can greatly affect measurements. Therefore, it is important to correct for changes caused by such things as axial loading and friction of the stratum. Sand, for instance, will many times increase the cone temperature as much as 86^{o} (30^{o}C). Therefore, if there is a sand layer above a clay layer it is advised to stop after the sand layer to let the cone cool to an insitu/normal temperature. While temperature would appear harmless, a 41^{o} (5^{o}C) change in temperature may result in a 1.45 psi (10 kPa) change in q (Post and Nebbling 1995).

Inclination of the probe can alter true depth. Therefore, many of the probes will include a slope indicator (servo accelerometer) in the tip to correct for true depth.

Insitu stresses in a soil mass may be affected by site specific parameters that are obvious to the knowledgeable engineer. If, for instance, a large excavation has begun, there may be a reduction in horizontal pressure, which may alter results. Conversely, a large amount of fill may have been deposited near enough to the probe to increase horizontal pressure. There are no recognized methods to correct for these altering factors so the engineer will many times have to use experience to take into account any effect on total bore hole measurements.

The cone penetration provide characterization of thin layers, which in turn can be used to identify differing soils since the probe will sense a change in stratigraphy before reaching the boundary for this change. It may also be slow to recognize when it is leaving

a stratum so there will be delayed reaction. If the layer of soil is soft, accuracy will be far greater than if the material is stiff clay because of the delay in registering resistance changes. For this reason, thin sand layers in a clay section may not provide accurate cone resistance factors. Charts have been developed that add a factor to derive the corrected cone resistance factor as a function of layer thickness (Vreugdenhil et al. 1994).

After recording continuous measurements of the various parameters, it may be necessary to make corrections for a "best fit" line when at the bottom of the probe. This will lessen the chance of wide scatter that may suggest much more variance in the soil profile than actually exists (Lunne et al. 2002).

Since the test requires calculation of the involved area of the probe, it is necessary to check the diameter prior to starting a test to ensure wear has not lessened the area enough to alter the measurements. Dimensions and tolerance for cones have been established around the world where the International Test Procedure for Cone Penetration Test (IRTP) is the most recognized standard of practice (Lunne 1997).

It is important for the operator to observe plots taken from the penetration tests to ensure that these are usable in scale and format. Definition and clarity are very import to provide precision for each parameter. It is also recommended that a check of readouts be made that will require derivations of measurements. These readouts include: corrected cone resistance, corrected sleeve friction and the friction ratio of f_s/q_c. Another correction is performed when normalized excess pore water pressure (U) is determined using measured pore pressure.

$$U = (u_t - u_o)/(u_i - u_o) \quad (3.4)$$

where:

u_t = pore water pressure at time t

u_i = pore water pressure at time = 0

u_o = in situ equilibrium or hydrostatic pore water pressure

Even as advancements in modern tools and computers have been made, the operator is still crucial to obtain meaningful test data. They are capable of looking at outputs and knowing when information is relevant in a particular environment.

3.3.4.2 Interpretation/Derivation of Soil Parameters from Piezocone (CPTU)

Several important factors can be accurately interpreted from CPT tests based upon measured factors such as; pore pressure, cone resistance, temperature, moisture content, etc. Since this research is focused on underpinning elements in clays, only measurements in clay are discussed here.

For a prediction of soil density it is necessary to first derive the pore pressure parameter ratio, B_q.

$$B_q = (u_2 - u_o)/(q_t - \sigma_{vo}) \quad (3.5)$$

where:

u_2 = pore pressure between cone and friction sleeve

u_o = equilibrium pore pressure

σ_{vo} = total overburden stress

q_t = cone resistance corrected for unequal end area effects

A second factor is net cone resistance q_n:

$$q_n = q_t - \sigma_{vo} \text{ (Ton/sf) or (MPa)} \quad (3.6)$$

A chart has been developed (Larsson and Mulabdic 1991) that roughly plots densities (#/cf) or (kN/m^3) against the pore pressure ratio and net cone resistance in combination with the type of clay material.

An approximation of the overconsolidation ratio (OCR) can be derived using CPTU by several means. These include use of the measured undrained shear strength (s_u), shape of the CPTU profiled and directly using CPTU data.

Computation of OCR can be found using shear strength (s_u) that can be measured or estimated in conjunction with estimates or laboratory tests of plasticity index (I_p), effective vertical stress (σ'_{vo}) and coefficient of earth pressure at rest (K_o) and the computed ratio of s_u / σ'_{vo} (Schmertmann 1974, 1975). As stated above, the determination of OCR by these means is an approximation and should be confirmed with laboratory testing when possible. Because these estimates are very sensitive to other estimates such as the coefficient of permeability and hydraulic conductivity, overburden pressure, pore pressure, etc., the practitioner should confirm when relying on this factor.

There is no precise way to determine the in situ horizontal stress (σ_h) or the coefficient of lateral earth pressure at rest (K_o) from CPT in fine grained soils. There are methods of estimating this factor, however. These methods may include using OCR: $K = 0.1(q_t - \sigma_{vo})/ \sigma'_{vo}$ (Kulhawy and Mayne 1990), using pore pressure difference: Normalized Effective Overburden Pressure (PPAV) = $(u_1 - u_2)/ \sigma'_{vo}$ to then approximating K_o off a chart (Sully and Campanella 1991) and measure lateral pressure on the friction sleeve but with less than reliable results (Lunne et al. 1997).

Undrained shear strength is extremely important to predictions of axial capacities of piers and piles as evidenced by the empirical formulas for these predictions. With CPT

there are several ways to predict this in situ factor with the probe penetration. Each must, however, take into consideration the strain rate and a fact that no clay soil is isotropic but is in an anisotropic state where strength is directional (Holtz and Kovacs 1981).

With each of the many methods of prediction of this factor, there is a common relationship between tip resistance and shear strength.

$$q_c = (N_c)(s_u) + \sigma_o \qquad (3.7)$$

where:

q_c = tip resistance (psi)

N_c = theoretical cone factor

σ_o = the in situ total pressure (psi)

s_u = undrained shear strength (psi)

CPT provides two recognized methods of measuring strength characteristics such as undrained shear strength and effective friction angle. The two methods of interpretation of cone penetration testing are theoretical methods and empirical correlations.

With theoretical solutions, the cone penetration is a complex matrix of forces that must be correlated with equally difficult estimates of soil behavior, failure factors and boundary relationships to the probe. Because these factors must be correlated with laboratory testing to prove their accuracy, they are not a preferred method of prediction.

Empirical correlations for undrained shear strength (s_u) using CPT and CPTU rely upon an estimation of: total cone resistance, effective cone resistance or excess pore pressure.

With total cone resistance (q_c) the following formula is used for CPT:

$$s_u = (q_c - \sigma_{vo})/N_k \quad (3.8)$$

where:

s_u = undrained shear strength (psi)

q_c = measured cone resistance (psi)

σ_{vo} = in situ total pressure (psi)

N_k = empirical cone factor

With CPTU this formula has been improved to include corrections for pore pressure to measure cone resistance (q_t). N_k was also improved to included OCR and plasticity index (I_p) to a new factor N_{kt}. Values of N_{kt} are shown to vary with OCR and the plasticity index (Aas et al. 1986). This formula is (Lunne 1997):

$$N_{kt} = (q_t - \sigma_{vo})/s_u \quad \text{or } s_u = (q_t - \sigma_{vo})/N_{kt} \quad (3.9)$$

where:

N_{kt} = cone factor, which for this test was set at 15

q_t = corrected cone resistance = $q_c + (1\text{-}a)u_2$

a = area of cone = A_n/A_c

u_2 = pore pressure behind cone

σ_{vo} = in situ total vertical stress

The shear strength values calculated using this formula must be used cautiously because they may not be accurate in over consolidated clay soils. Improvements in the cone factor are being developed so the future may provide a greater accuracy factor.

With effective cone resistance, Campanella (1982) suggests the formula becomes:

$$s_u = q_e/N_{ke} = (q_t - u_2)/N_{ke} \quad (3.10)$$

where:

s_u = undrained shear strength (psi)

q_e = effective cone resistance (psi)

N_{ke} = cone factor

q_t = corrected cone resistance (psi)

u_2 = pore pressure behind cone (psi)

Problems with this system are similar to those of total cone resistance in that the factors are very sensitive to miscalculations of pore pressure that is not always accurately estimated by CPTU.

It appears the most accurate way to calculate shear strength is by using excess pore pressure (Δu), (Lunne 1997). Where:

$$s_u = \Delta u / N_{\Delta u} \qquad (\Delta u = u_2 - u_o) \qquad (3.11)$$

where:

s_u = undrained shear strength (psi)

Δu = excess pore water pressure (psi)

$N_{\Delta u}$ = cone factor determined by user

u_2 = pore pressure behind cone (psi)

u_o = in situ pore pressure (psi)

While piezocones (CPTU) should be used for greater accuracy, site specific factors are still important. This means that different factors should be utilized for different stratum on the site. It is recommended that total cone resistance be used when little is known about a new site with N_{kt} selected at the upper limit for a greater factor of safety. In very soft clays with no history for determination of q_t, s_u should be estimated

from the excess pore water pressure (Δu) using $N_{\Delta u}$ with a value selected from the upper limit. As with other interpretations, laboratory testing of soil borings will add to the test accuracy.

Clay sensitivity (S_t) is the ratio of undisturbed undrained shear strength to remolded undrained shear strength. CPT sleeve friction (f) is an approximation of remoulded undrained shear strength. In sensitive clays, however, it is difficult to measure sleeve friction, which makes the correlation not as accurate. A formula for estimating sensitivity as proposed by Schmertmann (1978) is:

$$S_t = N_s/R_f \qquad (3.12)$$

where:

S_t = sensitivity

N_s = is a constant

R_f = friction ratio of sleeve = $(f_t/q_t)(100\%)$ or $(f_s/q_t)(100\%)$

Use of the effective stress method is very important in the calculation of axial capacities of driven piles. CPT interpretations of the factors important to measuring effective stress have been proposed as follows (Lunne 1997):

$$q_t - \sigma_{vo} = N_m(\sigma'_{vo} + a) \qquad (3.13)$$

where:

$B_q = \Delta u / (q_t - \sigma_{vo})$

$N_m = (N_q-1)/(1+ N_u B_q)$

β = angle of plastification as charted to determine tan φ'

a = attraction

N_q = bearing capacity factor

$= \tan^2 (45 + \varphi'½) \times e^{(\pi - 2\beta)\tan \varphi'}$

U = excess pore pressure measured immediately behind cone

N = bearing capacity factor

$= 6 \tan \varphi' (1-\tan\varphi')$

Because of the difficulties in exactly determining the distribution of stresses and pore pressures around a cone, any such estimation of c' and φ can only be made with a correlation to site specific laboratory soil borings and laboratory testing to help reduce the many assumptions required from CPT.

Several attempts have been made to accurately measure the constrained modulus (M) using CPT data but none to date have accurately depicted this factor (Lunne 1997)(REF). Undrained Young's modulus (E_u) can be estimated using the undrained shear strength and a constant (n) that is dependent upon OCR, clay sensitivity and the choice of shear stress level and when possible the plasticity index (I_p).

The shear modulus (G) has been estimated from soil density and shear wave velocity (Mayne and Rix 1993).

$$G = \rho V_s^2 \qquad (3.14)$$

where:

G = small strain shear modulus

ρ = mass density of the soil = γ/g

V_s = shear wave velocity

Charts have been developed to estimate these factors. For heavily over-consolidated clays, the value can vary by up to 300% (Butcher and Powell 1995). Therefore, caution is advised.

Important to many foundation problems is the determination of the coefficient of consolidation (c) and the hydraulic conductivity or permeability (k). These factors are measured from the dissipation or decay of pore pressure in time after the stop in penetration. This is expressed by:

$$c_v = k\ (M/\gamma_w) \qquad (3.15)$$

Because of problems estimating the initial pore pressure distribution, soil disturbance due to penetration, and difficulty estimating the horizontal to vertical pressure dissipation as a result of soil anisotropy, the accuracy of determining the coefficient of consolidation is rough at best.

Equally difficult to interpret is the coefficient of permeability (k). While soil permeability can be estimated from the soil types listed in CPT classification charts, reliance on these interpretations are not always accurate.

3.3.4.3 Applications to Axial Capacity

The most frequently used in situ test as referenced by foundation engineers is the Standard Penetration Test (SPT). Correlations between SPT have been made for: unconfined compressive strengths (q_u), overburden pressure, relative density, and internal angle of friction (Das 1990). Because of the popularity of CPT, research has been done to correlate CPT and SPT parameters.

Studies to correlate SPT (N_{60}) to CPT's q_c have established the ratio as (Robertson 1986):

$$(q_c/p_a)/N_{60} \quad (3.16)$$

where:

q_c = measured cone resistance (for clays use q_t) (psi)

p_a = atmospheric pressure (14.65 psi)

N_{60} = SPT energy ratio

From this correlation, the soil behavior index type, I_c, is established as:

$$I_c = ((3.47\text{-}\log Q_t)^2 + (\log F_r + 1.22)^2)^{0.5} \quad (3.17)$$

where:

Q_t = the normalized cone penetration resistance and is dimensionless

F_r = the normalized friction ratio and is in percent.

The values of I_c provide a factor to compare with different soil types that are divided into Zones from 1 to 12.

With these factors, the following equation provides the CPT-SPT ratios (Lunne 1997 modified from Jefferies and Davis 1993):

$$(q_c/p_a)/N_{60} = 8{,}5\ (1 - I_c/4.6) \quad (3.18)$$

Jefferies and Davis (1993) indicate that the methods above likely produce a closer estimate of SPT N values because they are more reliable/repeatable.

Axial capacity of piles is a combination of skin friction (Q_s) plus end bearing (Q_b) values:

$$Q_{ult} = Q_s + Q_b \quad (3.19)$$

or:

$$Q_{ult} = f_p \times A_s + q_p \times A_p \quad (3.20)$$

where:

f_p = unit side friction

A_s = outer pile shaft area

q_p = unit end bearing

A_p = pile end area

Of the accepted methods, the effective stress β method has been the most accurate for predicting axial capacity in clay soils (Burland 1973). From this analysis, numerous CPT tests have been carried out that closely track with the effective stress method and appear to show that there is no better method of calculating axial capacity of piling than that provided by CPT. This is due in part because of the continuous profiling of the soil that provides much more information to calculate the capacity factors. Although there have been multitudes of studies and several sets of empirical formulas, two stand out as the best; Bustamante and Gianeselli (1982) and de Ruiter and Beringen (1979).

With the Bustamante and Gianeselli method both side friction and end bearing are calculated from the CPT factor of mean q_{ca} that is the pile unit end bearing q_p. The end bearing is then calculated as:

$$q_p = k_c \times q_{ca} \quad (3.21)$$

where:

q_{ca} = equivalent average cone resistance

k_c = end bearing coefficient

For pile skin friction, the value of q_c is divided by the friction coefficient α_{LCPC}:

$f = q_c / \alpha_{LCPC}$

Since only q_c is used to calculate both side friction and end bearing, this method may have an advantage because interpreting f_s in CPT data is sometimes difficult (Lunne 1997).

With the de Ruiter and Beringen method, unit end bearing q_p is calculated by measuring the average q_c over a distance of (0.7D to 4D) and 8D. The skin friction f_p is the product of α x s_u, which is a measure of q_c. Where α is a constant that varies between 0.5 for O.C. clay to 1.0 for N.C. clay. Bustamante and Gianeselli are the most conservative methods but both methods should be measured against local experience.

3.3.4.4 The CPT Logs for the Two Probes at this Site

Figures 3.20 and 3.21 present CPT measurements along with soil classification information. Corrected strength factors were used to determine shear strength parameters for each soil layer and these results are included in Table 3.6 and Table 3.7.

Table 3.6 - Summary of Results from CPT #1

Depth (ft)	q_t (psi)	f_s (psi)	R_f (%)	u (psi)	N (60)*	N1 (60)*	φ (deg)	Su (psi)	OCR
0'-5'	416	6	5	3	9	18	0	29	10
5'-10'	486	23	4	8	18	34	0	30	10
10'-14'	347	8	3	10	12	14	0	42	9.8
15	308	8	3	35	9	10	0	17	5
16'-28'	347	8	3	10	12	14	0	29	9.8
28'-39'	356	8	3	35	9	10	0	38	5
39'-43'	297	6	3	34	8	9	0	22	5

***Note: N values are estimated from CPT readings; q_t and f_s are tip and friction resistances, respectively; R_f - Friction ratio**

Table 3.7 - Summary of Results from CPT #2

Depth (ft)	qt (psi)	fs (psi)	Rf (%)	U (psi)	N (60)*	N1 (60)*	φ (deg)	Su (psi)	OCR
0'-5'	347	6	1	3	6	13	0	29	10
5'-10'	500	20	1.5	20	12	15	0	28	10
10'-14'	347	7	2.5	22	12	21	0	43	10
15'	305	5	2	35	8	12	0	18	6
16'-28'	347	7	2.5	22	12	21	0	30	10
28'-39'	305	5	2	35	8	12	0	37	6
39'-49'	305	5	2	90	8	8	0	20	4
49'-54'	694	3	0.5	20	12	10	0	16	3.5

***Note: N values are estimated from CPT**

Table 3.8 presents undrained shear strength S_u parameters interpreted from in situ cone penetration tests for the summer periods and borehole laboratory test data for upper 10 ft in the spring condition. The SPT data of last depth section was used for determining the undrained shear properties of the shale layer.

Table 3.8 – Undrained Soil Strength Parameters from CPT

	Spring 2005	Summer 2005
Depth of Section	**S_u (psi)**	**S_u (psi)**
0'-5'	10**	29
5'-10'	18**	28
10'-13'	42	42
15'	17	17
16'-28'	29	29
28'-39'	37	37
39'-49'	20	20
49'-55'	16	16
55'-60'	12	12
60'-75'	192*	192*

*Estimated from N value (Bowles, 1977)
**Provided by UU Triaxial Tests

Figure 3.22- CPT Rig Performing Test on Site

3.4 Installation of Reaction Piers and Tie-down Bars

To allow over thirty (30) days between installation of reaction piers and tie-down of the bars, reaction piers were drilled and poured in June of 2004. Reinforcing steel consisted of 5- #11's with #3 – 6 in. pitch stirrups from bottom to top. To ensure the steel stayed in proper position, plastic shoes were placed at the bottom of the vertical #11's and side rolling spacers were set on the stirrups for lateral alignment. Because of the extreme weight of the final cage, cage racks were required to suspend the vertical steel and the stirrups were rolled around the support chains so that each could be tied with tie wire with not only attachment between stirrups and vertical steel but also diagonal ties to keep the steel properly set (Figure 3.23).

Figure 3.23- Reinforcement Cages Being Tied for Reaction Piers

Figure 3.24- Installation of Reaction Piers

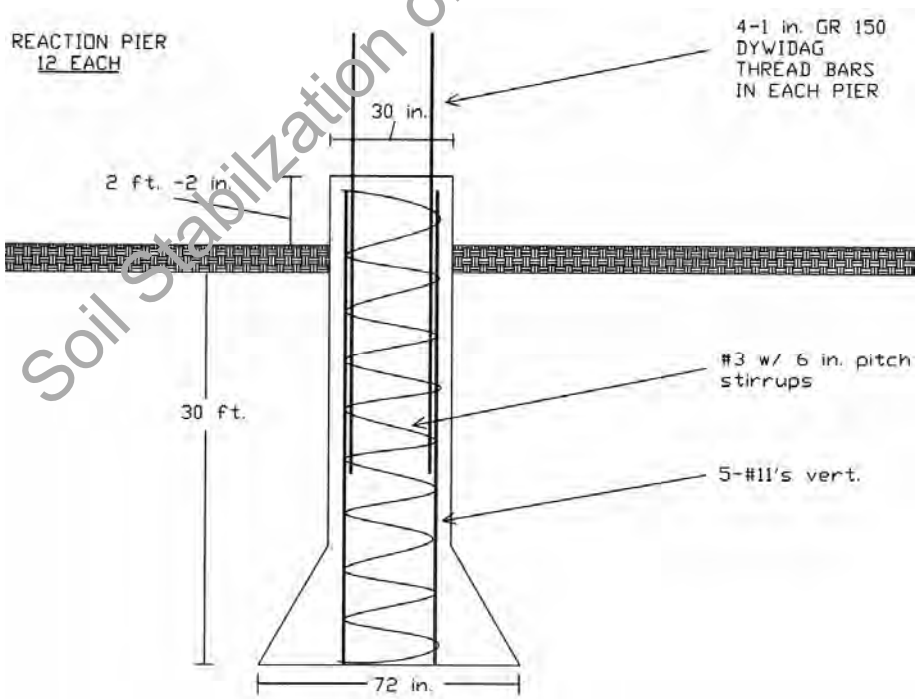

Figure 3.25 – Reaction Piers and Reinforcing Steel

To provide tie-down for the load test beams, four 1-in. Dywidag bars were set at 90^{o} positions around the reaction piers with a 10 ft embedment into the concrete just inside the steel pier cage. Because the north to south beams were run across the tie-down bars, two of the Dywidag bars were sectioned with a screw in coupling at the top of the concrete so that these two bars could be removed when testing the north to south direction.

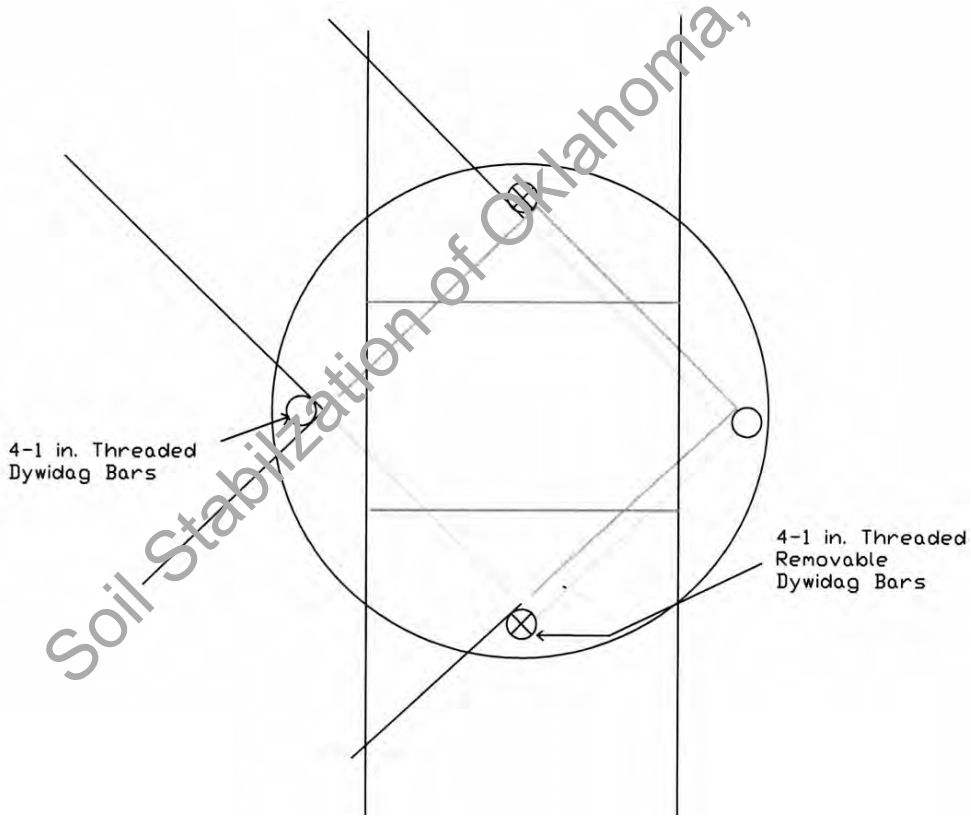

Figure 3.26 – Plan View of Reaction Piers and Tie-down Bars

Due to early planning, the site provided ample room for vehicles and machinery to operate around the test site. Arrangements for mowing the site, spreading excess soil,

and transporting it to low spots away from this site provided an excellent test site that contributed to smooth execution of the planned tests on underpinnings. The major disadvantage in clay soils is that the drive friction often prevents penetration to depths required to fully evaluate the stratagraphic lenses and the CPT probe is only able to penetrate into soft shale, which may not provide enough data to fully explore underpinning penetration depths for many foundations.

3.5 Transport and Setting of Reaction Beams

After concrete in the reaction piers had reached 28 day strength, the beams were transported to the site. Beams required for the pressed piling were set and strapped into place to provide resistance for installation of these elements. While the pressed concrete piles are designed to be driven directly under the grade beam, the preferred choice of the pressed steel contractor of this research is to bolt a bracket at the edge of the grade beam and then using resistance provided by the house to push the piles to the desired resistance. To emulate this condition, a bracket was welded to the beam and installation sleeves were used to resist bending moments caused by the push (Figure 3.38). Since the steel piles were set in one beam line in groups of three, only 3 welded brackets were required and the beam was moved as required for the next set.

Figure 3.27- Reaction Beams for Underpinning Testing

The larger beams were designated for the drilled shafts and augercast piles but were not set until time of testing. Because of the complexity of the reaction pier layout and beam configuration for efficiency of design, a considerable amount of crane standby time was necessary, but this helped reduce the overall cost of this experiment with the better utilization of the expensive reaction piers.

3.6 Installation of Test Subjects

Assurances for the privacy of the companies that installed their underpinning products required scheduling of times and days for their installation. Privacy in conjunction with equipment problems necessitated that the first half of underpinning subjects was installed over three weeks. Climatic conditions did not change, however, as the same precipitation frequency and duration was consistent over this installation period.

3.6.1 Drilled Straight Shafts

The first underpinning products installed were drilled straight and belled shafts. As depicted in the methodology section, these piers were 12 in. diameter and 15 ft deep, which represents standard specifications for most remedial underpinning and new construction of residential houses in this area. The standard drilling rig for this construction is the Texhoma 600 series. This rig is truck mounted and very maneuverable on not only the highways but also on a construction site. Two rigs were utilized for this project. The auger used for drilling the straight shafts was measured and found to be exactly 12 in diameter.

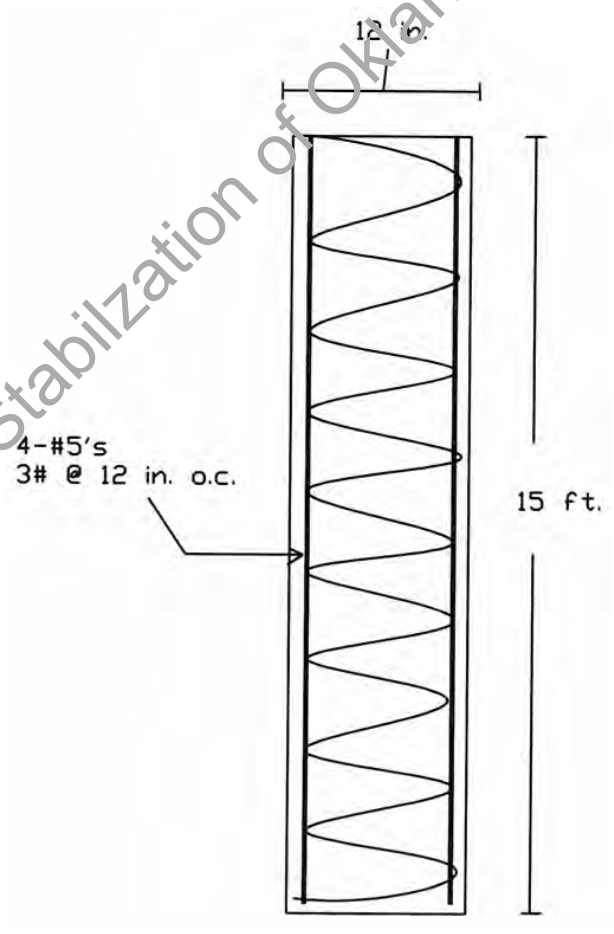

Figure 3.28 – Drilled Straight Shafts

The three pier holes required for this first half of the research were quickly drilled and checked for depth, vertical alignment and cleanliness. Drilling was monitored to make sure the drilling was continuous and uniform so rifling would not occur that might increase side friction and produce unreasonable ultimate capacities. As expected from the soil borings, no water was visible in the holes. Reinforcement consisting of 4- #5 vertical members was set with #3 – 6 in. square stirrups at a spacing of 12 in. o.c. to form a cage that was set into the holes and concrete was poured with the top screened off for a level surface. Reinforcing steel was made of grade 60 with the vertical steel providing 1% of the area of the pier as required for drilled shafts in expansive clay soils (FHWA 1999). Fiberglass side spacers were used to position the steel while the crane supported the cage until concrete placement was complete to a point approximately half way (Figure 3.30).

Figure 3.29- Drilled Shaft Installation

Concrete was specified at a 4,000 psi compressive strength, which is a common design to reduce potential material compression when the test load is applied. Concrete slump was specified at 8 in. with no aggregate larger than ¾ in. for good material flow so that all reinforcing steel would be engaged with no flaws in the pier structure. This concrete mix would be classified as a Texas Department of Transportation or TxDOT Class C with coarse aggregate grade 5.

Figure 3.30- Pouring of Concrete Piers

3.6.2 Drilled and Belled Shafts

Three belled piers were drilled to the same diameter and depth as the straight shafts but the bottom was under-reamed or belled with an attachment that widens the bottom to create more bearing capacity and also provide resistance to uplift forces that are experienced in expansive clay soils. The belling tool was measured at full extension

and showed to reach exactly 30 in. from tip to tip. When the belling tool was installed on the Kelly, the length of vertical travel of the Kelly stem was measured so that the driller would know when a complete extension had been achieved. Each bell required a minimum of 4 trips to ensure full extension and a clean hole. A regular drill bit was also run into the hole after completion of the bell to make sure no pier spoil was left on the bottom of the hole as a result of spilling out of the belling tool barrel.

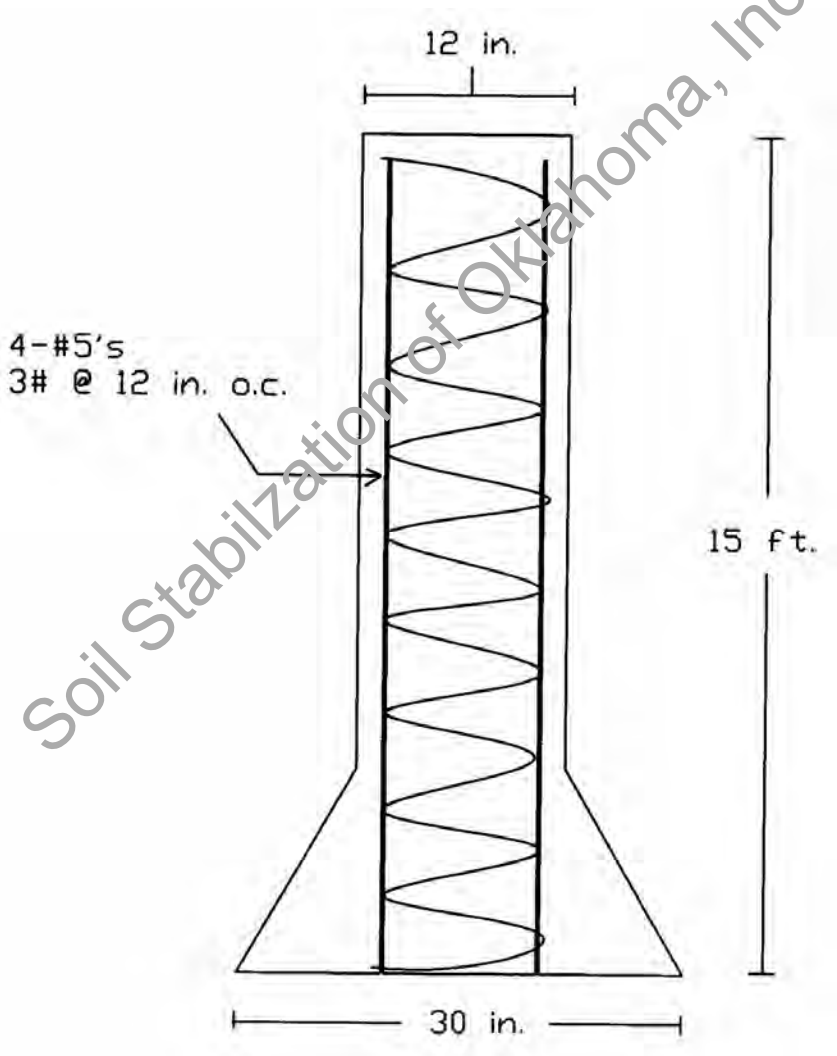

Figure 3.31 – Belled Drilled Shafts

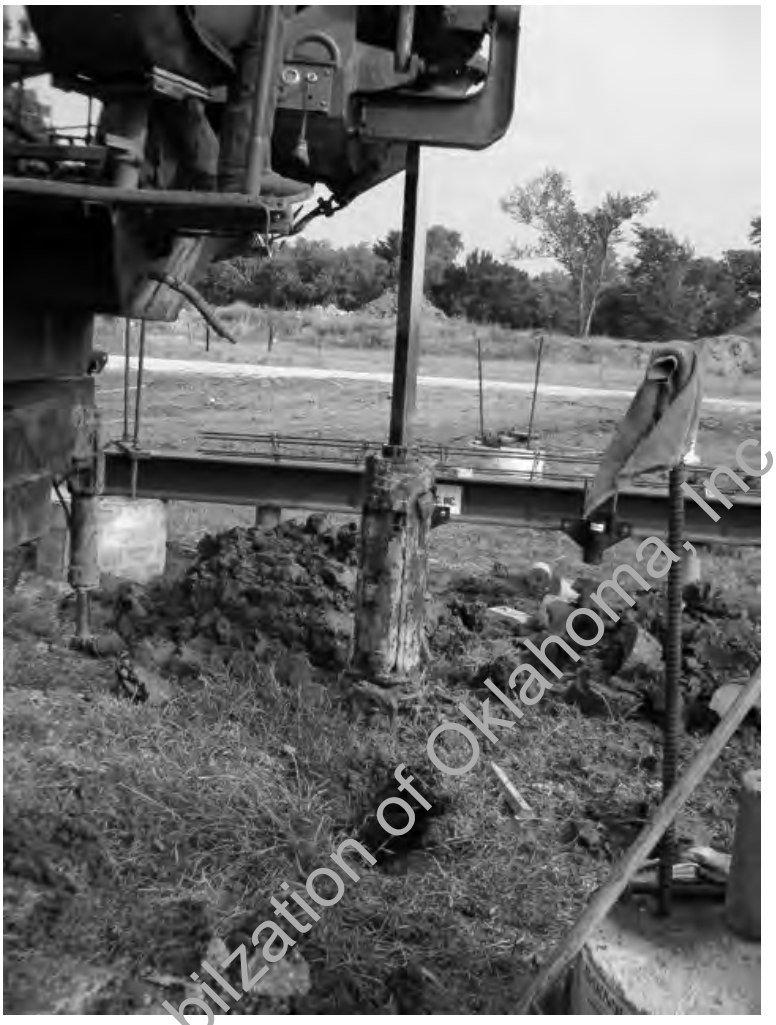

Figure 3.32- Installation of Belled Piers

The same steel, concrete and placement procedures were utilized to provide good quality control and there was no ground water visible in the hole at the time of placement. The rig used for this operation regularly drills new and remedial holes because of it's maneuverability around the site and versatility with the smaller residential holes.

3.6.3 Augercast piles

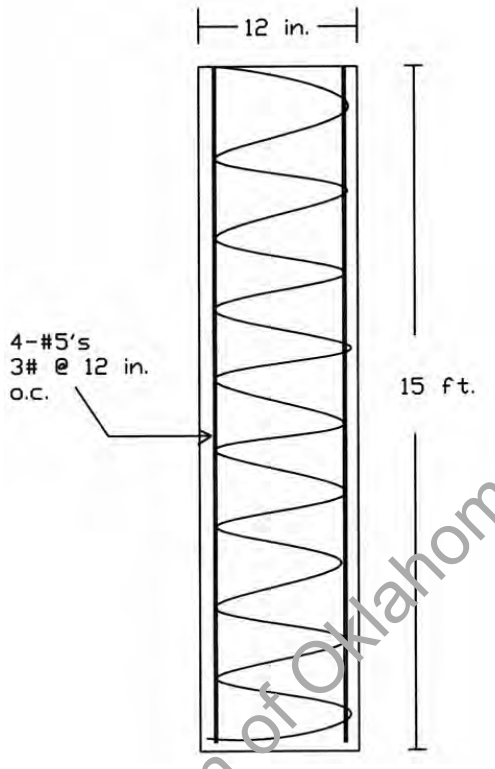

Figure 3.33 – Augercast Piles

Three augercast piles required stabbing a steel auger frame into the ground over the selected pile locations, hooking up the injection lines to the grout pump and starting the power units to power the continuous auger drive head. Prior to starting the auger, the grout pump was calibrated to make sure that the operator knew exactly how much grout by volume was pumped on each stroke. This required, using a 55 gallon barrel and counting strokes of the pump until the barrel was full to determine volume required to provide a quality hole. With this knowledge the operator knows when the grout has reached a level 4 ft above the bottom of hole so that augured soil can be pushed up ahead of the bit extraction and bore hole integrity can be maintained with no voids created in the shaft as a result of caving soil or misplaced auger excavations.

The soil conditions at this site show stiff clays, which did not cave with the drilled shafts. Therefore, the potential for caving was very low. Quality control measures were taken to ensure a competent shaft was installed. This process was repeated at each pile location and the same reinforcing steel cage as the one used in drilled shafts was lowered into the grouted area.

Figure 3.34- Installation of Augercast Piles

Since the soil at this site is a stiff expansive clay soil with no caving potential, lateral movement of the soil in the borehole was not considered to be a problem. When augercast piles are installed in sand, there is always a potential problem with mining the

soil up the auger by pulling is from outside the borehole, especially if the driller rotates the auger at a rapid penetration rate. The result is a loss in skin friction that may lower axial capacity below requirements for the pile (Brown 2005). To eliminate any chance of soil mining, the augercast contractor rotated the auger slowly (15 rpm) such that only the soil displacement volume of the auger and stem was removed from the hole and no rotating idling at the bottom was allowed prior to grout injection through the annulus.

The mix design was supplied by the augercast contractor and the local redi-mix concrete supplier provided a full design specification for review by both contractor and researcher. The mix design specifications were a minimum 10.39 sacks of Portland cement, compressive strength of 4 ksi, water/cement ratio of 0.427, maximum slump of 8 in. and no entrained air.

Table 3.9 - Augercast Mix Design

Material		S. P.	Lbs/cy	Ratio	Abs Vol/Yard
Cement	Type I	3.15	762	0.78	3.876
Flyash	Class F	2.33	215	0.22	1.478
Fine Agg	Trinity Ennis	2.64	952	0.395	5.779
Course Agg	Trinity Ennis	2.64	1460	0.605	8.863
Water		1	3	0.427	6.678
Admix #1	Grout Aid	lbs.	3	0	0.003
Admix #2		Fl Oz	0	0	0
Admix #3		lbs.	0	0	0
Entrained Air		%	0	0	0
Entrapped Air		%	1.2	0	0.324
		Totals:	3885.2		27.0 ft^3
		Unit Wt.	143.9 pcf		
		W/C #/#	0.427		50.0 gal/yd

3.6.4 Helical Anchors

Eight helical anchors were installed at locations depicted on the project map by excavating a small hole to start the bit and then applying torque pressure and adding extensions until a specified 5,000 ft-lbs torque was reached on each of the helical anchor installations. Two types of helical anchors, single helix (12 in.) or double helix (10 in. and 12 in.) are used in this research. For repeatability reasons, two of each type were installed but with the same maximum installation torque.

Anchors were installed with a driver that provided readout of torque to gauge pressures. The torque varies with gear ratio and hydraulic displacement but the method of calculation is the same for every drive head. The label on the driver unit shows: 2,500 psi = 4,278 ft-lb and 3,000 psi = 5,097 ft-lb. Therefore, 3,000 psi of pressure was chosen since we did not have to try and stop at a difficult unmarked point on the gauge pressure.

Figure 3.35- Installation of Helical Anchors

As seen from the driving depth chart, helical anchors of different depths for the same drive torque were installed at the site. Since this site is in an alluvial plain with differing soil stratum over the depth of the subsurface, differences in penetration depth are acceptable. However, these depths were small and acceptable as per the practicing engineers' experience in this area. These depths are consistent with those reported across the U.S. and Canada (Sharp, 2004). Zhang (1999) reports that axial compression capacity of helical anchors increases with the depth. This aspect was addressed in this research.

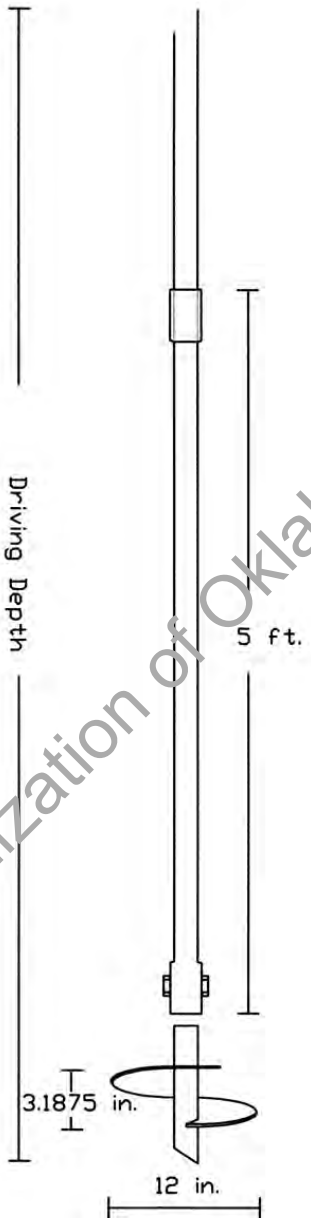

Figure 3.36 – Single Helix Anchor

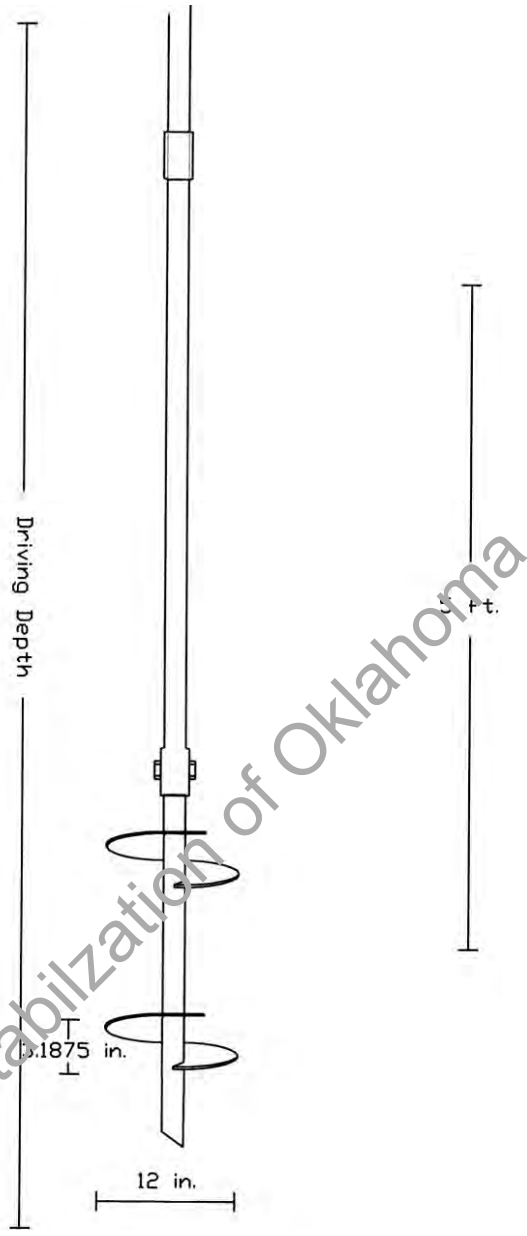

Figure 3.37 – Double Helix Anchor

The first two (2) helical anchors were installed with a single helix shaft (Figure 3.36), but the second 2 anchors were installed with double helix (10 in. helix and 12 in. helix set 3 ft apart as shown in Figure 3.37). The double helix is commonly used for vertical capacity when soil conditions are poor from a strength point of view. As

expected, the double helix did not penetrate to deeper zones due to increased shear strength created by the second helix.

Table 3.10 - Helical Installation Record

Installation Date	Pier #	Type	Drive Depth	Drive Pressure (psi)	Drive Torque (ft-lbs)
Sep.2004	27	Single	34'	3,000	5,097
Sep.2004	28	Single	45'	3,000	5,097
Sep.2004	31	Double	30'	3,000	5,097
Sep.2004	32	Double	28.5'	3,000	5,097
Apr. 2005	25	Single	34'	3,000	5,097
Apr. 2005	26	Single	26'	3,000	5,097
Apr. 2005	29	Double	27'	3,000	5,097
Apr. 2005	30	Double	32	3,000	5,097

In installing the helical anchors, one interesting phenomenon was noted. The efficiency of rotation into the ground was not consistent. This was observed by counting rotations into the ground to determine whether each turn coincided with vertical descent. To determine this factor, the vertical distance of the helix for a complete turn was measured to be 3-3/16 in. long (Figures 3.36 and 3.37). Therefore, if the rotation was completely efficient, then it would take 18.82 rotations to travel the 5 ft length of solid extension (60 in./3.1875).

As noted in the following table, this efficiency varied with depth. It should be noted that the top 11.67 ft (5 ft extension + 6.67 ft of stem with helix and one extension cord) was not counted in this calculation since there is some inefficiency when an anchor was moved into the ground.

Table 3.11 - Installation Inefficiency of Single Helix

		Rotation of Helix						
Pier #	Depths	0-11.67'	11.67'-16.67'	16.67'-21.67'	21.67'-26.67'	26.67'-31.67'	31.67'-36.67'	36.67'-41.67'
27	Single	No Count	41	19.5	19.5	21.5	-	-
28	Single	No Count	39	36.5	23	23	24.5	22
25	Single	No Count	26	24	23	22	-	-
26	Single	No Count	22	21	21	-	-	-

As noted above, the helix were driven lower than 31.67 ft and 36.67 ft but for purposes of measuring accuracy, only complete 5 ft lengths were recorded. The rotation observations in Table 3.11 are only for the single helix. The following table shows the double helix measurements for the four piles, but the inefficiency measure was very consistent.

Table 3.12 - Installation Inefficiency of Double Helix

		Rotation of Helix						
Pier #	Depth	0'-11.67'	11.67'-16.67'	16.67'-21.67'	21.67'-26.67'	26.67'-31.67'	31.67'-36.67'	36.67'-41.67'
31	Double	No Count	53	32	29	-	-	-
32	Double	No Count	47	29	31	-	-	-
29	Double	No Count	51	27	28	-	-	-
30	Double	No Count	57	36	29	-	-	-

It is obvious that the installation inefficiency in this soil for the double helix is worse than that of the single helix. Therefore, the disturbance factor for the double flight helix is much greater than the same of the single helix, when only a single auger screws into the ground. This would confirm that in stiff clay soils, inefficiency of the installation

creates an auguring effect that leaves some amount of void/disturbance behind the leading edge of the helix and greater disturbance of the soil under the second helix.

Since it is difficult to visualize the exact happenings behind the auger rotations of the helix, it is obvious that some of this action is similar to that of an auger bit drilling a pier hole as there is slippage below the helix, which creates a void/disturbance behind the auger as it rotates. Bobbitt et al. (1997) noted that the efficiency of rotation during installation is important to cause the least amount of disturbance to the soil. Adams and Radhakrishna (1971) and later Zhang (1999), showed the disturbance of clay reduced undrained shear strength considerably. It is also evident as the helix penetrates deeper into what appears to be denser soil, it increased efficiency. Therefore, it is important that the soil behind the helix provides enough resistance to overcome friction resistance to penetrate into the soil.

If the capacity of helical anchors does not meet existing empirical predictions, the possible creation of a trailing void and slipping of the auger will cause the primary load bearing element of the helix to be the point and leading edge of the flight. It is this engineer's experience in using helical piles for remedial repairs that each helix must be individually "seated" (pressure applied from house resistance to push the piling down until the house lifts) using the weight of the house to gain enough strength to provide support and lift the structure.

3.6.5 Pressed Steel Piles

With the reaction beams in place, the steel pressed piles could be hydraulically driven into position. This installation required welding of the steel bracket that normally is bolted to the concrete foundation beam. Installation drive pressure had been established

at 50 kips. The contractor first set the lead pipe with shear ring at the bottom, started pushing piles, and added 5 ft sections as the pipe progressed downward. As depicted on the project installation map, there was some variance in termination depth. The final axial load of 50 kips was targeted for all foundations. At the time of installation, the initial capacity was established at 50,640 lbs. The drive pressure was established at 3,000 psi on the gauge, which was easier to read but this calculated out at 50,640 lbs in lieu of 50,000 lbs.

Figure 3.38- Installation of Pressed Steel Piles

Monitoring of gauge pressure during installation revealed there were variations in soil resistance during the penetration. Most of these resistive layers/objects were weak

enough and the pile diameter was small enough that the installation was not prematurely stopped but it was evident that shear strength and cohesion was not linear and could inhibit the depth of larger piles such as the pressed concrete piles.

In order to test if the removal of structure load had any effect on later capacity (6 months after installation), three (3) of the initial six (6) pilings were left with no load from the test beam and three (3) were kept with a resistance to movement and were secured in place. This split test will determine if there is an impact with thixotropy or if these pilings will have set-up capacity to increase axial capacity even greater than installation pressure.

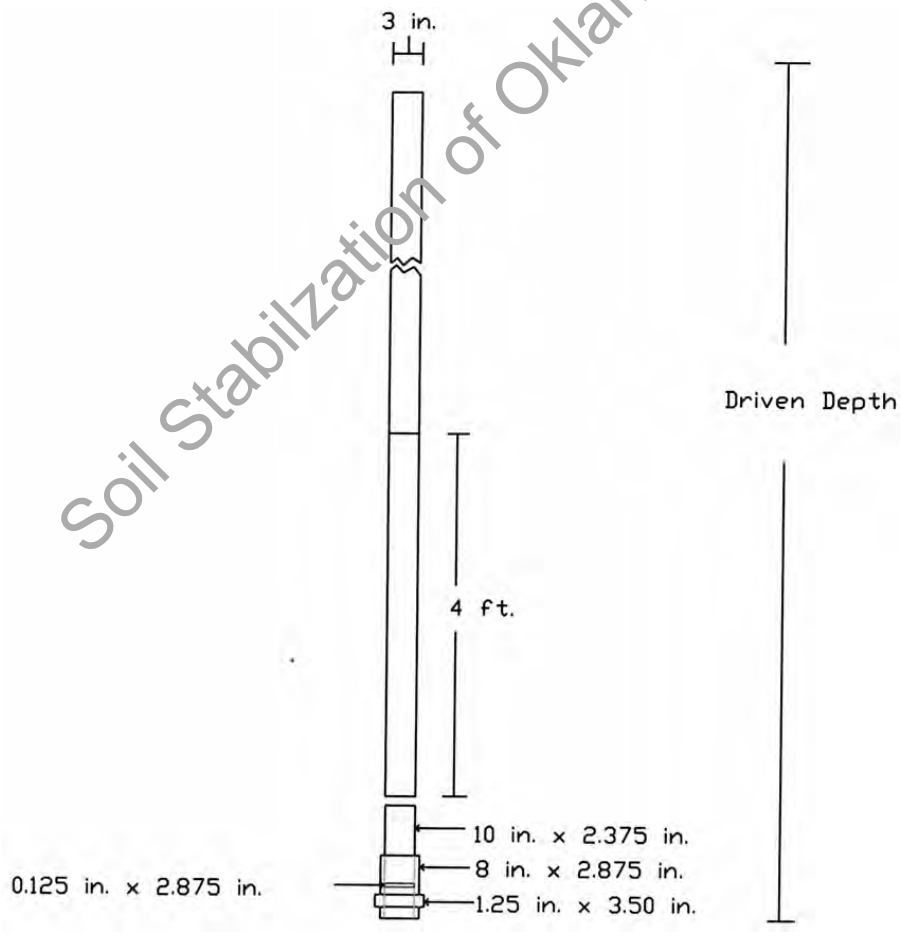

Figure 3.39 – Pressed Steel Pile

Table 3.13 - Pressed Steel Driving Records

Installation Date	Pile #	Gauge Pressure (psi)	Drive Force (lbs)	Final Depth
Sep. 2004	13	3,000	50,640	44'
Sep. 2004	14	3,000	50,640	70'
Sep. 2004	15	3,000	50,640	75'
Sep. 2004	22r	3,000	50,640	35'
Sep. 2004	23r	3,000	50,640	25'
Sep. 2004	24r	3,000	50,640	26
Apr. 2005	16	3,000	50,640	57'
Apr. 2005	17	3,000	50,640	64'
Apr. 2005	18	3,000	50,640	51'
Apr. 2005	19r	3,000	50,640	58'
Apr. 2005	20r	3,000	50,640	66'
Apr. 2005	21r	3,000	50,640	57'

3.6.6 Pressed Concrete Piles

To promote a typical comparison, the concrete pressed piles were hydraulically driven into position on the same beam line as the steel pressed piles and in close proximity. As evidenced with the steel pressed piles, there were zones of stiffer resistance at each of the driven concrete piles. Because the diameter is larger, however, some of these zones of resistance were stiff enough to max out the drive ram and stop advancement at some shallow depths. As an example, the depth for PC-1 and PC-2 varied 15 ft even though the distance between the pilings was only 4 ft and subsurface borings and CPT indicated homogeneous clay soil. As noted on the installation chart below, the drive pressure was held constant at 50 kips. Therefore, the variances in depth could only be explained by soil strength characteristics or other resistive obstructions. Here again, the initial axial load capacity was 50,000 pounds.

The procedure for pushing the concrete piles was to set a 6 in. × 12 in. precast pile section and push downward with a hydraulic jack until it was fully installed and then add

another cylinder and repeat the process. In lieu of a shear ring at the bottom, there was a 4 in. diameter round and 8 in. long precast section bottom section to help break up thin zones and help penetrate better.

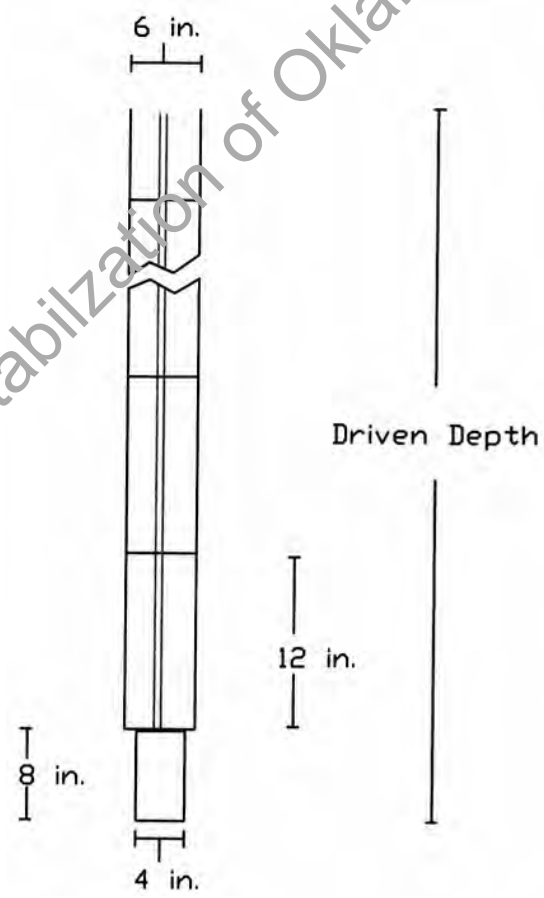

Figure 3.40 – Pressed Concrete Pile

Figure 3.41- Installation of Pressed Concrete Piles

It is also important to note that the driving sequence was: pile #1 followed by piles 2, 3, 6, 5, and 4. Therefore, there was no densification of soil with the initial pile driving. According to ASTM 1143, piles must be kept three (3) diameters apart to prevent group influence. These piles were actually eight (8) diameters apart. Therefore, there was no influence from adjoining piles.

Table 3.14 - Pressed Concrete Driving Records

Installation Date	Pile #	Gauge Pressure (tons)	Drive Force (lbs)	Final Depth
Sept.2004	1	25 tons	50,000	7.67'
Sept.2004	2	25 tons	50,000	10.17'
Sept.2004	3	25 tons	50,000	27.42'
Sept.2004	7r	25 tons	50,000	15.67'
Sept.2004	8r	25 tons	50,000	10.67'
Sept.2004	9r	25 tons	50,000	25.67'
Apr. 2005	4	25 tons	50,000	24.67'
Apr. 2005	5	22 tons	44,000	Broke/Abandoned
Apr. 2005	6	25.5 tons	51,000	19.67'
Apr. 2005	10r	25.5 tons	51,000	24.67'
Apr. 2005	11	23 tons	46,000	Broke/Abandoned
Apr. 2005	12r	25 tons	50,000	28.67'

Figure 3.42- Installation of all foundation elements complete in September 2004

3.7 Load Testing Set-Up

Because of the differences in underpinning types, a standard load test, ASTM D 1143-81 (Reapproved 1994) was chosen as the method for this field testing. This method is referred to as the "**Standard Test Method for Piles Under Static Axial Compressive Load".** As described in the introduction, "This standard has been prepared to cover routine methods of testing to determine if a pile has adequate bearing capacity".

Reaction piers/anchor piles are installed at both sides of the underpinnings. Steel rods extended from out of the reaction pier to tie-down a reaction beam such that a testing ram was installed between test subject and reaction beam to provide resistance to determine axial capacity. The test ram has been calibrated for this test. Since the test ram may indicate loads 10% to 20% greater than actual load transfer to the pier/pile, care must be taken to make sure there is even and equally distributed pressure imposed on the pile head (Figure 3.43).

To compensate for deflection of the steel reaction beams, steel angles/beams are placed on each side of the test member with a deflection gage to show actual deflection from its original position (ASTM D 1143, 4.1.1- 4.2.1). A 1 in. thick steel plate is set at the top of drilled piers and auger cast piles to distribute stresses. Potential for moments created around the helical anchor shaft and steel piles requires that a pipe be welded to the test plate to resist bending moments that might compromise the actual test results for true vertical pressure (ASTM D 1143, 3.1.1- 3.3.4). For the steel pipe and helical anchor there is a 3 in. inner diameter pipe welded to a 1 in. thick and 6 in. long round diameter steel plate, while the concrete piles are large enough to only require the 1 in. thick by 12 in. diameter round plate to transfer load from the test ram to the piling subject.

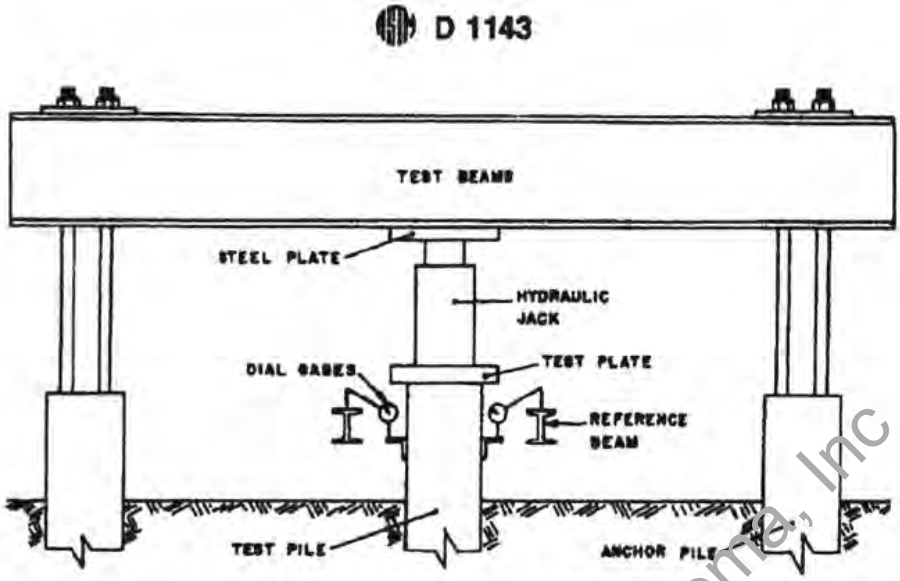

Figure 3.43 - Test Reaction Beams and Test Ram (ASTM D-1143)

Procedures for determination of axial capacity required a load was applied from the test ram and this load was increased in increments of 10 to 15% of the initial drive pressure and deflection was recorded until a maximum downward deflection had been measured that showed the pile failed by an inability to hold pressure. Deflection was plotted against test pressure to show actual failure of the shaft or pile (ASTM D1143-81) Pile load test interpretation in this manner is identified as the plunge method (US Army 1991). Each determined load was held for two (2) minutes and the deflection gauges were monitored during this time to ensure that deflection did not change. This method is termed as the Quick Test as delineated in ASTM D1143, which produces an accurate testing of axial capacity in a reasonable time period.

Figure 3.44 – Researcher Setting Coupled Tie-down Bar with Loader in Background

Figure 3.45 – Researcher Moving Beam into Place for Test

The following field test chart (Figure 3.46) was developed by the researcher and was used for this testing to measure deflection and applied load and determine ultimate capacity of each pier, pile or helical anchor. A separate chart was used for each foundation element and then transferred to the manuscript.

AXIAL LOAD CAPACITY TESTING LOG

JOB NAME: DATE:
ADDRESS: JOB NO.:

Test: ___________

			Gage		Gage		Remarks
Pier No.	Pressure	Load Lbs.	2.5 min		2.5 min		
							Measured in 1/100's of inch

COMMENTS

Figure 3.46 – Field Measurement Log

3.8 Reaction Piers and Beams

A common practice is to install reaction beams on each side of the element to be tested. For this research, the maximum axial compression test members are 12 in. diameter drilled and belled piers, 30 in. diameter drilled concrete piers with 72 in. bells installed with 4,000 psi concrete and 1 in. diameter dywidag bars installed to an embedment depth of 10 ft to resist pull out forces (Figure 3.25). Reinforcing steel bars of size #11 were used as longitudinal reinforcement. The #3 hoops were also used at a 6 in. pitch to compensate for moments around the shaft and any vibration forces induced during testing or installation.

As noted in Figure 3.26, 4-1 in. diameter dywidag bars were imbedded into the piers to allow strapping of the reaction beams at locations directly over the test subjects. For efficiency, two of the four Dywidag bars at each reaction pier were provided with couplings at the top such that the reinforcement bars could be removed or moved to allow for beams set at 60 degree angles to the north to south main beam line (Figure 3.25). The dywidag bars were designated as GR 150 THREADBARS and are rated for a maximum capacity of 1,020 kips (500 tons) with a 2 : 1 safety factor the resulting testing capacity of 510 kips (250 tons) as determined by ASTM A 722 (Dywidag). This factor of safety exceeds empirical capacities based upon soils information in the area and this research engineer's own experience with previous axial load capacity testing at the 2000 education workshop in Ft. Collins, Colorado.

The reaction beams were donated to this research and as evidenced in the photos, these "I" beams varied in length, height and flange width. To evaluate suitability for this testing, a structural program called RISA- 2D was used to calculate anticipated deflection

with an estimated maximum weight of 80 kips. Even the smallest beam passed the deflection criteria and would be used for the pressed piles and helical anchors. Another factor was that the larger beams had previously been used in a similar load test by Dr. Michael O'Neill with good success on even larger test subjects (30 in. x 30 in. x 60 in. bell) and capacities in excess of 200 kips.

The reaction beams were secured to the reaction piers with the Dywidag bars and specially fabricated strap channel. Dywidag nuts were used in conjunction with large washers to provide the necessary resistance for the beams to provide a secure locking. Blocking was also necessary to provide resistance to lateral slippage and rotation of the reaction beams.

3.9 Test Ram and Pump

The test equipment for this research was a 100-ton capacity ram and pump for testing foundations in the April 2005 test and a 200-ton capacity ram and pump for testing foundations in the August 2005 testing. This test ram is double acting, which means the pressure can be reversed to push the cylinder downward. The overall dimensions of the 100 ton cylinder were 12 in. diameter x 1 ft - 2 in. tall with a plunger that is 8 in. diameter (Figure 3.47). The 200 ton cylinder was 12 in. diameter x 1 ft - 8 in. tall that included a plunger that is 8 in. diameter. Use of this tester was donated for this testing by Con-Tech Systems who had no subjects for testing or economical benefit from this research. The Gauges and ram for the April testing were calibrated by Rone Engineering of Dallas, Texas on April 19, 2005 as evidenced by the calibration sheet for the one gauge used for this testing, see Figure 3.48. The April 2005 test ram was calibrated by RST Instruments of Coquitlam, British Columbia, Canada, see Figure 3.49

and Figure 3.50. Note* only one gauge was used for consistency. Because the test ram is 14 in. high and 20 in., when in place, all test subjects were kept a minimum of 24 in. below the reaction beam.

Figure 3.47- Test Equipment

As evidenced by the chart, there is an almost linear plot of gauge pressure to force and the dial is graduated in 100 psi increments up to a peak force of 10,000 psi. This results in a maximum output of 207,500 lbs of force for the 100 ton jack and 422,300 lbs of force for the 200 ton jack. With estimated maximum axial capacity of the belled piers being an approximate 180,000 lbs, an excess pressure to test capacity is well within expectations.

Because the pump is mechanical, gradual increases of pressure are easily maintained, which increases the sensitivity of the pressure increases and accuracy of the

measurements. With the fabricated 1 in. thick plate on top of the piers/pilings, the ram is protected and an even application of pressure is easily made.

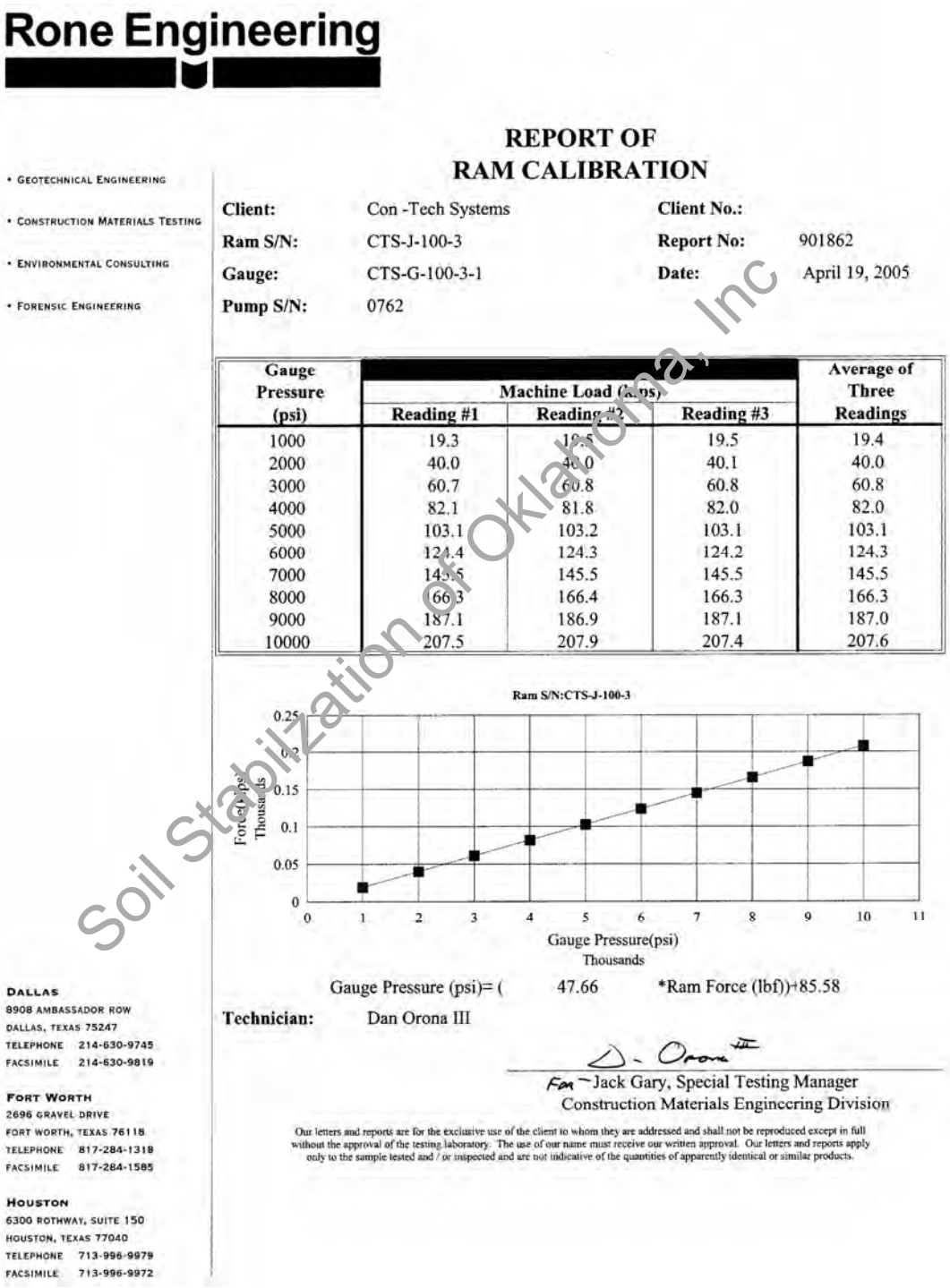

Rone Engineering

- Geotechnical Engineering
- Construction Materials Testing
- Environmental Consulting
- Forensic Engineering

REPORT OF
RAM CALIBRATION

Client: Con -Tech Systems **Client No.:**
Ram S/N: CTS-J-100-3 **Report No:** 901862
Gauge: CTS-G-100-3-1 **Date:** April 19, 2005
Pump S/N: 0762

Gauge Pressure (psi)	Machine Load (Lbs)			Average of Three Readings
	Reading #1	Reading #2	Reading #3	
1000	19.3	19.5	19.5	19.4
2000	40.0	40.0	40.1	40.0
3000	60.7	60.8	60.8	60.8
4000	82.1	81.8	82.0	82.0
5000	103.1	103.2	103.1	103.1
6000	124.4	124.3	124.2	124.3
7000	145.5	145.5	145.5	145.5
8000	166.3	166.4	166.3	166.3
9000	187.1	186.9	187.1	187.0
10000	207.5	207.9	207.4	207.6

Gauge Pressure (psi)= (47.66 *Ram Force (lbf))+85.58

Technician: Dan Orona III

For Jack Gary, Special Testing Manager
Construction Materials Engineering Division

Dallas
8908 Ambassador Row
Dallas, Texas 75247
Telephone 214-630-9745
Facsimile 214-630-9819

Fort Worth
2696 Gravel Drive
Fort Worth, Texas 76118
Telephone 817-284-1318
Facsimile 817-284-1585

Houston
6300 Rothway, Suite 150
Houston, Texas 77040
Telephone 713-996-9979
Facsimile 713-996-9972

Figure 3.48 – Test Ram Calibration for 100 Ton Jack and Gauge

RST Instruments Ltd.

200 - 2050 Hartley Ave., Coquitlam, British Columbia, Canada V3K 6W5

rst INSTRUMENTS

200 TON HYDRAULIC RAM CALIBRATION

CUSTOMER:	Con-Tech Systems	
DATE:	2-May-05	
W.O.#:	Q04309	
RAM SERIAL NUMBER:	**CTS-J-200-4**	
GAUGE SERIAL NUMBER:	**CTS-G-200-4-1**	
TEMPERATURE:	20 degrees	
EFFECTIVE RAM AREA:	42.23	SQ. INCHES

INDICATED PRESSURE (PSI)	APPLIED LOAD (KIPS) CALIBRATED AT 1 INCH STROKE			AVERAGE LOAD (KIPS)
	RUN 1	RUN 2	RUN 3	
0	0.0	0.0	0.0	0.0
1000	41.2	41.5	40.7	41.1
2000	82.4	82.1	81.4	82.0
3000	123.3	123.2	124.0	123.5
4000	165.5	165.5	165.5	165.5
5000	208.2	207.8	208.2	208.1
6000	251.3	251.3	251.3	251.3
7000	293.6	293.8	293.2	293.5
8000	337.2	337.0	337.1	337.1
9000	379.1	379.1	379.9	379.4
10000	422.0	422.3	422.5	422.3

CALIBRATED AGAINST RST STANDARD: MIP-01
CALIBRATED ANNUALLY TO NATIONAL STANDARDS

Applied Science Technologists and Technicians of British Columbia
22724
A.C.
AL CULLEY
AScT

Calibrated by: J. ALLAN

Figure 3.49 - Calibration of 200 Ton Test Ram and Gauges

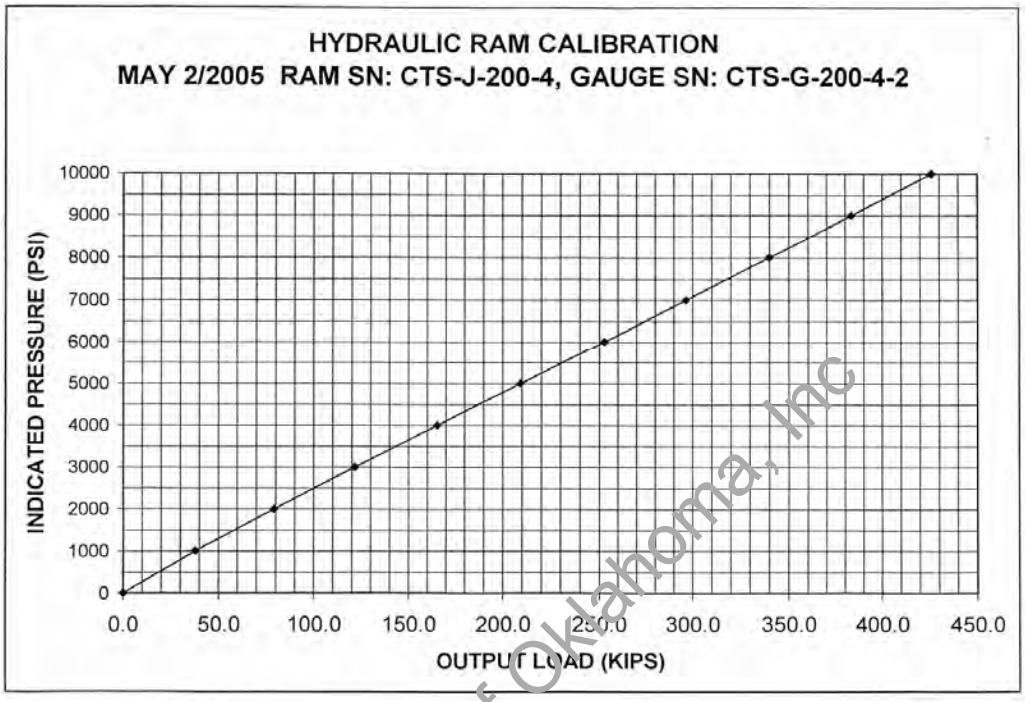

Figure 3.50 - Calibration Chart for 200 Ton Jack

3.10 Summary

This research project was designed to test the axial compression capacity of six commonly used underpinning techniques used for remedial home repairs. Four soil borings were conducted at differing times of the research schedule to provide a good profiling of soil conditions. Two CPT tests were also performed at each end of the project for further profiling and modeling of soil conditions. ASTM D-1143 was followed to test each of the underpinning foundations. The test lines were set at 60^{o} angles to provide the maximum number of test elements. Reaction piers were installed around the site with tie-down bars to secure the reaction beams for compression testing of each pier, pile and helical anchor. All six (6) foundation types were installed with spacing between the

reaction piers at a minimum 3 diameters apart so that soil modification as a result of foundation installation would not affect neighboring test values. Test equipment was calibrated and deflection gauges set to measure deflection with respect to load.

CHAPTER 4

AXIAL CAPACITY TESTING OF FOUNDATIONS

4.1 Introduction

In this chapter, test results from axial compression load tests performed on the present underpinning foundations were presented. Each foundation element was installed at different seasonal periods (wet and dry seasons) and tested in the opposite seasonal period. Hence, results explain the variation in seasonal installation and their impact on final load test results.

4.2 Axial Load Test Results

4.2.1 Straight Drilled Shafts

Testing of the three straight drilled shafts installed in August of 2004 was conducted on April 26, 2005. Set-up and test procedure was in accordance with ASTM D1143 method (also known as the Quick Test). Loading pressure was applied from the test ram in gradual amounts, while deflection on each side of the test plate was monitored from dial gauges placed upon the drilled shaft. Each loading pressure was held for a time period of 2.5 minutes or until the deflection readings remained the same. In both cases, the longer time period was close to 2.5 minutes before increasing the loading to the next increment. Loading pressure increments were made in consistent increments to properly determine the ultimate load. The pressure and strain gauge measurement were then recorded at each time.

Figure 4.1 - Field Testing of the Straight Shafts

The following Tables 4.1, 4.2, 4.3 and Figure 4.2 presents recorded results from testing of the three drilled straight shafts with failure axial capacity along with displacement gauge readings.

Table 4.1 - Test Results For 'Dry to Wet' Straight Drilled Shafts: Pier #43

Installation Date	Pier #	Depth	Initial Pressure(psi)	Final Pressure(psi)	Initial Deflection(in)	Final Deflection(in)	Ultimate Capacity(lb)
Aug.2004	43	15'	1,000	1,000	0	0	
			2,000	2,000	0.011	0.011	
			3,000	3,000	0.027	0.027	
			4,000	4,000	0.038	0.038	
			5,000	5,000	0.073	0.073	
			5,100	5,050	0.35	0.359	
			5,100	5,050	0.473	0.497	104,160
			3,000	3,000	0.488	0.488	
			1,500	1,500	0.423	0.423	
			0	0	0.373	0.374	

Table 4.2 - Test Results For 'Dry to Wet' Straight Drilled Shafts: Pier #44

Installation Date	Pier #	Depth	Initial Pressure(psi)	Final Pressure(psi)	Initial Deflection(in)	Final Deflection(in)	Ultimate Capacity(lb)
Aug.2004	44	15'	1,000	1,000	0	0	
			2,000	2,000	0	0	
			3,000	3,000	0.012	0.012	
			4,000	4,000	0.028	0.028	
			5,000	4,900	0.101	0.101	
			5,000	4,900	0.149	0.149	
			5,000	4,900	0.221	0.231	
			5,000	4,900	0.247	0.253	100,990
			3,000	3,000	0.253	0.256	
			1,500	1,500	0.233	0.232	
			0	0	0.205	0.205	

Table 4.3 - Test Results For 'Dry to Wet' Straight Drilled Shafts: Pier #42

Installation Date	Pier #	Depth	Initial Pressure(psi)	Final Pressure(psi)	Initial Deflection(in)	Final Deflection(in)	Ultimate Capacity(lb)
Aug.2004	42	15'	1,000	1,000	0	0	
			2,000	2,000	0	0	
			3,000	3,000	0.028	0.028	
			4,000	4,000	0.046	0.046	
			5,000	5,000	0.059	0.061	
			6,000	6,000	0.07	0.07	
			6,200	6,100	0.085	0.085	
			6,200	6,100	0.125	0.028	
			6,200	6,100	0.2	0.211	126,410
			4,000	4,000	0.211	0.211	
			2,000	2,000	0.203	0.203	
			0	0	0.154	0.154	

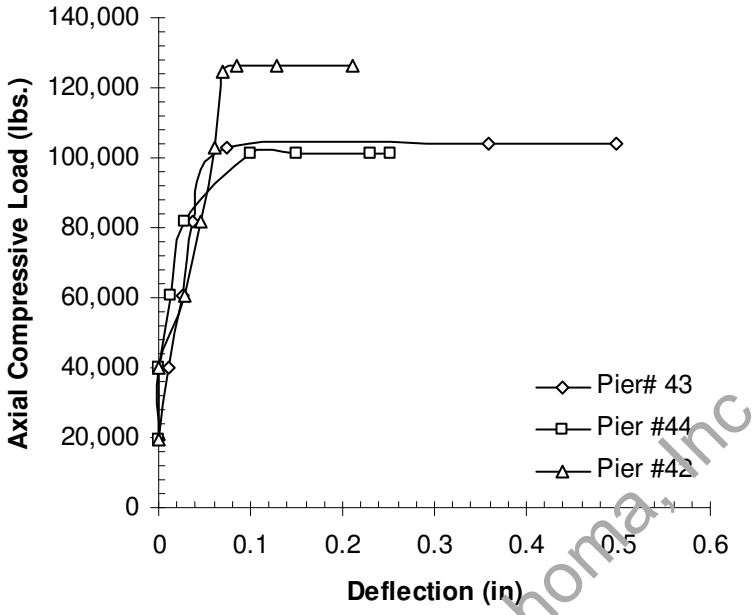

Figure 4.2 - Load vs. Deflection Plots for Shafts Installed in August and Tested in April

Another set of three straight drilled shafts were installed in April of 2005 and were tested on August 17 and 18, 2005.

The following Tables 4.4, 4.5, 4.6 and Figure 4.3 was recorded from testing of the three drilled straight shafts with failure pressure indicated and corresponding axial capacity below gauge reading:

Table 4.4 - Test Results For 'Wet to Dry' Straight Drilled Shafts: Pier #39

Installation Date	Pier #	Depth (ft)	Initial Pressure(psi)	Final Pressure(psi)	Initial Deflection(in)	Final Deflection(in)	Ultimate Capacity(lbs)
Apr. 2005	39	15	500	500	0.02	0.02	
			1,000	1,000	0.035	0.035	
			1,500	1,500	0.05	0.05	
			2,000	2,000	0.06	0.063	
			2,500	2,500	0.08	0.09	
			2,600	2,600	0.1	0.112	
			2,700	2,600	0.14	0.16	
			2,700	2,600	0.18	0.21	
			2,700	2,600	0.23	0.27	
			2,700	2,600	0.342	0.381	106,600
			2,000	2,000	0.381	0.381	
			1,500	1,500	0.371	0.371	
			1,000	1,000	0.365	0.365	
			500	500	0.345	0.345	
			0	0	0.32	0.32	

Table 4.5 - Test Results For 'Wet to Dry' Straight Drilled Shafts: Pier #40

Installation Date	Pier #	Depth (ft)	Initial Pressure (psi)	Final Pressure (psi)	Initial Deflection (in)	Final Deflection (in)	Ultimate Capacity (lbs)
Apr. 2005	40	15	500	500	0.021	0.021	
			1,000	1,000	0.06	0.06	
			1,500	1,500	0.077	0.077	
			2,000	2,000	0.09	0.09	
			2,500	2,500	0.1	0.105	
			3,000	3,000	0.121	0.123	
			3,100	3,000	0.16	0.162	
			3,100	3,000	0.192	0.195	
			3,100	3,000	0.227	0.232	123,000
			2,000	2,000	0.21	0.21	
			1,000	1,000	0.166	0.166	
			0	0	0.145	0.145	

Table 4.6 - Test Results For 'Wet to Dry' Straight Drilled Shafts: Pier #41

Installation Date	Pier #	Depth (ft)	Initial Pressure (psi)	Final Pressure (psi)	Initial Deflection(in)	Final Deflection(in)	Ultimate Capacity(lbs)
Apr. 2005	41	15	500	500	0.l0	0.1	
			1,000	1,000	0.2	0.22	
			1,500	1,500	0.3	0.32	
			2,000	2,000	0.055	0.058	
			2,500	2,500	0.1	0.112	
			2,600	2,500	0.332	0.338	
			2,600	2,500	0.4	0.411	
			2,600	2,500	0.523	0.555	102,500
			2,000	2,000	0.554	0.544	
			1,500	1,500	0.506	0.505	
			1,000	1,000	0.473	0.473	
			500	500	0.44	0.439	
			0	0	0.402	0.402	

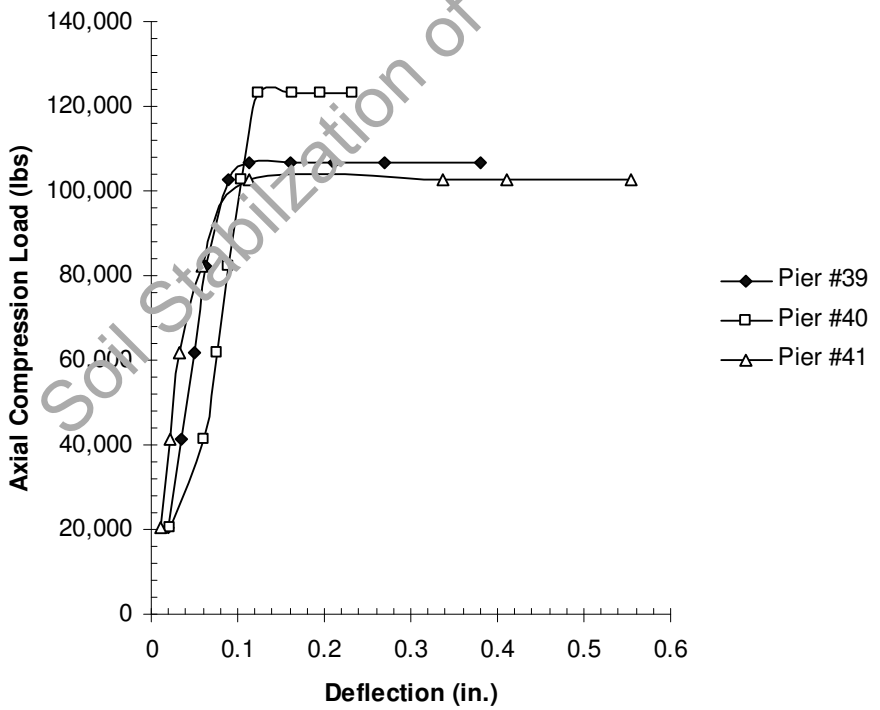

Figure 4.3 - Load vs. Deflection Plots for Shafts Installed in April and Tested in August

4.2.2 Drilled Belled/Under-reamed Shafts

Tests were conducted on three drilled belled shafts installed in August of 2004 on April 26, 2005. Set-up and test procedure was in accordance with ASTM D1143 (Quick Test). Pressure was applied to the foundation from the test ram in incremental magnitudes and the deflection on each side of the foundation was monitored. Pressure or load increment was kept the same for 2.5 minutes or until the deflection readings remained the same, which ever was longer. Then the next load increment was applied and the deflection readings from the gauge measurement were then recorded.

Figure 4.4 – Load Testing of Belled Shafts

Tables 4.7, 4.8, 4.9 and Figure 4.5 present load-deformation results of the three drilled belled shafts with failure pressure indicating the ultimate axial capacity of the shafts.

Table 4.7 - Test Results for 'Dry to Wet' Belled Drilled Shafts: Pier #36

Installation Date	Pier #	Depth	Initial Pressure (psi)	Final Pressure (psi)	Initial Deflection (in.)	Final Deflection (in.)	Ultimate Capacity (lbs)
Aug.2004	36	15'	1,000	1,000	0	0	
			3,000	3,000	0	0	
			5,000	5,000	0.16	0.16	
			6,000	6,000	0.33	0.33	
			7,000	7,000	0.57	0.57	
			8,000	8,000	0.112	0.119	
			8,200	8,200	0.14	0.14	
			8,400	8,400	0.158	0.158	
			8,600	8,600	0.181	0.187	
			8,800	8,700	0.21	0.213	
			8,800	8,700	0.315	0.325	
			8,800	8,700	0.41	0.423	
			8,800	8,700	0.447	0.456	**180,790**
			8,000	8,000	0.447	0.447	
			6,000	6,000	0.432	0.432	
			4,000	4,000	0.421	0.421	
			2,000	2,000	0.402	0.402	
			1,000	1,000	0.39	0.389	
			0	0	0.304	0.304	

Table 4.8 - Test Results for 'Dry to Wet' Belled Drilled Shafts: Pier #37

Installation Date	Pier #	Depth	Initial Pressure (psi)	Final Pressure (psi)	Initial Deflection (in)	Final Deflection (in)	Ultimate Capacity (lbs)
Aug. 2004	37	15'	1,000	1,000	0	0	
			3,000	3,000	0	0	
			4,000	4,000	0	0	
			5,000	5,000	0	0	
			6,000	6,000	0	0	
			7,000	7,000	0.012	0.012	
			7,500	7,500	0.057	0.059	
			8,000	8,000	0.087	0.093	
			8,200	8,200	0.112	0.119	
			8,400	8,300	0.222	0.231	
			8,400	8,300	0.312	0.319	
			8,400	8,300	0.383	0.397	**172,540**
			8,000	8,000	0.397	0.397	
			6,000	6,000	0.397	0.397	
			4,000	4,000	0.388	0.388	
			2,000	2,000	0.378	0.378	
			1,000	1,000	0.369	0.369	
			0	0	0.303	0.303	

Table 4.9 - Test Results for 'Dry to Wet' Belled Drilled Shafts: Pier #38

Installation Date	Pier #	Depth	Initial Pressure (psi)	Final Pressure (psi)	Initial Deflection (in)	Final Deflection (in)	Ultimate Capacity(lbs)
Aug. 2004	38	15	1,000	1,000	0	0	
			3,000	3,000	0	0	
			5,000	5,000	0.011	0.011	
			6,000	6,000	0.017	0.017	
			7,000	7,000	0.043	0.043	
			7,500	7,500	0.077	0.077	
			8,000	8,000	0.101	0.103	
			8,200	8,100	0.137	0.149	
			8,200	8,100	0.21	0.21	
			8,200	8,100	0.333	0.349	**168,380**
			8,000	8,000	0.349	0.349	
			6,000	6,000	0.349	0.349	
			4,000	4,000	0.332	0.332	
			2,000	2,000	0.311	0.311	
			1,000	1,000	0.278	0.278	
			0	0	0.223	0.223	

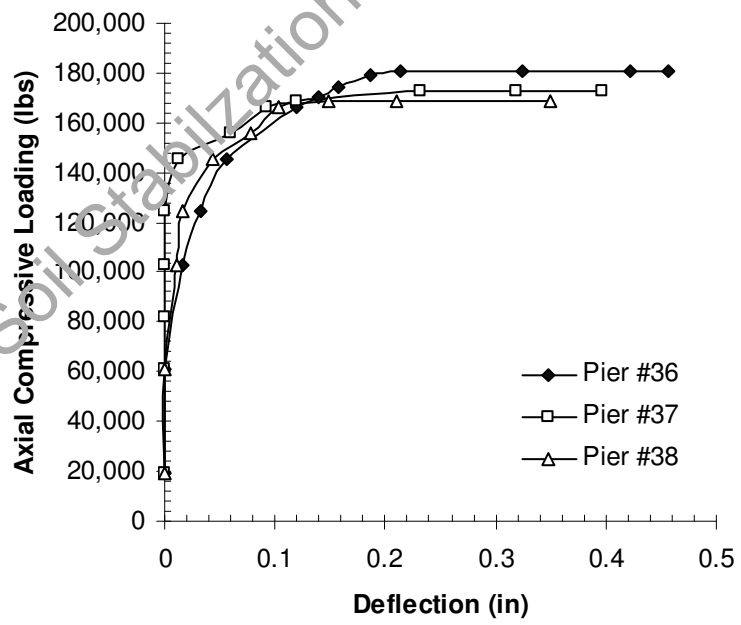

Figure 4.5 Load vs. Deflection Plots for Shafts Installed in August and Tested in April

Tests were conducted on three drilled belled shafts installed in April of 2005 on August 17 and 18, 2005. Set-up and test procedure was in accordance with ASTM D1143 (Quick Test). Pressure was applied to the foundation from the test ram in incremental magnitudes and the deflection on each side of the foundation was monitored. Pressure or load increment was kept the same for 2.5 minutes or until the deflection readings remained the same, which ever was longer. Then the next load increment was applied and the deflection readings from gauge measurement were recorded.

Tables 4.10, 4.11, 4.12 and Figure 4.6 present load-deformation results of the three drilled belled shafts with failure pressure indicating the ultimate axial capacity of the shafts.

Table 4.10 - Test Results for 'Wet to Dry' Belled Drilled Shafts: Pier #33

Installation Date	Pier #	Depth	Initial Pressure (psi)	Final Pressure (psi)	Initial Deflection (in)	Final Deflection (in)	Ultimate Capacity(lbs)
Apr. 2005	33	15	500	500	0.032	0.032	
			1,000	1,000	0.06	0.06	
			1,500	1,500	0.091	0.091	
			2,000	2,000	0.1	0.1	
			2,500	2,500	0.106	0.114	
			3,000	3,000	0.116	0.125	
			3,500	3,500	0.128	0.128	
			4,000	4,000	0.179	0.181	
			4,200	4,000	0.321	0.351	
			4,200	4,000	0.422	0.448	
			4,200	4,000	0.616	0.689	165,500
			3,000	3,000	0.616	0.616	
			2,000	2,000	0.606	0.606	
			1,000	1,000	0.553	0.533	
			500	500	0.573	0.573	
			0	0	0.523	0.523	

Table 4.11 - Test Results for 'Wet to Dry' Belled Drilled Shafts: Pier #34

Installation Date	Pier #	Depth	Initial Pressure (psi)	Final Pressure (psi)	Initial Deflection (")	Final Deflection (")	Ultimate Capacity (lbs)
Apr. 2005	34	15	500	500	0.012	0.012	
			1,000	1,000	0.037	0.037	
			1,500	1,500	0.05	0.05	
			2,000	2,000	0.088	0.088	
			2,500	2,500	0.096	0.096	
			3,000	3,000	0.111	0.113	
			3,500	3,500	0.141	0.145	
			4,000	4,000	0.191	0.201	
			4,100	4,000	0.221	0.232	
			4,100	4,000	0.276	0.281	
			4,100	4,000	0.286	0.298	165,500
			3,000	3,000	0.256	0.256	
			2,000	2,000	0.22	0.22	
			1,000	1,000	0.2	0.2	
			0	0	0.155	0.155	

Table 4.12 - Test Results for 'Wet to Dry' Belled Drilled Shafts: Pier #35

Installation Date	Pier #	Depth	Initial Pressure (psi)	Final Pressure (psi)	Initial Deflection (")	Final Deflection (")	Ultimate Capacity (lbs)
Apr. 2005	35	15	500	500	0.001	0.001	
			1,000	1,000	0.001	0.001	
			2,000	2,000	0.004	0.004	
			3,000	3,000	0.011	0.011	
			3,500	3,500	0.022	0.022	
			4,000	3,800	0.1	0.111	
			4,000	3,800	0.251	0.257	
			4,000	3,800	0.291	0.302	157,060
			3,000	3,000	0.302	0.302	
			2,000	2,000	0.264	0.264	
			1,000	1,000	0.254	0.254	
			0	0	0.209	0.209	

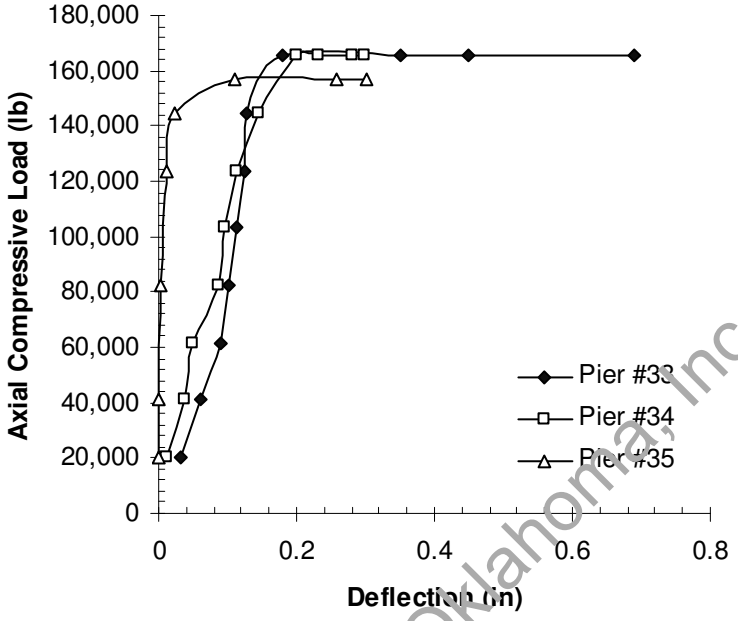

Figure 4.6 Load vs. Deflection Plots for Shafts Installed in April and Tested in August

4.2.3 Augercast Piles

Testing on three augercast piles installed in September of 2004 was conducted on April 26, 2005. The same test procedures described in the earlier sections were followed for these tests.

Figure 4.7 – Field Testing of Augercast Piles

Table 4.13, 4.14, 4.15 and Figure 4.8 present both load and deformation data, including the ultimate capacity of the foundation in lbs.

Table 4.15 – Test Results for 'Dry to Wet' Augercast Piles: Pile #50

Installation Date	Pile #	Depth	Initial Pressure (psi)	Final Pressure (psi)	Initial Deflection (in.)	Final Deflection (in.)	Ultimate Capacity (lbs)
Aug. 2004	50	15	1,000	1,000	0.007	0.007	
			2,000	2,000	0.043	0.045	
			3,000	3,000	0.057	0.061	
			4,000	4,000	0.075	0.078	
			4,500	4,500	0.101	0.105	
			5,000	4,900	0.291	0.322	
			5,000	4,900	0.478	0.512	
			5,000	4,900	0.731	0.811	**100,990**
			3,000	3,000	0.811	0.811	
			1,500	1,500	0.799	0.799	
			500	500	0.778	0.778	
			0	0	0.711	0.711	

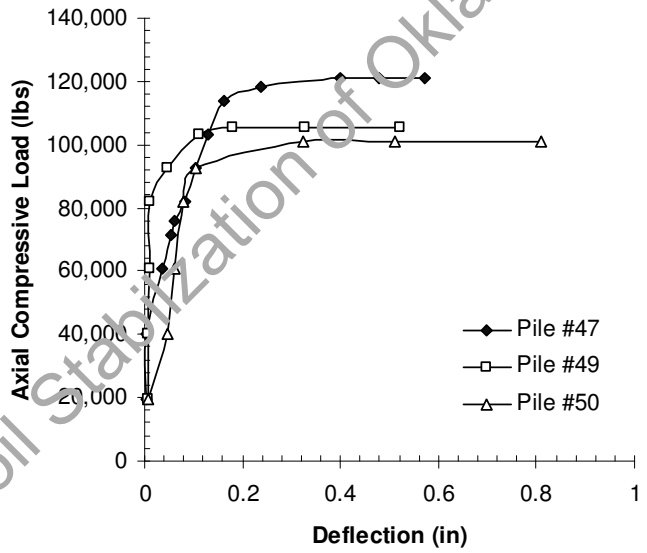

Figure 4.8 - Load vs. Deflection Plots for Augercast Piles Installed in August and Tested in April

Test on three other augercast piles installed in April of 2005 were performed on August 17 and 18, 2005. Figure 4.16, 4.17, 4.18 and Table 4.6 present both load and deformation.

Table 4.18 – Test Results for Wet to Dry' Augercast Piles: Pile #48

Installation Date	Pile #	Depth	Initial Pressure (psi)	Final Pressure (psi)	Initial Deflection (in.)	Final Deflection (in.)	Ultimate Capacity (lbs)
Apr. 2005	48	15	500	500	0.032	0.032	
			1,000	1,000	0.051	0.051	
			1,500	1,500	0.071	0.071	
			2,000	2,000	0.087	0.088	
			2,500	2,500	0.102	0.105	
			2,800	2,600	0.211	0.218	
			2,700	2,600	0.331	0.34	
			2,700	2,600	0.521	0.535	106,760
			2,000	2,000	0.521	0.521	
			1,500	1,500	0.511	0.511	
			1,000	1,000	0.5	0.5	
			500	500	0.479	0.479	
			0	0	0.401	0.401	

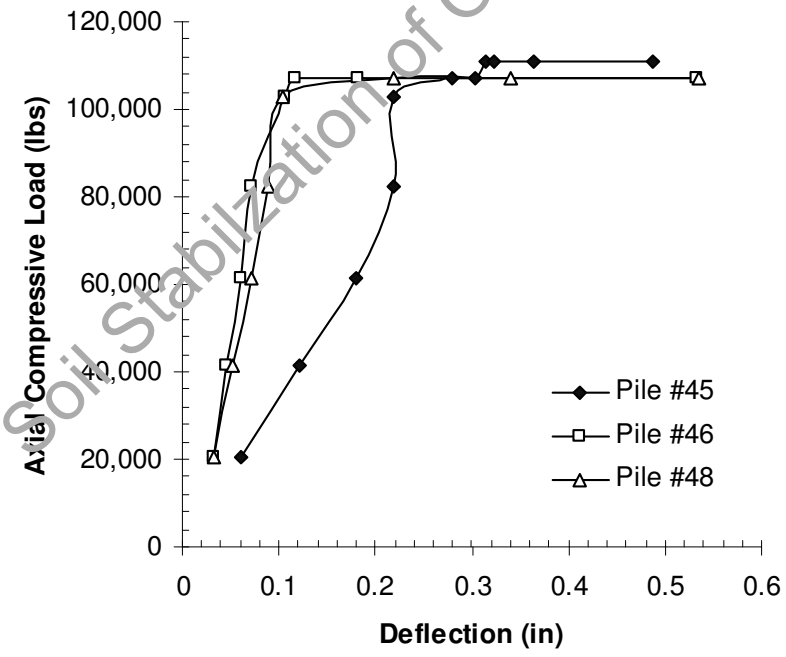

Figure 4.9 - Load vs. Deflection Plots for Augercast Piles Installed in April and Tested in August

4.2.4 Helical Anchors

Testing of the four helical anchors installed in September of 2004 was conducted on April 21, 2005. It should be noted here that the notation 'H-1' indicates a single flight 12 in. helical anchor and notation 'H-2' indicates a double helical anchor with helix of 10 in. and 12 in. The same test procedures described in the earlier sections were followed for these tests.

Figure 4.10 - Field Testing of Helical Anchors

Tables 4.19, 4.20, 4.21, 4.22 and Figures 4.11 and 4.12 present both load and deformation data, including the ultimate capacity of the foundation in lbs. All results are presented separately for the single and double helical anchor. These tests were referred to as 'dry to wet' helical anchors.

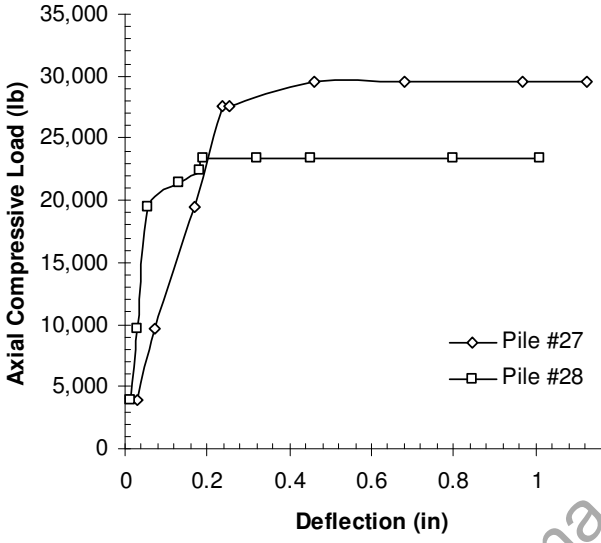

Figure 4.11 - Load vs. Deflection Plots for Single Flight Helical Piles Installed in August and Tested in April

Table 4.21 – Test Results for 'Dry to Wet' Helical Anchors: Helix #31

Double Helix H-2

Installation Date	Pile #	Depth	Initial Pressure (psi)	Final Pressure (psi)	Initial Deflection (in.)	Final Deflection (in.)	Ultimate Capacity (lbs)
Sept.2004	31	30	200	200	0.025	0.025	
			500	500	0.054	0.054	
			1,000	1,000	0.07	0.073	
			1,200	1,200	0.121	0.121	
			1,400	1,400	0.187	0.187	
			1,500	1,400	0.23	0.23	
			1,500	1,400	0.52	0.591	
			1,500	1,400	0.88	0.878	**27,580**
			1,000	1,000	0.878	0.878	
			600	600	0.809	0.809	
			300	300	0.773	0.773	
			0	0	0.669	0.669	

Table 4.22 – Test Results for 'Dry to Wet' Helical Anchors: Helix #32

Installation Date	Pile #	Depth	Initial Pressure (psi)	Final Pressure (psi)	Initial Deflection (in.)	Final Deflection (in.)	Ultimate Capacity (lbs)
Sept.2004	32	28.5	200	200	0.027	0.028	
			300	300	0.027	0.031	
			500	500	0.035	0.039	
			700	700	0.053	0.054	
			1,000	1,000	0.121	0.123	
			1,200	1,200	0.178	0.182	
			1,300	1,300	0.25	0.252	
			1,400	1,400	0.38	0.387	
			1,500	1,400	0.43	0.438	
			1,500	1,400	0.563	0.567	
			1,500	1,400	0.783	0.789	**27,580**
			1,000	1,000	0.775	0.775	
			600	600	0.713	0.713	
			300	300	0.689	0.689	
			0	0	0.676	0.676	

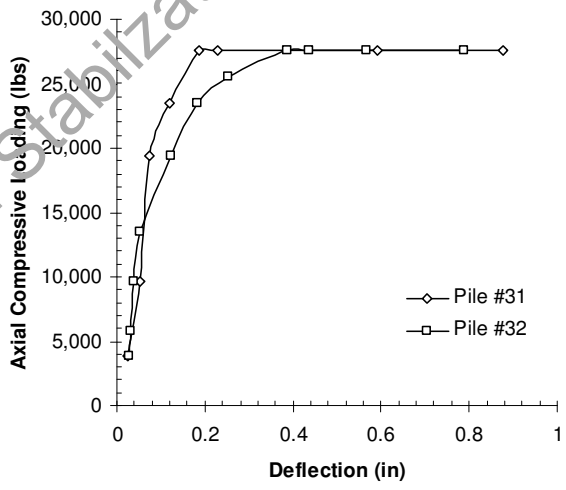

Figure 4.12 - Load vs. Deflection Plots for Double Flight Helical Piles Installed in August and Tested in April

The second set of tests on the rest of four helical anchors installed in April of 2005 was attempted on August 16 and 17, 2005. The same test procedures described in the earlier sections were followed for these tests. Tables 4.23, 4.24, 4.25, 4.26 and Figures 4.13 and 4.14 present both load and deformation data, including the ultimate capacity of the foundation in lbs. These foundations were referred to as 'wet to dry' helical anchors.

Table 4.23 – Test Results for 'Wet to Dry' Helical Anchors: Helix #25

Single Helix H-1

Installation Date	Pile #	Depth	Initial Pressure (psi)	Final Pressure (psi)	Initial Deflection (in.)	Final Deflection (in.)	Ultimate Capacity (lbs)
Apr. 2005	25	34	100	100	0.112	0.112	
			200	200	0.12	0.121	
			300	300	0.173	0.173	
			400	400	0.233	0.225	
			500	500	0.255	0.256	
			600	550	0.45	0.455	
			600	600	0.47	0.472	
			650	600	0.49	0.495	
			650	600	0.53	0.577	24,720
			500	500	0.577	0.577	
			300	300	0.534	0.534	
			100	100	0.456	0.457	

Table 4.24 – Test Results for 'Wet to Dry' Helical Anchors: Helix #26

Single Helix H-1

Installation Date	Pile #	Depth	Initial Pressure (psi)	Final Pressure (psi)	Initial Deflection (in.)	Final Deflection (in.)	Ultimate Capacity (lbs)
Apr. 2005	26	26	100	100	0.121	0.121	
			200	200	0.178	0.178	
			300	300	0.188	0.19	
			400	400	0.211	0.211	
			500	500	0.231	0.245	
			600	600	0.318	0.338	
			700	620	0.377	0.401	
			700	620	0.512	0.581	
			700	620	0.791	0.899	25,544
			500	500	0.881	0.881	
			300	300	0.812	0.812	
			100	100	0.701	0.701	
			0	0	0.625	0.625	

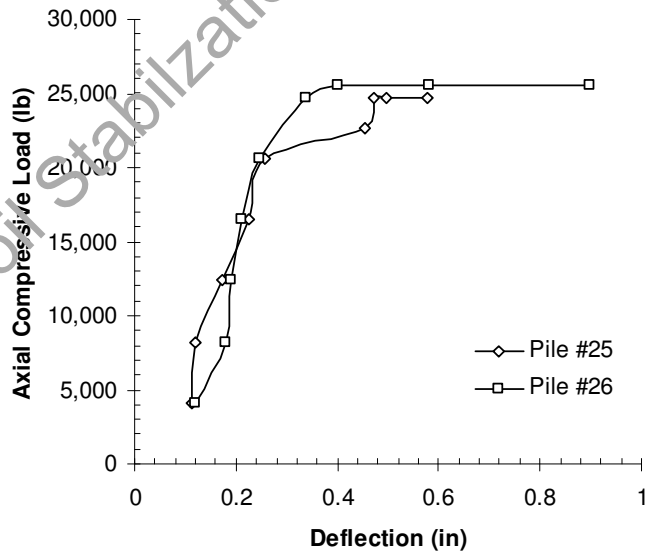

Figure 4.13 - Load vs. Deflection Plots for Single Flight Helical Piles Installed in April and Tested in August

Table 4.25 – Test Results for 'Wet to Dry' Helical Anchors: Helix # 29

Double Helix H-2

Installation Date	Pile #	Depth	Initial Pressure (psi)	Final Pressure (psi)	Initial Deflection (in.)	Final Deflection (in.)	Ultimate Capacity (lbs)
Apr. 2005	29	27	100	100	0.101	0.101	
			200	200	0.15	0.152	
			300	300	0.156	0.156	
			400	400	0.185	0.187	
			500	500	0.205	0.209	
			600	600	0.265	0.271	
			700	650	0.362	0.367	
			700	650	0.385	0.389	
			700	650	0.43	0.436	
			700	650	0.53	0.537	
			700	650	0.72	0.821	26,780
			500	500	0.816	0.816	
			300	300	0.806	0.806	
			100	100	0.791	0.791	
			0	0	0.746	0.746	

Table 4.26 – Test Results for 'Wet to Dry' Helical Anchors: Helix # 30

Double Helix H-2

Installation Date	Pile #	Depth	Initial Pressure (psi)	Final Pressure (psi)	Initial Deflection (in.)	Final Deflection (in.)	Ultimate Capacity (lbs)
Apr. 2005	30	32	100	100	0.06	0.06	
			200	200	0.1	0.1	
			300	300	0.133	0.133	
			400	400	0.175	0.175	
			500	480	0.2	0.2	
			500	500	0.23	0.23	
			600	500	0.25	0.25	
			600	600	0.28	0.287	
			700	680	0.3	0.304	
			700	680	0.402	0.412	
			700	680	0.65	0.651	28,016
			500	500	0.622	0.622	
			300	300	0.56	0.56	
			100	100	0.501	0.501	
			0	0	0.453	0.453	

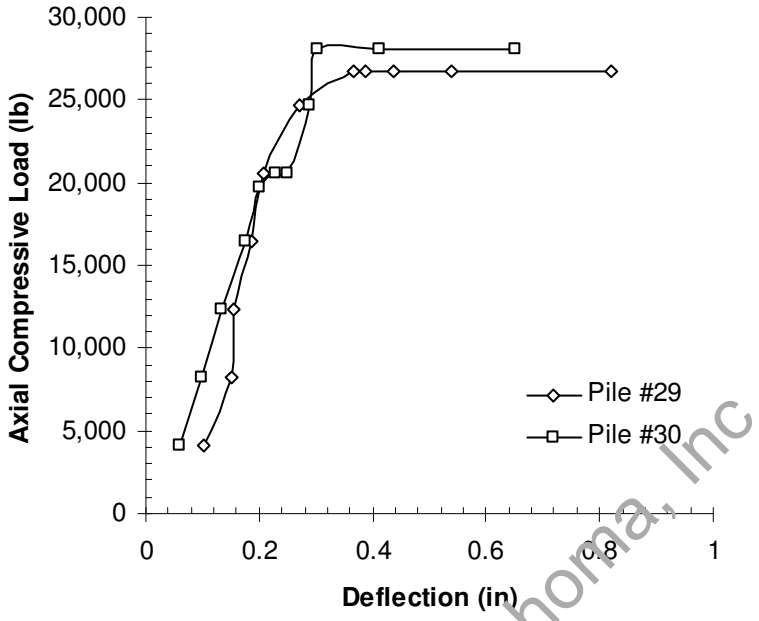

Figure 4.14 - Load vs. Deflection Plots for Double Flight Helical Piles Installed in April and Tested in August

4.2.5 Pressed Steel Pilings

In the case of pressed steel pilings, tests were conducted on all six piles as per the same procedures. The pressed steel piles were installed in September of 2004 and tested on April 21, 2005. The same test procedures described in the earlier sections were followed for testing the pressed steel piles.

Figure 4.15 - Field Testing of the Pressed Steel Piles

Tables 4.27, 4.28, 4.29, 4.30, 4.31, 4.32 and Figure 4.16 present both load and deformation data, including the ultimate capacity of the pressed steel piles in lbs.

Table 4.27 – Test Results for 'Dry to Wet' Pressed Steel Piles: Pile #22

Installation Date	Pile #	Depth	Initial Pressure (psi)	Final Pressure (psi)	Initial Deflection (in.)	Final Deflection (in.)	Ultimate Capacity (lbs)
Sept.2004	22r	35	200	200	0.01	0.01	
			500	500	0.08	0.08	
			1,000	1,000	0.115	0.115	
			1,500	1,500	0.208	0.208	
			1,800	1,800	0.28	0.28	
			2,000	2,000	0.305	0.305	
			2,200	2,200	0.358	0.358	
			2,400	2,400	0.425	0.425	
			2,600	2,400	0.5	0.5	
			2,500	2,400	0.611	0.75	
			2,500	2,400	0.821	0.833	**48,320**
			2,000	2,000	0.833	0.833	
			1,000	1,000	0.816	0.816	
			500	500	0.798	0.798	
			0	0	0.735	0.735	

Table 4.28 – Test Results for 'Dry to Wet' Pressed Steel Piles: Pile #23

Installation Date	Pile #	Depth	Initial Pressure (psi)	Final Pressure (psi)	Initial Deflection (in.)	Final Deflection (in.)	Ultimate Capacity (lbs)
Sept.2004	23r	25	200	200	0.04	0.04	
			500	500	0.67	0.67	
			1,000	1,000	0.081	0.081	
			1,500	1,500	0.105	0.105	
			1,800	1,650	0.2	0.24	
			1,800	1,650	0.275	0.533	
			1,800	1,650	0.778	0.943	**33,000**
			1,000	1,000	0.943	0.943	
			500	500	0.923	0.923	
			0	0	0.876	0.876	

Table 4.29 – Test Results for 'Dry to Wet' Pressed Steel Piles: Pile #24

Installation Date	Pile #	Depth	Initial Pressure (psi)	Final Pressure (psi)	Initial Deflection (in.)	Final Deflection (in.)	Ultimate Capacity (lbs)
Sept.2004	24r	26	200	200	0.009	0.009	
			500	500	0.043	0.043	
			1,000	1,000	0.08	0.085	
			1,500	1,500	0.092	0.093	
			2,000	2,000	0.143	0.143	
			2,200	2,200	0.17	0.175	
			2,400	2,400	0.2	0.209	
			2,500	2,500	0.231	0.243	
			2,600	2,600	0.24	0.24	
			2,800	2,600	0.275	0.377	
			2,800	2,600	402	0.656	
			2,700	2,600	0.767	0.833	**52,480**
			2,000	2,000	0.833	0.833	
			1,000	1,000	0.812	0.812	
			500	500	0.734	0.734	

Table 4.30 – Test Results for 'Dry to Wet' Pressed Steel Piles: Pile #13

Installation Date	Pile #	Depth	Initial Pressure (psi)	Final Pressure (psi)	Initial Deflection (in.)	Final Deflection (in.)	Ultimate Capacity (lbs)
Sept.2004	13	44	200	200	0.2	0.2	
			500	500	0.35	0.37	
			1,000	1,000	0.074	0.077	
			1,500	1,500	0.123	0.127	
			1,700	1,700	0.146	0.167	
			2,000	2,000	0.201	0.223	
			2,200	2,100	0.303	0.354	
			2,200	2,100	0.454	0.582	
			2,200	2,100	0.687	0.723	**42,000**
			2,000	2,000	0.723	0.723	
			1,000	1,000	0.713	0.713	
			500	500	0.689	0.689	
			0	0	0.623	0.623	

Table 4.31 – Test Results for 'Dry to Wet' Pressed Steel Piles: Pile #14

Installation Date	Pile #	Depth	Initial Pressure (psi)	Final Pressure (psi)	Initial Deflection (in.)	Final Deflection (in.)	Ultimate Capacity (lbs)
Sept.2004	14	70	200	200	0.04	0.04	
			500	500	0.115	0.115	
			1,000	1,000	0.15	0.15	
			1,500	1,500	0.25	0.25	
			1,800	1,800	0.337	0.337	
			2,000	2,000	0.4	0.4	
			2,100	2,050	0.71	0.792	
			2,100	2,050	0.82	0.931	**41,000**
			2,000	2,000	0.931	0.931	
			1,000	1,000	0.921	9,921	
			500	500	0.903	0.903	
			0	0	0.834	0.834	

Table 4.32 – Test Results for 'Dry to Wet' Pressed Steel Piles: Pile #15

Installation Date	Pile #	Depth	Initial Pressure (psi)	Final Pressure (psi)	Initial Deflection (in.)	Final Deflection (in.)	Ultimate Capacity (lbs)
Sept.2004	15	75	200	200	0.023	0.023	
			500	500	0.03	0.3	
			1,000	1,000	0.06	0.06	
			1,500	1,500	0.104	0.104	
			1,800	1,800	0.167	0.167	
			2,000	2,000	0.191	0.191	
			2,100	2,100	0.23	0.23	
			2,200	2,200	0.26	0.26	
			2,300	2,300	0.285	0.285	
			2,400	2,400	0.291	0.291	
			2,500	2,400	0.305	0.415	
			2,500	2,400	0.603	0.805	**48,320**
			2,000	2,000	0.805	0.805	
			1,000	1,000	0.789	0.789	
			500	500	0.776	0.776	
			0	0	0.712	0.712	

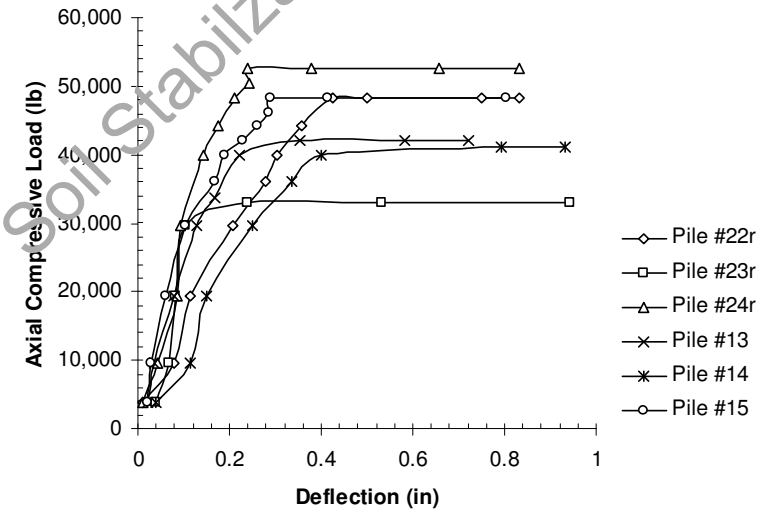

Figure 4.16 - Load vs. Deflection Plots for Pressed Steel Piles Installed in September and Tested in April

As evidenced by the pile layout arrangement, there was 26 ft difference in driving depth between piles that were only 5 ft apart. While this spacing distance is far greater than the prescribed requirement of 3 diameters (0.75 ft), an even more obvious observation is the fact that driving sequence showed no correlation between a previously driven pile and a pile 5 ft away. As an example, pile #13 was driven to a depth of 44 ft while pile #14, 5 ft to the side, was installed afterward but was driven 70 ft. Therefore, there was no perceptible occurrence of soil densification for a subsequently driven pile. In view of the shallow depths reached by some of these piles, it would appear that seasonal dryness and subsequent increased shear strength of some subsurface layers created tip resistance that prevented deeper penetration. A review of the Cone Penetration tests showed that there was far greater driving resistance at the north end of the project than the south end. Therefore, here again tip resistance appears to be the determining factor is establishing driving depth. It is interesting to note, however, that all pressed steel piles terminated in clay with much lower N values than those mediums with sand dispersion. Therefore, with steel piles skin friction is an important factor.

Testing of the six pressed steel pilings installed in April of 2005 was conducted on August 16, 2005. The same test procedures described in the earlier section were followed for testing these pressed steel piles. Tables 4.33, 4.34, 4.35, 4.36, 4.37, 4.38 and Figure 4.17 present both load and deformation data, including the ultimate capacity of the pressed steel piles in lbs.

Table 4.33 – Test Results for 'Wet to Dry' Pressed Steel Piles: Pile # 16

Installation Date	Pile #	Depth	Initial Pressure (psi)	Final Pressure (psi)	Initial Deflection (in.)	Final Deflection (in.)	Ultimate Capacity (lbs)
Apr. 2005	16	57	100	100	0.001	0.001	
			200	200	0.04	0.04	
			300	300	0.08	0.08	
			400	400	0.117	0.117	
			500	500	0.15	0.15	
			600	600	0.162	0.162	
			700	700	0.232	0.232	
			800	800	0.296	0.296	
			900	900	0.333	0.333	
			1,000	1,000	0.386	0.386	
			1,100	1,000	0.42	0.42	
			1,100	1,000	0.44	0.44	
			1,100	1,000	0.47	0.47	
			1,100	1,000	0.504	0.511	
			1,100	1,000	0.53	0.536	
			1,100	1,000	0.7	0.804	41,200
			700	700	0.8	0.8	
			400	400	0.58	0.58	
			200	200	0.48	0.48	
			0	0	0.465	0.465	

Table 4.34 – Test Results for 'Wet to Dry' Pressed Steel Piles: Pile # 17

Installation Date	Pile #	Depth (ft)	Initial Pressure (psi)	Final Pressure (psi)	Initial Deflection (in)	Final Deflection (in)	Ultimate Capacity (lbs)
Apr. 2005	17	64	100	100	0.101	0.101	
			200	200	0.142	0.142	
			300	300	0.156	0.156	
			400	400	0.176	0.176	
			500	500	0.23	0.23	
			600	600	0.27	0.27	
			700	700	0.326	0.326	
			800	800	0.432	0.432	
			900	820	0.721	0.816	
			900	820	1.112	1.207	
			900	820	1.321	1.407	33,784
			700	700	1.222	1.222	
			400	400	1.112	1.112	
			200	200	1.011	1.011	
			0	0	0.989	0.989	

Table 4.35 – Test Results for 'Wet to Dry' Pressed Steel Piles: Pile # 18

Installation Date	Pile #	Depth (ft)	Initial Pressure (psi)	Final Pressure (psi)	Initial Deflection (in)	Final Deflection (in)	Ultimate Capacity (lbs)
Apr. 2005	18	51	100	100	0	0	
			200	100	0.101	0.101	
			300	300	0.131	0.132	
			400	400	0.172	0.172	
			500	500	0.18	0.181	
			600	600	0.27	0.27	
			700	700	0.318	0.328	
			800	800	0.391	0.391	
			900	900	0.468	0.472	
			1,000	900	0.539	0.544	
			1,000	900	0.565	0.573	
			1,000	900	0.61	0.617	37,080
			700	700	0.6	0.6	
			400	400	0.501	0.501	
			200	200	0.41	0.41	
			0	0	0.376	0.376	

Table 4.36 – Test Results for 'Wet to Dry' Pressed Steel Piles: Pile # 19

Installation Date	Pile #	Depth (ft)	Initial Pressure (psi)	Final Pressure (psi)	Initial Deflection (in)	Final Deflection (in)	Ultimate Capacity (lbs)
Apr. 2005	19	58	100	100	0	0	
			200	200	0.064	0.064	
			300	300	0.11	0.113	
			400	400	0.141	0.143	
			500	500	0.18	0.186	
			600	600	0.22	0.225	
			700	700	0.268	0.272	
			800	800	0.322	0.326	
			900	900	0.39	0.393	
			1,000	940	0.476	0.485	
			1,000	940	0.482	0.494	
			1,000	960	0.52	0.526	
			1,000	960	0.7	0.713	
			1,000	960	0.901	0.912	39,552
			700	700	0.906	0.906	
			400	400	0.831	0.831	
			200	200	0.802	0.802	

Table 4.37 – Test Results for 'Wet to Dry' Pressed Steel Piles: Pile # 20

Installation Date	Pile #	Depth (ft)	Initial Pressure (psi)	Final Pressure (psi)	Initial Deflection (in)	Final Deflection (in)	Ultimate Capacity (lbs)
Apr. 2005	20	66	100	100	0	0	
			200	200	0.02	0.02	
			300	300	0.07	0.072	
			400	400	0.113	0.118	
			500	500	0.142	0.147	
			600	600	0.204	0.31	
			700	700	0.285	0.29	
			800	800	0.362	0.371	
			900	900	0.44	0.451	
			1,000	910	0.7	0.73	
			1,000	910	0.9	0.923	
			1,000	910	1.141	1.157	37,492
			700	700	1.141	1.141	
			400	400	1.024	1.024	
			0	0	0.911	0.911	

Table 4.38 – Test Results for 'Wet to Dry' Pressed Steel Piles: Pile # 21

Installation Date	Pile #	Depth (ft)	Initial Pressure (psi)	Final Pressure (psi)	Initial Deflection (in)	Final Deflection (in)	Ultimate Capacity (lbs)
Apr. 2005	21	57	100	100	0.002	0.002	
			200	200	0.004	0.004	
			300	300	0.101	0.101	
			400	400	0.148	0.148	
			500	500	0.171	0.176	
			600	600	0.218	0.228	
			700	700	0.246	0.254	
			800	700	0.3	0.303	
			800	780	0.321	0.333	
			900	840	0.392	0.392	
			1,000	920	0.55	0.57	
			1,000	970	0.611	0.621	
			1,000	970	0.7	0.726	
			1,000	970	0.77	0.792	39,964
			700	700	0.786	0.786	
			400	400	0.776	0.776	
			100	100	0.716	0.716	
			0	0	0.698	0.698	

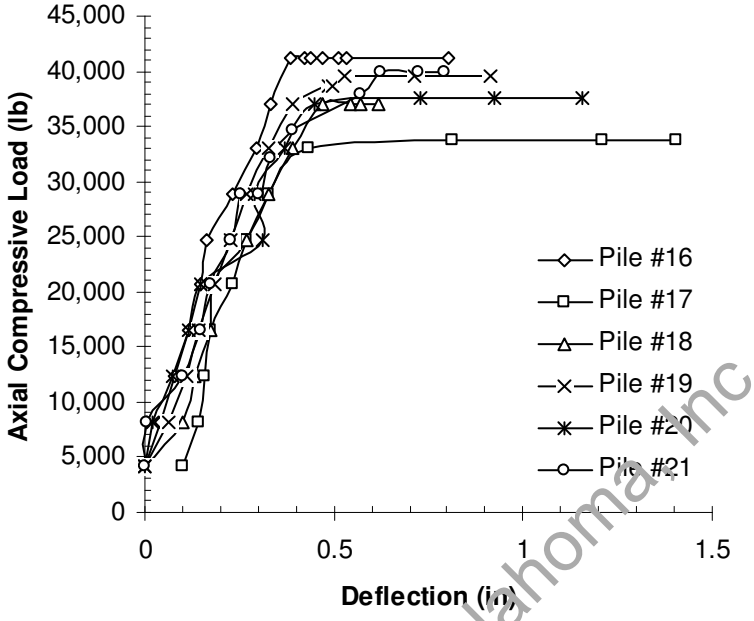

Figure 4.17 Load vs. Deflection Plots for Pressed Steel Piles Installed in April and Tested in August

4.2.6 Pressed Concrete Pilings

In the case of pressed concrete pilings, tests were conducted on all six piles as per the same procedures. The pressed concrete piles were installed in September of 2004 and were tested on April 20, 2005. The same test procedures described in the earlier sections were followed for testing the pressed concrete piles.

Figure 4.18 - Field Testing of the Pressed Concrete Piles

Table 4.39, 4.40, 4.41, 4.42, 4.43, 4.44 and Figure 4.19 present both load and deformation data, including the ultimate capacity of the pressed concrete piles in lbs.

Table 4.39 – 'Dry to Wet' Testing of Pressed Concrete Piles: Pile # 1

Installation Date	Pile #	Depth	Initial Pressure (psi)	Final Pressure (psi)	Initial Deflection (in.)	Final Deflection (in.)	Ultimate Capacity (lbs)
Sept.2004	1	7.67	200	200	0.006	0.006	
			500	500	0.02	0.02	
			750	750	0.05	0.054	
			1,000	1,000	0.086	0.086	
			1,200	1,200	0.1	0.106	
			1,400	1,400	0.135	0.135	
			1,500	1,400	0.175	0.18	
			1,500	1,400	0.185	0.2	
			1,500	1,400	0.321	0.356	**29,000**
			1,000	1,000	0.356	0.356	
			500	500	0.337	0.337	
			0	0	0.309	0.309	

Table 4.40 – 'Dry to Wet' Testing of Pressed Concrete Piles: Pile # 2

Installation Date	Pile #	Depth	Initial Pressure (psi)	Final Pressure (psi)	Initial Deflection (in.)	Final Deflection (in.)	Ultimate Capacity (lbs)
Sept.2004	2	10.17	200	200	0.006	0.006	
			500	500	0.006	0.006	
			1,000	1,000	0.006	0.006	
			1,500	1,500	0.008	0.008	
			1,750	1,750	0.018	0.018	
			1,800	1,800	0.022	0.022	
			2,000	1,850	0.04	0.1	
			2,000	1,850	0.202	0.211	**37,000**
			1,000	1,000	0.202	0.202	
			500	500	0.189	0.189	
			0	0	0.167	0.167	

Table 4.41 – 'Dry to Wet' Testing of Pressed Concrete Piles: Pile # 3

Installation Date	Pile #	Depth	Initial Pressure (psi)	Final Pressure (psi)	Initial Deflection (in.)	Final Deflection (in.)	Ultimate Capacity (lbs)
Sept.2004	3	27.42	200	200	0.005	0.005	
			500	500	0.005	0.005	
			1,000	1,000	0.02	0.02	
			1,425	1,425	0.04	0.04	
			2,000	2,000	0.04	0.04	
			2,250	2,250	0.04	0.04	
			2,500	2,500	0.04	0.04	
			2,700	2,700	0.04	0.04	
			3,000	3,000	0.045	0.045	
			3,100	3,100	0.048	0.048	
			3,200	3,200	0.05	0.05	
			3,300	3,300	0.053	0.053	
			3,400	3,400	0.066	0.07	
			3,500	3,400	0.115	0.15	
			3,500	3,400	0.231	0.254	**68,566**
			3,000	3,000	0.254	0.254	
			2,000	2,000	0.233	0.233	
			1,000	1,000	0.211	0.211	
			0	0	0.167	0.167	

Table 4.42 – 'Dry to Wet' Testing of Pressed Concrete Piles: Pile # 7

Installation Date	Pile #	Depth	Initial Pressure (psi)	Final Pressure (psi)	Initial Deflection (in.)	Final Deflection (in.)	Ultimate Capacity (lbs)
Sept.2004	7r	15.67	200	200	0.006	0.006	
			500	500	0.009	0.009	
			1,000	1,000	0.009	0.009	
			1,500	1,500	0.022	0.022	
			1,750	1,750	0.024	0.024	
			2,000	2,000	0.028	0.028	
			2,200	2,200	0.038	0.038	
			2,400	2,400	0.056	0.056	
			2,500	2,500	0.093	0.093	
			2,600	2,500	0.127	0.18	
			2,600	2,500	0.253	0.267	**50,400**
			2,000	2,000	0.265	0.265	
			1,000	1,000	0.248	0.248	
			500	500	0.234	0.234	
			0	0	0.187	0.187	

Table 4.43 – 'Dry to Wet' Testing of Pressed Concrete Piles: Pile # 8

Installation Date	Pile #	Depth	Initial Pressure (psi)	Final Pressure (psi)	Initial Deflection (in.)	Final Deflection (in.)	Ultimate Capacity (lbs)
Sept.2004	8r	10.67	200	200	0.004	0.004	
			500	500	0.004	0.004	
			1,000	1,000	0.024	0.024	
			1,200	1,200	0.031	0.031	
			1,400	1,400	0.04	0.043	
			1,500	1,500	0.047	0.047	
			1,700	1,700	0.06	0.06	
			1,800	1,800	0.06	0.06	
			1,900	1,900	0.068	0.068	
			2,000	1,950	0.15	0.25	
			2,000	1,950	0.333	0.41	**39,000**
			1,000	1,000	0.407	0.407	
			500	500	0.387	0.387	
			0	0	0.334	0.334	

Table 4.43 – 'Dry to Wet' Testing of Pressed Concrete Piles: Pile # 9

Installation Date	Pile #	Depth	Initial Pressure (psi)	Final Pressure (psi)	Initial Deflection (in.)	Final Deflection (in.)	Ultimate Capacity (lbs)
Sept.2004	9r	25.67	200	200	0.006	0.006	
			500	500	0.006	0.006	
			1,000	1,000	0.01	0.01	
			1,500	1,500	0.024	0.024	
			2,000	2,000	0.04	0.04	
			2,500	2,500	0.055	0.055	
			3,000	3,000	0.09	0.09	
			3,200	3,200	0.1	0.1	
			3,300	3,300	0.11	0.118	
			3,400	3,400	0.121	0.281	
			3,500	3,400	0.287	0.652	
			3,500	3,400	0.781	0.899	**68,000**
			3,000	3,000	0.899	0.899	
			2,000	2,000	0.875	0.875	
			1,000	1,000	0.834	0.834	
			0	0	0.756	0.756	

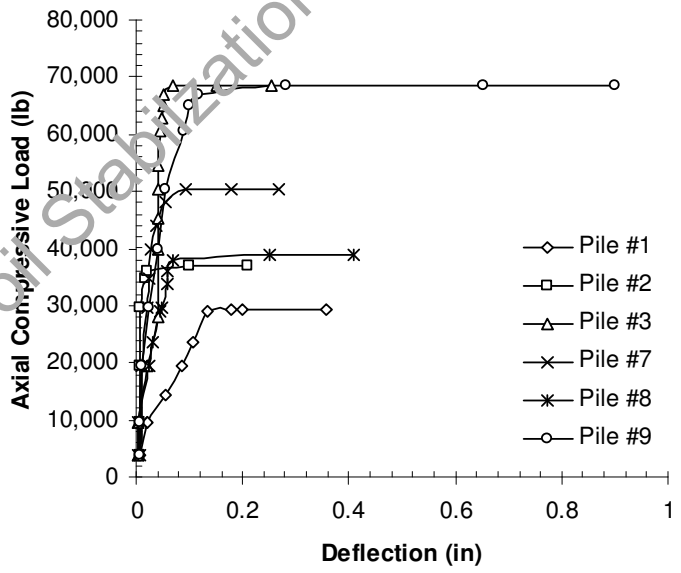

Figure 4.19 - Load vs. Deflection Plots for Pressed Concrete Piles Installed in September and Tested in April

As evidenced by the pile layout arrangement, there was a considerable difference in driving depth, which was as high as 20 ft though the piles were only separated by a distance of 5 ft. While this spacing distance is larger than the prescribed requirement of 3 diameters (1.5 ft), an even more obvious observation is the fact that driving sequence showed no correlation between a previously driven pile and a pile that is driven 5 ft from the previously driven pile. For an example, pile #2, which is 5 ft from pile #3 was driven to a depth of 10.17 ft while pile #3, 5 ft to the side, was installed afterward but was driven 27.42 ft. In a completely reverse order, pile #9 was driven to a depth of 25.67 ft whereas as near pile 8 was driven only to 10.67 ft. This indicates there was no perceptible occurrence of soil densification from a previously driven pile to a newly driven near the previous pile. In view of the shallow depths reached by some of these piles, it would appear that seasonal dryness and subsequent increased shear strength of subsurface layers might have created stiffer soil resistance that prevented deeper penetration. The following Tables 4.45, 4.46, 4.47, 4.48, 4.49, 4.50 and Figure 4.20 present test results conducted on the 'wet to dry' pressed concrete piles.

Table 4.45 – 'Wet to Dry' Testing of Pressed Concrete Piles: Pile #4

Installation Date	Pile #	Depth	Initial Pressure (psi)	Final Pressure (psi)	Initial Deflection (in.)	Final Deflection (in.)	Ultimate Capacity (lbs)
Apr. 2005	4	24.67	100	100	0.01	0.01	
			200	200	0.016	0.016	
			300	300	0.018	0.018	
			400	400	0.024	0.024	
			500	500	0.028	0.03	
			600	600	0.034	0.036	
			700	700	0.042	0.044	
			800	800	0.052	0.054	
			900	900	0.061	0.064	
			1,000	1,000	0.069	0.071	
			1,100	1,100	0.076	0.079	
			1,200	1,200	0.087	0.09	
			1,300	1,300	0.094	0.098	
			1,400	1,400	0.109	0.12	
			1,500	1,400	0.22	0.231	
			1,500	1,400	0.401	0.431	
			1,500	1,400	0.602	0.636	57,940
			1,000	1,000	0.597	0.597	
			500	500	0.577	0.577	
			0	0	0.506	0.506	

Table 4.46 – 'Wet to Dry' Testing of Pressed Concrete Piles: Pile #5

Installation Date	Pile #	Depth	Initial Pressure (psi)	Final Pressure (psi)	Initial Deflection (in.)	Final Deflection (in.)	Ultimate Capacity (lbs)
Apr. 2005	5	22					

Note* Broke Below the surface at driving depth of 22ft and could not be recovered so pile was abandoned

Table 4.47 – 'Wet to Dry' Testing of Pressed Concrete Piles: Pile #6

Installation Date	Pile #	Depth	Initial Pressure (psi)	Final Pressure (psi)	Initial Deflection (in.)	Final Deflection (in.)	Ultimate Capacity (lbs)
Apr. 2005	6	19.67	100	100	0.012	0.012	
			200	200	0.028	0.028	
			300	300	0.04	0.042	
			400	400	0.052	0.055	
			500	500	0.056	0.058	
			600	600	0.06	0.062	
			700	700	0.064	0.068	
			800	800	0.068	0.072	
			900	900	0.075	0.078	
			1,000	1,000	0.082	0.083	
			1,100	1,100	0.084	0.086	
			1,200	1,200	0.088	0.092	
			1,300	1,300	0.095	0.099	
			1,400	1,400	0.102	0.108	
			1,500	1,500	0.11	0.115	
			1,600	1,400	0.122	0.122	
			1,600	1,500	0.222	0.242	
			1,600	1,500	0.254	0.257	
			1,600	1,500	0.454	0.454	61,800
			1,000	1,000	0.45	0.45	
			500	500	0.426	0.426	
			0	0	0.356	0.356	

Table 4.48 – 'Wet to Dry' Testing of Pressed Concrete Piles: Pile #10

Installation Date	Pile #	Depth	Initial Pressure (psi)	Final Pressure (psi)	Initial Deflection (in.)	Final Deflection (in.)	Ultimate Capacity (lbs)
Apr. 2005	10	24.67	100	100	0.02	0.02	
			200	200	0.038	0.04	
			300	300	0.04	0.041	
			400	400	0.062	0.065	
			500	500	0.066	0.068	
			600	600	0.075	0.077	
			700	700	0.085	0.088	
			800	800	0.098	0.102	
			900	900	0.11	0.114	
			1,000	1,000	0.126	0.127	
			1,100	1,100	0.134	0.138	
			1,200	1,200	0.147	0.154	
			1,300	1,300	0.158	0.162	
			1,400	1,400	0.17	0.177	
			1,500	1,500	0.19	0.193	
			1,600	1,600	0.205	0.222	
			1,700	1,600	0.241	0.285	
			1,700	1,600	0.305	0.408	
			1,700	1,600	0.47	0.718	65,920
			1,200	1,200	0.708		
			800	800	0.686	0.686	
			400	400	0.636	0.636	
			0	0	0.567	0.567	

Table 4.49 – 'Wet to Dry' Testing of Pressed Concrete Piles: Pile #11

Installation Date	Pile #	Depth	Initial Pressure (psi)	Final Pressure (psi)	Initial Deflection (in.)	Final Deflection (in.)	Ultimate Capacity (lbs)
Apr. 2005	11	26					

Note* Broke Below the surface at driving depth of 26ft and could not be recovered so pile was abandoned

Table 4.50 – 'Wet to Dry' Testing of Pressed Concrete Piles: Pile #12

Installation Date	Pile #	Depth	Initial Pressure (psi)	Final Pressure (psi)	Initial Deflection (in.)	Final Deflection (in.)	Ultimate Capacity (lbs)
Apr. 2005	12	28.67	100	100	0.015	0.018	
			200	200	0.052	0.055	
			300	300	0.075	0.075	
			400	400	0.088	0.09	
			500	500	0.112	0.114	
			600	600	0.12	0.123	
			700	700	0.128	0.132	
			800	800	0.134	0.136	
			900	900	0.154	0.155	
			1,000	1,000	0.155	0.163	
			1,200	1,200	0.176	0.196	
			1,300	1,300	0.198	0.205	
			1,400	1,400	0.207	0.21	
			1,500	0	1.145	1.145	61,800**

Note Piling broke at the top. Therefore, no rebound readings could be taken.**

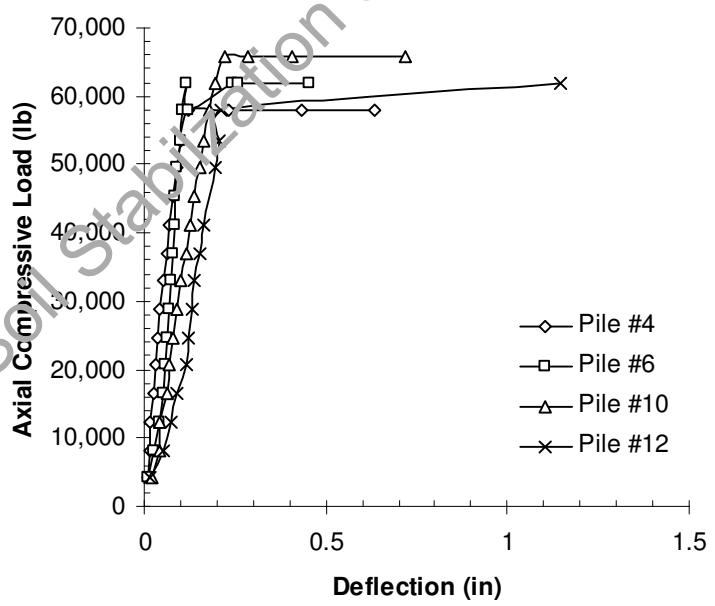

Figure 4.20 Load vs. Deflection Plots for Pressed Concrete Piles Installed in April and Tested in August

It should be noted here that at the time of installation, all pressed pilings had a 50,000 lb axial capacity. The letter "r" after the type of piling signifies the piling was restricted from upheaval from time of installation to time of testing. No determination was made as to the reason for destruction of pilings during the driving process. In each case, however, the piling was probably broken below the surface such that alignment problems or poor concrete capacity could not be attributed as a cause or causes of the foundation failure. Shallow excavation to an approximate depth of 3 ft below the surface did not reveal any rupture point, but the piling shaft was starting to drift away from the vertical axis. Therefore, the point of problem was likely to be below the 3 ft level.

In the next chapter, available empirical and semi-empirical models were used to estimate the pile or pier capacities and these results are compared with measured axial loads of this chapter.

4.3 Summary

Axial capacity testing of each underpinning element showed both strengths and weaknesses and their responses to seasonal moisture changes. There was negligible difference in measured ultimate capacity of straight drilled shafts and augercast piles of the same lengths. The belled shaft showed the highest axial capacity followed by the drilled straight shaft and augercast pile. Deflection at the point of an ultimate capacity was slightly higher for the augercast pile than for the straight drilled shaft. In a comparison of all foundation systems, the deflection of the underpinning at the point of ultimate capacity was highest for the pressed steel pilings followed by the helical anchors.

There was a minor or very little difference in ultimate axial compression capacities of the single and double helix systems. Pressed pilings showed consistent ultimate capacity when they were installed in the wet period and they penetrated to deeper depths with the same installation pressure that was used in the dry period. These results for pressed concrete pilings are only valid for a system where a grouted steel rod was installed in the pile for lateral rigidity.

CHAPTER 5

AXIAL CAPACITY PREDICTIONS

5.1 Introduction

In this chapter, an attempt is made to analyze various empirical and semi-empirical models to predict the axial load capacities of the present underpinnings. These predicted capacities are compared with measured ultimate axial loads to evaluate the prediction capabilities of these existing models. Soil properties from laboratory and in situ tests are used in the load prediction models. Effects of seasonal installation on both predicted and measured loads of underpinnings are addressed.

5.2 Interpretations of Ultimate Axial Loads

5.2.1 Drilled Straight Shafts

Cone penetration tests provided a cross section for establishment of soil properties for this site. Four soil borings supplied supplementary information that was complimentary to CPT data and allowed accurate computations of wet season soil properties. These results were used to predict axial capacity of foundations. Formulas 2.3, 2.4 and 2.5, which were presented in chapter 2, are summarized as follows:

$$R_{TN} = R_{SN} + R_{BN}$$

$$R_{BN} = 9 \times s_u \times A_b$$

$$R_{SN} = \sum f_{maxi} \times \pi \times D \times L$$

It should be mentioned here that terms such as 'Dry to Wet' condition refers to underpinnings installed in dry season and tested in wet season. 'Wet to Dry' condition refers to underpinnings installed in 'Wet' season and tested in 'Dry' season. Projections for the drilled straight shafts based upon the applicable soils and their undrained shear strength information are presented in the following tables:

Table 5.1 – Straight Shafts, 'Dry to Wet' Condition

Section Depth (in)	Su (psi)	Circumference (in)	α coeff.	R_{SN}, lbs
60 (0-5 ')	10	37.7	0.55	12441
60 (5-10 ')	28	37.7	0.55	34834.8
36 (10-13 ')	42	37.7	0.55	31351.32
24 (13-15 ')	17	37.7	0.55	8459.88
				87087
Base Resistance, lbs, R_{BN}			N^*_c	R_{BN}
	17	113.09	9	17302.77
Predicted Total Capacity, lbs, R_{TN}				104389.77

Table 5.2 – Straight Shafts, 'Wet to Dry' Condition

Section Depth (in)	Su (psi)	Circumference (in)	α coeff.	Side Resistance, lbs R_{SN}
48 (0-4 ')	0	37.7	0.55	0
12 (4-5 ')	20	37.7	0.55	7215.78
60 (5-10 ')	28	37.7	0.55	34834.8
36 (10-13 ')	42	37.7	0.55	31351.32
24 (13-15 ')	17	37.7	0.55	8459.88
				81861.78
Base Resistance, lbs, R_{BN}			N^*_c	R_{BN}
	17	113.09	9	17302.77
Predicted Total Capacity, lbs, R_{TN}				99164.55

The observations made at the time of testing and measurement along the shafts revealed that the soil had shrunk away from the shaft to a point of 4 ft below the ground. Therefore, the top 48 in. or 4 ft was only eliminated from the calculations. This is consistent with the approach used to estimate axial loads for drilled shaft, which do not account for the upper 5 ft of side friction. Remedial and construction piers are typically residential foundations and are placed under an approximate 18 in. of soil. Piers in such conditions may not experience soil shrinking away from the perimeter to such depths.

In clay soil, the O'Neill and Reese method for drilled shafts discounts the top 5 ft of the shaft because of possible lack of contacts between pier and soil, immobilization of side friction to full magnitudes, and probable active depths and considered this upper layer as a non-contributing zone. Soil surrounding these shafts shrank away from the shaft. This shrinkage was visually observed since the piers were extended slightly above the ground surface and due to a severe drought during the time of summer testing. A thin steel wire (1/16 in. diameter) was pushed adjacent to the pier to a depth between 3 ft. and 4 ft. below the surface (Figures 5.1, 5.2 and 5.3). Therefore, the upper 4 ft. of the soil was eliminated from skin friction consideration.

Figure 5.3- Length of Steel Rod Length Used to Push Next to Shaft

It should be noted here that the soil samples collected from the dry period showed higher undrained shear strengths than the same depth samples collected from the wet spring periods. Increased shear strength was, however, accounted for in the segment below 4 ft. Predictions by the drilled shaft models showed a close match with measured load results (Tables 5.3 and 5.4) and small differences between both values are attributed to the use of non-contributing zones for practical reasons. Also, test results from different seasonal installation indicated slightly different values with 'wet to dry' condition, which can be regarded as low ultimate loads.

The question for future calculations is how to address the non-contributing upper

zone due to skin friction reduction in expansive clay soils such as the ones encountered in this research. If soil sampling and laboratory testing were performed during the wet season, then it would appear that the 5 ft non-contributing zone reduction would result in lower axial compression capacities. If, however, soil testing was performed during the dry season when the zone of seasonal moisture change creates an increase in shear strength, then the 5 ft reduction would be warranted.

Another factor to consider is that in a normal setting the pier is not exposed beyond the surface. In such cases, soil drying may move away soil from piers to a maximum depth of 2 ft. Such depths should be properly established from future research studies. Otherwise, reduction of skin friction of the upper 5 ft can be construed as overly conservative approach when estimating ultimate capacities of drilled shafts.

Table 5.3 –Comparison of Predicted to Tested Capacity of Straight Drilled Shafts, 'Dry to Wet' Condition

Pier #	Depth(ft)	Predicted Capacity, lbs	Measured Capacity, lbs
42	15	104,390	126,410
43	15	104,390	104,160
44	15	104,390	100,990

Table 5.4 –Comparison of Predicted to Tested Capacity of Straight Drilled Shafts, 'Wet to Dry' Condition

Pier #	Depth(ft)	Predicted Capacity, lbs	Measured Capacity, lbs
39	15	99,165	106,600
40	15	99,165	123,000
41	15	99,165	102,500

5.2.2 Drilled and Belled Shafts

Based upon the soil properties, axial capacity of drilled belled piers can be calculated as follows:

$$R_{TN} = R_{BN} + R_{SN} \quad (5.1)$$

$$R_{BN} = 9 \times s_u \times A_b \quad (5.2)$$

$$R_{SN} = \sum f_{maxi} \times \pi \times D \times L \quad \text{with the side of the bell not considered} \quad (5.3)$$

Predictions of ultimate loads for the drilled straight shafts based on the present soil information are presented in the following tables 5.5 and 5.6 for different seasonal soil conditions:

Table 5.5 – Belled Shafts, 'Dry to Wet' Condition

Section Depth (in)	Su (psi)	Circumference (in)	α coeff.	Side Resistance, lbs R_{SN}
60 (0-5')	10	37.7	0.55	12441
60 (5-10 ')	18	37.7	0.55	22393.8
30 (10-12.5 ')	42	37.7	0.55	26126.10
30 (12.5-15 ')	0	37.7	0.55	0
				60960.90
Base Resistance, lbs, R_{BN}			N^*_c	R_{BN}
	17	706.86	9	108149.58
Predicted Total Capacity, lbs, R_{TN}				169110.48

Table 5.6 – Belled shafts, 'Wet to Dry' Condition

Section Depth (in)	Su (psi)	Circumference (in)	α coeff.	Side Resistance, lbs R_{SN}
48 (0-4 ')	0	37.7	0.55	0
12 (4-5 ')	29	37.7	0.55	7215.78
60 (5-10 ')	28	37.7	0.55	34834.8
30 (10-12.5 ')	42	37.7	0.55	26126.1
30 (12.5-15 ')	0	37.7	0.55	0
				68176.68
Base Resistance, lbs, R_{BN}			N^*_c	R_{BN}
	17	706.86	9	108149.58
Predicted Total Capacity, lbs, R_{TN}				176326.26

Note* observations made at time of testing and measurement along beside shafts revealed that the soil had shrunk away from the shaft to a point 4' below the ground. Therefore, the top 48" was eliminated from the calculations.

Both predicted and measured loads are presented in Tables 5.7 and 5.8 for different seasonal periods. For drilled and belled shafts the normal design allowance is to eliminate friction from the top 5 ft. of shaft and the bottom zone of one diameter of shaft and the periphery of the bell. Test results indicate that a better match was made for ultimate axial compressive capacity of piers tested in wet seasons when the shaft friction at the periphery of the bell was only excluded. This implies that there is shaft contact with upper layers during the wet seasonal periods. When testing in the dry season, there is the added deduction of the upper 4 to 5 ft, which resulted in a good match between predicted and measured axial loads.

Table 5.7 –Comparison of Predicted to Tested Capacity of Belled Drilled Shafts, 'Dry to Wet' Condition

Pier #	Depth(ft)	Predicted Capacity, lbs	Measured Capacity, lbs
36	15	169,110	180,790
37	15	169,110	172,540
38	15	169,110	168,380

Table 5.8 –Comparison of Predicted to Tested Capacity of Belled Drilled Shafts, 'Wet to Dry' Condition

Pier #	Depth(ft)	Predicted Capacity, lbs	Measured Capacity, lbs
33	15	176,326	165,500
34	15	176,326	165,500
35	15	176,326	157,060

5.2.3 Augercast Piles

Steps described in the German standard for axial capacity of augercast piles are the same as those of the drilled shaft (O'Neill 1994). This means that the axial capacity predictions of the augercast piles will be similar to straight drilled shafts of section 5.2. This method is accepted by several practitioners, especially in clay soils (O'Neill 1994).

Table 5.9 – Comparison of Predicted to Tested Capacity of Augercast Piles, 'Dry to Wet' Condition

Pier #	Depth(ft)	Predicted Capacity, lbs	Measured Capacity, lbs
47	15	104,390	121,120
49	15	104,390	105,220
50	15	104,390	100,990

Table 5.10 –Comparison of Predicted to Tested Capacity of Augercast Piles, 'Wet to Dry' Condition

Pier #	Depth(ft)	Predicted Capacity, lbs	Measured Capacity, lbs
45	15	99,165	110,030
46	15	99,165	106,760
48	15	99,165	106,760

5.2.4 Helical Anchors

Helical anchor manufacturer's specifications and other testing provide several formulas for estimation of axial capacity of helical anchors/pier (Seeder 2004; Carville 1994; Hoyt and Clemence 1989). One of the used approaches as presented in chapter 2 (equation 2.6) uses the following equations:

$$Q = K \times T \tag{5.4}$$

where:

K is the average installation torque, which is between 3 and 10 for pipe shafts. Determining the value of K is subjective and this is the primary obstacle in producing an accurate estimate of axial capacity of helical anchors. Conservative recommendations suggest using a K factor of 10 #/ft-# for 3.5 in. diameter or less cylindrical pipe shafts. T is the average installation pressure over the last three feet (4,800 ft-lbs.), which would predict the following axial capacity:

$$Q = (10 \text{ lb/ft-lb})\ (4{,}800 \text{ ft-lb}) = 48{,}000 \text{ lbs}$$

The AB Chance design manual provides a chart for estimation of ultimate capacity and details of this chart is presented in Chapter 2, (Figure 2.1). For a blow count of 18 (soil boring SPT measurement for the depth where the helix was terminated), the axial capacity would be 18,000 lbs. There is another recommendation that when soils

information is not available then the ultimate capacity should be estimated at 10 times the torque pressure, which would be the 48,000 lbs as presented above.

Based on the above calculations as specified by industry, there is a wide variation in the prediction estimations for axial pile capacities. Therefore, use of more accepted formula is preferred. Equation 2.13 from chapter 2 is presented as follows:

Individual Bearing Method

$Q_{ult} = \sum (A_{hx} \times N_c \times S_u) + A_{shaft} \times \alpha \times S_u$

This method was followed in the present research calculations, which are presented in the following.

Helical Piles Installed in August, 2004 and Tested in April, 2005.

For the double helix installed to a depth of 30 ft (H-2, #31) the following projection of axial capacity would apply based upon soil borings and subsequent laboratory testing.

Q_{ult} = {[(10 in.)(10 in.)(π)/4]-[7.06 in^2]} x [(9)(29 #/in^2] + {[(12 in.)(12 in.)(π)/4]-

[7.06 in^2] x (9)(29 #/in^2) + [(27ft)(12 in./ft)(3 in.)(π)](0.30)(29 #/in^2)

= 71.49 in^2 (9)(29#/in^2) + 106.03 in^2(9)(29 #/in^2) + (27ft)(113.09 in^2 /ft)(0.30)(29#/in^2)

= 18,656.28 + 27,675.81 + 26,564.84

= 72,896.93 lbs

Since this value is much large than the actual test results, it is important to explain reasons for this difference.

It should be noted that observations are made during installation, which revealed that the penetration to rotation was not efficient (Tables 3.11 and 3.12). Therefore, it is important to note that the concept of soil destructuring be used to allow for a reduction in

axial capacity prediction formulae. With lack of sufficient penetration efficiency, the upper helix was not completely seated on the clay medium but seated on a combination of initial slicing and cross slicing with the second helix, thus receiving response from a large disturbed soil/shaft contact area.

There is also an obvious lack of soil contact area with the lower helix if the installation action becomes a process of auguring and not pulling into the soil. In addition to the reductions in the capacity of the second helix, shaft friction would also be reduced by a similar factor. There is also some initial movement in clays with even small loads, which suggest that this destructuring factor would reduce both shaft and vertical helix compression sufficiently to create downward movement. It is also important to note that soil moisture was increased from the time of installation to the time of testing for the initial four piles and this resulted in the reduction of shear strength.

This reduction factor is subjective but can be quantified with additional testing and observations of installation efficiency. Future research in this field should address this aspect. An assumption is made by the author by assuming an 80% disturbance effect in the present ultimate capacity predictions. This observation of using deduction for soil disturbance behind the helix is based upon field disturbances noted during the operations of this underpinning foundation system. Hence, the following revised ultimate capacity formulation was used in this case:

Q_{ult} = 18,656.28 + (27,675.8)(0.20) + (26,564.8)(0.20)

= 18,656.28 + 5,535.16 + 5,312.97

= 29,504.41 lbs

The predicted loads are in agreement with actual load test results. This agreement implies that a more realistic empirical formula was developed, which can be used to better predict axial load capacities in expansive clay soils.

28.5 ft deep double helix (H-2, #32) with maximum shear of 29 #/in^2

Q_{ult} = 18,656.28 + 27,676.82(0.20) + 25,089.02(0.20)

= 18,656.28 + 5,535.16 + 5,017.80

= 29,209.24 lbs

34 ft deep single Helix (H-1, #27) with maximum shear of 27 #/in^2

Q_{ult} = 25,765.29 + 28,396.90 (0.20)

= 31,444.67 lbs

45 ft deep single Helix (H-1, #28) with maximum shear of 22 #/in^2

Q_{ult} = 20,995.45 + 31,348.55 (0.20)

= 27,265.16 lbs

Table 5.11 – 'Dry to Wet' Testing of Helical Anchors/Predicted vs. Actual

Pile #	Type (dbl/single)	Depth (ft)	Predicted Capacity(lbs)	Measured Capacity(lbs)
27	single	34'	31,645	29,550
28	single	45'	27,265	23,640
31	double	30	29,504	27,580
32	double	28.5'	29,209	27,580

An obvious observation from the present comparisons is that the double helix configuration appears to provide a more consistent axial capacity with the driving depth. As with depositional stratum in an alluvial plain, there is some inconsistency associated with soil strength parameters at this site. This would appear to explain certain inconsistency in shear strength of soil, which would be the primary reason for such a

wide difference in the single helix axial capacities. Also the use of disturbance factor to account for soil disturbance resulted in an accurate prediction of axial capacity.

Helical Piles Installed in April, 2005 and Tested in August, 2005.

Ultimate loads are predicted using the 'Individual Bearing Plate Method' and the disturbance factor for the trailing helix and shaft. These comparisons are made between ultimate loads and predicted loads and these results are presented in Table 5.12.

Table 5.12 – 'Wet to Dry' Testing of Helical Anchors/Predicted vs. Actual

Pile #	Type (double/single)	Depth (ft)	Predicted Capacity (lbs)	Measured Capacity (lbs)
25	single	34	31,645	24,720
26	single	26	23,182	25,544
29	double	27	28,914	26,780
30	double	32	29,898	28,016

It is obvious that the disturbance factor approach leads to an accurate prediction of capacity. With single helix piles the primary problem in the analysis is the approximate determination of shear strength of the soil at strains corresponding to those around the helical anchors.

5.2.5 Pressed Steel Piles

Based on soils properties, ultimate load capacity predictions for pressed steel piles would be calculated as follows using equation 2.17 from chapter 2:

$$Q_u = R_s + R_t \qquad (5.5)$$

$$= f_s \times A_s + q_t \times At$$

$$= \sum f_s \times A_s + q_t \times At$$

Based on the α method, the sleeve friction can be calculated using equation 2.20 from chapter 2:

$fs = c_a = \alpha \times c_u$ α from Figure 2.6

Ca from Figure 2.5

Table 5.13 - Soil Properties for Pressed Steel Piles -'Wet Condition'

Cross Section of Boring Logs using alpha from Fig. 9.18							
Soil Layer Depth	Shear Su (psi)	Shear Su (kPa)	A	Adhesion Ca (psi)	Adhesion Ca (kPa)	Adhesion Ca (psi)	Adhesion Ca (kPa)
0'-5'	10	69	0.95	9.5	65.55	8.99	62
5'-10'	18	124	0.95	17.1	111.6	10.44	72
10'-13'	42	290	0.3	12.6	87	7.25	50
13'-15'	17	117	0.75	12.75	87.75	10.59	73
20'-30'	32	221	0.3	9.6	66.3	7.25	50
30'-40'	40	276	0.3	12	82.8	7.25	50
40'-50'	19	131	0.6	11.4	78.6	10.15	70
50'-60'	22	152	0.4	8.8	60.8	9.28	60

Table 5.14 - Soil Properties for Pressed Steel Piles -'Dry Condition'

Cross Section of Boring Logs Using alpha from Fig. 9.18							
Soil Layer Depth	Shear Su (psi)	Shear Su (kPa)	A	Adhesion Ca (psi)	Adhesion Ca (kPa)	Adhesion Ca (psi)	Adhesion Ca (kPa)
0'-5'	29	200	0.95	10.29	71.03	7.54	52
5'-10'	28	193	0.3	14.9	102.83	7.25	50
10'-13'	42	290	0.45	9.76	67.29	7.25	50
13'-15'	17	117	0.45	9.49	65.44	10.59	73
20'-30'	32	221	0.3	9.61	66.29	7.25	50
30'-40'	40	276	0.3	14.25	98.32	7.25	50
40'-50'	19	131	0.3	8.92	61.55	10.15	70
50'-60'	22	152	0.99	10.73	74.02	9.28	64

Adhesion (C_a) from Figure 9.18 of the FHWA manual was used for a more conservative approach but the variance between $\alpha \times C_u$ was negligible as shown above. From this adhesion factor, axial capacity of pressed piles was estimated. Total Stress Method (α method) was adopted in this analysis. Details of this method can be found in the literature (FHWA 1996).

Table 5.15 - Prediction of 70 ft. Pressed Pile Capacity Based Upon Soil Properties

Side Resistance, lbs, R_{SN}		Steel Piles	Dry to Wet		
Pile #	**Depth (in)**	**Ca (psi)**	**fs- section**	**As (sq in)**	**∑fsAs**
14	60 (0-5')	8.99	539.4	9.03	4870.782
	60 (5-10')	10.44	626.4	9.03	5656.392
	60 (10-15')	8.4	504	9.03	4551.12
	60 (15-20')	8.4	504	9.03	4551.12
	120(20-30')	7.25	870	9.03	7856.1
	120(30-40')	7.25	870	9.03	7856.1
	120(40-50')	10.15	1218	9.03	10998.54
	120(50-60')	9.28	1113.6	9.03	10055.81
	120(60-70')	9.28	1113.6	9.03	10055.81
	70 ft				66451.77
Base Resistance, lbs, R_{BN}					
Pile #	Cu at tip	As (sq in)	Nc	Rt	
14	21.75	6.49	9	1270.4175	
Predicted Total Capacity, lbs, R_{TN}					67722.19

Based on this theoretical model the ultimate load estimated is 63 kips. For this same pile, the measured ultimate load was 41 kips showing significant differences between predicted and measured results. The following tables list both predicted and measured installed capacities. Measured or actual capacities are based on the load tests performed in the field at different time periods with different in situ soil conditions. It should be noted here that the installation was stopped when the load to push the piling material reached 50 kips. Hence, this load at the time of installation was taken as the ultimate load of this pile foundation.

Table 5.16 – Empirical Predictions of Axial Capacity of Pressed Steel Piles Using Soil Properties for 'Dry to Wet' Condition.

Pile #	Depth(ft)	Predicted Capacity (lb)	Measured Capacity (lb)	Installation Capacity (lb)
13	44	35,302	42,000	50,640
14	70	67,722	41,000	50,640
15	75	69,608	48,320	50,640
22	35	33,954	48,320	50,640
23	25	25,435	33,000	50,640
24	26	26,220	52,480	50,640

Table 5.17 – Empirical Predictions of Axial Capacity of Pressed Steel Piles Using Soil Properties for 'Wet to Dry' Conditions.

Pile #	Depth(ft)	Predicted Capacity (lb)	Measured Capacity (lb)	Installation Capacity (lb)
16	57	48,993	41,200	50,640
17	64	56,032	33,784	50,640
18	51	42,960	37,080	50,640
19	58	49,999	39,552	50,640
20	66	58,043	37,492	50,640
21	57	48,998	39,964	50,640

Calculations were also completed for each piling using adhesion values determined by the product of $\alpha \times S_u$, but the results showed very little improvement.

It is clear from the above results presented in the table that driven pile interpretation methods developed for the expansive clays for the pressed piles tend to predict capacities that are not in agreement with measured load capacities or installed load capacities. This requires further revision of the interpreted capacities using different approaches, including the use of CPT profiles from the same area.

A comparison of the CPT for the two probes shows a sudden spike in tip resistance between 6 ft and 10 ft and also in the vicinity of 30 ft. This spike would

confirm that the tip resistance may have been the overriding factor in determining not only axial capacity, but also the depth of penetration for pressed piles. As noted above, the installation capacity was 50 kips. When going from a dry season to a wet season, however, there was a loss in capacity for all but one of the pilings, which is a significant consideration for these pilings. The loss in capacity at one piling was inconsistent with the factors of safety on the other four pilings, which yielded consistent but low capacities. Since the present pressed pilings went beyond the zone of seasonal moisture change or active depth of this site, there appears to be less influence of an increase in moisture content on the measured capacities of pressed piles.

Another important observation is that the depth of penetration for pressed steel piles is more uniform when installed in wet season conditions than in dry seasons. The average length of piles installed in wet conditions is higher than the same in dry conditions. Though this pile length difference is expected, it raises an important question with respect to the approach used to install these piles in dry seasons. What would be consistent pile lengths needed to carry the intended loads in other seasonal environments?

It has been suggested by several researchers and European code practices that a direct approach using cone penetration test results should be used for estimating capacities of driven piles (Briaud 1988). A similar approach was followed using CPT soundings from this site and this approach provided reasonably good predictions.

Tables 5.18 and 5.19 present CPT results and a typical calculation to predict the pile capacities.

Table 5.18 – Cone Penetration Tests Results for Direct Tip Resistance and Side Friction

	CPT- 1		CPT-2	
Depth (ft)	**qt (psi)**	**fs (psi)**	**qt (psi)**	**fs (psi)**
0'-5'	416	6	347	6
5'-10'	486	22	500	23
10'-30'	347	9	347	7
30'-41'	356	8	305	6
41'-49'			305	5
49'-54'			694	3

Table 5.19 - Prediction of 70 ft Pressed Steel Pile Capacity Based Upon CPT, 'Dry to Wet Condition"

Side Resistance, lbs, R_{SN}	**Steel Piles**				
Pile #	**Depth (in)**	**fs (psi)**	**fs-section (psi)**	**As (sq in)**	**∑fsAsD**
14	60 (0-5')	6	360	9.03	3250.8
	60 (5-10')	22	320	9.03	11919.6
	60(10-15')	8	480	9.03	4334.4
	60(15-20')	8	480	9.03	4334.4
	120(20-30')	7	840	9.03	7585.2
	120(30-40')	5	600	9.03	5418
	120(40-50')	5	600	9.03	5418
	120(50-60')	5	600	9.03	5418
	120(60-70')	3	360	9.03	3250.8
	70 ft				50929.2
Base Resistance, lbs, R_{BN}					
Pile #	qt at tip	As (sq in)	Rt		
14	300	6.49	1947		
Predicted Total Capacity, lbs, R_{TN}					52876.2

Tables 5.20 and 5.21 present these results for steel piles. Results interpreted from CPT values are similar to those using borehole based soil property data.

Table 5.20 – Empirical Predictions of Axial Capacity of Pressed Steel Piles Using CPT for 'Dry to Wet' Condition.

Pile #	Depth(ft)	Predicted Capacity Using CPT Data	Predicted Capacity Using Soil Properties	Actual Capacity lbs	Installation Capacity lbs
13	44	40,989	35,302	42,000	50,640
14	70	52,876	67,722	41,000	50,640
15	75	54,501	69,608	48,320	50,640
22	35	34,133	33,954	48,320	50,640
23	25	29,884	25,435	33,000	50,640
24	26	30,642	26,220	52,480	50,640

Table 5.21 – Empirical Predictions of Axial Capacity of Pressed Steel Piles Using CPT for 'Wet to Dry' Condition

Pile #	Depth(ft)	Predicted Capacity in lbs Using CPT Data	Predicted Capacity in lbs Using Soil Properties	Actual Capacity lbs	Installation Capacity lbs
16	57	38,789	48,993	41,200	50,640
17	64	41,128	56,032	33,784	50,640
18	51	36,189	42,960	37,080	50,640
19	58	39,223	49,999	39,552	50,640
20	66	41,662	58,043	37,492	50,640
21	57	38,789	48,993	39,964	50,640

Overall, axial capacity predictions vary considerably even with the CPT method and they are different from the measured axial load capacities. This difference indicates that the present methods similar to those used for driven piles tend to predict higher capacities than the measured loads and hence such use of the driven pile estimation method for pressed piles should be thoroughly examined. This discrepancy is attributed to the differences in installation procedures between driven piles and pressed piles. One is similar to dynamic driving mechanism and the other is more close to quasi-static penetration mechanism. One would expect the CPT, which is similar to the pressed piles,

will probably yield better results if calibrated using different material constants than those developed for driven piles.

5.2.6 Pressed Concrete Piles

Using the same format and empirical formulas as delineated in the above section, the prediction of axial capacity of pressed concrete piles can be estimated as follows:

Based upon soil properties, capacity predictions would be calculated as follows:

$$Q_u = R_s + R_t$$

$$= f_s \times A_s + q_t \times A_t$$

$$= \sum f_s \times A_s + q_t \times At$$

Using the α method as recommended by driven pile literature (FHWA 1996):

$fs = c_a = \alpha \times c_u$ α from Figure 2.5

c_a from Figure 2.6

The material coefficients used between soil and pressed pile material, which is concrete in this case, will be different than for steel piles but the application and method of estimation will be the same.

Tables 5.22 and 5.23 present cohesion and adhesion from subsoil layers in different units, psi and kPa. Table 5.24 presents a typical prediction of axial load for the pressed concrete pile.

Table 5.22 Soil Properties for Pressed Concrete Piles 'Wet Condition'

Cross Section of Boring Logs using alpha using Fig. 9.18							
Soil Layer Depth	Shear Su (psi)	Shear Su (kPa)	A	Adhesion Ca (psi)	Adhesion Ca (kPa)	Adhesion Ca (psi)	Adhesion Ca (kPa)
0'-5'	10	69	0.95	9.5	65.55	10.15	70
5'-10'	18	124	0.3	17.1	111.6	12.04	83
10'-13'	42	290	0.45	12.6	87	8.4	60
13'-15'	17	117	0.45	12.75	87.75	12.47	86
20'-30'	32	221	0.3	0.6	66.3	8.4	60
30'-40'	40	276	0.3	12	82.8	8.4	60
40'-50'	19	131	0.3	11.4	78.6	11.6	80
50'-60'	22	152	0.99	8.8	60.8	9.86	68

Table 5.23 Soil Properties for Pressed Concrete Piles 'Dry Condition'

Cross Section of Boring Logs using alpha from Fig. 9.18							
Soil Layer Depth	Shear Su (psi)	Shear Su (kPa)	A	Adhesion Ca (psi)	Adhesion Ca (kPa)	Adhesion Ca (psi)	Adhesion Ca (kPa)
0'-5'	29	200	0.95	10.29	71.03	8.4	60
5'-10'	28	193	0.3	14.9	102.83	8.4	60
10'-13'	42	290	0.45	9.76	67.29	8.4	60
13'-15'	17	117	0.45	9.49	65.44	12.47	86
20'-30'	32	221	0.3	9.61	66.29	8.4	60
30'-40'	40	276	0.3	14.25	98.32	8.4	60
40'-50'	19	131	0.3	8.92	61.55	11.6	80
50'-60'	22	152	0.99	10.73	74.02	9.86	68

Table 5.24 - Prediction of Pressed Concrete Pile Capacity Based Upon Soil Properties for 'Dry to Wet' Condition

Side Resistance, lbs, R_{SN}					
Pile #	Depth (in)	Ca (psi)	fs-section	As (sq in)	∑fsAs
9	60 (0-5')	10.15	609	18.85	11479.65
	60 (5-10')	12.04	722.4	18.85	13617.24
	60 (10-15')	8.4	504	18.85	9500.4
	60 (15-20')	12.47	748.2	18.85	14103.57
	68(20-25.7)	8.7	591.6	18.85	11151.66
	25.67 ft				59852.52
Base Resistance, lbs, R_{BN}					
Pile #	Su at tip	As (sq in)	Nc	Rt	
9	32	28.27	9	2141.76	
Predicted Total Capacity, lbs, R_{TN}					67994.28

Tables 5.25 and 5.26 present capacities from different seasonal conditions. The predicted capacity of concrete pressed pile #9 is close to 60 kips where as the actual pile load test resulted in an axial capacity of 68 kips. The majority of the pressed piles have yielded higher ultimate loads than those interpreted. Additionally, from dry to wet testing, three out of six pressed concrete piles experienced higher loads than installed loads and the other three yielded lower loads than installed loads

Table 5.25 – Empirical Predictions of Axial Capacity of Pressed Concrete Piles Using Soil Properties, 'Dry to Wet' Condition

Pile #	Depth(ft)	Predicted Capacity (lbs)	Measured Capacity (lbs)	Installation Capacity (lbs)
1	7.67	31,426	29,000	50,000
2	10.17	34,319	37,000	50,000
3	27.42	71,474	68,566	50,000
7	15.67	41,398	50,400	50,000
8	10.67	39,596	39,000	50,000
9	25.67	67,994	68,000	50,000

Table 5.26 – Empirical Predictions of Axial Capacity of Pressed Concrete Piles Using Soil Properties, 'Wet to Dry' Condition

Pile #	Depth(ft)	Predicted Capacity (lbs)	Measured Capacity (lbs	Installation Capacity (lbs)
4	24.67	60,316	57,940	50,000
6	19.67	48,000	61,800	50,000
10	24.67	60,316	65,920	50,000
12	28.67	67,860	61,800	50,000

The piles pushed below the zone of seasonal moisture change have shown higher capacities due to increase in shear strength or cohesion during dry seasons. The three piles above the depths of seasonal moisture change (normally considered 12 ft in this area), lost a significant amount of capacity (22% to 42%) when tested in wet conditions. Since dry seasonal times normally produce an increase in shear strength in the active zone the result is that pile depths will be smaller when installed during this season. However, in the wet season, due to loss of shear strength from moisture increase their axial capacities are reduced.

When tested in dry conditions, all piles yielded higher loads than those used during installation. Such variation and lack of consistent prediction of ultimate loads indicate the need for further research and better estimation procedures for calculating

predicted capacities of these piles. Use of driven pile methods tends to provide results that are not in sync with measured loads. Similar to the previous section, axial capacities are predicted using CPT data and methodology (Tables 5.27, 5.28 and 5.29). Please note in this approach, side friction measured from CPT was directly used as side friction for pressed piles. Such approach is considered acceptable since both CPT and pressed piles do experience similar penetration mechanisms, i.e. quasi-static penetrations.

Table 5.27 – Prediction of 25.67 ft Pressed Concrete Pile Capacity Based Upon CPT, 'Dry to Wet' Condition

Side Resistance, lbs, R_{SN}					
Pile #	**Depth (in)**	**fs (psi)**	**fs-section (psi)**	**As (sq in)**	**∑fsAsD**
9	60 (0-5')	6	360	18.85	6786
	60 (5-10')	22	1320	18.85	24882
	60 (10-15')	8	480	18.85	9048
	60 (15-20')	8	480	18.85	9048
	68(20-25.7')	7	476	18.85	8972.6
		5	0	18.85	0
		5	0		0
		5	0		0
		3	0		0
	25.67 ft				58736.6
Base Resistance, lbs, R_{BN}					
Pile #	q_t at tip	As (sq in)	Rt		
9	347	28.27	9809.7		
Predicted Total Capacity, lbs, R_{TN}					68546.3

Table 5.28 – Empirical Predictions of Axial Capacity of Pressed Concrete Piles Using CPT for 'Dry to Wet' Condition

Pile #	Depth(ft)	Predicted Capacity in lbs Using CPT Data	Predicted Capacity in lbs Using Bore Hole Data	Actual Capacity In lbs	Installation Capacity In lbs
1	7.67	34,191	31,426	29,000	50,000
2	10.17	46,105	34,319	37,000	50,000
3	27.42	71,845	71,474	68,566	50,000
7	15.67	51,732	41,398	50,400	50,000
8	10.67	44,795	39,596	39,000	50,000
9	25.67	68,546	67,994	68,000	50,000

Table 5.29 – Empirical Predictions of Axial Capacity of Pressed Concrete Piles Using CPT for 'Wet to Dry' Condition.

Pile #	Depth(ft)	Predicted Capacity in lbs Using CPT Data	Predicted Capacity in lbs Using Bore Hole Data	Actual Capacity In lbs	Installation Capacity In lbs
4	24.67	66,963	60,316	57,940	50,000
6	19.67	58,970	48,000	61,800	50,000
10	24.67	66,963	60,316	65,920	50,000
12	28.67	70,450	67,860	61,800	50,000
5*					
11*					

*Pilings broke during installation

As evidenced by the above table, the pressed concrete pilings can be predicted somewhat closer to measured capacities when CPT side friction results are used. This approach performs better than those based on undrained soil strength data but it still requires further calibration and verification. The reasons for better agreement are

attributed to the similar quasi-static penetration mechanisms used to push the cone penetrometer and pressed concrete pile.

The important finding from this investigation is that the use of installation capacity is not necessarily resulted in as an ultimate load for all seasons. Rather this method resulted in different depths when installed in dry seasons and produces uniform depths in wet seasons. Due to such high variation in installation depth and their dependency on seasonal installation procedures, as well as lack of calibrated engineering models to predict the axial capacities of the pressed piles, engineers should use their judgment in the selection and use of this method. Further research in this method will help in answering some of these limitations.

5.3 Summary

Prediction of drilled shafts and augercast piles were made with good accuracy using undrained cohesive properties of soil layers. Strength properties of upper strata have a major bearing on predicted axial compression capacity due to differences in strength of upper layers (0’ to 10’). Helical anchors were accurately predicted using the individual bearing plate method but with the double helix there was a need to adjust the trailing helix with a disturbance factor. This approach reduced helix area contribution to ultimate axial capacity. Prediction of pressed steel pilings does not appear to be accurate when using soil strength properties. The method that provided better predictions of pressed pilings’ capacities is the method that has used CPT side friction data for pilings friction resistance.

CHAPTER 6

COMPARISONS BETWEEN PREDICTED AND MEASURED CAPACITY

6.1 Introduction

This chapter compares predicted values for the different underpinning elements to test results for this research. There is also a comparison between all foundations with respect to axial compression results and deflection at time of ultimate capacity.

It should be mentioned that the observations noted here are based on a few underpinning foundations tested in this research. Though more numbers of data from testing underpinnings would have been ideal and statistically important, the present numbers tested are practically sufficient to deduce crucial observations on the axial load transfer performance of these foundations.

6.2 Comparison of Predicted to Measured Axial Capacity

6.2.1 Straight Drilled Shafts

Predictions of axial compressive capacity for the straight drilled shafts were made using the soil information compiled from soil property data interpreted from CPT results. As shown in Tables 6.1 and 6.2 as well as Figures 6.1 to 6.4, the predictions are close to the measured axial loads except for one pier, which exceeded prediction capacity from both ‘dry to wet’ and ‘wet to dry’ testing conditions. As noted in the soil borings and also with the CPT, there are lenses in this soil that have higher shear strength and this results in higher resistance for piers that are installed through these hard discontinuous layers.

Table 6.1 - Predicted vs. Tested Capacity for Straight Shafts, 'Dry to Wet' Condition

Pier #	Depth(ft)	Predicted Capacity (lb)	Actual Capacity (lb)
42	15	104,390	126,410
43	15	104,390	104,160
44	15	104,390	100,990

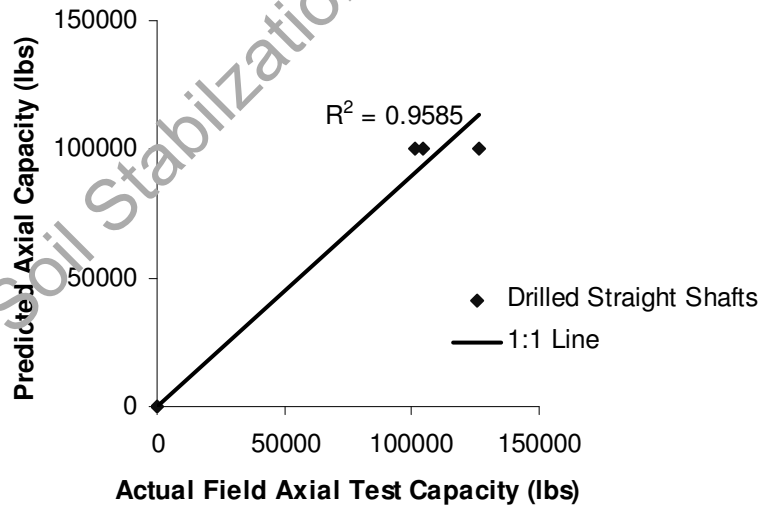

Figure 6.1 - Comparisons of Predicted to Measured Axial Capacities of Straight Shafts, 'Dry to Wet' Condition

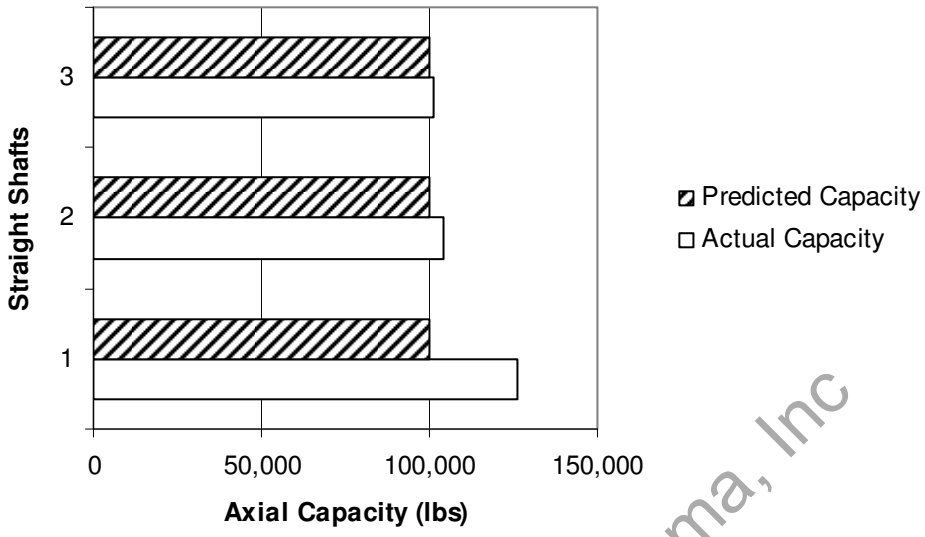

Figure 6.2 - Comparisons of Predicted to Measured Axial Capacities of Straight Shafts, 'Dry to Wet' Condition

Table 6.2 - Predicted vs. Tested Capacity for Straight Shafts 'Wet to Dry' Condition

Pier #	Depth(ft)	Predicted Capacity (lbs)	Actual Capacity (lbs)
39	15	99,165	106,600
40	15	99,165	123,000
41	15	99,165	102,500

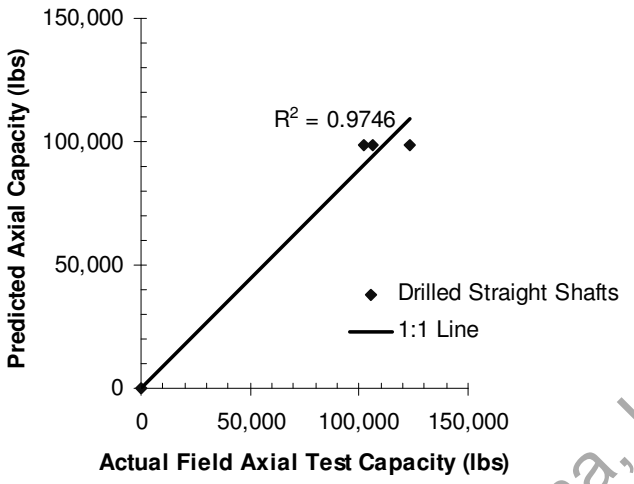

Figure 6.3 - Comparisons of Predicted to Measured Axial Capacities of Straight Shafts, 'Wet to Dry' Condition

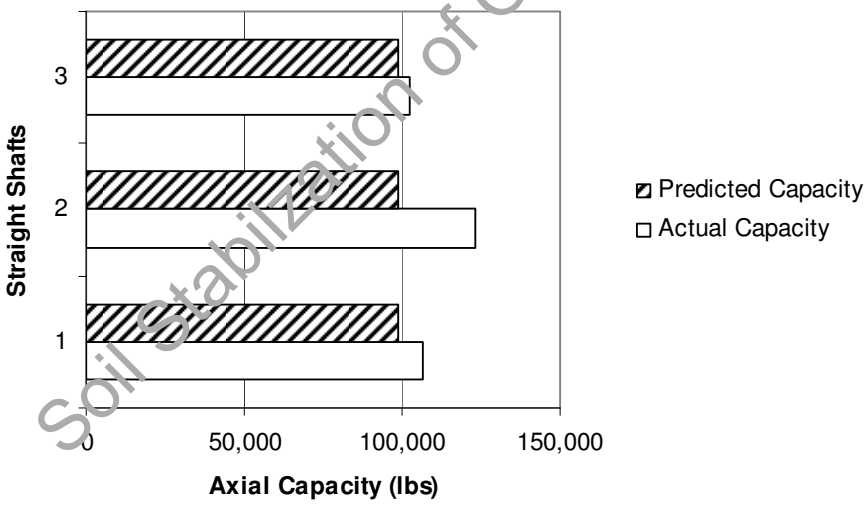

Figure 6.4 - Comparisons of Predicted to Measured Axial Capacities of Straight Shafts, 'Wet to Dry' Condition

Figures 6.1 and 6.3 would have been ideal when the number of tests are higher than 10. The R^2 comparisons in such cases would provide explanations on the prediction capacities of the models used. Here, in this research, this type of comparison figure is still used, just to show the existence of a trend or a correlation between predicted capacities and actual measured capacities. Based on the results shown in Figures 6.1 and 6.3, it can be mentioned that the existing theoretical model to predict axial loads of straight shafts is providing very good predictions for straight piers tested in both seasonal conditions of this research.

6.2.2 Drilled Belled/Under-reamed Shafts

Predictions of Axial Compressive Capacity for the drilled belled shafts were made using soil property data interpreted from CPT results. Tables 6.3 and 6.4 as well as Figures 6.5 to 6.8 present predicted and measured capacities of the present belled shafts.

Table 6.3 - Predicted vs. Tested Capacity for Drilled Belled Shafts, 'Dry to Wet' Condition

Pier #	Depth(ft)	Predicted Capacity (lbs)	Actual Capacity (lbs)
36	15	169,110	180,790
37	15	169,110	172,540
38	15	169,110	168,380

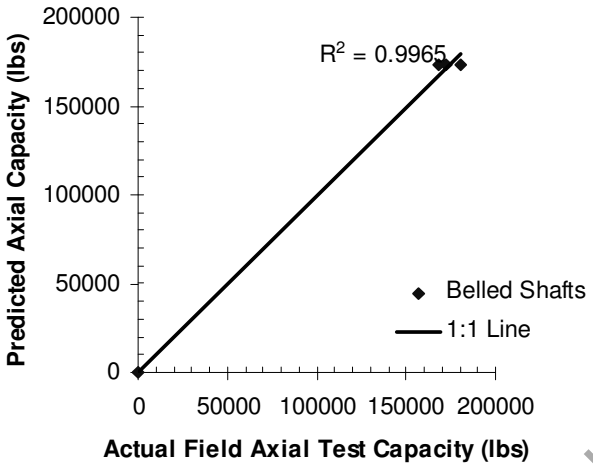

Figure 6.5 - Comparisons of Predicted to Measured Axial Capacities of Drilled Belled Shafts, 'Dry to Wet' Condition

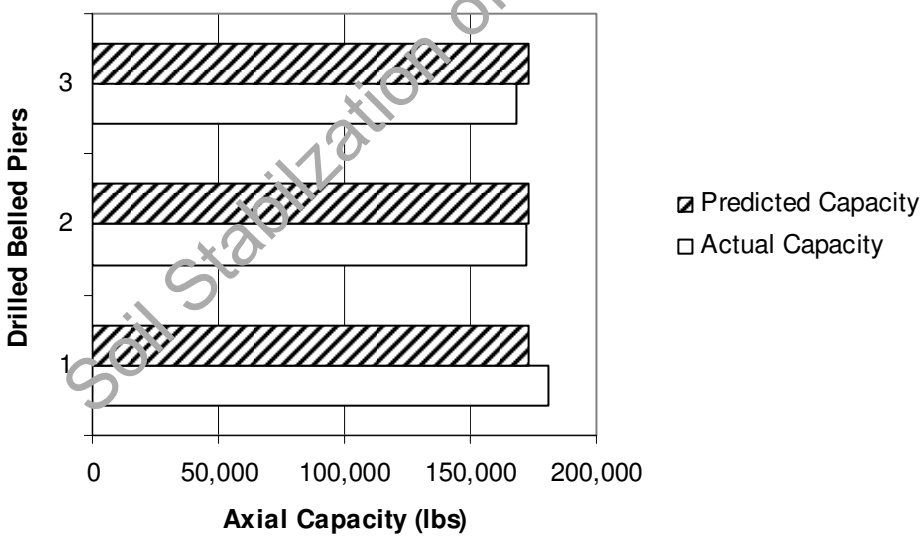

Figure 6.6 - Comparisons of Predicted to Measured Axial Capacities of Drilled Belled Shafts, 'Dry to Wet' Condition

Table 6.4 - Predicted vs. Tested Capacity for Drilled Belled Shafts, 'Wet to Dry' Condition

Pier #	Depth(ft)	Predicted Capacity (lbs)	Actual Capacity (lbs)
33	15	176,326	165,500
34	15	176,326	165,500
35	15	176,326	157,060

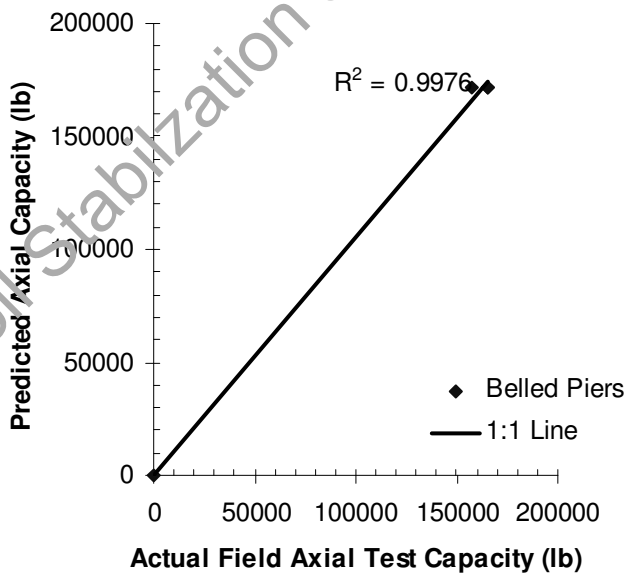

Figure 6.7 - Comparison of Predicted to Measured Axial Capacity Drilled Belled Shafts, 'Wet to Dry' Condition

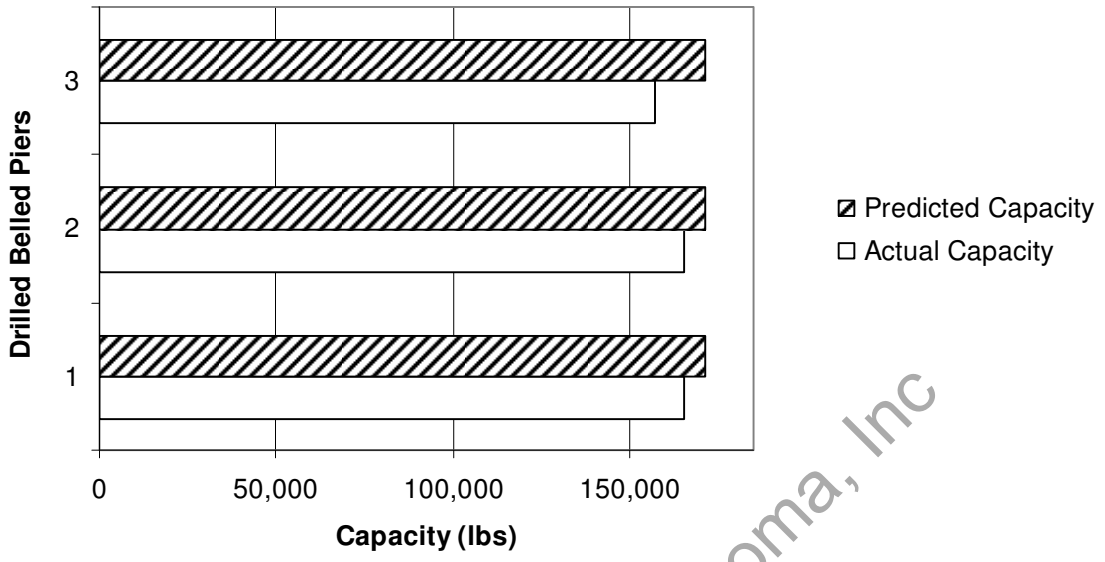

Figure 6.8 - Comparisons of Predicted to Measured Axial Capacity Drilled Belled Shafts, 'Wet to Dry'

As shown by the comparisons in Figure 6.5 and 6.7, a strong correlation exists between measured and predicted capacities of belled piers, implying that the procedure provided by O'Neill and Reese resulted in accurate predictions of measured axial loads of the belled piers. Overall, prediction analyses of both types of drilled shafts (straight and belled) installed at different seasonal conditions showed that the prediction models can be confidently used to design these shafts in expansive soil conditions.

6.2.3 Augercast Piles

Predictions of Axial Compressive Capacity for the augercast piles were made using soil information from CPT data in the same manner as those used for straight shafts and these results were used in Tables 6.5 and 6.6 as well as Figures 6.9 to 6.12. Two of

these piles tested were close to the same predicted loads, with one pile showing a slightly high ultimate capacity.

Table 6.5 - Predicted vs. Tested Capacity for Augercast Piles, 'Dry to Wet' Condition

Pier #	Depth(ft)	Predicted Capacity (lbs)	Actual Capacity (lbs)
47	15	104,390	121,120
49	15	104,390	105,220
50	15	104,390	100,990

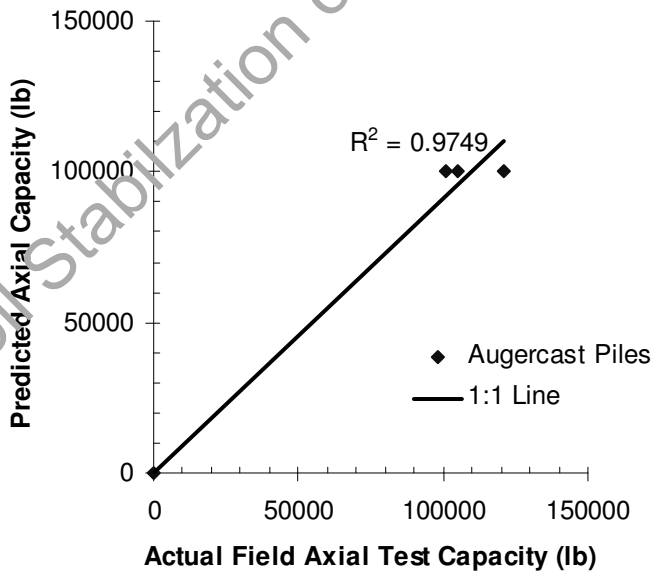

Figure 6.9 - Comparison of Predicted to Measured Axial Capacity of Augercast Piles, 'Dry to Wet' Condition

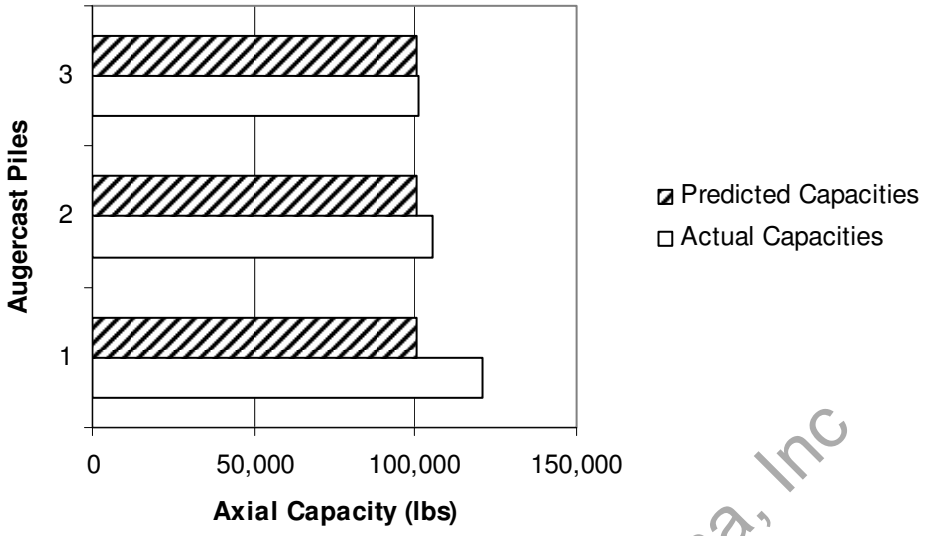

Figure 6.10 - Comparison of Predicted to Measured Axial Capacity of Augercast Piles, 'Dry to Wet' Condition

Table 6.6 Predicted vs. Tested Capacity for Augercast Piles, 'Wet to Dry' Condition

Pier #	Depth(ft)	Predicted Capacity (lbs)	Actual Capacity (lbs)
45	15	99,165	110,030
46	15	99,165	106,760
48	15	99,165	106,760

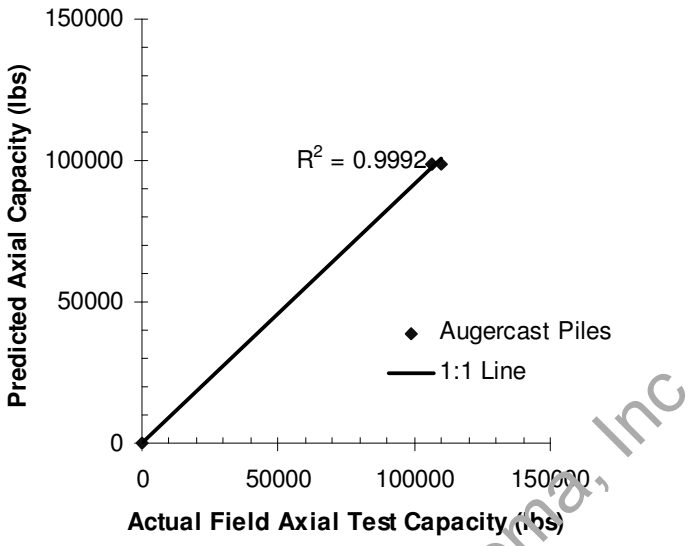

Figure 6.11 - Comparison of Predicted to Measured Axial Capacity of Augercast Piles, 'Wet to Dry' Condition

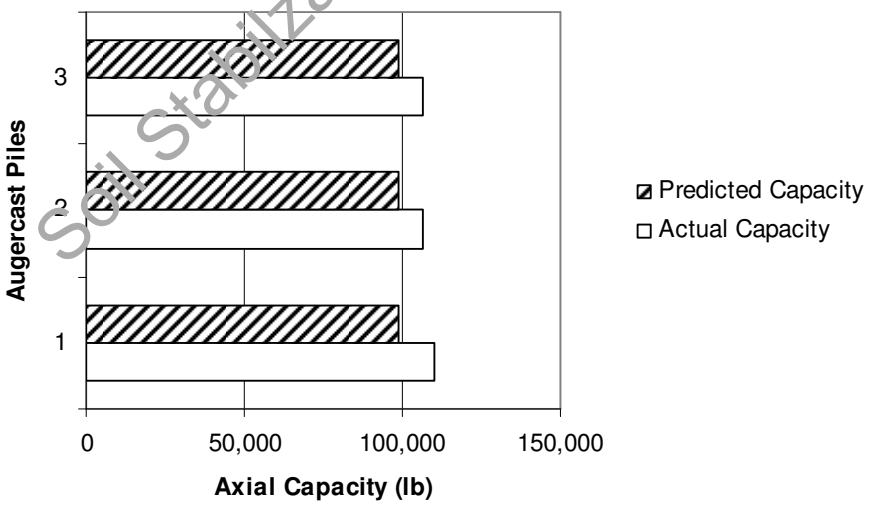

Figure 6.12 - Comparison of Predicted to Measured Axial Capacity of Augercast Piles, 'Wet to Dry' Condition

Overall, the prediction of axial capacity was accurate using the same formulae for augercast piles as those used for the drilled straight shafts. Therefore, it can be reasonable that in clay soil, with open hole shafts, capacities should be the same for both augercast piles and straight drilled shafts.

6.2.4 Helical Anchors

Predictions of Axial Compressive Capacity for the helical anchors were made using soil boring information from four borings on site in accordance with the Individual Bearing Plate Method and the added factoring of a disturbance factor for the double flight helix piles. As shown below in Tables 6.7 and 6.8 as well as in Figures 6.13 to 6.16, this method of predicting capacities was close to measured capacities on this site.

Table 6.7 - Predicted vs. Tested Capacity for Helical Anchors, 'Dry to Wet' Condition

Pile #	Type (dbl/single)	Depth (ft)	Predicted Capacity (lbs)	Actual Capacity (lbs)
27	single	34'	31,645	29,550
28	single	45'	27,265	23,640
31	double	30	29,504	27,580
32	double	28.5'	29,209	27,580

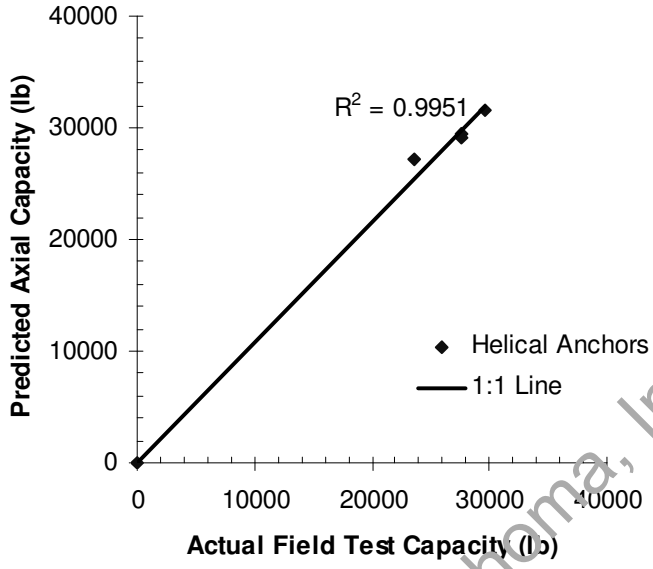

Figure 6.13 Comparison of Predicted to Measured Axial Capacity of Helical Anchors, 'Dry to Wet' Condition

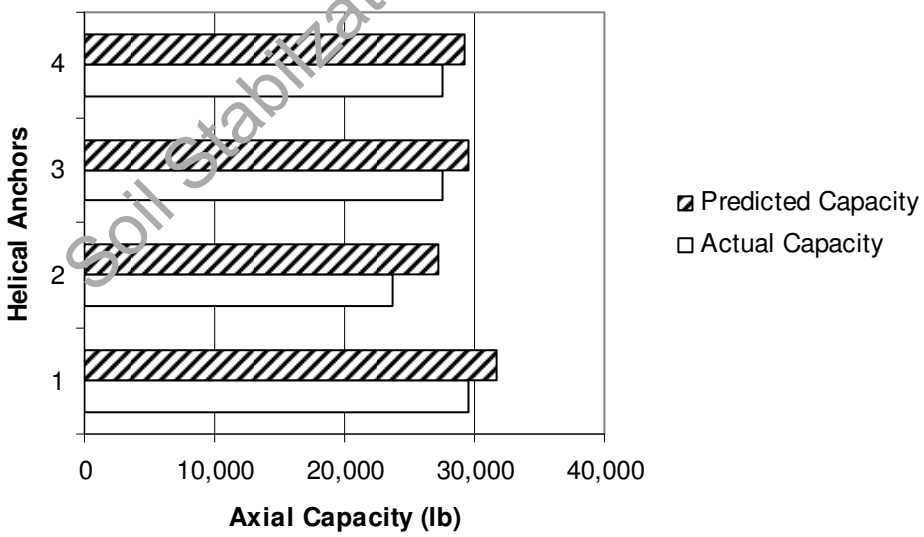

Figure 6.14 - Comparison of Predicted to Measured Axial Capacity of Helical Anchors, 'Dry to Wet' Condition

Table 6.8 - Predicted vs. Tested Capacity for Helical Anchors, 'Wet to Dry' Condition

Pile #	Type (dbl/single)	Depth (ft)	Predicted Capacity (lbs)	Actual Capacity (lbs)
25	single	34	31,645	24,720
26	single	26	23,182	25,544
29	double	27	28,914	26,780
30	double	32	29,898	28,016

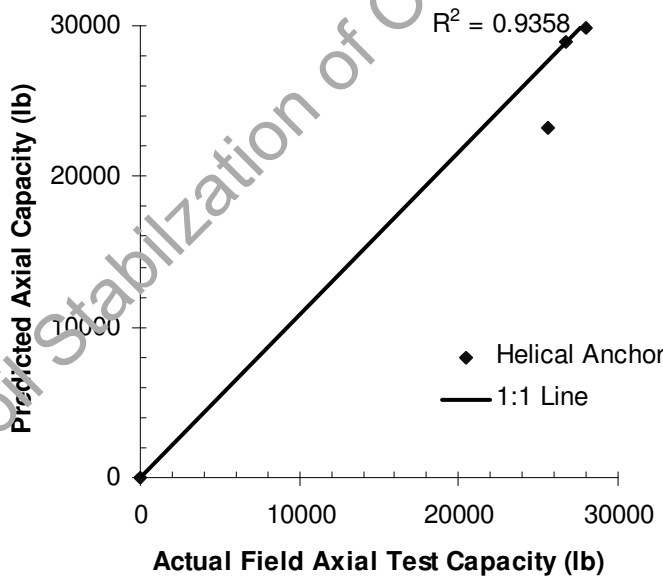

Figure 6.15 - Comparison of Predicted to Measured Axial Capacity of Helical Anchors, 'Wet to Dry' Condition

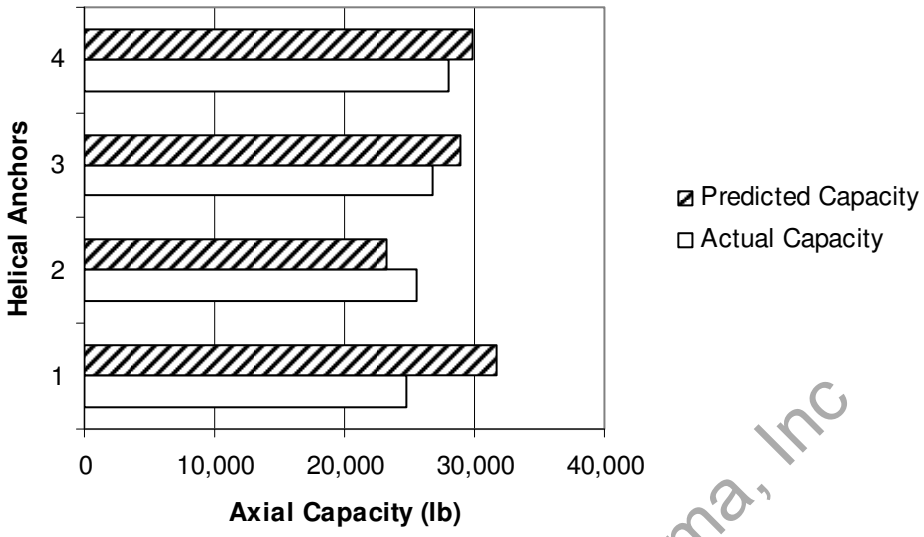

Figure 6.16 - Comparison of Predicted to Measured Axial Capacity of Helical Anchors, 'Wet to Dry' Condition

As shown by the comparison plots of Figures 6.13 and 6.15, predictions of the helical anchors were good using soil information along with the added factor on the double helix of a disturbance factor. Due to extensive soil sampling being taken at five feet intervals, there is always the possibility that lenses with high or low shear strength may exist. This can influence the performance of the helical anchor and this is probably reflected in the single helix that gains most of its strength from end resistance. The following figures show this discrepancy by breaking out the single and double performance comparison with predicted capacities.

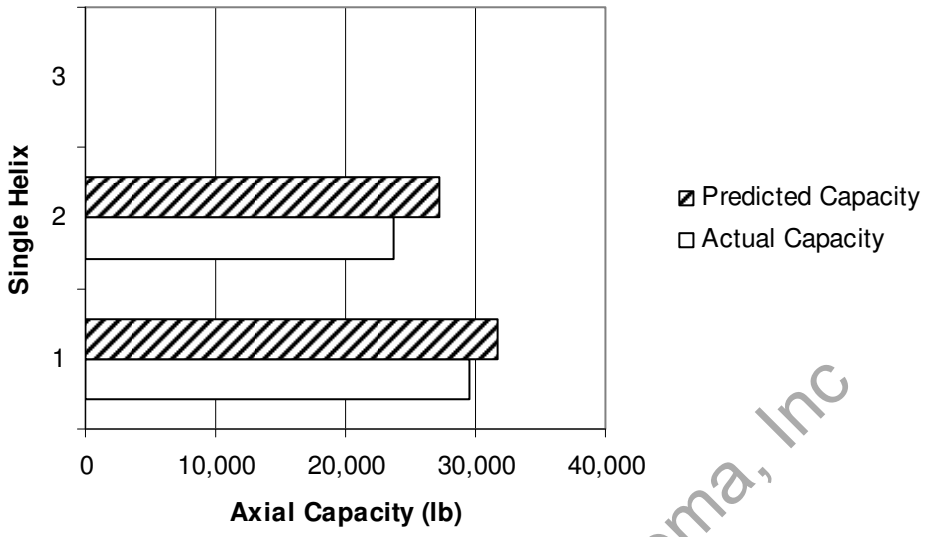

Figure 6.17 - Comparison of Predicted to Measured Axial Capacity of Single Helical Anchors, 'Dry to Wet' Condition

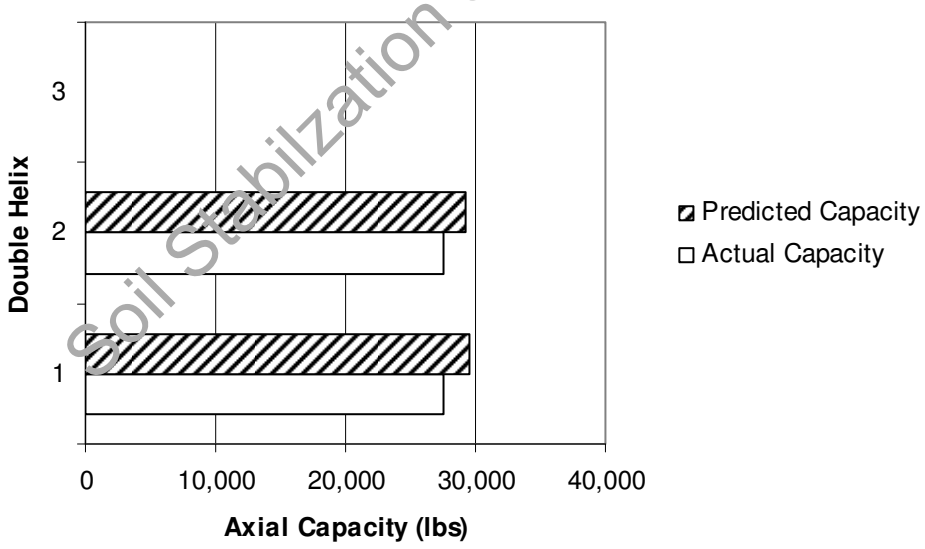

Figure 6.18 - Comparison of Predicted to Measured Axial Capacity of Double Helical Anchors, 'Dry to Wet' Condition

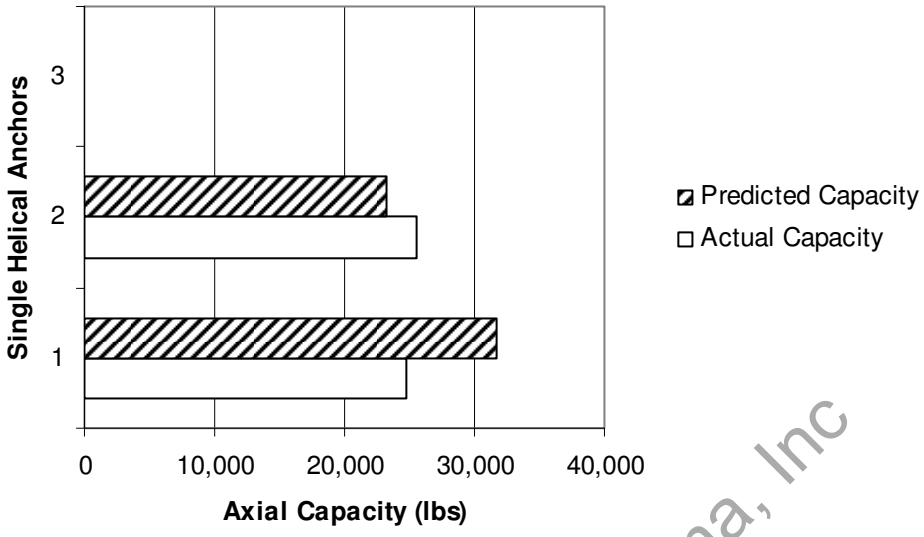

Figure 6.19 - Comparison of Predicted to Measured Axial Capacity of Single Helical Anchors, 'Wet to Dry' Condition

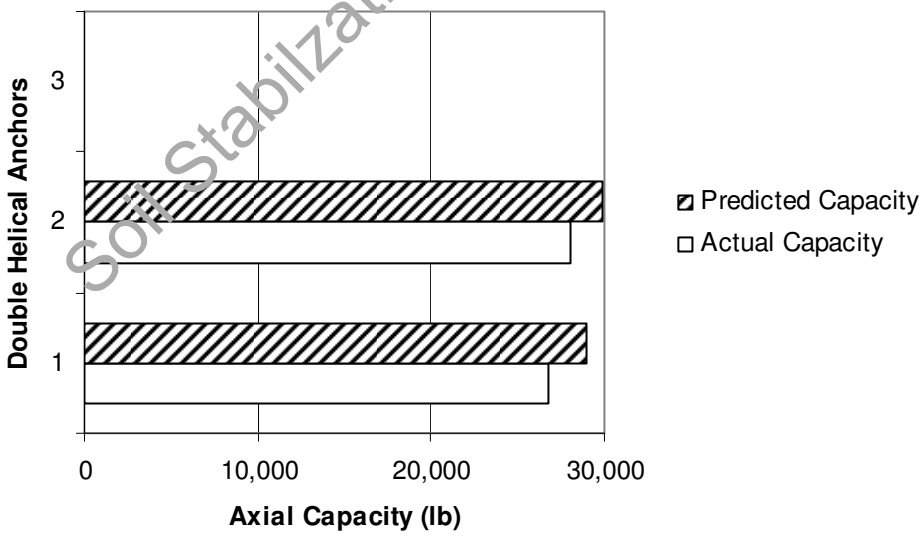

Figure 6.20 - Comparison of Predicted to Measured Axial Capacity of Double Helical Anchors, 'Wet to Dry' Condition

Figures 6.17-6.20 show that the predictions are good for both helical types with slightly lower values being predicted for single helix piles. In the case of double helix pile, predictions are improved via the use of the individual plate method with a disturbance factor that accounted for the trailing helix and shaft by closely simulating the penetration mechanism around the double helix pile. In the case of single helix, however, there appears to be difficulty in predicting the shear strength around the flat plate of the helix. As a result, predictions are slightly on low side. Nevertheless, both prediction methodologies provided reasonably good interpretation of axial load capacities.

6.2.5 Pressed Steel Piles

Predictions of axial compressive capacity for the pressed steel piles were made using soil properties measured from soil strata. Load capacities are then determined by following the total stress (α) method. The following observations are based on the comparisons between predicted and actual field load tests on the foundations. Predictions shown here are based on soil properties determined from borehole sample test data.

Table 6.9 - Predicted vs. Tested Capacity for Pressed Steel Piles Using Soil Properties, 'Dry to Wet' Condition

Pile #	Depth(ft)	Predicted Capacity (lbs)	Actual Capacity (lbs)	Installation Capacity (lbs)
13	44	35,302	42,000	50,640
14	70	67,722	41,000	50,640
15	75	69,608	48,320	50,640
22	35	33,954	48,320	50,640
23	25	25,435	33,000	50,640
24	26	26,220	52,480	50,640

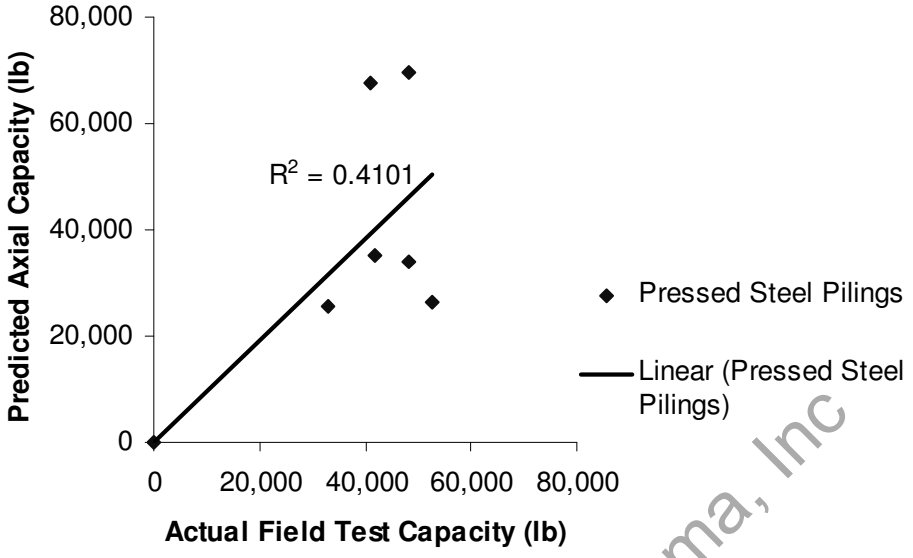

Figure 6.21 - Comparison of Predicted to Measured Axial Capacity of Pressed Steel Piles Using Soil Properties, 'Dry to Wet' Condition

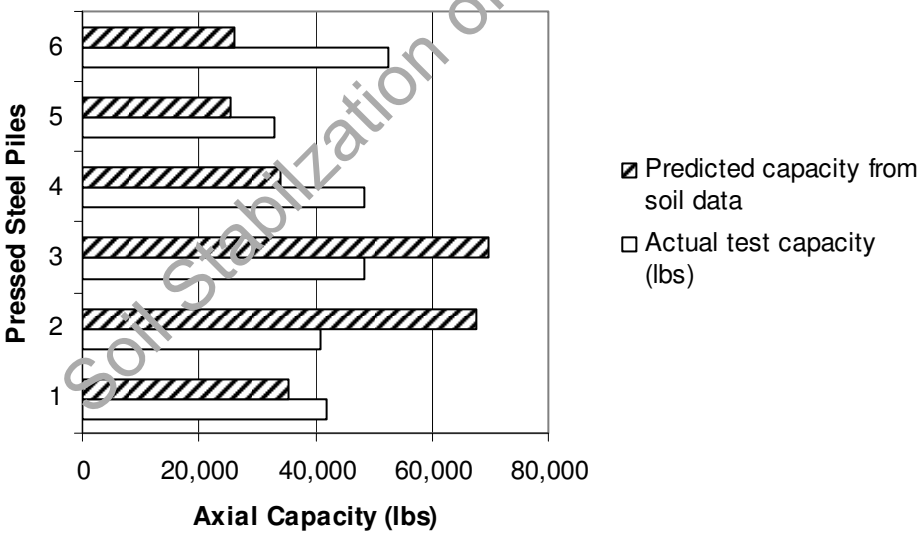

Figure 6.22 - Comparison of Predicted to Measured Axial Capacity for Pressed Steel Piles Using Soil Properties, 'Dry to Wet' Condition

Table 6.10 - Predicted vs. Tested Capacity for Pressed Steel Piles Using Soils Properties, 'Wet to Dry' Condition

Pile #	Depth(ft)	Predicted Capacity (lbs)	Actual Capacity (lbs)	Installation Capacity (lbs)
16	57	48,993	41,200	50,640
17	64	56,032	33,784	50,640
18	51	42,960	37,080	50,640
19	58	49,999	39,552	50,640
20	66	58,043	37,492	50,640
21	57	48,993	39,964	50,640

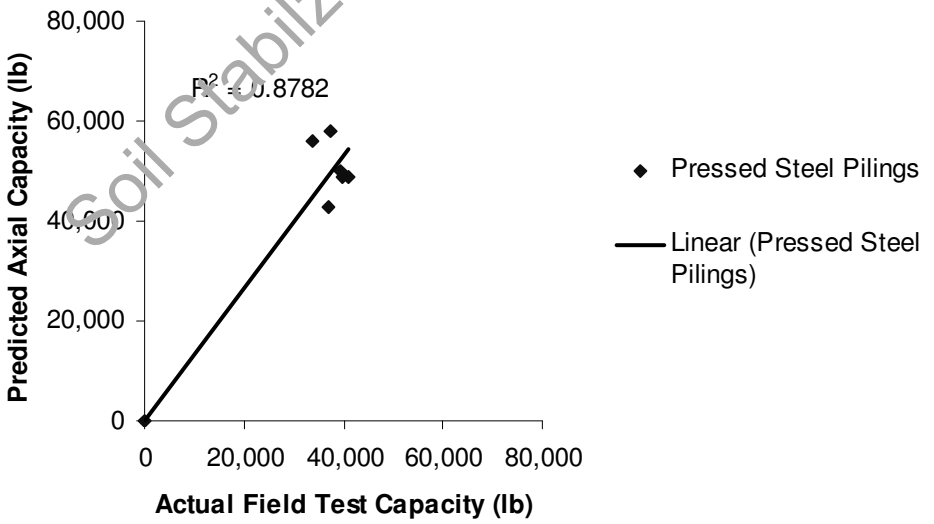

Figure 6.23 - Comparison of Predicted to Measured Capacity of Pressed Steel Pilings Using Soil Properties, 'Wet to Dry' Condition

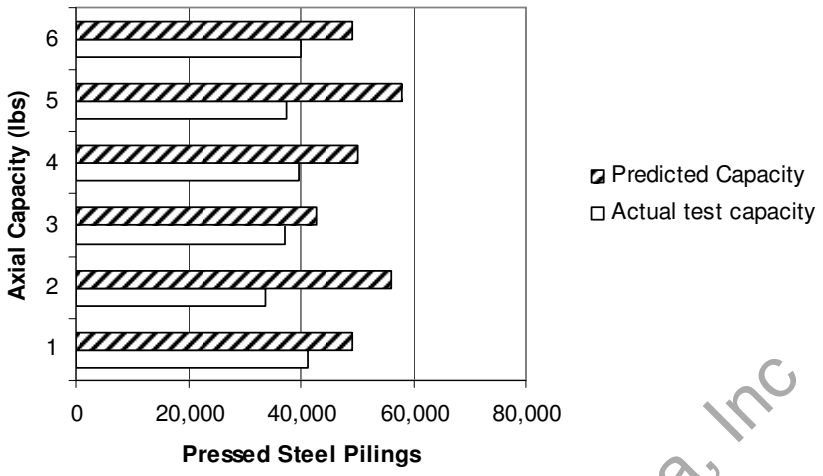

Figure 6.24 Comparison of Predicted to Measured Field Capacity of Pressed Steel Pilings Using Soil Properties, 'Wet to Dry' Condition

An important finding from these figures is that the prediction of axial capacity using soil properties did not result in accurate predictions. The following tables and results show similar comparisons with prediction capacities from CPT side friction test data. These predictions are close to measured loads suggesting the significance using shear strengths of residual state to be used for side friction calculations. It should be noted that this variation is attributed to penetration mechanisms that result in soil being in residual state with the pressing mechanism.

Table 6.11 Predicted vs. Measured Capacities for Pressed Steel Piles Using CPT, 'Dry to Wet' Condition

Pile #	Depth (ft)	Predicted Capacity (lbs)	Actual Capacity (lbs)	Installation Capacity (lbs)
13	44	40,989	42,000	50,640
14	70	52,876	41,000	50,640
15	75	54,501	48,320	50,640
22	35	34,133	48,320	50,640
23	25	29,884	33,000	50,640
24	26	30,642	52,480	50,640

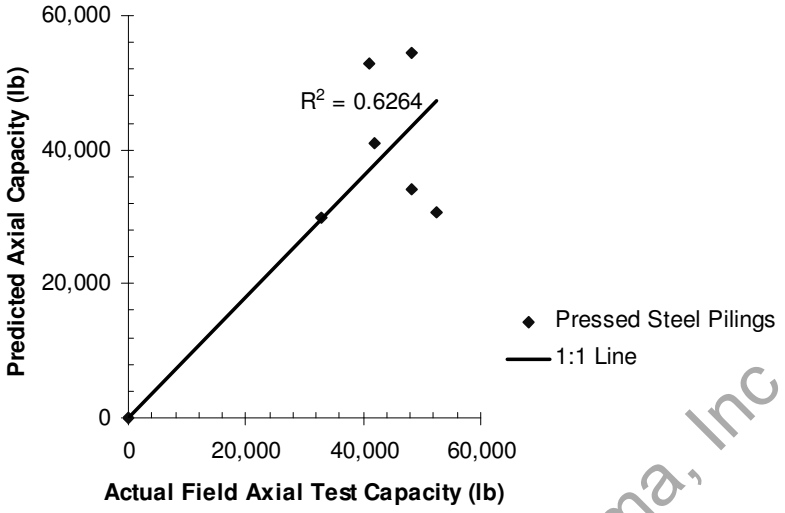

Figure 6.25 - Comparison of Predicted to Measured Axial Capacity of Pressed Steel Pilings Using CPT, 'Dry to Wet' Condition

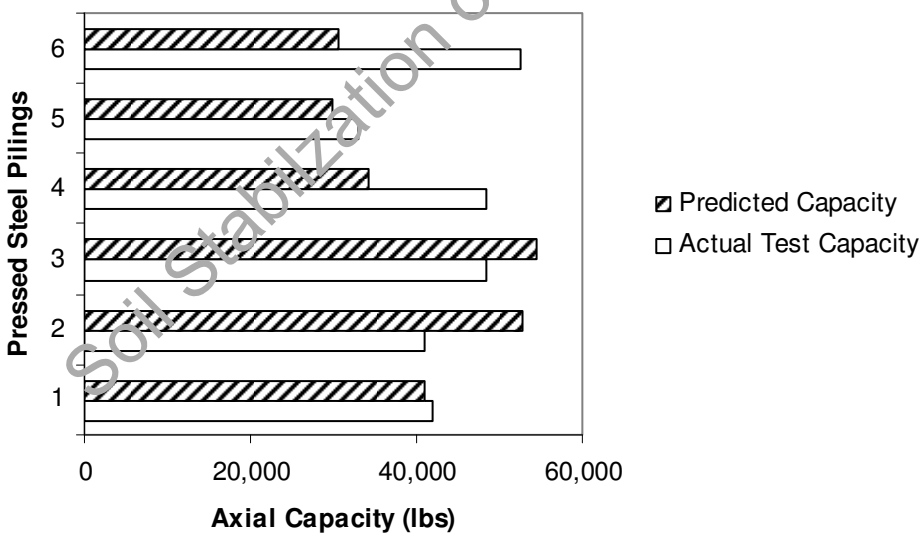

Figure 6.26 - Comparison of Predicted to Measured Axial Capacity of Pressed Steel Piles Using CPT, 'Dry to Wet' Condition

Table 6.12 - Predicted vs. Measured Capacity for Pressed Steel Piles Using CPT, 'Wet to Dry' Condition

Pile #	Depth(ft)	Predicted Capacity (lbs)	Actual Capacity (lbs)	Installation Capacity (lbs)
16	57	48,000	41,200	50,640
17	64	50,926	33,784	50,640
18	51	44,749	37,080	50,640
19	58	48,542	39,552	50,640
20	66	51,576	37,492	50,640
21	57	48,000	39,964	50,640

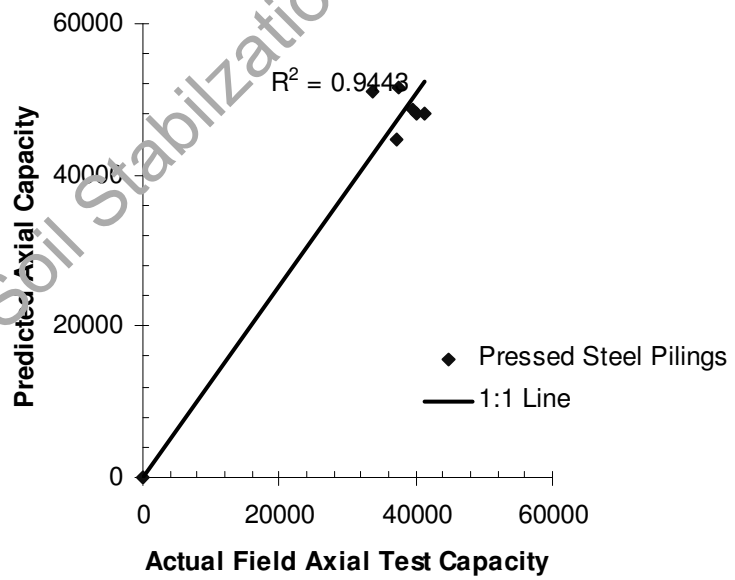

Figure 6.27 - Comparison of Predicted to Measured Field Capacity of Pressed Steel Piles using CPT, 'Wet to Dry' Condition

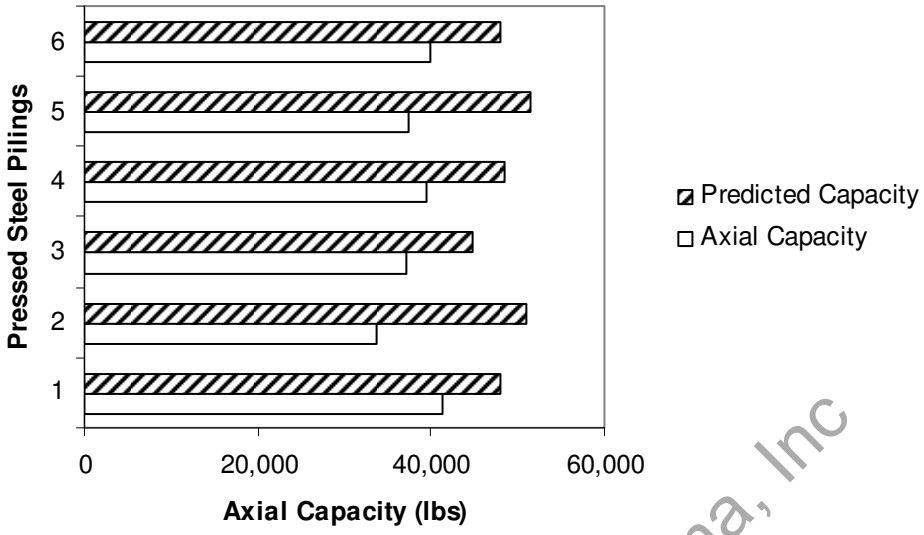

Figure 6.28 - Comparison of Predicted to Measured Axial Capacity of Pressed Steel Piles Using CPT, 'Wet to Dry' Condition

As evident from these figures (Figures 6.25 to 6.28) and tables, prediction of axial capacity using continuous CPT friction data has provided better predictions. Certain problems in these interpretations do exist and these are attributed to the presence of strong lenses in the soil with higher shear strength, which may result in establishing of a piling of short length. As a result, when moisture returns to this area from rainfall infiltration, shear strength decreases and as a results, the piling with short length will be able to support only reduced axial capacity.

The final outcome of this analysis is that a continuous soil profiling is needed for better estimation of axial capacities of pressed steel piles. The CPT is consistent and simulates the penetration mechanism around pressed steel piles, which are pressed into the ground using segmental cylinders of steel pipe in a continuous pressing operation.

6.2.6 Pressed Concrete Piles

Predictions of Axial Compressive Capacity for the pressed concrete piles were attempted using both soil properties and CPT side friction information (Tables 6.13 and 6.14 as well as Figures 6.29 to 6.32). The following explains a comparison of these predictions along with the measured capacities.

Table 6.13 - Predicted vs. Measured Capacities for Pressed Concrete Piles Using Soil Properties, 'Dry to Wet' Condition

Pile #	Depth (ft)	Predicted Capacity (lbs)	Actual Capacity (lbs)	Installation Capacity (lbs)
1	7.67	31,426	29,000	50,000
2	10.17	34,319	37,000	50,000
3	27.42	71,474	68,566	50,000
7	15.67	41,398	50,400	50,000
8	10.67	39,596	39,000	50,000
9	25.67	67,994	68,000	50,000

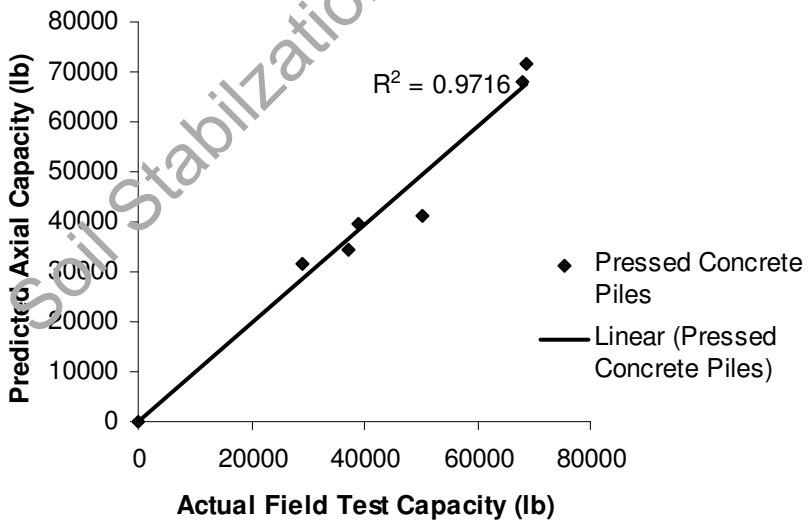

Figure 6.29 – Comparisons of Predicted to Measured Axial Capacity Using Soil Properties, 'Dry to Wet' Condition

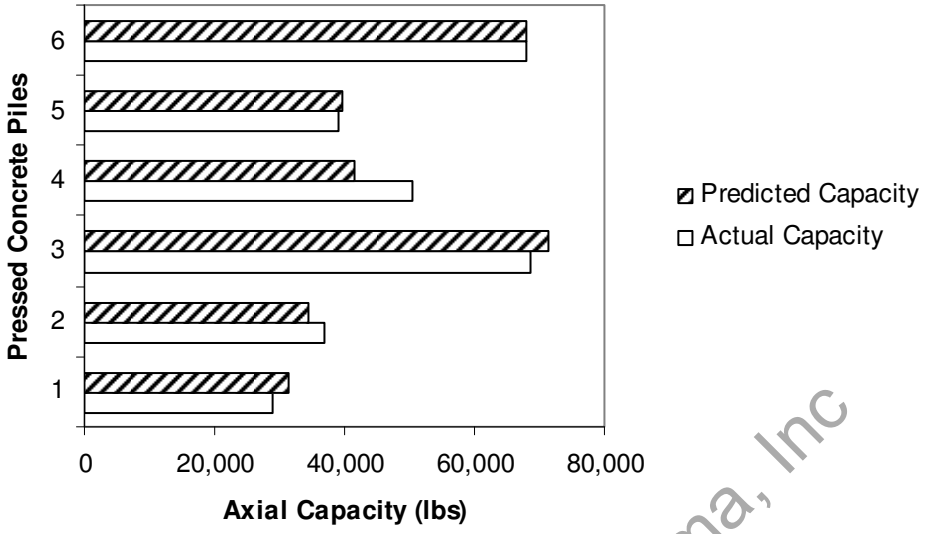

Figure 6.30 – Comparisons of Predicted to Measured Axial Capacity Using Soil Properties, 'Dry to Wet' Condition

Table 6.14 Predicted vs. Tested Capacity for Pressed Steel Piles Using Soil Properties, 'Wet to Dry' Condition

Pile #	Depth(ft)	Predicted Capacity (lbs)	Actual Capacity (lbs)	Installation Capacity (lbs)
4	24.67	60,316	57,940	50,000
6	19.67	48,000	61,800	50,000
10	24.67	60,316	65,920	50,000
12	28.67	67,860	61,800	50,000

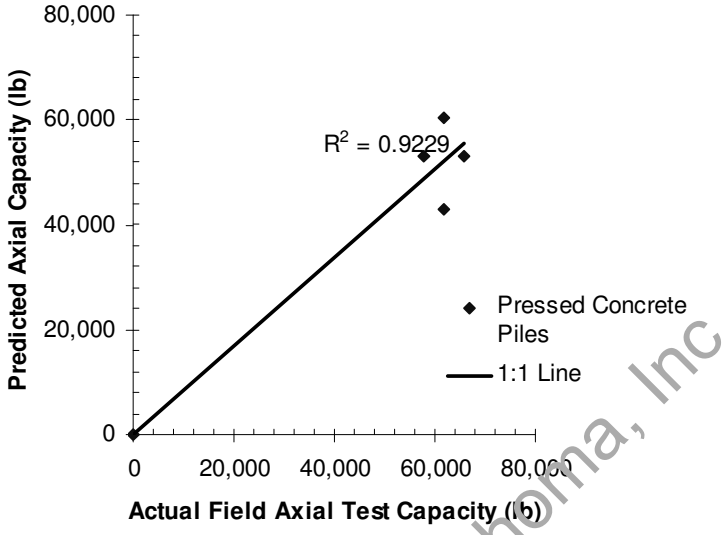

Figure 6.31 - Comparisons of Predicted to Measured Axial Capacity Using Soil Properties, 'Wet to Dry' Condition

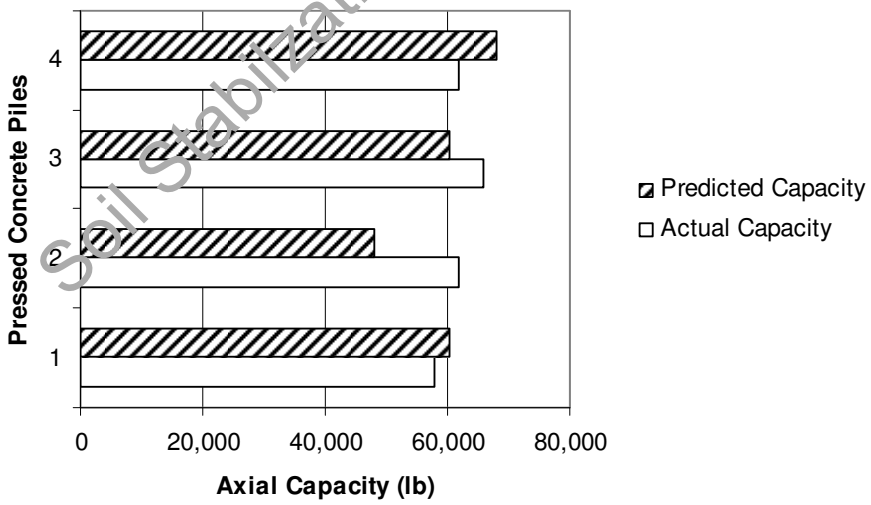

Figure 6.32 - Comparisons of Predicted to Measured Axial Capacity Using Soil Properties, 'Wet to Dry' Condition

Now predictions were made using CPT data for the pressed concrete pilings for this test.

Table 6.15 - Predicted vs. Tested Capacity for Pressed Concrete Piles Using CPT, 'Dry to Wet' Condition

Pile #	Depth(ft)	Predicted Capacity (lb)	Actual Capacity (lb)	Installation Capacity (lb)
1	7.67	34,191	29,000	50,000
2	10.17	46,105	37,000	50,000
3	27.42	71,845	68,566	50,000
7	15.67	51,732	50,400	50,000
8	10.67	44,795	39,000	50,000
9	25.67	68,546	68,000	50,000

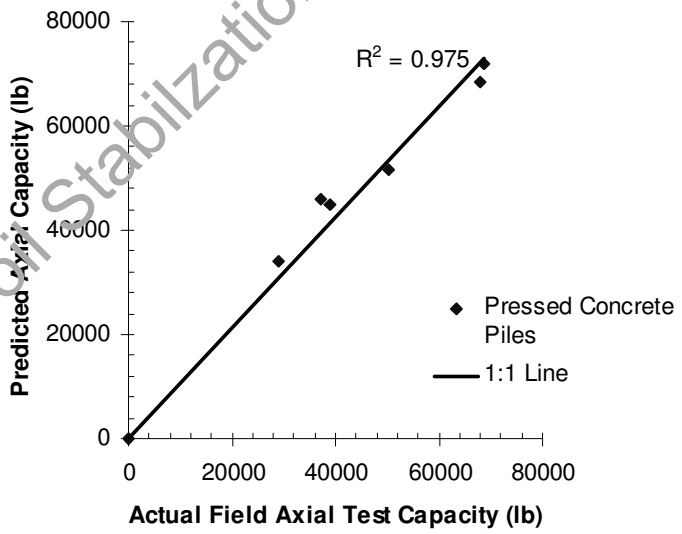

Figure 6.33 - Comparison of Predicted Capacity to Measured Axial Capacity Using CPT, 'Dry to Wet' Condition

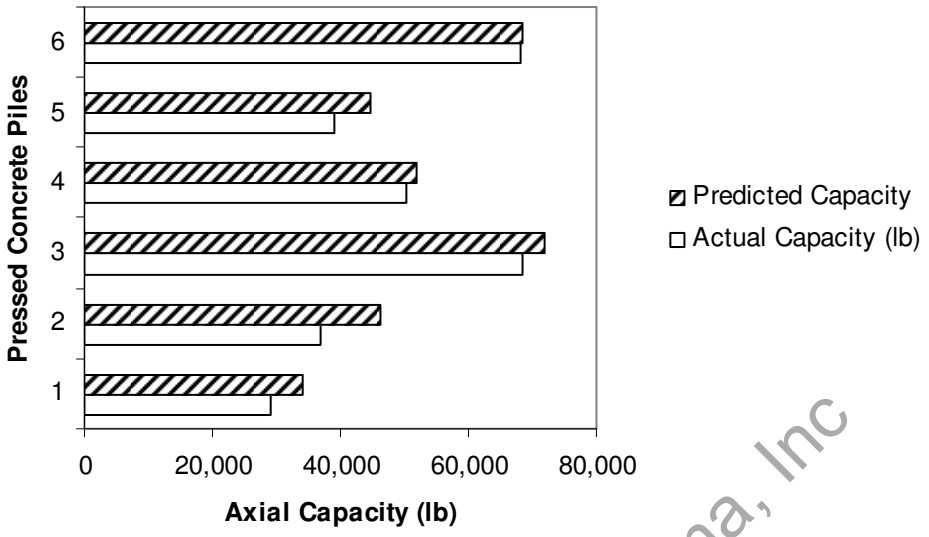

Figure 6.34 - Comparison of Predicted Capacity to Measured Axial Capacity Using CPT, 'Dry to Wet' Condition

Table 6.16 - Predicted vs. Tested Capacity for Pressed Concrete Piles Using CPT, 'Wet to Dry Condition

Pile #	Depth(ft)	Predicted Capacity (lbs)	Actual Capacity (lbs)	Installation Capacity (lbs)
4	24.67	66,963	57,940	50,000
6	19.67	58,970	61,800	50,000
10	24.67	66,963	65,920	50,000
12	28.67	70,450	61,800	50,000
5* 11*				

*** Pilings Broke During Installation**

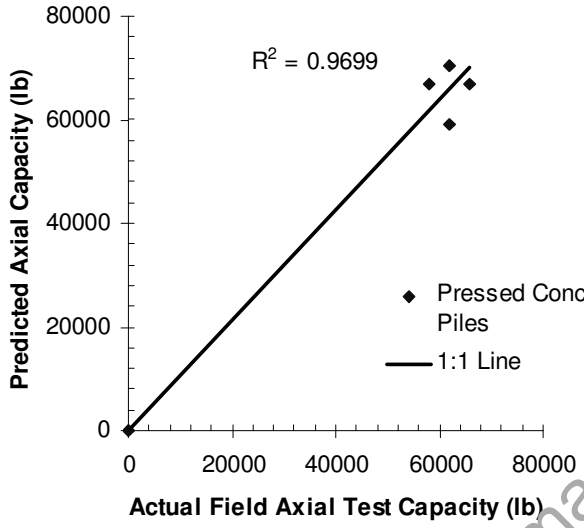

Figure 6.35 - Comparison of Predicted to Measured Axial Capacity Using CPT, 'Wet to Dry' Condition

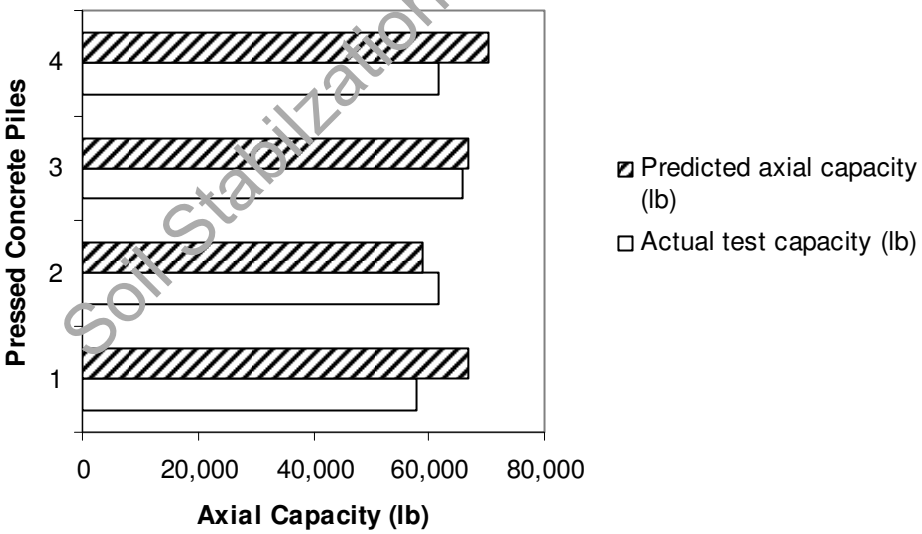

Figure 6.36 - Comparison of Predicted to Measured Axial Capacity Using CPT, 'Wet to Dry' Condition

This interpretation based on soil properties was good for pressed piles and the same with CPT data provided better predictions of the capacities for the same piles. As shown above, the CPT based approach is the best predictor of axial capacity, probably because the test is similar to the installation of the pressed concrete piles, which are similar to quasi-static in operation. Hence the CPT approach based interpretation method accounted for variations in shear strength of soils including properties of thin lenses in subsoil strata. As a result, the predictions here are close to measured results. Hence, for pressed concrete piles, both interpretation methods are recommended.

Reasons for soil property based interpretation for pressed concrete piles are close to measured results (unlike in pressed steel piles) is due to incorporation of higher side friction terms for converting them to adhesion to account for higher roughness of concrete materials.

6.3 Summary

As detailed in this chapter, predictions of drilled shafts (straight and belled) and augercast piles are good indicating current predictive models providing reasonable predictions. Predictions of helical anchor capacities are also acceptable using the individual bearing plate method. With multiple helixes, there is a disturbance factor that must be employed to better predict the ultimate axial compressive capacities. Prediction of axial capacity of the pressed steel piles is not accurate using soil properties but using CPT, the predictions are improved. Pressed concrete pile predictions can be made using soil properties; however these axial capacity predictions are more accurate when the CPT friction data is used.

CHAPTER 7

OVERALL AXIAL CAPACITY COMPARISON

7.1 Introduction

In this chapter, several comparisons were made among the underpinnings used in this research. The main intent of these comparisons is to explain the seasonal variations on the axial load capacities of the foundations as well as to explain the effects of the type of foundation on the final load capacities.

7.2 Effects of Seasonal Variations

As mentioned earlier, this study was a first time attempt to address the ultimate load capacities of underpinning foundations installed in dry (summer) and wet (spring) seasons. It should be noted here that the tests were conducted in the alternate seasons, i.e. installed in wet or spring season and tested in dry or summer season.

7.2.1 'Dry Season to Wet Season'

Table 7.1 and Figure 7.1 present axial load capacities of the underpinning elements installed in summer season and tested in spring or wet season.

Table 7.1 - Comparison of Axial Capacities of Different Underpinning Methods, 'Dry to Wet Season'

Straight Shafts	Belled Shafts	Augercast Piles	Helical Piles	Pressed Steel Piles	Pressed Concrete Piles
104,160	180,790	121,120	29,550	48,320	29,000
100,990	172,540	105,220	23,640	33,000	37,000
126,410	168,380	100,990	27,580	52,480	68,566
			27,580	42,000	50,400
				41,000	39,000
				48,320	68,566

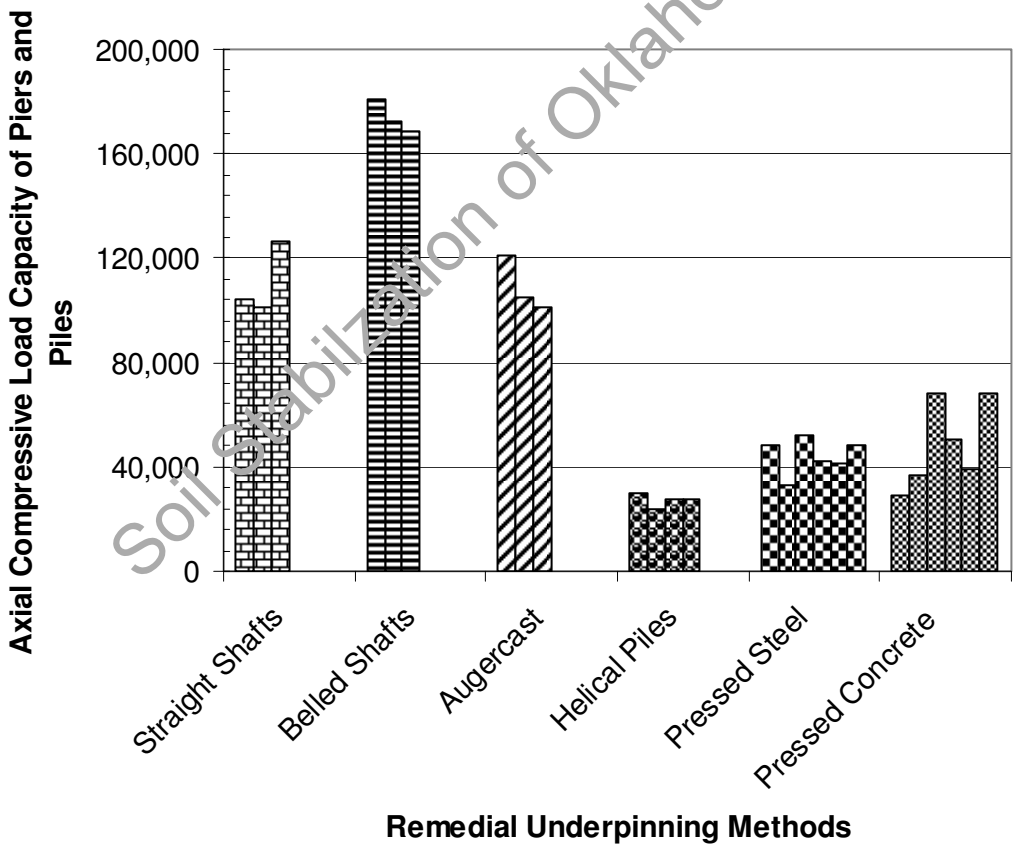

Figure 7.1 - Comparison of all Underpinning Methods, 'Dry to Wet' Condition

It should be noted that the lengths and diameters of each of the foundations are different and hence exact comparisons based on their predictions should not be addressed. Results in Figure 7.1 indicate that the drilled shafts (straight and belled) and augercast piles yielded higher capacities among the present underpinning methods. All these foundations were installed in August 2004 and tested in April 2005.

Belled shafts yielded highest capacities with predominant loads contributed from the bell portion. Among the helical and pressed piles, pressed concrete capacities are not uniform whereas pressed steel piles provided similar load capacities. Helical piles provided lower capacities and their lengths are between those of the pressed concrete and pressed steel foundations.

7.2.2 Wet Season to Dry Season

Table 7.2 and Figure 7.2 present axial load capacities of the underpinning elements installed in spring season and tested in summer or dry season.

Table 7.2 - Comparison of Axial Capacities of Different Underpinning Methods, 'Wet to Dry' Condition

Straight Shafts	Belled Shafts	Augercast Piles	Helical Piles	Pressed Steel Piles	Pressed Concrete Piles
106,600	165,500	110,030	24,720	41,200	57,940
123,000	165,500	106,760	25,544	33,784	61,800
102,500	157,060	106,760	26,780	37,080	65,920
			28,016	39,552	61,800
				37,492	
				39,964	

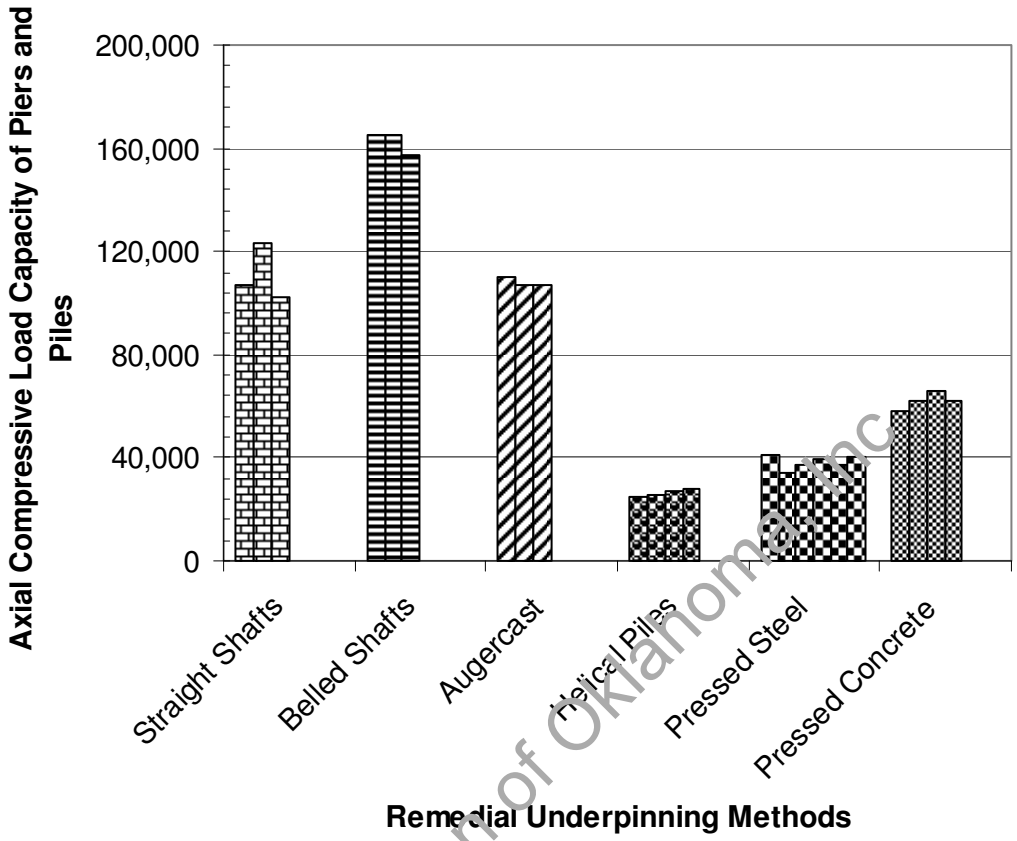

Figure 7.2 - Comparisons of All Underpinning Methods (Wet to Dry Condition)

Again, both drilled shafts (straight and belled) and augercast piles yielded higher capacities among the underpinning methods installed in April 2005 and tested in August 2005. All foundations showed a much more consistent capacity when they were tested during this seasonal environmental condition. Also the lengths of each of the underpinnings of this seasonal group are higher or the same when compared to the earlier seasonal group, since the foundations were installed in a wetter season when the soils are soft in nature and allowed a deeper penetration into the clay soil.

There was negligible difference between ultimate axial compression capacity in straight drilled shafts and augercast piles. This condition is expected since both foundation installation methods have some similarities. Therefore, the skin friction allowance for the straight drilled shafts should be included similar to the augercast piles in clay soil.

7.3 Overall Comparisons

The following table 7.3 compares all foundations across various seasons.

Table 7.3 - Comparison of All Underpinning Systems Across All Seasons

Straight Shafts	Belled Shafts	Augercast Piles	Helical Piles	Pressed Steel Piles	Pressed Concrete Piles
104,160	180,790	121,120	29,550	48,320	29,000
100,990	172,540	105,220	23,640	33,000	37,000
126,410	168,380	100,990	27,580	52,480	68,566
106,600	165,500	110,030	27,580	42,000	50,400
123,000	165,500	106,760	24,720	41,000	39,000
102,500	157,060	106,760	25,544	48,320	68,566
			26,780	41,200	57,940
			28,016	33,784	61,800
				37,080	65,920
				39,552	61,800
				37,492	
				39,964	

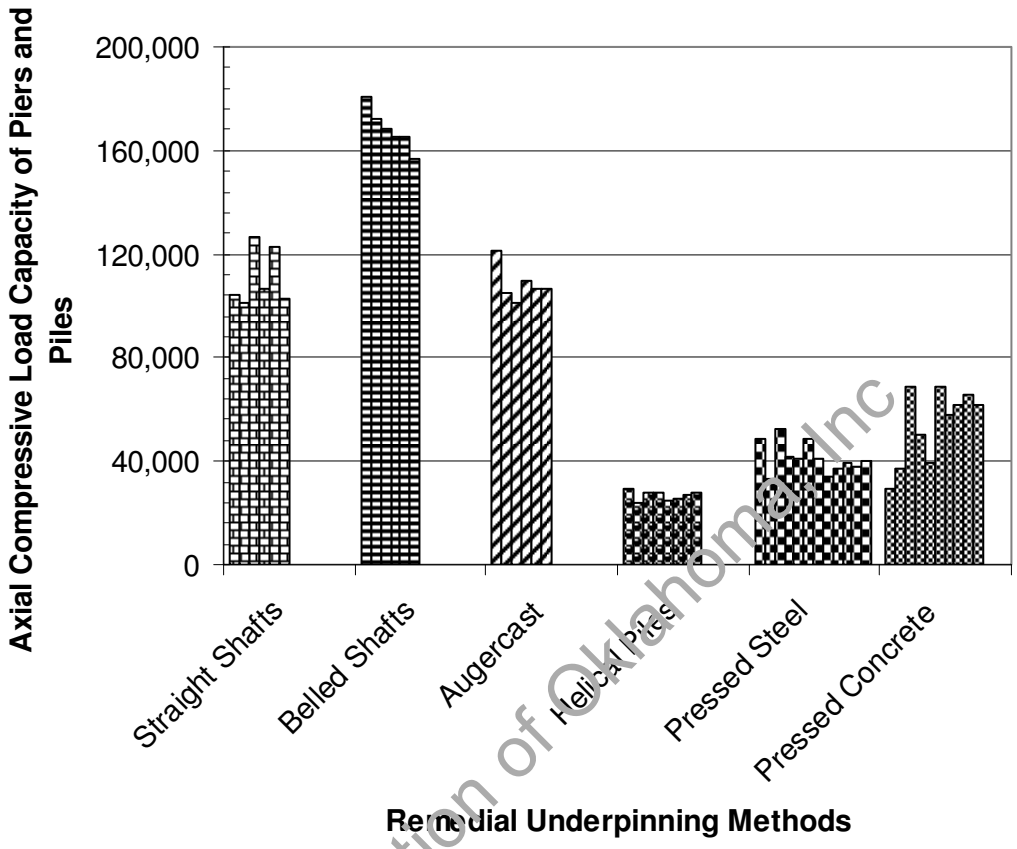

Figure 7.3 - Comparisons of Different Underpinning Methods Across All Seasons

Regardless of the season, the drilled shafts and augercast pilings show consistent capacities and higher ultimate axial loads than the rest of the underpinning techniques tested in this research. With the pressed concrete pilings, the depth of penetration is a key element in recording a high axial compression capacity. In the case of pressed steel pilings, there is considerable variation among the lengths of pressed pile systems.

Helical piles did not show any dependency on the type of seasonal installation. Since these foundations derive their capacities from residual shear strength parameters

below the helix(s) and not along the pipe stem, seasonal moisture changes do not appear to have a measurable effect on their ultimate capacity.

7.4 Load Versus Deflection at Failure

It was recognized during the test that the different methods showed different deflection patterns leading up to the ultimate failure load. To further understand these deformations, average load at failure was plotted against deflection at the initial ultimate capacity.

Table 7.4 - Load vs. Deflection for Different Underpinning Methods- 'Dry to Wet' Season

Average Load at Failure	Average Deflection at Failure	Underpinning Type
110,520	0.182	straight shafts
173,903	0.198	belled shafts
109,110	0.3	augercast piles
27,088	0.306	helical piles
44,187	0.39	pressed steel
48,755	0.155	pressed concrete

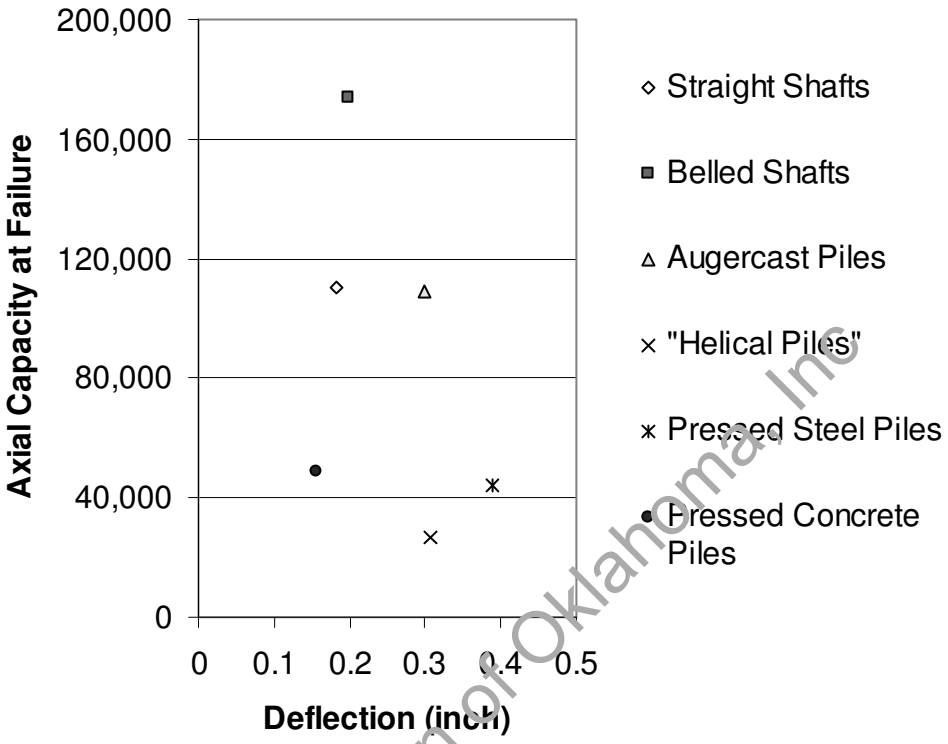

Figure 7.4 - Load vs. Deflection for Different Underpinning Groups 'Dry to Wet' Season

Table 7.5 - Load vs. Deflection for Different Underpinning Methods- 'Wet to Dry' Season

Average Load at Failure	Average Deflection at Failure	Underpinning Type
110,700	0.116	straight shafts
162,687	0.164	belled shafts
107,850	0.217	augercast piles
26,265	0.386	helical piles
38,179	0.591	pressed steel
61,865	0.199	pressed concrete

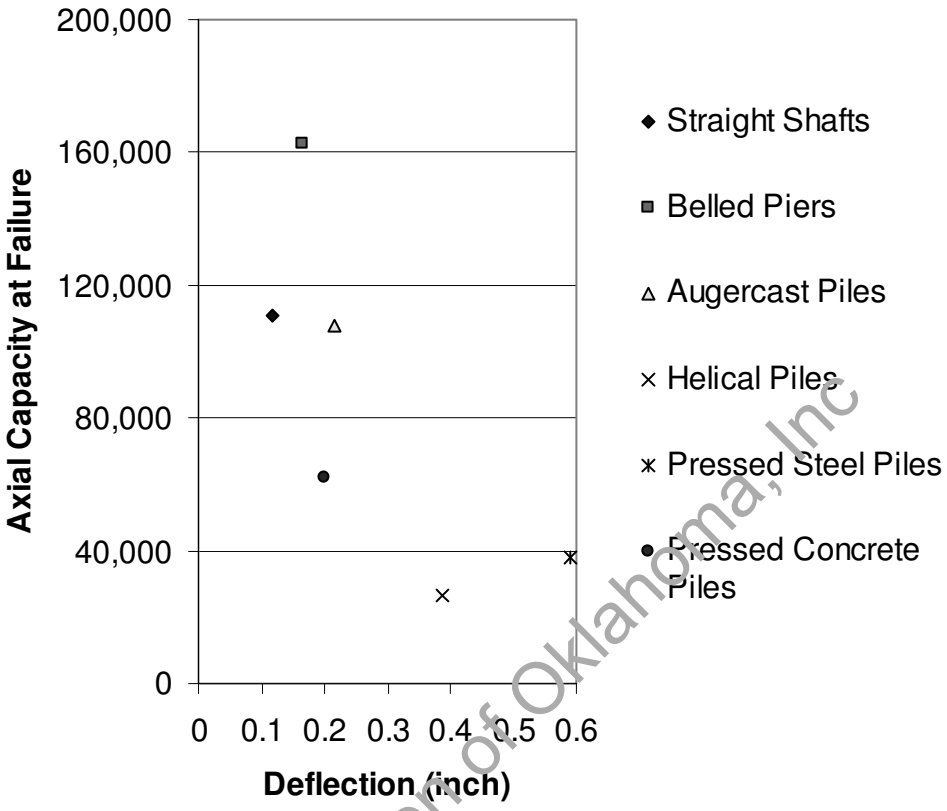

Figure 7.5 - Load vs. Deflection for Different Underpinning Groups Wet to Dry Season

Table 7.6 - Overall Comparison of all Methods and Both Seasons

Average Load at Failure	Average Deflection at Failure	
110,610	0.149	straight shafts
168,295	0.181	belled shafts
108,480	0.258	augercast piles
26,677	0.346	helical piles
41,183	0.491	pressed steel
55,310	0.177	pressed concrete

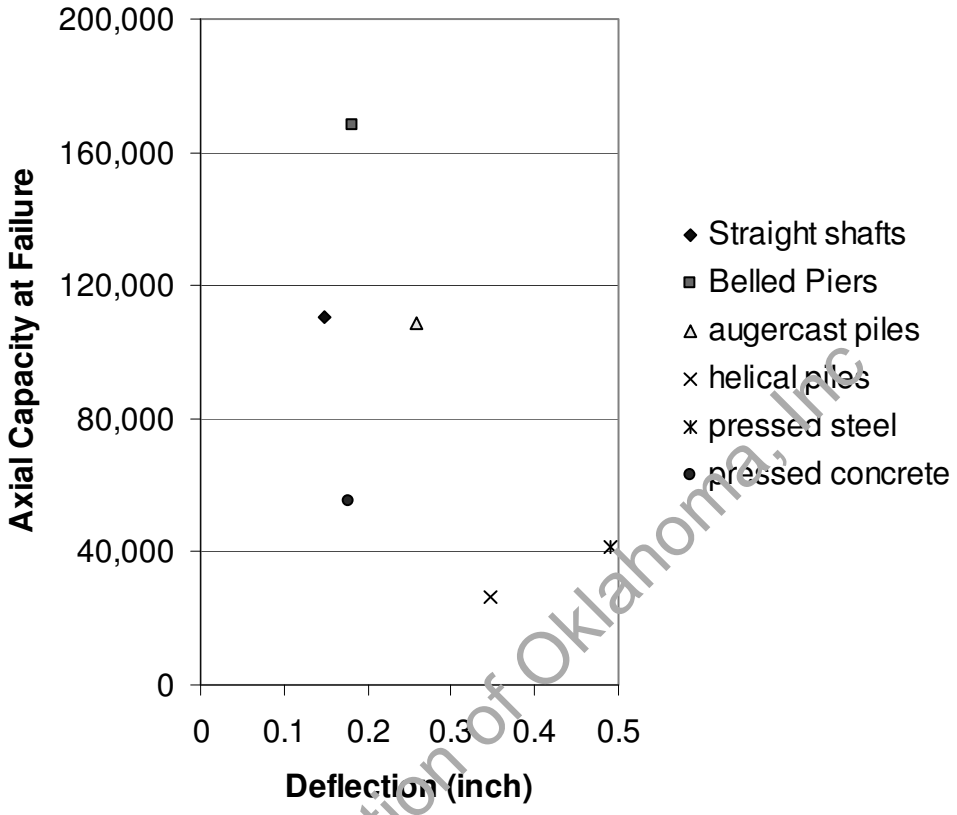

Figure 7.6 - Loads vs. Deflection for Different Underpinning Groups and Both Seasons

The deflection point at ultimate capacity was slightly greater for the augercast pile than for the straight or belled shaft. This may be attributable to installation procedures where spoil from the hole is removed by grout pumping and not by visual cleaning of the hole with an auger bit as is the case with the drilled shafts. It should also be noted that this difference may only be measurable because these holes are relatively short where end bearing has a higher contribution to ultimate capacity.

As shown in the tables and on the figures above, the pressed steel and helical piles showed the greatest amount of deflection in reaching their ultimate load. These results mirror this engineer's own personal experience in using helical piles for remedial work on foundations of houses. The pressure that was required to "seat" the helical piles prior to applying a load to lift a house appears to be similar to these test results. The amount of deflection recorded for this test, however, was much less than this engineer has witnessed in previous observations. This difference in deflection was probably the result of a connection method used by a different supplier where a looser connection separated slightly as the helix pulled the bar into the ground and created tension in the stem, which was then compressed downward when a load was applied.

It should be noted that the design engineer must consider the amount of deflection recorded to get to ultimate capacity in this underpinning system when deciding to use helical piles for new construction since there is no opportunity to "seat" the pile prior to receiving the building load.

It is also obvious that the pressed steel pile records a considerable amount of deflection prior to reaching its ultimate strength, which is probably the result of a small diameter piling and much less material skin friction than concrete elements. The pressed concrete pilings showed similar deflection behavior to the drilled piers. Therefore, it appears that material skin friction is a key element in side friction of a piling in clay soil.

7.5 Summary

This chapter presented an overall comparison between the foundation systems across seasonal moisture changes. The drilled straight shafts and augercast piles provided similar capacities with the belled piers showing the highest capacity of any underpinning

system. Helical anchors showed the lowest capacity but their capacities were very consistent. Pressed steel pilings showed the largest deflection prior to reaching ultimate capacity and their capacities varied a considerable amount.

The pressed concrete pilings showed a large variation primarily because some of the pilings installed in the dry period could not be pushed beyond the active zone. When the pressed concrete pilings were installed below the active zone, however, they performed similarly to drilled shafts, but with proportionally less ultimate capacity in comparison with their size.

CHAPTER 8

SUMMARY AND CONCLUSIONS

8.1 Introduction

Foundation distress and subsequent failure will continue to be a problem for homeowners, especially when they are built in expansive clay soils. As a result, underpinning to mitigate deflection problems for slab-on-grade foundations in contact with these expansive soils will continue to be remedial measures adapted in the field. Because of the wide spread use of piers, piling and helical piers, this research was undertaken to address the axial load transfer mechanisms in these foundations. This research will be helpful to provide insights to the practitioner, engineers and homeowners while deciding the proper method of underpinnings for foundation repairs. It should also be mentioned that the research results and conclusions can be further corroborated by conducting additional studies on different expansive soil sites.

The major conclusions and summary information from the present study are summarized in the following section.

8.2 Summary and Conclusions

The following conclusions and summary information was obtained from this research conducted on six different underpinning systems installed in an expansive soil zone.

8.2.1 Summary

1. Predictions of axial compression capacity of the drilled shafts, belled piers and augercast piles were close to measured capacities. Hence, the pier or pile capacity procedures using the FHWA-IF-99-025 design manual (FHWA 1999) are considered reliable methods for estimations of axial capacities of these foundations in expansive soil media.
2. Use of a 60^{o} layout plan for field testing of large numbers of piers and piles was proven to be effective and efficient in the field load testing operation.

8.2.2 Conclusions

1. There was a negligible difference between ultimate axial compression capacity in the straight drilled shafts and augercast piles. The skin friction allowance for the drilled shafts should be the same as the one allowed for augercast piles in clay soil. Also, the deflection readings at ultimate capacity were slightly greater for the augercast pile than for the straight or belled shaft. This difference may be attributed to construction procedures in that the augercast pile normally does not produce a clean bottom surface whereas in a drilled shaft, the bottom surface can be inspected before placing concrete by either looking in the hole or running a camera in the case of open holes and by probing when pouring under slurry.
2. There was a negligible difference in ultimate axial compression capacities of the majority of drilled underpinnings between 'dry to wet' and 'wet to dry' seasonal conditions. While shear strength in upper layers did increase while

going from ‘wet to dry’ season, drying induced soil shrinkage from the pier/pile (near surface) might have mitigated the increases in axial capacity.

3. Time of soil sampling has a major bearing on predicted axial compression capacity. If insitu or soil sampling tests is made during the dry season, shear strength parameters might have been increased for upper clayey layers due to desiccation related drying. Conversely, the wet season strength parameters are low and may provide lower, but conservative design parameters.
4. This research also indicates that the non-contributing depth of soil considered for shafts appeared to be important when foundation tests were performed in dry season. The non-contributing lengths from thin wire measurements show that they vary from 3 ft to 4 ft, slightly less than the recommended 5 ft value. If soil sampling and testing is attempted in the wet season, this research indicates that the total shaft depth should be included in the predictions of axial capacity since soil around the upper layers is in contact with shafts.
5. Installation of helical piles shows that the installation process of the helix in clayey medium may not pull into the ground efficiently to prevent augering of the helix and thus producing a trailing section of loose soil. Therefore the helical anchors will many times require seating using pressure from a structure in order to obtain the maximum capacity of the helical piles. With the presence of this void, larger deflection in helical piles installed in new construction jobs must be anticipated in clay soils and the design engineer must allow for this deflection accordingly.

6. In this research, when the installation torque was constant and same for helical piles, there was minor or very little difference in ultimate axial compression capacity between single and double helix piles. The double helix piling did, however, produce a more consistent ultimate capacity.
7. There was no obvious or major difference in the ultimate axial capacities of the helical piles installed in 'dry to wet' and 'wet to dry' conditions.
8. The Individual Bearing Plate method proved reasonable approach in estimating capacity of the single helix. With the double helix, however, it is necessary to apply a disturbance factor to be included in the axial capacity formulation to simulate disturbed state of soil condition. This disturbance factor was found to be an approximate 80% for this research. Therefore, contributing axial capacity support of the trailing helix was only 20% of the leading helix capacity as measured by area of helix and shear strength of soil.
9. Pressed steel pilings show the greatest amount of deflection prior to reaching their ultimate capacity. Both pressed concrete and steel piling systems yielded consistent at their ultimate capacity when they were installed during the wet period. Deeper penetration depths for these pressed piles were obtained, which indicate that the final capacity of these piles depend on length of the pile, and installation as well as testing seasonal conditions.
10. Pressed concrete pilings appear to perform in an identical fashion as those of drilled concrete piers but with an obvious reduction in axial load capacity due to smaller size of the pressed concrete pile dimensions.

11. When pressed concrete pilings were installed shallower than the zone of seasonal moisture change (between 10 ft and 15 ft for this test), they tend to loose most of the installation capacity, i.e. up to 42% of the installation load. When these same pilings are installed below 15 ft in this soil and in these climatic conditions, they have gained 37% over installation capacity.
12. Three of the final six pressed concrete pilings were broken either during installation or during testing. It is not known if this failure was due to the movements of reaction beam or due to bending moments caused by lateral soil shrinkage around the piling during the dry period.
13. The pressed concrete pilings used in this research were installed with a #4 reinforcing steel bar passed through the center of the piles with the hole filled with Portland cement grout. Both reinforcement and grouting enhance lateral load resistance as well as flexural capacity of this foundation system. Hence, the present pressed concrete pile results are valid for this type of pressed concrete pile system. The performance of pressed concrete pilings without any reinforcement or bonding may have problems simply due to lesser tensile and flexural resistances.
14. Predicting axial compression capacity of pressed steel pilings does not appear to be accurate when using soil properties from laboratory tests on samples collected from the field. When the continuous CPT profiling with side friction measurements was used to estimate the capacities, they appear to match with the measured ultimate loads. This correlation is especially strong when the pilings were installed sufficiently below the active zone. This indicates that

soil is around pressed piles are in residual shear strength state, which is well captured by the side friction of CPT. Also, the mechanisms of penetration for pilings and CPT are similar and hence there is a strong correlation between side friction estimation in both methods.

15. Overall comparisons of the six underpinning methods show that the belled shaft has the highest axial load capacity followed by the straight shaft and augercast piles. Though cost comparisons are not included here, it can be qualitatively mentioned that the costs of drilled shafts and augercast piles for underpinning can be significantly high in expenses when compared to the rest of the underpinning methods. However, the final selection of the underpinning foundation system should not be based on the cost of installation and construction of them. Such practice may lead to further problems to residential structures in the future.

8.3 Recommendations for Future Studies

The following areas of research are suggested for future studies.

1. Testing of pressed steel and concrete should be attempted using standard installation pressures that would emulate a one story house. These standard pressures appear to be at installation load, between 25,000 lbs and 35,000 lbs.
2. Testing of pressed steel and pressed concrete pilings in expansive clay soil to measure uplift movement and/or pressures.

3. Testing of non-joined pressed concrete pilings to determine axial load capacity and influence of active soil uplift movement against the segmental piling string.
4. Testing of pressed steel and concrete pilings in sandy soil to determine axial compressive capacity over time and water table drawn-down.
5. Further testing of pressed steel and pressed concrete pilings with projections using CPT site data.
6. Comparative testing of augercast piles and drilled straight shafts should be done in sandy soils using both casing and slurry installation for the drilled shafts to compare axial compressive capacity with these installation techniques.
7. Testing of straight drilled shafts should be attempted in expansive clay soils using casings to overcome caving conditions to address if the increase in shaft diameter mitigates perceived skin friction loss along the casing perimeter.
8. Additional testing of drilled shafts across seasons with installation and time of soil testing (in situ or bore hole) to determine/confirm if time of soil testing has an effect on total shaft length consideration.

APPENDIX A

TYPICAL UU TRIAXIAL MOHR CIRCLES

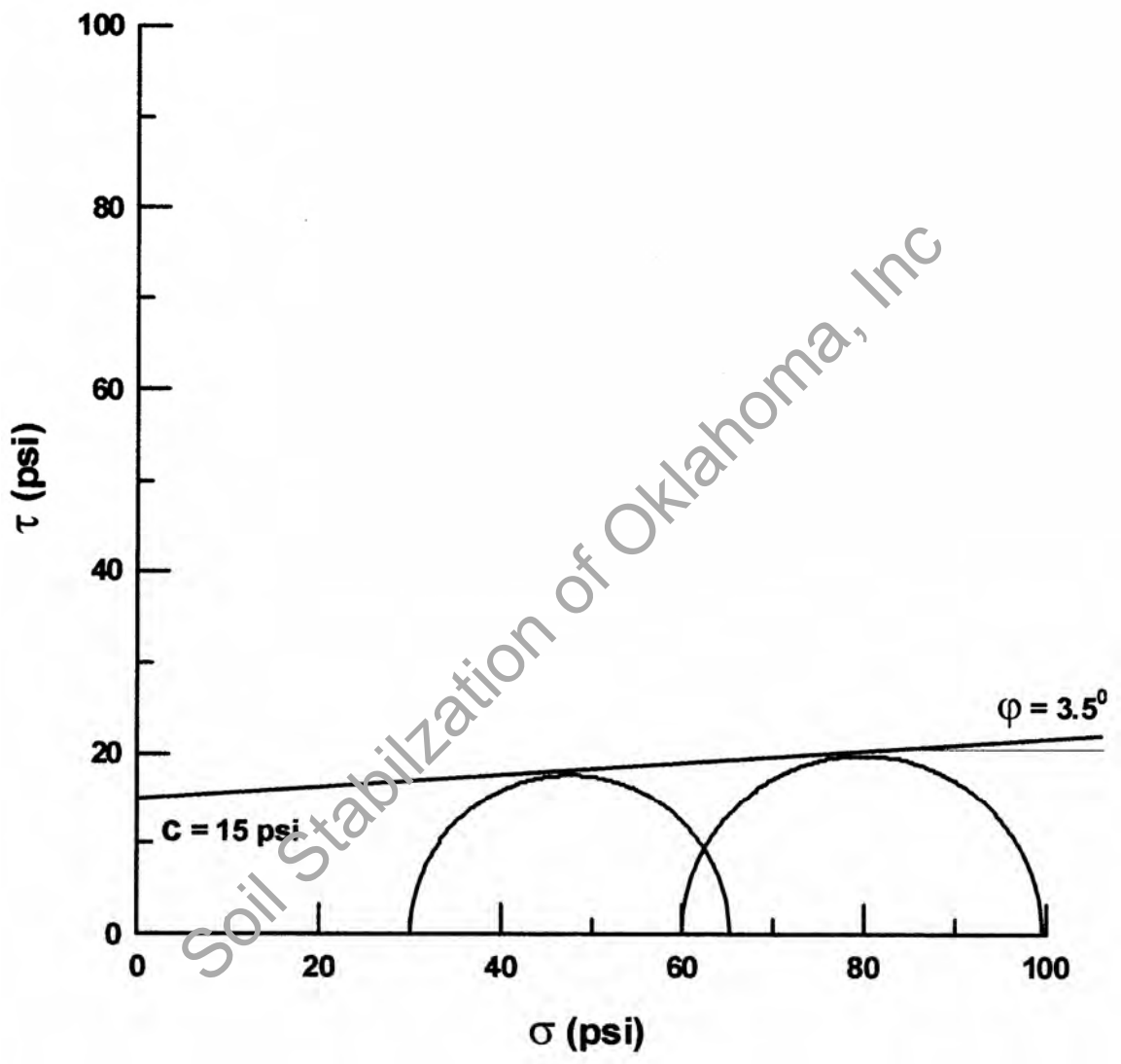

Figure A1 - UU Triaxial Tests Determination of φ and c_u with Two Soil Samples. Boring #2, 45ft to 50ft

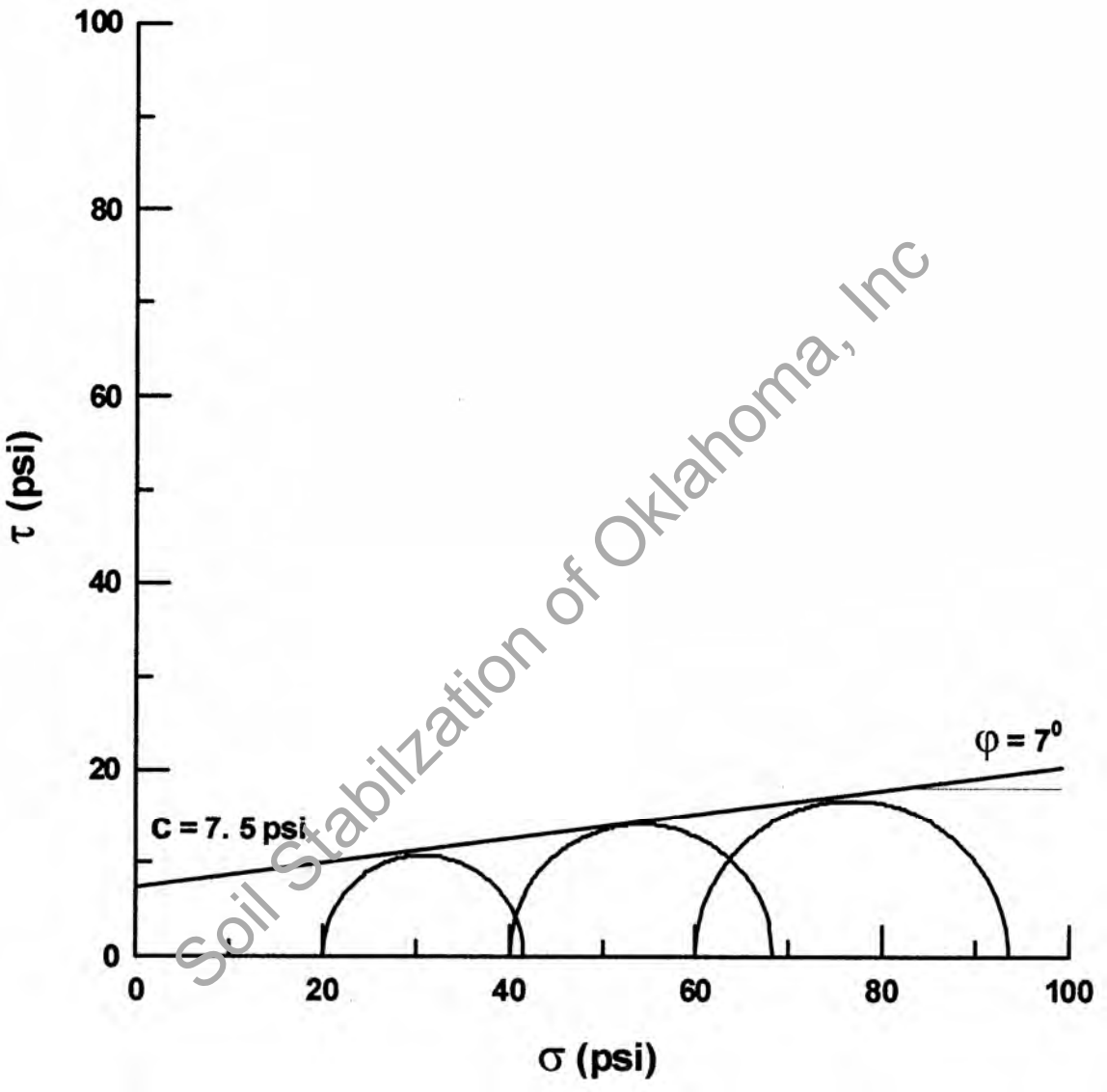

Figure A2 - UU Triaxial Tests Determination of φ and c_u with Three Soil Samples. Boring #3, 0 to 5ft

CONTRIBUTIONS IN KIND AND MONEY

This project would not have been possible without the combined contributions of the following individuals who donated services, material, equipment, time and money. The magnitude of their contribution was a very humbling event and told me how much they wanted to be apart of this ground breaking research. To have the support of the engineering community across the United States told me this research was important. Support from the foundation underpinning industry to the magnitude reflected below, however, told me that this testing had been needed for a long time and would potentially change the industry. At the very least, this research will create a climate for additional testing that will lead to many more worthwhile discoveries that will not only help an industry but bring greater value to the residential foundation repair market and ultimately increase value to the homeowner and help protect and remediate their greatest value.

1. ADSC, Industry Advancement Fund- Seed money
2. ADSC, South Central Chapter- cash sponsorship
3. Advanced Foundation Repair, Dallas, Texas- 12 pressed concrete piles

4. Allied Drilling company, Ft. Worth, Texas- drilling shafts and belling piers for testing
5. ATS Drilling, Ft. Worth, Texas- Reinforcing steel for reaction piers
6. Cameron Machine Shop- Miscellaneous Welding and fabricating
7. Con-Tech Systems, LTD- Donation of 100 ton test ram for use to test in April, 2005 and August 2005
8. Custom Crete Concrete- Concrete for reaction piers
9. Dywidag Corporation- 48 reaction bars, machining of bars, engineering and couplings
10. Fox Foundation Repair, Dallas, Texas- pier/pile test plates
11. Fugro Geotechnical Engineers, Dallas, Texas- 4 soil borings
12. Greg In Situ, Houston, Texas – 2 CPT logs and generated analysis
13. Illini Drilled Foundation, Danville, Illinois- augercast piles
14. Lindamood Excavating, Irving, Texas- Hydralift for moving of beams
15. McKinney Drilling Co., Ft. Worth, Texas- Drilling reaction piers
16. Ram Jack Foundation Repair, Dallas, Texas- 12 pressed steel piles, 4 helical anchors and miscellaneous welding and fabricating
17. N.L. Schutte, Dallas, Texas- Reaction Beams
    29 days crane service
18. S & W Foundation Contractors, Richardson, Texas- augercast and drilled pier labor and trucking
19. Texas Shafts, Ft. Worth, Texas- Tying of steel and crane service to set reinforcing steel for reaction piers

20. Mike Trotter General Contractor and the Trotter Companies, Doraville, Georgia.

21. Farrell, Ed – donation of ranch land for test for 16 months and not requiring clean-up of site.

22. Clayton and Johnnie Stephens- time, labor and coordination

BIOGRAPHICAL INFORMATION

W. Tom Witherspoon was born in Dallas, Texas on February 1, 1949. He received his B.S. in Civil Engineering from Southern Methodist University in Dallas, Texas in 1971. He then received a Masters of Management and Administrative Science from the University of Texas at Dallas in 1979. He did graduate studies in Geotechnical Engineering at Southern Methodist University in 1979 and 1980 as a doctoral candidate. He began doctoral studies at the University of Texas at Arlington in August of 2002 and completed all requirements for the Degree of Doctor of Philosophy in Civil Engineering and received the Degree on May 13, 2006.

Mr. Witherspoon's Professional Licenses include:

Licensed Professional Engineer – Texas

Registered Professional Land Surveyor – Texas

Licensed Irrigator – Texas

Registered Sanitarian – Texas

Professional Geoscientist (Soil Science) - Texas

Certified Structural Repair Specialist – U.S.

Certified Foundation Repair Specialist – U.S.

Mr. Witherspoon has authored one book (Residential Foundation Performance 2000) and two standards for the Foundation Repair Association (Foundation Maintenance 2001 and Expectations of Underpinning 2001).